



Authors

Prof. Tapan Saha

Dr. Mithulan Nadarajah

Dr. Jahangir Hossain

Mr. Tareq Aziz and

Mr. Sudarshan Dahal

---

# **INTELLIGENT GRID**

## **RESEARCH CLUSTER-PROJECT 1**

Control Methodologies of Distributed Generation  
for Enhanced Network Stability and Control

## CONTENTS

<b>1.-----EXECUTIVE SUMMARY</b>	<b>12</b>
1.1. Modelling and analysis	13
1.2. Voltage stability	13
1.3. Small signal stability	14
1.4. Reactive Compensation	14
1.5. Control methodologies for the enhancement of small signal stability	15
1.6. Results and Outcomes	15
1.7. Small Signal Stability Assessment with DG Units	19
1.8. Control Methodologies for Distributed Generation	22
1.9. Final conclusions	25
<b>2.-----INTRODUCTION</b>	<b>28</b>
2.1. Review of power system modelling	29
2.2. Review of system stability	32
2.3. Review of control methodologies	36
2.4. Summary	43
<b>3.-----MODELLING OF DISTRIBUTION SYSTEMS WITH DISTRIBUTED GENERATORS</b>	<b>45</b>
3.1. Distributed Generators	45
3.2. Load modelling	51

<b>3.3. Static Var compensator (SVC)</b>	<b>53</b>
<b>3.4. Static synchronous compensator (STATCOM)</b>	<b>54</b>
<b>3.5. Summary</b>	<b>56</b>
<b>4.-----ENHANCEMENT OF VOLTAGE STABILITY WITH DG UNITS</b>	<b>57</b>
Investigation of effective voltage stability indices	59
<b>4.1. System Loadability</b>	<b>60</b>
<b>4.2. Reactive power margin</b>	<b>60</b>
<b>4.3. Voltage Sensitivity Factor</b>	<b>60</b>
<b>4.4. L-Index</b>	<b>60</b>
<b>4.5. Impact of load model on voltage stability indices</b>	<b>62</b>
<b>4.6. Static load model</b>	<b>62</b>
<b>4.7. Test system and load composition</b>	<b>63</b>
<b>4.8. Improvement of static voltage stability margin with DG placement</b>	<b>67</b>
<b>4.9. Ranking of bus strength based on voltage stability indices</b>	<b>68</b>
<b>4.10. Determining the size of induction generators</b>	<b>75</b>
<b>4.11. Enhancement of static and dynamic voltage stability in view of present grid standard</b>	<b>79</b>
<b>4.12. Grid interconnection requirements and standards</b>	<b>80</b>
<i>4.12.1. Reactive power generation capability</i>	<i>80</i>
<i>4.12.2. Steady state voltage; continuous operation range</i>	<i>80</i>
Interconnection system response to abnormal voltage	81

<b>4.13. Methodology</b>	<b>81</b>
4.13.1. 3.4.3 <i>Solution algorithm</i>	82
<b>4.14. System model</b>	<b>83</b>
<b>4.15. Optimal capacitor placement</b>	<b>83</b>
<b>4.16. Results and analysis</b>	<b>83</b>
4.16.1. <i>Load composition and load curves</i>	84
4.16.2. <i>Distributed Generators and their size</i>	85
4.16.3. <i>Optimal capacitor placement and sensitivity indices</i>	86
<b>4.17. Voltage recovery and STATCOM placement</b>	<b>87</b>
<b>4.18. Summary of voltage stability study</b>	<b>93</b>
<b>4.19. Software platform</b>	<b>95</b>
<b>5.----SMALL SIGNAL STABILITY ASSESSMENT WITH DG UNITS</b>	<b>97</b>
<b>5.1. Methodology</b>	<b>97</b>
<b>5.2. Simulation results</b>	<b>100</b>
<b>5.3. Oscillatory modes observed in distribution system</b>	<b>101</b>
<b>5.4. Participation factor</b>	<b>102</b>
<b>5.5. Impact of penetration</b>	<b>103</b>
<b>5.6. Impact of penetration on mode participations</b>	<b>104</b>
<b>5.7. Impact of penetration on eigenvalue sensitivity</b>	<b>105</b>
<b>5.8. Time domain analysis</b>	<b>108</b>

<b>5.9.</b>	<b>Influence of composite loads on oscillatory stability</b>	<b>110</b>
<b>5.10.</b>	<b>Identification of critical modes</b>	<b>111</b>
<b>5.11.</b>	<b>Identification of most influential load</b>	<b>112</b>
<b>5.12.</b>	<b>Load Representation by composite load model</b>	<b>114</b>
<b>5.13.</b>	<b>Influence of composite load model on oscillation of generators</b>	<b>115</b>
<b>5.14.</b>	<b>Composite load modelling of multiple loads</b>	<b>117</b>
<b>5.15.</b>	<b>Impact of percentage of motor load</b>	<b>119</b>
<b>5.16.</b>	<b>Impact of the size of an induction motor</b>	<b>119</b>
<b>5.17.</b>	<b>Impact of lower order model</b>	<b>121</b>
<b>5.18.</b>	<b>Critical modes</b>	<b>122</b>
<b>5.19.</b>	<b>Identification of the most influential load</b>	<b>123</b>
<b>5.20.</b>	<b>Influence of composite loads on loadability</b>	<b>124</b>
<b>5.21.</b>	<b>Influence of load composition on loadability</b>	<b>125</b>
<b>5.22.</b>	<b>Identification of significant buses</b>	<b>127</b>
<b>5.23.</b>	<b>Impact of capacitor placement</b>	<b>129</b>
<b>5.24.</b>	<b>Placement of SVC</b>	<b>131</b>
<b>5.25.</b>	<b>Comparison of SVC and shunt capacitor placement</b>	<b>132</b>
<b>5.26.</b>	<b>Summary</b>	<b>135</b>
<b>6.----</b>	<b>CONTROL METHODOLOGIES FOR DISTRIBUTED GENERATION</b>	<b>140</b>
<b>6.1.</b>	<b>Controlling a capacitor bank using a thyristor control reactor (TCR)</b>	<b>141</b>

<b>DESIGN OF SUPPLEMENTARY CONTROLLER FOR PV GENERATORS</b>	<b>149</b>
6.2. Robust decentralised control for flexible DG integrations	164
6.3. Summary	174
6.4. Software section	176
<b>7.----CONCLUSIONS AND KEY FINDINGS FROM THIS PROJECT</b>	<b>177</b>
7.1. Key findings	177
<b>8.----APPENDIX-A</b>	<b>181</b>
8.1. List of publications from this project	182
<b>9.----REFERENCES</b>	<b>184</b>
<b>10.--REFERENCE LIST</b>	<b>193</b>

## LIST OF FIGURES

Figure 1: Steady state equivalent circuit of induction generator	
Figure 2: Transient equivalent circuit of induction generator .....	46
Figure 3: Schematic diagram of DDWG .....	47
Figure 4: A schematic diagram of grid connected PV system.....	49
Figure 5: Relationship between DC link voltage and output power of a PV array .....	50
Figure 6: A composite dynamic load model.....	51
Figure 7: Transient equivalent circuit of induction motor.....	52
Figure 8: Block diagram of SVC control .....	54
Figure 9: Basic STATCOM model .....	55

Figure 10: Block diagram of STATCOM controller.....	56
Figure 11: P-V curve: Enlargement of voltage stability margin .....	58
Figure 12: Sample Q-V curve and reactive power margin .....	59
Figure 13: Single line diagram of 16-bus test distribution system. ....	64
Figure 14: Q-V curves for extreme types of loads. ....	66
Figure 15: Reactive power margin with typical load composition.....	67
Figure 16: Reactive power margin of load buses of the test system.....	69
Figure 17: Voltage Sensitivity Factor of load buses of the test system. ....	69
Figure 18: Change in Reactive Power Margin in weak area with inclusion of IG .....	71
Figure 19: Change in Reactive Power Margin in weak area with inclusion of IG .....	71
Figure 20: Variation in Loadability with the change of Synchronous machine size .....	72
Figure 21: Variation in Loadability with the change of Synchronous machine size .....	73
Figure 22: Change in Grid losses and Reactive power intake with Synchronous machine size .....	74
Figure 23: Change in Grid losses and reactive power intake with Induction machine size.....	76
Figure 24: Flow chart: determination of type, size and location of reactive power controller .....	82
Figure 25: Single line diagram of 43 bus test system. ....	84
Figure 26: Voltage at Bus 3 for peak load (16 bus system) .....	89
Figure 27: Voltage at Bus 6 for peak load (16 bus system) .....	89
Figure 28: Voltage at Bus 5 for peak load (16 bus system) .....	90
Figure 29: Voltage at Bus 4 for base load (43 bus system). ....	91
Figure 30: Voltage at Bus 50 for base load (43 bus system). ....	91
Figure 31: Voltage at Bus 4 for peak load (43 bus system). ....	92
Figure 32: Voltage at Bus 50 for peak load (43 bus system). ....	92

Figure 33: Single line diagram of the 16 bus test distribution system .....	101
Figure 34: Eigenvalues of the 16 bus test distribution system. ....	101
Figure 35: Eigen sensitivities with generation for increased penetration.....	106
Figure 36: Eigen sensitivities with loading for increased penetration. ....	107
Figure 37: Response of voltage controlled synchronous generator for increased penetration. ....	108
Figure 38: Response of power factor controlled synchronous generator for increased penetration (power factor = unity). ....	109
Figure 39: Response of power factor controlled synchronous generator for increased penetration (power factor = 0.8, lag). ....	109
Figure 40: Comparison of eigenvalue sensitivities of different modes with respect to active power loading. ....	111
Figure 41: Comparison of eigenvalue sensitivities of different modes with respect to reactive power loading. ....	112
Figure 42: Real part of critical modes with different load models.....	115
Figure 43: Response of rotor speed of SG2 (100% motor).....	116
Figure 44: Response of rotor speed of induction generator (100% motor). ....	117
Figure 45: Comparison of real part of critical modes for composite load modelling at single load and three loads. ....	118
Figure 46: Real part of critical modes with different motor ratio. ....	119
Figure 47: Comparison of real part of critical modes for composite load modelling with 'large' and 'small' induction motor. ....	120
Figure 48: Comparison of real part of critical modes for composite load modeling with third and first order induction motor model. ....	121
Figure 49: Comparison of time domain responses for third order and first order models of induction motor. ....	122
Figure 50: Trajectories of oscillatory modes and HB condition. ....	122

Figure 51: Load ranking at HB point of system loading .....	123
Figure 52: Load ranking at base load of test distribution system. ....	124
Figure 53: System loadability with composite loads at different buses .....	124
Figure 54: System loadability with composite load models at multiple loads. ....	125
Figure 55: Variation of loadability with motor ratio of composite loads.....	126
Figure 56: Modes of voltage stability .....	128
Figure 57: Magnitudes of the weakest modes with different capacitor locations. ....	129
Figure 58: Oscillatory modes with and without capacitor at Bus 3. ....	130
Figure 59: Change in real part of oscillatory modes with different capacitor placements. ....	131
Figure 60: Participation factors of SVC states on system modes with different locations of SVC. ....	132
Figure 61: Comparison of real part shift with shunt capacitor and SVC at Bus 3. ....	133
Figure 62: Comparison of response of voltage at Bus 3 with and without shunt controller.....	134
Figure 63: Comparison of response of rotor speed of generator at Bus 3 with shunt capacitor and SVC. ....	134
Figure 64: Controllability factors of susceptance modulation of shunt capacitors of the test distribution system for the critical mode. ....	144
Figure 65: A schematic diagram of thyristor-controlled reactor for controlling the susceptance of a capacitor bank .....	145
Figure 66: Block diagram of the distribution system with converter control.....	146
Figure 67: Impact of controller location on damping ratio of the critical modes.....	146
Figure 68: Impact of controller on time domain response of the system. ....	147
Figure 69: Block diagram of the distribution system with converter control and additional controller. .....	148
Figure 70: Comparison of damping ratios of different modes with and without controllers.....	148

Figure 71: Single line diagram of a case distribution system.....	150
Figure 72: d- axis current controller.....	151
Figure 73: q-axis current controller.....	151
Figure 74: Residues of system when d-axis current of PV is modulated. ....	152
Figure 75: Residues of system when q-axis current of PV is modulated. ....	152
Figure 76: Variation of damping ratio of critical mode with controller gain. ....	154
Figure 77: Comparison of damping ratios with and without controller.....	154
Figure 78: Comparison of time domain responses of voltage at Bus 10 with and without controller. .....	155
Figure 79: Comparison of time domain responses of DC-link voltage with and without controller. .....	156
Figure 80: Scheme for rotor current control.....	157
Figure 81: Residues of system when d-axis rotor current of DFIG is modulated. ....	158
Figure 82: Residues of system when d-axis rotor current of DFIG is modulated. ....	159
Figure 83: Comparison of open loop gains of the original and the shaped plant.....	160
Figure 84: Comparison of responses of original and reduced controller. ....	161
Figure 85: Comparison of damping ratios of the modes with and without robust controller.....	161
Figure 86: Comparison of time domain response of the bus voltage with and without robust controller.....	162
Figure 87: (a) Control strategy for DFIG.....	165
Figure 88: Block diagram of decentralised control.....	167
Figure 89: Terminal voltage of DFIG for three-phase fault at Bus 7. ....	170
Figure 90: Terminal voltage of DFIG (solid line proposed control and dotted line conventional control).....	172

Figure 91: Terminal voltage of DFIG during islanding (solid line proposed control and dotted line PI).....	173
Figure 92: Speed response of DFIG during islanding (solid line proposed control and dotted line PI).....	174
Figure 93: Terminal voltage of PV during islanding (solid line proposed control and dotted line PI). .....	174

## LIST OF TABLES

Table 1: Sample of load exponents	63
Table 2: Random load composition	64
Table 3: Typical load composition [3]	64
Table 4: Weak bus detection for extreme load types	65
Table 5: Weak bus detection for intermediate load types	66
Table 6: Weak Buses	70
Table 7: Strong Buses	70
Table 8: Optimal Size of Synchronous Generator	75
Table 9: Optimal Size of Induction Generator	76
Table 10: Minimum Size of Compensator	77
Table 11: Combined Effect on voltage profile and LOADING margin by SG AND IG	77
Table 12: Combined EFFECTS on voltage profile and loading margin by SG, IG and PV Panel	78
Table 13: Interconnection system response to abnormal voltages [107]	81
Table 14: Typical load composition [159]	85
Table 15: Peak load data [166]	85
Table 16: Distributed Generation: capacity and location	86

Table 17: Optimal capacitor solution for the 16 bus system	87
Table 18: Optimal capacitor solution for 43 bus system	87
Table 19: Voltage recovery timeS for 16 bus system (peak load)	90
Table 20: Voltage recovery time for 43 bus system (base load)	92
Table 21: Voltage recovery time for 43 bus system(peak load)	93
Table 22: the oscillatory modes existing in the distribution system	102
Table 23: Participation factors of state variables	103
Table 24: Impact of the penetration of renewable resources on participation factors of state variables	104
Table 25: SUMMARIES of Generators of the System	110
Table 26: THE OSCILLATORY MODES OF THE DISTRIBUTION SYSTEM	110
Table 27: Critical Modes sensitivity At Different Loadings of Distribution System	113
Table 28: TYPICAL INDUCTION MOTOR DATA	126
Table 29: THE OSCILLATORY MODES OF THE DISTRIBUTION SYSTEM	127
Table 30: THE OSCILLATORY MODES OF THE DISTRIBUTION SYSTEM	127
Table 31: BUS PARTICIPATION FACTOR	128
Table 32: OSCILLATORY MODES EXISTING IN THE TEST SYSTEM	141
Table 33: DOMINANT GENERATORS AND STATES FOR DIFFERENT MODES	142
Table 34: PARAMETERS OF THE POWER FACTOR CONTROLLER.	153
Table 35: COMPARISON OF DAMPING RATIOS AT DIFFERENT OPERATING CONDITIONS OF THE DISTRIBUTION SYSTEM.	163
Table 36: PENETRATION LEVELS AT DIFFERENT OPERATING MODES	170
Table 37: Penetration levels using proposed controls	172

## 1. EXECUTIVE SUMMARY

There has been an immense interest in incorporating distributed generation (DG) into medium voltage (MV) and low voltage (LV) distribution networks in recent years. During the last decade the penetration of renewable energy-based DG units has increased significantly. Wind and solar are the natural renewable power choices for many countries such as Germany, Spain, Denmark and the UK and they have successfully integrated large wind farms into existing electricity infrastructures. In Australia, with a 2020 target of 20% renewable energy, the future grid must be prepared for the consequences of intermittency and other related technical challenges. In recent years non-renewable small-scale embedded and/or co-generation has also been the focus for many small and medium-sized industries and commercial entities.

Whether they are powered by renewable or non-renewable energy, DG units bring many new challenges for power systems operators needing to integrate these units into existing distribution systems. These challenges include: bidirectional power flow, less inertial generation and unregulated/intermittent behaviours. These challenges mean that instability is one of the key issues and DG units have a significant impact on the system and equipment in both steady state operation and in dynamic operation. They affect reliability, power quality, stability and safety. Because of the close proximity of the DG units to loads and to their controllers in medium and low voltage networks, dynamic interaction is a more complex issue than it is in larger systems. Hence, assessing and responding to stability issues are important tasks for accommodating the higher penetration of DG units and for the secure operation of the electricity systems. DG units embedded with different technologies, and with different steady state and dynamic characteristics, can improve or impair system stability depending on how the challenges they pose are dealt with.

This research project focused primarily on the enhancement of voltage stability and small signal stability of MV and LV power systems in the presence of DG units. The overall objectives of this research project were to:

- investigate the impact of distributed generation units on voltage regulation and dynamic stability
- determine the optimal size and location of the static and dynamic compensation devices and DG units in order to enhance the system stability and reduce losses
- coordinate DG with available voltage control devices in order to ensure that the system retains the appropriate voltage regulation and mitigate the possible negative effects of DG placement on stability

- develop appropriate control methodologies for the robust and flexible integration of DG units without violating system constraints.

### 1.1. Modelling and analysis

We conducted a comprehensive review of the literature on the modelling of distributed generators, including synchronous generators, wind generators and inverter operated static generators (such as solar PV generators). In a stable power system, the electrical output of generating units is continually adjusting so that it matches the electrical load of the system. So load characteristics play a very important role in power system stability. Static load models are relevant to load flow studies as these express active and reactive steady state powers as functions of the bus voltages (at a given fixed frequency). These models are typically categorised as polynomial, exponential and frequency dependent models. Studies of power systems stability often require load dynamics to be accurately modelled. The study of systems with large concentrations of motors also requires the representation of load dynamics. Typically, induction motors consume 60% to 70% of the total energy supplied by a power system. Therefore, the dynamics attributable to motors are usually the most significant aspects of the dynamic characteristics of system loads.

### 1.2. Voltage stability

Although the integration of distributed generation has a number of advantages like voltage support, power loss reduction, opportunity to utilise local energy resources and better peak load management, it may give rise to some instability issues because of the nature of sources and loads related with DG units. As more and more DG units penetrate into power systems, these instability issues need to be addressed to evaluate their impact. Moreover, the high  $R/X$  ratio of distribution networks makes them more vulnerable to voltage collapse. Consequently, the location and sizing of DG units has become one of the most important concerns for power system stability. The introduction of DG affects power flow, which in turn affects feeder voltage profiles and influences voltage and reactive power control in the distribution system. At present, most strategies for voltage control and protection in MV and LV networks are based on the assumption that these networks are unidirectional power flow systems. The connection of DG requires the use of voltage and reactive power control equipment in order to ensure that the system will maintain proper voltage regulation. Before a DG unit can be connected to an existing power system, the low voltage ride through (LVRT) capability must be assessed.

### 1.3. Small signal stability

With the integration of different renewable energy resources, dynamic elements such as generators and controllers generate oscillatory modes, which need to be handled carefully to ensure the stability of a system. Because they depend on wind speed and solar radiation, DG units that run on renewable energy pose new challenges to the stability, operation and control of power systems when they are run in parallel with conventional synchronous generators. This has led to an increased need to consider rotor oscillations and stability of power supply.

Generators in transmission systems are usually equipped with power system stabilisers (PSS) for ensuring small signal stability, while generators in emerging MV and LV systems (wind and solar generators) usually do not have such stabilising functionality. Owing to the close proximity of these generators and their controllers, dynamic interaction in a distribution system is a complex issue. As a result, not only electromechanical modes but also some control modes become prominent issues for small signal stability.

### 1.4. Reactive Compensation

The steady state voltage level at each load connection point is one of the most important parameters for maintaining the quality of supply. The equipment used for voltage and reactive power control are switched shunt capacitors, on load tap changer (OLTC) transformers and step voltage regulators. Static volt-ampere reactive (VAr) Compensators (SVC) and Static Synchronous Compensators (STATCOMs) can improve voltage stability and regulate steady state voltages. Distributed compensators installed on the distribution side of a power delivery transformer have significant advantages over the lumped compensation that has traditionally been placed at transmission and sub-transmission levels. STATCOM or SVC, which can be connected at distribution level voltage without the need for transformers, makes it possible to directly connect small Static VAr Systems (SVS) to distribution buses. This offers a number of advantages over placing the traditional single bulk SVS at the transmission or sub-transmission level. Static voltage stability margin can be enhanced using adequate reactive power support at an appropriate bus/node and this can shift the point of collapse.

The impact of introducing DG units into an existing power system can be positive or negative depending on the characteristics of the distribution system and of the DG units. Power flow direction may reverse and the distribution network may become an active system with power flow

and voltage determined by both generation and load. Voltage control issues in a power system have a strong correlation with reactive power compensation by both static and dynamic compensators. Determining the optimum size and location of static compensators (such as capacitor banks) is an important task in reactive power planning. On the other hand, SVC and STATCOM have inbuilt potential to offer both dynamic reactive power compensation for transient voltage stability improvement and for steady state voltage regulation.

Grid requirements and standards are the key drivers that shape the conventional control strategies to allow faultless integration of DG in the main grid. Post fault voltage recovery time at the DG bus is the crucial part of these standards, as the DG is required to trip if recovery time exceeds a certain limit. Small-scale DG units with limited reactive power generation capability suffer most with regard to recovery voltage with current grid code practices.

### 1.5. Control methodologies for the enhancement of small signal stability

Control methodologies have to be redefined for new renewable and non-renewable distributed resources. The correct location of controllers is very important for their best economic and technical performance. A number of approaches have been investigated to locate shunt controllers with appropriate control schemes to meet grid standards.

### 1.6. Results and Outcomes

#### 1.6.1. Enhancement of Voltage Stability with DG units

A voltage stable power system is capable of maintaining post-fault voltages near the pre-fault values. If a power system is unable to keep the voltage within acceptable limits, the system undergoes voltage collapse. The most important factors determining the voltage stability of a power system are characteristics of the load, the reactive compensation devices and the voltage control equipment of the network. Voltage instability is often considered to be a local area phenomenon associated with the lack of reactive power in a significant part of the power network. Therefore, the incorporation of VAR sources can increase the static voltage stability margin (VSM), which is defined as the distance between the nose point and the operational limit point of a traditional Q-V curve. VAR sources such as capacitor banks, SVC and STATCOMs are key components for improving the voltage stability. The study of voltage stability in this research work can be explained through the following steps:

- investigating effective voltage stability indices
- improving static voltage stability margins by proper DG placement

- enhancing static and dynamic voltage stability in view of present grid standards.

#### 1.6.2.

#### 1.6.3. *Reactive Power Margin*

The reactive power margin of a particular bus indicates how much the loading on that bus can be increased before its loading limit is exceeded and voltage collapse takes place. A 16-bus distribution system was extensively used in this study. This system consisted of a total load of  $P_L=28.7$  MW and  $Q_L=17.3$  MVar respectively. In this report, simulations were performed using DigSilent Power Factory 14.0, PSSE32 and results were verified using the research analytical tool PSAT and a user defined block in a Matlab environment. A wide variation of load composition was simulated through different sets of load models, which included both extreme and intermediate conditions. Three types of extreme load models were considered along with three intermediate combinations represented by the ZIP load model. Irrespective of load composition, the reactive power margin index worked as a reliable index for identifying the weakest and strongest bus in a system.

#### 1.6.4. *Ranking of Bus Strength Based on Voltage Stability Indices*

A methodology was developed based on Q-V curve analysis to determine the location and size of two major classes of DG – synchronous (SG) and induction generators (IG). The methodology considered the reactive power issues of the system and of these machines. P-V analysis was also carried out to investigate the loadability of the system. This methodology was able to rank the buses, which leads to the final selection of sites for SG and IG for an overall improvement of reactive power reserve and loadability. Ranking of buses was performed by calculating their reactive power margins and voltage sensitivity factors (VSFs). When an amount of reactive power equal to the reactive power margin is drawn from a bus by applied load then the system may experience voltage collapse.

#### 1.6.5. *Selecting the proper locations for Synchronous and Induction Generators*

Weak buses with low reactive power margins are already operating with a deficiency in reactive power. So if some DG units, which consume reactive power, are placed on these buses it will cause voltage problems and instability. However, we can use the large reactive margins of 'strong buses' to help these types of DG units. This study clearly demonstrates that the inclusion of IGs at the 'weak buses' does not improve the reactive power margin or strength of these buses. It is obvious that with the inclusion of SGs at a bus, losses in the system start to decrease, but beyond the optimal size of DG units the grid losses may increase again and may exceed the base case

loss. So the optimal size of SG should be chosen based on loss minimisation. When synchronous generator-based DG units are placed in the system and the total reactive power demand of the system is delivered from that SG, there will be zero reactive power flow from the rest of the grid into the DG connected system. Any SG with a rated value lower/greater than this optimal value will result in a greater amount of real and reactive power losses in the system.

#### *1.6.6. Determining the Size of Induction generator*

With the inclusion of an induction generator into a system, the loadability of the system starts to decrease after a certain machine size. So the optimal size of the induction generator corresponds to maximum loadability. The inclusion of an induction machine in the distribution system usually results in a greater amount of grid loss, as mentioned earlier, and this amount of loss is always more than with an SG in the system. Also, the reactive power consumption through the grid tends to increase with increasing machine size. With an IG connected to the system, if the volatile primary resource (e.g. wind and solar) becomes zero then the real power injection also becomes zero. But the reactive power consumption is still there, which creates a significant amount of grid loss which is greater than the base case. To keep the loss always lower than the base case loss, it is important to provide reactive power compensators on buses with IGs, which can support the worst case. Depending on the available resources, there might be various types of DG units available in the same distribution system. From the results, it can be summarised that with an increasing size of SG machine, both the loadability and voltage profile improve significantly.

Results from this study show that for the enhancement of the static voltage stability margin, SG needs to be placed at a weak bus and IG needs to be placed at a bus near to a substation which is strong enough to support reactive power requirement of the IG. In recent years grid requirements and standards have been developed to shape conventional control strategies and maintain static as well as dynamic voltage stability throughout DG-integrated systems. The technical regulations or specific standards define the maximum permitted variation of every bus bar voltage under both transient and steady state conditions. The augmentation of both static and dynamic stability has been studied in this research project.

#### *1.6.7. Enhancement of static and dynamic voltage stability in view of present grid standards*

The post fault voltage recovery time at the DG bus is the crucial part of available standards as it requires that DG trips if recovery time exceeds a certain limit (2 s according to IEEE 1547 report). Determining the optimum location and size of static compensators (such as capacitor banks) is one of the foremost tasks in reactive power planning. When they are of the correct size and when

they are in the correct position, SVCs and STATCOMs have the inbuilt potential to offer both dynamic reactive power compensation for transient voltage stability improvement and steady state voltage regulation. A sensitivity-based approach to deciding the appropriate location and size of high-cost dynamic compensators such as STATCOMs has been proposed. This novel approach not only reduces the loss but also ensures faster recovery time and thus improves uptime of DG units. The feasibility of the methodology was demonstrated on two distribution systems with different network and load configurations.

#### 1.6.8. *Grid interconnection requirements and standards*

Grid codes were specified for wind power plants and for other distributed generators under both steady state and dynamic conditions. Normally, the operation requirements for DG units are specified at the point of common coupling. In general, the steady state operation requirements include: power factor requirements for the DG units; steady state voltage operating ranges; frequency operating ranges; and voltage quality. In order to achieve increased real power generation in the system, different grid codes around the world have proposed limited reactive power capability of DG units. For example, IEEE Std 1547-2003 does not allow DG units to regulate voltage at the point of common coupling actively. In Australia, distributed generators with a capacity of less than 30MW shall not actively regulate the voltage at a coupling point and the power factor must lie between unity and 0.95 (leading) for both 100% and 50% real power injections. The steady state voltage level at each load connection point is one of the most important parameters for the quality of supply, and the inclusion of DG has not affected this requirement. In general it is expected that the voltage of the DG bus and the load bus should remain within the range of  $\pm 10\%$  of nominal voltage. IEEE std. 1547-2003 states that any DG unit should cease energising the electric power system during abnormal system conditions according to the clearing times (Voltage range  $V < 0.5\text{pu}$ -clearing time 0.16 s, Voltage range  $0.5 \leq V < 0.88\text{ pu}$ -clearing time 2 s, Voltage range  $1.1 < V < 1.2\text{ pu}$ -clearing time 1 s and voltage range  $V \geq 1.2\text{ pu}$ -clearing time 0.16 s). The clearing time listed is a maximum threshold for any DG with a capacity of 30 kW or less. For DG units with generation capacities greater than 30 kW, the listed clearing time is a default value (2 s) though this can vary with different utility practices.

A methodology was developed for the placement of reactive compensation devices with the objectives of minimising grid losses and satisfying grid code requirements. Steady state voltage requirements (at generator and load terminals) are set as the constraints for the objective function. Time domain stimulation was also performed under conditions that introduced various faults into the system. This was done to check the dynamic voltage restoring capability of the generator and

load bus. A dynamic compensator (in this case a STATCOM) is required only if static compensators fail to meet the grid requirements. If this situation occurred, a new sensitivity index  $dV/dI_R$  (along its direction, i.e. either positive or negative) was used to find out the best location among optimal capacitor nodes to replace that capacitor with a STATCOM. After replacing the optimal capacitor with a STATCOM on the bus with the highest sensitivity, the voltage recovery time was calculated with time domain simulation for the generator and load buses. Performance of  $dV/dI_R$  was compared with an existing sensitivity index  $dV/dQ$  and other methods of implementing reactive power compensation.

To test the effectiveness of the proposed methodology, two distribution test systems with different configuration and load compositions were considered in this part of the research. The first distribution system used in this work was a 23 kV radial distribution system with 16 nodes and the second test system was an IEEE 43 bus mesh distribution system, with total real and reactive power loads of 21.76MW and 9MVAR respectively.

The findings suggest that a STATCOM should be placed at the bus with the highest inductive  $dV/dI_R$  to support the voltage recovery requirements of DG units in the system. This scheme works efficiently as during the post fault recovery, capacitive VAR is required which is made available by a STATCOM. For a small radial system like a 16 bus system it a STATCOM was not even necessary to support voltage recovery, though wrong placement of a STATCOM led to longer recovery times. But for the 43 bus system with large mesh configuration, a STATCOM was required at both base and peak loading conditions to enable the voltage recovery to occur within the specified time. The proposed approach helped in placing capacitor banks and STATCOM in a distributed manner to improve voltage profile at DG and load bus. The new sensitivity index  $dV/dI_R$  proved to be effective in detecting the appropriate location of STATCOM in the presence of fixed compensation. As a result, small scale DG units could remain connected to the grid under abnormal conditions, thus improving their uptime.

### 1.7. Small Signal Stability Assessment with DG Units

Traditional distribution systems are passive systems in which power flows in one way only and they consume power from the substations. However, the increasing penetration of distributed generating (DG) sources and other controllers for enhancing power quality are transforming the traditional distribution systems into more active systems, where there are possibilities for dynamic interactions among DG units and controllers. The dynamic interactions may lead to low damped

and low frequency oscillations, raising the issue of small signal stability. Small signal stability analysis is typically performed with the help of eigenvalue analysis of the linearised model of a power system around the operating point of interest. Eigenvalue analysis results can be supplemented with nonlinear time domain simulation for small disturbances such as load increases. Eigenvalue analysis can be used to determine acceptable renewable energy penetration before the system loses small signal stability. The limiting criteria for penetration could be either the damping ratio or a point of Hopf bifurcation condition, which triggers the onset of oscillation and limits the loading.

It is interesting to note that the oscillatory frequencies of critical modes are around 3 Hz, which is more than the frequency of electromechanical modes of large generators observed in transmission systems, where typical values are 0.1 to 2 Hz. When a large number of generators are scattered in a large distribution system, this may create some small groups of generators oscillating against each other, creating a problem of inter-area oscillations. The time domain simulation also confirms the frequency of oscillations obtained from modal analysis.

Many countries aim to supply at least 20% of their load demand by renewable energy within the next 10 years. Based on this, our research investigated three cases for small signal stability analysis.

- Base case: This is the case of the existing scenario.
- 20% wind
- 20% solar

One of our objectives was to determine the contributions of different types of generators on different oscillation modes. Participation factor and eigenvalue sensitivity approaches were chosen for analysis. This helps us choose the most effective generator to control in order to suppress unwanted oscillations in the distribution system. We found wind generators have a significant impact on the dynamics of systems and solar generators have less impact than wind penetration. The impact of solar PVs on low frequency electromechanical oscillations should be very low as photovoltaic generators do not have rotating parts. The increased penetration of wind and solar power has a positive impact on the oscillation damping of the voltage controlled synchronous generator. However, the given DG penetration is not always sufficient to ensure the stability of the system and in such cases an additional controller for a DG unit can be designed for system stability enhancement.

Loads are considered to be the major driver of small signal stability. Each load at a node may consist of a wide variety of loads, including induction motor loads. In this research, a sensitivity based approach was used to rank the load buses to select the most influential bus for composite load modelling on power system oscillatory stability. The proposed indices for load ranking can be computed numerically using perturbations in active and reactive power loads. The results were verified and compared by modelling the high ranked and low ranked loads using composite load models. Also, we examined the impact on small signal stability of varying the composition of the composite load model. The conclusions drawn are summarised as follows.

A distribution system with DG units may have a number of oscillatory modes. Of these, the modes which are highly sensitive at different operating conditions of a system may be selected as critical modes for load ranking. The sensitivity-based indices introduced in this work can identify the critical modes of the distribution system. Also, the indices can be used to rank the loads based on their relative influence on small signal stability of the distribution system.

It is recommended to use a composite load model to reflect the load dynamics of a distribution system. The rotor oscillations of both synchronous and induction generators are better damped when loads are modelled with the composite load model. Hence, composite load modelling gives accurate results for small signal stability.

It is obvious that the selection of a load model will have an influence on stability assessment of a distribution system. Each distribution system has its unique composition of loads, which ultimately influences the results of stability assessment, including the dynamic loading margin. Appropriate load modelling in a distribution system is very important for system planning and operation.

Oscillatory stability can be improved by adding damping on the critical mode and this can be done with a wide variety of devices and controllers. However, some important questions to be addressed are what controller or device, at which location and what is the control approach? We developed an approach to locating shunt controllers to enhance the small signal stability of distribution systems with DG units. First, we ranked buses to determine the best locations of shunt compensators for enhancing voltage stability. Then, we selected the location for a shunt compensator that had the least detrimental impact on oscillation damping. A minimum eigenvalue shift based index was used for placement of a static shunt compensator such as a capacitor. A participation factor was used as an index to locate a dynamic compensator such as an SVC. The following conclusions were made based on the observations.

Oscillatory modes exist in a distribution network with integrated DG units. All the modes must be well damped to ensure small signal stability of a system.

$V - Q$  Sensitivity analysis can be used to rank the buses of a distribution system for compensator placement. Then, installation of a shunt compensator at a high ranked bus effectively improves the overall voltage stability of the system. On the other hand, such a compensator may weaken the damping of oscillatory modes. A shift of eigenvalues towards the imaginary axis of a complex plane may occur.

Placing a shunt compensator for voltage stability enhancement does not necessarily enhance small signal stability as well. But, the location, which causes the least movement of eigenvalues towards the imaginary axis, is the best location for small signal stability. The least eigenvalue shift corresponds to the highest magnitude of participation factor of dynamic compensator such as SVC.

Shunt compensators sometimes introduce negative damping, creating a small signal stability problem in a distribution system. The installation of a dynamic compensator such as an SVC gives less negative damping of oscillatory modes as compared to a static compensator such as capacitor of the same rating. Also, SVC performances are better for transient and steady state responses of bus voltage and generator rotor angle against system disturbances.

Hence, SVC is a better choice than a shunt capacitor of the same rating for small signal stability enhancement of a distribution system. A controller in addition to the primary voltage controller of an SVC can be designed for the SVC to eliminate its negative damping effect. Future power distribution requires extra expandability and flexibility in the integration of DG. This is why the control strategy in the interconnected grids should be combined with a control methodology using inverters. The next section describes methodologies for controlling converters in DG units, for example, DFIG, DDWG and PV systems for the enhancement of stability under both small and large disturbances.

## 1.8. Control Methodologies for Distributed Generation

The main technical challenges to increased penetration of DG units into an existing grid are voltage regulation, power quality, protection, dynamic voltage and small signal stabilities. There are a number of approaches for enhancing the network stability of DG systems such as designing a shunt controller for a selected capacitor bank and designing additional controllers for DG units such as PVs and DFIGs. A coordinated control approach for different DG units is also proposed

and discussed in this study. A number of cases are analysed to gain a deeper insight into those issues. A number of control algorithms are proposed that can significantly enhance the penetration level.

First, we have developed an approach to control a shunt capacitor bank in order to adjust the damping of the critical modes. Next, we have proposed a supplementary control for PV generators for augmenting small signal stability. We then presented a robust control algorithm for a doubly-fed induction generator (DFIG) for enhancing small disturbance stability. As well as designed a robust decentralized control approach for different types of DG including DFIGs, PV generators and direct drive wind generators (DDWGs) in order to enhance both dynamic voltage and transient stabilities for the flexible integration of DG units.

#### *1.8.1. Controlling a Capacitor Bank using Thyristor CONTROL REACTOR (TCR)*

Flexible AC transmission system (FACTS) controllers are employed in conventional transmission systems for stability enhancement. However, the mechanically switched capacitor banks used to support node voltages in conventional distribution networks are incapable of handling the dynamics of a distribution network with DG's. Furthermore, capacitor banks are reported to be detrimental to oscillation damping. Hence, dynamic compensation devices such as FACTS with supplementary control loops may be required to ensure the small signal stability of a distribution network. Alternatively, instead of investing in an additional device, existing capacitor banks may be utilised by combining them with a TCR to ensure small signal stability by dynamically controlling their susceptance. This combination is popularly known as an SVC. The SVC at a particular bus will have the highest controllability factor for shunt susceptance modulation. Hence, controlling the susceptance of this capacitor is the most effective place for damping control of the critical mode.

A methodology was investigated and an additional controller was designed to achieve a desired damping ratio of the critical mode. Adding an additional controller can improve the damping of the critical mode and keep fluctuations within an acceptable range. The primary controller has an impact on all the modes of the system, while the proposed additional controller does not affect the damping of other modes, except the critical one. Hence, adding another damping controller can enhance the damping of a particular mode of interest without compromising the damping of other modes.

### 1.8.2. Design of Supplementary Controller for PV Generators

Oscillatory instabilities in the form of low frequency oscillations are highly undesirable. These oscillations must have acceptable damping ratios to ensure stable operation of a power system. In transmission systems, various controllers such as power system stabilizers (PSS), SVC and STATCOM are used for oscillation damping. However, installing such devices in a low voltage distribution system may not always be technically and economically attractive. Instead, one of the DG units in the system may be controlled to improve system stability. Given the structure of DG units (such as PV and DFIG), which are dominated by controllers, one of the controllers of DG units may be used to improve the oscillation damping. The network used in our study consisted of synchronous generators, a fixed speed induction generator, a DFIG and a PV. A control methodology was tested for a PV system to enhance the damping of low frequency oscillations.

We evaluated the effectiveness of the controller by observing the damping ratios before and after installing the controller for the PV. The supplementary controller effectively improved the damping ratio of critical modes to the targeted value (minimum 5%). Time domain simulation also confirmed the findings from modal analysis. For a number of renewable energy based distributed generators, outputs depend upon the weather conditions. A PV system generates power based on available solar irradiation and temperature. Hence, oscillation damping from a PV generator is not possible on a cloudy day, unless there is a provision for energy storage. In such a scenario, a wide area coordinated control of a number of DG units and reactive power compensators may be designed. Any of the DG units may then utilize their available energy to support oscillation damping based on wide area measurement data.

### 1.8.3. Control of DFIG

Given the structure of a DFIG-based wind generation system, which is dominated by controllers, one of the controllers of DFIG may also be employed for improving the oscillation damping. The network is assumed to consist of synchronous generators, a squirrel cage induction generator, a PV generator and a DFIG-based generator. The impact of DFIG power on a low frequency mode was systematically assessed and a robust control methodology was proposed for a DFIG system to enhance the damping of low frequency oscillations. As a DG unit, DFIG is usually operated in a desired power factor. It is obvious that active and reactive power output of a DFIG is determined by terminal voltage and input current. In a distribution network, terminal voltage is governed by the operating condition of the distribution network and input current is determined by the availability of

real power on the generator shaft. Therefore, it is convenient to control rotor currents to obtain a desired ratio of active to reactive power.

#### 1.8.4. *Robust coordinated control of DG units*

The controllers designed by classical control techniques have their validity restricted to a nominal operating point at which the system is linearised. But a power system constantly experiences changes in operating conditions due to variations in load generation patterns and variations in transmission networks. Moreover, some uncertainty is introduced into the power system model due to inaccurate approximation of the power system parameters, neglecting high frequency dynamics and assumptions made in the modelling process. Hence, it is desirable to have a robust damping controller to ensure adequate damping under various system operating conditions. The use of DG units could be significantly enhanced if they operate in a voltage control mode instead of the unity power factor recommended by the IEEE 1547 standard. Transient voltage variations and dynamic voltage instability can also limit DG penetration, although voltage rise is a major constraint when accommodating DG units. The simulation results show that the proposed robust control method can augment the potential penetration of DG units without requiring network reinforcements or violating systems operating constraints.

### 1.9. **Final conclusions**

With the increased penetration of DG units, early tripping of a DG unit due to local disturbances can deteriorate the stability of the whole system. To address this issue, grid standards have been developed, which require system stability under steady state and fast voltage recovery under abnormal conditions. In this research, a grid compatible methodology was developed to control voltage and reactive power. Small signal instability could lead to oscillatory instability problems and is considered to be a more significant problem than transient instability.

A methodology was developed for the determination of the optimal location and size of synchronous and induction generator-based DG units, considering their reactive power capabilities. The methodology is based on a reactive power margin index which was found to be reliable for identifying suitable locations for various DG units. Placing synchronous generators (SG) on weak buses improves voltage stability and increases the loadability of the distribution system and the rate of increase of loadability with SG is greater at a “weak bus” than at a “strong bus”. To avoid reduction of loadability and to improve voltage stability, induction generator based DG units need to be placed at strong buses. This methodology can be used by distribution companies in

planning the most suitable location and appropriate sizes of DG units along with other practical considerations.

A complete methodology based on a new index was formulated for the steady state and post fault voltage recovery. The index complies with current grid codes and standards. The index is based on the sensitivity of terminal voltage with respect to the reactive current injection. Grid codes demand voltage recovery within a short time (e.g. 2sec in IEEE grid code 1547 and in AEMO requirements) after a fault takes place near to a generator bus. The methodology developed in this research, can calculate the minimum number of shunt compensation devices and appropriate sitting (capacitor bank and/or STATCOM) required preventing DG units from tripping and allowing them to remain connected. The appropriate location of DG units can in most cases improve voltage stability. However, for a weakly connected network, the proper placement of compensation devices needs to be considered. Moreover, in many cases, fixed capacitors help to improve the voltage profile in the steady state as well as under abnormal conditions. However, in a few cases, a shunt FACTS device is required to ensure fast voltage recovery. This methodology and index will be useful for distribution utilities for planning capacitor and shunt FACTS reactive power compensation devices in an optimal and economic manner.

Distribution networks with DG units oscillate with a frequency around 3 Hz under certain operating conditions. This frequency of oscillation is higher than that found in transmission systems. DG units, not only the conventional synchronous generators but also induction generators, can participate in the oscillation either in a positive or negative way. DG units enhance damping of oscillatory modes by positively participating in oscillation. While this is a positive result for utilities who want to increase DG penetration, it is important that further investigations be undertaken into power quality and protection issues for higher penetration of DG units in distribution systems.

The composition of a load has a significant impact on small signal stability and this impact is more pronounced when DG units are present in the system. The percentage of load that is induction motor load and its size influences the damping on critical modes. An increase in percentage of induction motor load increases the damping ratio of the critical mode. Moreover, a detailed dynamic model of an induction motor yields a more accurate result of small signal stability compared to a simplified model. Hence, in order to get more accurate damping performance results, power industries need to model the impact of induction motors in detail.

Shunt compensation devices such as capacitor banks, SVCs and STATCOMs are normally installed for voltage stability enhancement. However, the placement of such compensating devices

can have an influence on small signal stability. Static reactive power compensating devices may compromise the small signal stability of a network. For example, a shunt capacitor yields a poorer damping ratio on critical mode. On the other hand, DG units installed with appropriate control mode in a network can be utilised to enhance small signal stability of the network so that distribution utilities don't have to invest in expensive controllers. Given the controller-dominated structure of renewable energy based DG units such as solar and wind, one or more of the controllers may be employed to support oscillation damping. For example, pole placement control strategy for shunt capacitor bank, lead/lag control of solar photovoltaic and robust control of DFIG can be used as shown in the report for the enhancement of small signal stability. The controller designed in this research improved the damping ratio from 2% to the minimum desired value, i.e. 5%.

The penetration level of DG units is generally constrained by a voltage rise problem in distribution systems. However, transient voltage variations and dynamic voltage instability can also limit DG penetration in stressed systems. When DG units operate in voltage control mode instead of at the unity power factor recommended by the IEEE 1547 standard, more DG units can be accommodated. A robust coordinated control method was developed in this research for enhancing the dynamic stability of PVs, DFIGs and DDWG-based DG units. This method can increase the potential penetration of DG units without requiring network reinforcements or violating a system's operating constraints.

## 2. INTRODUCTION

Globally, the electricity industry is in transition from large integrated utilities providing power at regulated rates to an industry that incorporates competitive companies selling unbundled power at market-based rates [1]. This change has led to increased interest in the development of renewable energy generation and of combined heat and power (CHP) distributed generation (DG) units. Distributed generation has been defined as “any small scale electrical power generation technology that provides electric power at or near the load site; it is either connected to the distribution system, or directly to the customer’s facilities, or both” [2]. The Institute of Electrical and Electronics Engineers (IEEE) defines distributed resources (DR) as sources of electric power that are not directly connected to a bulk power transmission system and which include generator and energy storage technologies [3]. These DR units include those which use both renewable and non-renewable resources with outputs ranging from some kW to a few MWs [4]. Wind power, solar power, small hydropower and CHP plants are among the most rapidly developing distributed generation technologies. Reduction of grid loss, less investment costs in line connection, efficient asset utilisation and utilising green technologies are some of the potential benefits of DG in a deregulated electricity market [5].

DG is gaining more and more attention worldwide as an alternative to large-scale centralised generators. In recent years, wind and solar based power generation have become very attractive alternatives to traditional power generation technologies. Countries such as Germany, Spain, Denmark and the UK have successfully integrated large wind farms using existing infrastructures. As of mid 2010, Europe had commissioned 333 MW of offshore wind turbines and had a total installed capacity of 2.3 GW. Renewable energy capacity throughout the world and in the United States has more than tripled between 2000 and 2009 [6]. In Australia, the penetration level of renewable energy to the national electricity grid is still very small. However, with a 2020 vision of 20% renewable energy, the future grid must be prepared for the consequences of intermittency and other technical challenges. Distributed Generators (DG) have a significant impact on systems and equipment in terms of steady state and dynamic operation, reliability, power quality, stability and safety for both customers and electricity suppliers. A comprehensive literature review has been undertaken to find the gaps in the existing literature, which will be addressed in this research project.

## 2.1. Review of power system modelling

The analysis of stability limits requires modelling of networks. This modelling needs to consider different penetration levels of DG units to adequately evaluate their impacts on the stability of networks.

### 2.1.1. *Distributed Generator modelling for load flow*

A power system is a complex nonlinear system with interconnected dynamic devices and hence mathematical modelling is a challenging task. To date, much analysis has been performed on distribution power flow with the presence of Distributed Generation units. In general, most studies have modelled the DG units as generator buses (PV) or load (PQ) nodes for power flow calculations [7],[8],[9]. In [10], a helpful list of DG models was presented which considered the machine operation and the type of interface/connection to the grid for power flow analysis.

### 2.1.2. *Distributed Generator modelling for dynamic study*

System stability can be assessed by using appropriate models of different components such as generators, controllers, and networks. The increasing use of renewable energy resources has introduced induction generators consuming reactive power (such as conventional wind generators) and inverter operated static generators (such as solar PV generators).

### 2.1.3. *Synchronous Generators*

Conventional synchronous generators are popular in cogeneration, small hydro and some wind power applications. Permanent magnet synchronous generators (PMSGs) are also gaining popularity in various distributed generation applications, particularly for wind energy conversion (WEC). PMSGs are expected to offer many advantages to emerging distribution systems for reactive power management and efficient energy conversion from variable energy resources such as wind. Until now, the majority of synchronous generators used in distributed generation applications have been of a conventional type. Hence, small signal stability issues with conventional synchronous generators are considered in this research. The issues of rotor oscillation in conventional synchronous machines are well known [11]. Since the generators connected to distribution systems do not take part in frequency regulation, the mechanical torque of the generators is assumed to be constant. Usually synchronous generators are connected to MV systems as constant active power sources operating at power factor control mode [12].

However, depending upon their capability they may support the voltage by providing reactive power as well. In this research both voltage and power factor control mode operations of synchronous generators have been considered. For voltage control modes, reactive power limits have been defined.

#### 2.1.4. Induction Generators

Induction generators are popularly employed in wind power generation applications, small and micro hydro and some thermal plants. With the increased penetration of induction machines in a power system, the rotor oscillation in induction machines is also an important issue [13]. An advance in induction generator design has changed the way they impact on system stability. For example, the contributions of squirrel cage induction generators (SCIGs) and doubly fed induction generators (DFIG) on transient stability are different [14]. In this work, both types of induction generators have been considered. Squirrel cage induction generators are assumed to consume reactive power from the system. The reactive power support for an SCIG is partially supplied by a shunt capacitor, whose rating is equal to one-third of the active power created by the generator. On the other hand, doubly fed induction generators are assumed to operate at a constant power factor with the help of converters. Similar to synchronous generators, the mechanical torque in DFIGs is assumed to be constant. For dynamic analysis, SCIG has been modelled using the third order induction machines model [15]. Similarly, DFIGs are modelled by a third order induction machine model as well as a dynamic model of converters.

#### 2.1.5. PV generators

One of the popular DG units in present power distribution systems is the solar photovoltaic (PV) system. The technology of PV systems is different to that of conventional synchronous and induction generators. Unlike conventional generators, PV systems do not have rotating mechanical parts and their system dynamics are dominated by controllers [16]. Analysis of the impact of PV on the stability of a distribution network requires the use of an appropriate model of a PV system. A number of studies discuss the modelling of photovoltaic systems [16],[17],[18]. Some of these works employ detailed modelling for transient stability studies [16]. Approximate models are used for small signal and steady state stability analysis [18],[19]. A comparison of a detailed model and approximate models for assessment of small signal stability is presented in [18]. In [18] it is recommended that approximate models are accurate enough to represent the small signal behavior of a power system. Similarly, some researchers have discussed the impact of PV

systems on the transient and small signal stability of power systems [16],[18]. In many cases, PV systems have been reported to improve the damping of low frequency oscillations.

#### 2.1.6. Load modelling

In a stable power system, the electrical output of generating units continuously matches the electrical load of the system. So load characteristics play a very important role in the study of power system stability. The load model can either static or dynamic. In MV and LV systems, voltages vary widely along system feeders as there are fewer voltage control devices; therefore, the voltage-current (V–I) characteristics of the load are more important in load flow studies of low and medium voltage systems [20]. Static load models are relevant to load flow studies as these express active and reactive steady state powers as functions of the bus voltages (at a given fixed frequency). These are typically categorised as polynomial, exponential and frequency dependent models [21], [22], [23]. One of the most complete static load models combining both voltage and frequency dependence is given in [24].

Studies of inter-area oscillations, voltage stability and long-term stability often require load dynamics to be modelled. The study of systems with large concentrations of motors also requires the representation of load dynamics. Typically, induction motors consume 60% to 70% of the total energy supplied by a power system [25]. Therefore, the dynamics attributable to motors are usually the most significant aspects of the dynamic characteristics of system loads. The dynamic loads which are basically considered as induction motors are represented by third order models based on Stanley's equations [26, 27]. Mathematically the combination of static and dynamic loads needs to be shown by the composite load model [28], which combines both static (ZIP) load and induction motor load with  $\alpha$  as the percentage of induction motor load.

#### 2.1.7. System modelling in general

The key point in power system modelling is the choice of model for a particular case study. Real life observations of the behaviour of power systems have shown that for up to a few seconds after a major disturbance, a system behaves as a non-linear system. So a non-linear model is required to simulate the results of large disturbances of short duration. But after a few seconds, or in the case of small disturbances, the system can be treated as a linear system which suggests it is appropriate to use linear models for power system simulation [25], [29]. For stability studies, power systems are modelled using a set of differential equations and a set of algebraic equations as in [25]. In general, elements that should be considered when modelling power systems for various

stability studies are generators (synchronous and asynchronous), generator controllers, transformers, transmission/distribution lines and loads. When the models are presented with appropriate mathematical relationships and once they are properly understood, these models will be employed for power system stability analysis.

## 2.2. Review of system stability

### 2.2.1. Voltage stability assessment

Although distributed generation integration has a number of advantages including voltage support, improved power quality, power loss reduction, opportunity to utilise local energy resources and a smoother load peak [1], it may give rise to some instability issues because of the nature of the sources and loads related with DG units. As more and more DG units penetrate into the power system, these stability issues are being met with greater efforts and advanced techniques by researchers evaluating the impact of these incoming DG units [4], [30]. A comprehensive study of possible operating problems and challenges in connecting distributed generation to the low and medium voltage electric power grid can be found in [31]. The impact of DG interconnection on the voltage profile has been discussed by many researchers. Assessments of this impact need to account for system characteristics such as machine size, line length, load distribution and the location and interconnection of the DG units [32], [33]. The high R/X ratio of the distribution networks makes them more vulnerable to voltage collapse [34]. With the increased share of DG in distribution systems, allocation and sizing of DG units has become one of the most important concerns for power system stability. Inappropriate selection of location and size of DG may lead to increased system loss and an unacceptable voltage profile. This situation has been found in several studies [35], [36]. Appropriate location and size of DG might be helpful to mitigate these problems and improve voltage stability [37], [38].

Two of the essential factors influencing the interaction between DG units and the grid are the technology utilised in DG, and the mode of DG control and operation. As mentioned earlier in the modelling section, the following three generation technologies are normally used for distributed generation: synchronous generators, asynchronous generators and power electronic converter interfaces. Comparisons of the impacts of those generator technologies on the operation of power systems has been made in [30], and [39]. These comparisons consider the ability of the technologies to generate reactive power. It is found that the inclusion of inverters and converters in static distributed generators can introduce or amplify the harmonic components in the system [40]. However, inverter-interfaced DG units can provide the means to suppress both problems. Some

recent work has demonstrated, through analysis and experiment, that control functions can be added to DG inverters to provide forms of reactive power compensation and harmonic suppression as ancillary services [19].

Short circuit capacity in MV and LV networks will also increase with the introduction of DG units [41]. The short circuit withstand capacity of installed distribution equipment is selected based on the maximum short circuit level without DG in the distribution network [42]. As a result, it is becoming a common practice to disconnect DG when a fault occurs. However, disconnecting all DGs when a fault occurs would make the system unreliable, particularly since most faults on overhead distribution lines are temporary. Lack of proper static and dynamic reactive power planning may result in slow voltage recovery which results in disconnection of DG units according to grid standards [43].

The introduction of DG affects power flow, which in turn affects feeder voltage profiles and influences the voltage and reactive power control in the distribution system. At present, most operation and control in MV and LV networks, such as voltage control and protection, are based on the assumption that these networks are unidirectional power flow systems [44], [45]. The connection of DG requires coordination with available voltage and reactive power control equipment in the system in order to ensure that these systems will not lose proper voltage regulation. Although voltage stability is the major concern in MV and LV systems, small signal stability has also become a critical issue of renewable energy-based electricity distribution systems.

#### *2.2.2. Small signal stability assessment*

With the integration of different renewable energy resources, control devices and continuous load growth, the structure of the electricity systems is becoming more complex [46]. There are several concerns as to the stable operation of MV and LV networks under various operating conditions and disturbances. It has become important for assessment of low voltage ride through (LVRT) capability to be undertaken before a DG unit can be connected to an existing power system [47],[48]. Similarly, DG units must operate within acceptable voltage and power factor deviations. The integration of dynamic elements such as generators and controllers generates oscillation modes which need to be handled carefully to ensure the stability of a system. In distribution and sub-transmission systems the generators and controllers are in closer proximity to each other than

the elements in transmission systems. Such proximity may induce interactions among the machines leading to low frequency oscillations and improper tuning of controllers [49], [50].

The use of renewable energy resources has introduced new types of generators into electricity distribution systems. The power injection from these generators depends upon the weather conditions; that is, wind speed and levels of solar radiation. When these generators are operated in parallel with conventional synchronous generators, they impose new challenges to stability, operation and control of the power system and its components [12]. With the increasing penetration of induction machines such as wind generators, the concern regarding rotor oscillations and stability of the network has increased. Studies [51-53] have reported that induction machine rotor oscillations have been studied less than synchronous machine rotor oscillations. On the other hand, solar photovoltaic generators are basically treated as inverter-based active power generators without rotating mechanical parts and are modelled as static generators in stability simulation [54]. Some studies show that the penetration of induction generators increases the damping of the power system by effectively reducing the inertia of the system [55, 56]. Similar results are reported with when PV generators are involved [57]. However, in those studies the conventional synchronous generators have been replaced by equivalent induction or PV generators. The results of the analysis depend on the generator model used. For example, in the case of doubly fed induction generator (DFIG) applications, the controllers decouple the mechanical modes with electrical modes [58]. However, for squirrel cage induction generators (SCIG) there is a strong coupling among rotor mechanical and electrical modes [59]. Hence, DFIG and SCIG generators act differently in system stability; that is the stability results obtained by employing DFIG are not the same as those obtained by employing SCIG.

The existing literature deals mainly with the small signal stability of large transmission systems focusing on large generators [57, 58]. The generators considered are regulated to support the stability of transmission networks. To date, most of the works on small signal stability are on transmission systems, which is characteristically different from MV and LV systems. For example, the dynamics of a transmission network is governed by large synchronous generators while the dynamics of emerging distribution/sub-transmission networks will be affected by different types of generators such as synchronous, induction, and static generators and by their controllers. In a large transmission system, generators are scheduled for reactive power support for voltage stability. On the other hand, DG units of small capacity are not required to support the reactive power of the network, according to the interconnection guidelines for DG units set by utilities such

as the Australian Energy Market Operator (AEMO) [47]. Generators in a transmission system are usually equipped with power system stabilisers (PSS) for small signal stability while wind and solar generators in emerging MV and LV systems usually do not have such stabilizing functionality. Owing to the close proximity of the generators to each other and to their controllers, dynamic interaction in distribution systems is a more complex issue. As a result, not only electromechanical modes but also some control modes become prominent issues for small signal stability. Consequently, issues of oscillatory instability may threaten the secure operation of emerging distribution systems. Small signal stability has become a major concern of renewable energy-based electricity systems in addition to the usual concerns such as voltage stability, protection and power quality. Hence, assessment and enhancement of small signal stability for the secure operation of the emerging electricity systems becomes an important task for accommodating the higher penetration of renewable energy-based distributed generation.

In many studies, the voltage stability analysis of power systems has been performed using bifurcation analysis. Bifurcation is obtained when a system reaches its stability limit as a parameter of the system is changed. To correctly capture all the bifurcation phenomena, bifurcation studies should be done considering all system dynamics and not only voltage controls [60]. An overview of local bifurcation theory and its application to power system voltage stability analysis is presented in [61]. The relationship between bifurcations, and their usefulness and limitations in power systems stability analysis through a thorough analysis of several examples is presented in [60].

Bifurcation theory deals with sudden changes in system behaviour as certain system parameters such as system loading are varied. The change may be brought about by merging together two distinct equilibrium points, one stable and the other unstable, leading to saddle node bifurcation (SNB), or by a pair of complex conjugate eigenvalues crossing the imaginary axis leading to Hopf bifurcation (HB). In the present study, the HB limit is considered for dynamic loadability determination. The HB limit is reached when a limit cycle and equilibrium coalesce as a function of a parameter. The importance of Hopf bifurcation has been increasingly recognised as it has become clear that the stability of the equilibrium can be lost by this mechanism well before it reaches the point of collapse. In this research, this kind of bifurcation is of particular interest as the scope of this work covers the dynamic interaction of different machines in the distribution network. Calculating the Hopf bifurcation requires the computation of the system eigenvalues to detect the crossing of the imaginary axis since the Jacobean does not become singular in this case. Furthermore, to discern which type of Hopf has taken place (subcritical or supercritical), one needs

to run a costly transient simulation or use special techniques that take into consideration additional nonlinear terms in the system, a very expensive procedure when dealing with relatively large systems. Nevertheless, for PQ load models and typically small resistive losses in the transmission system, Hopf bifurcations are unlikely to occur.

In a system consisting of induction motor loads, Hopf bifurcation analysis has been performed to study the induction motor load impact on system stability. In [62], bifurcations were examined in the total dynamic system model using induction motor loads (dynamic loads) and constant power loads. In [63], bifurcations were performed for a power system model consisting of two generators feeding a load, which is represented by an induction motor in parallel with a capacitor and a combination of constant power and impedance PQ load. Numerical bifurcation techniques can be used to assess the stability limit and transfer capability limits of a system. Studies with numerical bifurcation techniques can be found in many studies. In [64] various indices are proposed and studied to detect and predict oscillatory instabilities in power systems. The available transfer capability (ATC) constrained by dynamic stability utilising the bifurcation approach is presented in [65]. The Hopf bifurcation limit has been considered for determination of the dynamic ATC including induction motors. In [66], the authors explain the motor stalling as a possible saddle-node bifurcation (SNB) of equilibrium equations. The selection of appropriate control methodologies for DG units plays an important role in maintaining stability in distribution systems.

## 2.3. Review of control methodologies

### 2.3.1. Control methodologies for the enhancement of voltage stability

The steady state voltage level at each load connection point is one of the most important parameters for maintaining the quality of supply. Technical regulations or specific contracts define the allowed voltage range that bounds the maximum permitted variation of voltage at every bus. In a conventional distribution system, the desired operating voltage is maintained by controlling the voltage or reactive power flow that in turn controls voltage drop [25]. The equipment used for voltage and reactive power control are switched shunt capacitors, on load tap changer (OLTC) transformers and step voltage regulators [67]-[68]. SVC and/or STATCOM offer reactive power compensation for transient voltage stability improvement as well as steady state voltage regulation [69], [70]. Generally, a multilevel inverter-based distribution static synchronous compensator (D-STATCOM) is spatially located in a distribution system. This distributed approach suggests that several SVC/STATCOM placements at MV distribution level (11kV and 22 kV) is appropriate instead of placing bulk SVC at a high voltage level (132kV and above) with a transformer [71],

[72], [73]. Distributed compensators installed on the distribution side of a power delivery transformer can provide significant benefits over lumped compensation that has traditionally been placed at transmission and sub-transmission levels. The benefits of distributed compensators on the distribution side of a substation include lower VAR requirements, better voltage regulation in load centres, lower rating transformer requirement and increased reliability. These benefits have been found in [71] and [73]. With the availability of STATCOMs or SVCs (the cheaper option) which can be connected at distribution-level voltages without the need for transformers, it has been proven that small Static VAR Systems (SVS) directly connected to distribution buses offer a number of advantages over the traditional single bulk SVS placement at transmission or sub-transmission level. SVC placement on distribution buses offers reliable operation for (N-1) contingency operation along with savings in MVARs and transformer MVA. This methodology didn't account for the presence of DG. All substation loads assume a 90% power factor with a constant PQ load and that the distribution transformer is not considered as OLTC. SVS is placed at every bus at a 25kV level without considering any optimisation process for the selection.

The static voltage stability margin can be enhanced using adequate reactive power support at an appropriate bus/node and hence shift the point of collapse. Various reactive compensation devices are used by the utilities for this purpose, each of which has its own characteristics and limitations. However, the distribution utility is interested in achieving this goal with the most beneficial compensation device [74], [69]. Historically, synchronous condensers connected at the sub-transmission and transmission buses have been used to supply the continuously adjustable capacitive or inductive currents to support the voltages at the load centres. Because of the precedent set by synchronous condensers, the SVSs, which have largely replaced them, still tend to be located at the sub-transmission and transmission buses.

The introduction of distributed generation units into an existing power system can significantly impact the flow of power and the voltage conditions in the customers' and the utility's equipment. These impacts may be either positive or negative depending on the characteristics of both the distribution system and the DG units. Due to significant penetration of DG, power flow may reverse and the distribution network may become an active system with power flow and voltage determined by both generation and load [1]. This bi-directional power flow in turn results in significant changes to voltage control mechanism in the distribution network [75], [76], [77]. This section summarises how some distribution systems which include DG utilise reactive power compensators to maintain voltage throughout the system.

It is well known that voltage control issues in a power system have a strong correlation with reactive power compensation. Both static and dynamic compensators play an important role in voltage stability. Optimum allocation of static compensators (such as capacitor banks), taking into account location and size, is one of the foremost components in reactive power planning [78]. On the other hand, SVC and STATCOM have an inbuilt potential to offer both dynamic reactive power compensation for transient voltage stability improvement and steady state voltage regulation for DG integrated systems. For example, in a wind turbine integrated system, dynamic reactive power compensation is provided by a STATCOM or SVC located at the point of the wind turbine connection [79], [80]. With a voltage source converter (VSC), STATCOM has the least delay associated with thyristor firing, resulting in faster operation compared to an SVC [81]. However, these studies only emphasised the role of SVC and STATCOM in improving voltage profile of DG bus.

In a few studies, the reactive power capability of large-scale DG has been utilised to mitigate voltage problems. In [82], Tanaka proposes a decentralised voltage control for DG integrated systems utilising the reactive power generation capability of inverter-based DG units. Foster, in [83], utilises the reactive power of Doubly Fed Induction generators (DFIGs) with a capability chart to mitigate issues that arise during voltage dip. The use of existing reactive power sources in systems which contain wind turbines to maintain voltage at a point of common coupling using offline optimisation strategies has been the focus of research work by Keane [84]. The role of DFIG-based wind turbines for stability improvements has been investigated by Nunes [85]. A typical wind farm consists of various reactive power controllers and is based on the generation at any time of the day. Various controllers attempt to maintain the voltage such that the wind turbines are free to generate maximum reactive power. The tap changers are key controllers in such a voltage control exercise and [33] suggests a control strategy involving DFIG and a tap changer. The possibility of using the reactive power generation capability of inverter-based distributed generation (such as solar panels and pluggable hybrid electric vehicles) to support voltage has been studied in [86] although this form of generation is not supported under the present grid standard. In [87], the inverter is controlled to perform as a multi-function device to improve different power quality features throughout the grid.

The integration of large-scale DG in a distribution system leads toward coordinated control. In a few studies, On Load Tap Changing Transformers (OLTC) along with the reactive power

generation capability of DG units has been utilised to maintain the voltage profile at a point of common coupling under all operating conditions [88], [89], [83], [84], [90]. Coordination between OLTC and the reactive power production of DG has been proposed by Caldon in [88]. A proper coordination between OLTC, substation switched capacitors and feeder switched capacitors has been proposed by Viawan and Conti in order to obtain optimum voltage and reactive power control [34], [91], [89], [92]. In the method they propose, DG operating at constant voltage reduces OLTC operations per day and voltage fluctuation in the system. Yi Wang [93] suggests a coordinated control strategy for DFIG and Fixed Speed Induction Generator (FSIG) turbines under unbalanced grid conditions. Yi Wang [93] also demonstrated the effectiveness of this control strategy through simulation results. Li Wang [94] proposes an approach in which a line-commutated back-to-back HVDC link connects induction generator-based wind turbine generation systems to the grid. The line-commutated converter in this system allows users to comply with grid interconnection standards.

Taking account of the renewable energy intermittency problem and islanding modes of operation, energy storage-based control methodologies have been developed by a number of researchers. Teleke [95], [96] deals with the optimal control of battery-based energy storage, which helps in making wind farm power output more predictable and thus allows them to behave as conventional generators. Muyeen [97] presents an energy capacitor system (ECS) to smooth the output power fluctuations of a variable speed wind farm. A suitable and economical topology of ECS, composed of a current controlled voltage source inverter, a DC–DC buck-boost converter and an electric double layer capacitor (EDLC) bank including control strategies, is developed in that study. In Muyeen's study, the simulation results are described in light of the US grid code, set by Federal Energy Regulatory Commission (FERC) [98]. Balaguer [99] proposes a controller with two interface controls: one for grid connected operation and the other for intentional islanding operation for a static generator-based power system. The proposed control scheme maintains grid standards under both operation modes.

One of the most common power quality problems reported in practice is voltage fluctuation. At the point of common coupling of the distributed generator, this problem is sometimes inevitable because of the variable nature of renewable energy sources. This can be mitigated by any of a number of technologies but the fast response of the D-STATCOM makes it an ideal solution [100]. The optimum location and size of the compensation device is required to mitigate power quality problems of consumers with the least capital cost. In [101], two case studies of D-STATCOM are

presented, with and without the presence of DG. The presence of DG reduces the size of the D-STATCOM. Molinas [102] addresses the gearbox issue (torque transients due to grid fault) for fixed speed wind turbines with the help of STATCOM. Flicker management is an issue associated with wind turbines connected to grids, hence modelling of wind turbines and their control algorithms plays a very important role. Saad-Saoud [103], proposes a model for a simple induction generator as a set of the first order differential equations and their integration for flicker analysis. Investigations into STATCOM and wind farms with fixed wind speed turbines have been carried out by Saad-Saoud [104]. In [105], coordination between DG and switched capacitors is presented in order to ensure that the voltage rise caused by DG will not result in any over-voltage with energised capacitors.

Grid requirements and standards are the key drivers that shape the conventional control strategies to allow seamless integration of DG in the main grid. Post-fault voltage recovery time at the DG bus is the crucial part of these standards as it requests DG to trip if recovery time exceeds a certain limit [106], [43], [107]. Small-scale DG units with limited reactive power generation capability suffer most with regard to recovery voltage under current grid code practices. Hence, a system operator becomes responsible for maintaining the voltage profile within an acceptable range at all nodes and under all operating conditions. A sensitivity-based approach has been proposed in [108] to decide and limit the location of high cost dynamic compensator devices such as STATCOM to recover voltage at all buses of interest.

### *2.3.2. Control methodologies for the enhancement of small signal stability*

The low damped modes of oscillation in a power system may be effectively damped by the appropriate location of shunt controllers [109], [110]. Conventional distribution systems are highly compensated with shunt capacitors for voltage stability improvement. In recent years, Flexible AC Transmission System (FACTS) controllers such as SVCs and DSTATCOM are also used to achieve efficient voltage and power quality control [111]. It is well known that the application of shunt compensators enhances the voltage stability of a power system. However, shunt compensators have been reported to degrade the small signal stability in some cases by contributing negative damping to system oscillation [112],[113]. On the other hand, controllable devices such as SVCs can support small signal stability if primary controller parameters are carefully selected [113]. Therefore careful attention should be given to minimising the detrimental impact on small signal stability while selecting a control methodology for voltage stability improvement.

An important issue of distribution system control is the location of the controller. The correct location is very important for the best economic and technical performance of a controller. There are a number of approaches to locate shunt controllers in a power system. Modal analysis has been proposed by [114] to determine the suitable location for voltage stability enhancement. Similarly, residue and controllability factor-based methods have been proposed in [109] and [110] to locate shunt controllers for small signal stability enhancement. In [115], an extended eigenvector-based method has been used. The application of residues and controllability indices are possible when the input and output of the controllers are defined externally. Furthermore, these methods are suitable when some controllers are to be selected from among a large number of controllers in a power system to add supplementary damping controllers [110],[113] and [115]. On the other hand, the application of extended eigenvectors needs computation of the sparse Jacobian matrix, which consists of a system admittance matrix as one of its components. Handling a large and sparse matrix, in turn, needs more computational effort. In this work, the appropriate location of shunt compensators is identified by the Q-V sensitivity technique. Then the best location is identified by using the participation factor of the SVC state on the critical mode.

In these works, controllers are designed by both the classical lead/lag compensation and robust techniques. The controllers designed by the classical control technique have their validity restricted to a nominal operating point at which the system is linearised. However, a power system constantly experiences changes in operating conditions due to variations in load generation patterns and variations in transmission networks. In addition, some uncertainty is introduced into the power system model due to inaccurate approximation of the power system parameters, neglecting high frequency dynamics and assumptions made in the modelling process. Hence it is desirable to have a robust damping controller to ensure adequate damping under various system operating conditions. In this research, the Glover-McFarlane loop shaping design has been employed for robust controller design [116]. Optimal design has been preferred, as this technique has less computational burden as compared to other robust control techniques [117].

In conventional power systems, various advanced compensating devices such as FACTS devices as well as stabilizers are commonly used for stability enhancement. However, these devices are not very common in distribution networks due to their complex design and costs. On the other hand there are uncertainties in power generation from DG units, which are usually not regulated in a distribution network. So, conventional approaches may not always be suitable for ensuring the

stability of emerging distribution networks. Alternatively, different approaches for controlling DG units, network devices or loads can be options for stability improvement. This work broadly covers additional aspects of stability assessment and enhancement opportunities in emerging renewable energy-based electricity distribution systems.

Installation of shunt control devices in a low voltage distribution system may not always be technically and economically attractive. Instead, one of the DG units in the system may be controlled to improve system stability [118]. Given the structure of DFIG-based wind generation systems and photovoltaic generators, which are dominated by controllers, one of their controllers may be employed for improving the oscillation damping.

Several research efforts have been devoted to utilise DFIG for stability enhancement of power systems. According to [85] the DFIG, equipped with a four-quadrant AC-to-AC converter increases the transient stability margin of a power network compared to the fixed-speed wind systems based on squirrel cage generators. In [119], it is shown that a DFIG equipped with power electronic converters and fault ride through capability will have no adverse effect on the stability of a weak grid. Reference [120] focuses on the operational mode of variable speed wind turbines that could enhance the transient stability of the nearby conventional generators. The effect of wind farms on the modes of oscillation of a two area, four-generator power system is analysed in [121].

Reference [55] advocates that the generator types used in wind turbines should not take part in power system oscillations. Rather, the penetration of wind power will have a damping effect due to a reduction in the size of synchronous generators that engage in power system oscillations. The congestion phenomenon at a weak grid and reduced damping are reported in [122], in the case of increased wind power penetration. Hughes et al. [123] used a power system stabilizer (PSS) in a DFIG with a rotor side converter to damp power system oscillations. The control is based on flux magnitude and angle control (FMAC), where the rotor flux magnitude controls the reactive power/voltage while the rotor flux angle controls the active power/torque. Since the stator voltage-oriented or flux-oriented vector control is used widely in DFIG [124] the investigation of the oscillation damping capability in vector control based DFIG is of practical value. In [125], the DFIG penetration was added to the classic inter-area oscillation test system. The authors investigated the function of a supplementary damping control loop added at the rotor voltage point. In [126] the authors established that in a vector control scheme, active power modulation can best help to damp low frequency oscillations. Though several efforts have been made to utilise DFIG for stability enhancement, the application of DFIG controller damping of system oscillations has not

been well studied yet. This work attempts to design a robust controller for DFIG to enhance small signal stability of emerging distribution networks.

Similarly, a number of works have studied dynamic models, stability, and/or the control of three-phase, single-stage PV systems [127],[128]. Reference [127] has elegantly developed a reduced order model for a PV system. The model and the proposed controllers are based on the voltage mode control strategy and they can be conveniently incorporated into time domain power system simulation studies. However the paper does not provide a stability analysis or controller design methodology. A number of works [128], [129] have adopted the current mode control strategy. Reference [129] identifies the control loops and the transfer functions of the PV system, but does not report any analysis of the stability or interactions with the line/loads. Reference [130] has adopted an analysis approach similar to that taken in [129], with an emphasis on the impact of grid impedance on closed-loop stability and not on the interaction between the PV system and the distribution network. In [128], the behaviour of a three-phase, single-stage PV system is studied, with an emphasis on the maximum power point tracking (MPPT) strategy rather than on the control or stability of the PV system. There have been a number of attempts to analyse a PV system for small signal stability. However, the impact of PV on the oscillation of distribution networks and the advantage of a PV controller for system damping is not well addressed in the literature. The present work proposes a controller for PV to support damping of low frequency oscillations in emerging distribution networks.

## 2.4. Summary

This chapter summarises an extensive literature review on voltage stability and small signal stability in the presence of DG units in power systems. With the emergence of new renewable and non-renewable distributed resources, control methodologies have also been redefined. Conventionally, the generators connected to an integrated power system are synchronous generators. However, many renewable resources do not employ synchronous generators for power conversion. Instead, they use inverter-based storage type generators (which do not have rotors) and induction generators which have rotor speeds different from the system frequency. Also, system dynamics are already affected by the dynamic nature of different loads connected to the distribution system. A review of stability and control assessment shows that different dynamic devices with various dynamic characteristics integrated into the same synchronised system will pose a big challenge to system stability. Hence, proper power system modelling is mandatory in order to analyse the actual impact of DG on a power system and develop required control

mechanisms considering grid standards. The next chapter details the system modelling considered in our work.

### 3. MODELLING OF DISTRIBUTION SYSTEMS WITH DISTRIBUTED GENERATORS

For the analysis of the dynamic stability responses, the elements of a power system are captured using the following differential and algebraic equations (DAE):

$$\begin{cases} \dot{x} = f(x, y, l, p) \\ 0 = g(x, y, l, p) \end{cases} \quad (2.1)$$

where  $x$  is a vector of state variables,  $y$  is a vector of algebraic variables, and  $l$  and  $p$  are uncontrollable and controllable parameters, respectively.

In general, the components that should be considered in the power distribution system for various stability studies are distributed generators, transformers, transmission lines (including subtransmission lines), compensators and loads. The models utilised for various elements of the distribution system in this research are explained below.

#### 3.1. Distributed Generators

Distributed generators (DG units) can be fuelled by a variety of sources from traditional to renewable energy and they are classified into three types as far as the electricity production is concerned. The three types are synchronous, induction and static generators.

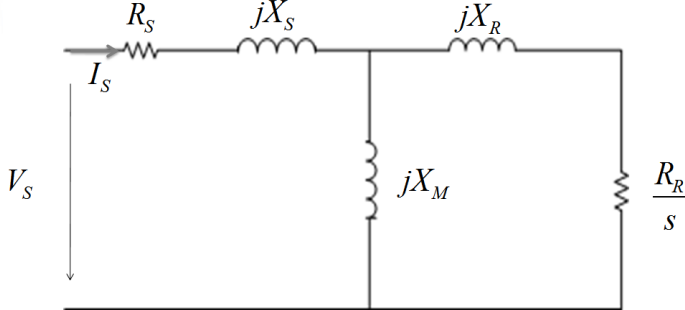
##### 3.1.1. Synchronous generators

Most of the distributed generation applications today employ synchronous generators for energy conversion and electricity production [12]. This type of DG unit can be used in thermal, hydro and wind power applications for energy conversion. Since the DG units are connected to the distribution system they do not take part in frequency control and the mechanical torque of the generator is assumed to be constant. In transient stability analysis, synchronous generators are represented by a sixth order model [131]. Usually, synchronous generators are connected to distribution systems as constant active power sources operating at the power factor control mode. However, depending upon their capability, they may support the voltage by providing reactive power as well. In this research, both types of operations of synchronous generator were considered. For voltage control mode, the reactive power limit has been defined.

##### 3.1.2. Induction Generators

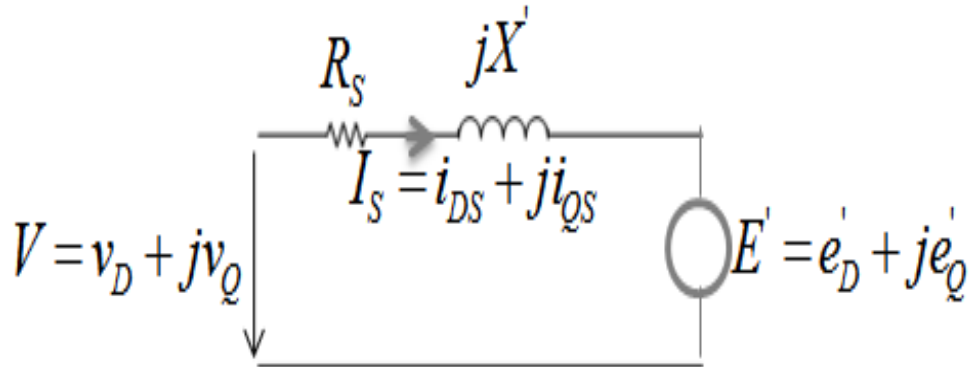
Induction generators are popularly employed in wind power generation applications, small and micro hydro generators and some thermal plants [12, 15], [132]. As is the case for synchronous generators, the mechanical torque is assumed to be constant. The squirrel cage induction generator (SCIG) model has been considered. The steady state equivalent circuit of an SCIG is shown in Figure 1.

Figure 1: Steady state equivalent circuit of induction generator



In stability analysis, the SCIGs are modelled by a third order model neglecting the stator flux dynamics [15]. The model can be represented by a transient voltage source behind transient impedance as shown in Fig. 2.2. In Figure 2,  $V_D$  and  $V_Q$  are direct (d) axis and quadrature (q) axis terminal voltages, respectively.

Figure 2: Transient equivalent circuit of induction generator



$$\text{where } \begin{cases} v_D = R_s i_{DS} - X' i_{QS} + e'_D \\ v_Q = R_s i_{QS} + X' i_{DS} + e'_Q \end{cases} \quad (2.2)$$

The real part of transient impedance is stator resistance and the imaginary part is the transient reactance which is given by (2.3).

$$X' = X_s + X_M \parallel X_R = X_s + \frac{X_M \cdot X_R}{X_M + X_R} \quad (2.3)$$

The induction generator model is expressed by three dynamic equations as given in (2.4).

$$\begin{cases} \frac{de'_D}{dt} = -\frac{\omega_E R_R}{X_R + X_M} \left( e'_D + \left( \frac{X_M^2}{X_M + X_R} \right) i_{QS} \right) + s\omega_E e'_Q \\ \frac{de'_Q}{dt} = -\frac{\omega_E R_R}{X_R + X_M} \left( e'_Q + \left( \frac{X_M^2}{X_M + X_R} \right) i_{DS} \right) - s\omega_E e'_D \\ 2H \frac{d}{dt} \left( \frac{\omega_R}{\omega_{BASE}} \right) = T_{MECH} - T_{EM} \end{cases} \quad (2.4)$$

where  $\omega_E$  is the system frequency,  $\omega_{BASE}$  is the base frequency,  $s$  is the slip, and  $H$  is the acceleration constant of the induction generator.  $T_{EM}$  is the electromagnetic torque developed and  $T_{MECH}$  is the mechanical torque obtained from external force (such as wind).

In (2.4),  $e'_D$  and  $e'_Q$  are  $d$  – axis and  $q$  – axis back emfs (electromotive forces) induced in the induction generator.

$$\begin{cases} e'_D = \frac{-\omega_E}{\omega_{BASE}} \frac{X_M}{X_M + X_R} \psi_{QR} \\ e'_Q = \frac{\omega_E}{\omega_{BASE}} \frac{X_M}{X_M + X_R} \psi_{DR} \end{cases} \quad (2.5)$$

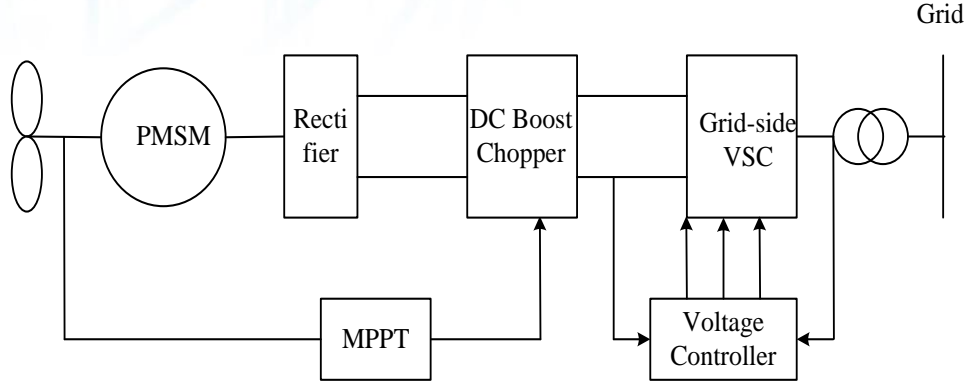
where  $\psi_{DR}$  and  $\psi_{QR}$  are the rotor fluxes. The fluxes are related to stator and rotor currents as

$$\begin{cases} \psi_{DS} = (X_S + X_M) i_{DS} + X_M i_{DR} \\ \psi_{QS} = (X_S + X_M) i_{QS} + X_M i_{QR} \\ \psi_{DR} = (X_R + X_M) i_{DR} + X_M i_{DS} \\ \psi_{QR} = (X_R + X_M) i_{QR} + X_M i_{QS} \end{cases} \quad (2.6)$$

### 3.1.3. Modelling of direct drive wind generator

Figure 3 is a simple diagram of a directly driven wind generator (DDWG) system. The AC power output from the generator is converted into DC power through diode rectifier circuits. The grid side connection is realised by a self-commutated pulse-width modulated (PWM) converter that imposes a pulse-width modulated voltage to the AC terminal.

Figure 3: Schematic diagram of DDWG



This direct drive permanent magnet synchronous generator uses constant excitation. The dynamic model of the DDWG is given by [133]:

$$L_s \frac{di_{ds}}{dt} = -v_{ds} - R_s i_{ds} + L_s \omega i_{qs} \quad (2.20)$$

$$L_s \frac{di_{qs}}{dt} = -v_{qs} - R_s i_{qs} - L_s \omega i_{ds} + \omega \psi$$

(2.21)

where  $v_{ds}$  and  $v_{qs}$  are the  $d$  and  $q$  axis components of the stator voltage, respectively;  $i_{ds}$  and  $i_{qs}$  are the  $d$  and  $q$  axis stator current, respectively;  $R_s$  is the resistance of the stator;  $L_s$  is the inductance of the stator;  $\omega$  is the generator's electrical speed; and  $\psi$  is the magnet flux.

As the permanent generator is directly connected to the turbine, the model of the drive train can be represented by the one mass model given by:

$$H_{tot} \frac{d\omega_t}{dt} = T_M - T_e \quad (2.22)$$

where  $\omega_t$  is the turbine speed,  $H_{tot}$  is the inertia constant of the whole drive system;  $T_M$  is the mechanical torque of the turbine and  $T_e$  is the electromagnetic torque of the generator.

The DDWG is connected to the grid via a full-scale back-to-back converter. The active power flow through the converter is balanced via the DC link which is modelled as:

$$C v_{dc} \frac{dv_{dc}}{dt} = v_{Dg} i_{Dg} + v_{Qg} i_{Qg} + v_{ds} i_{ds} + v_{qs} i_{qs} \quad (2.23)$$

where  $i_{Dg}$  and  $i_{Qg}$  are the  $d$  and  $q$  axis currents of the grid side converter, respectively;  $v_{Dg}$  and  $v_{Qg}$  are the  $d$  and  $q$  axis voltages of the grid side converter, respectively;  $v_{dc}$  is the terminal voltage of the converter,  $i_{dc}$  is the current of the converter; and  $C$  is the capacitance of the capacitor.

### 3.1.4. Static Generators (PV Systems)

Solar PV cells generate a DC current which is converted into AC by a power electronics inverter with appropriate control. The power electronic converters decouple the PV system dynamics from network dynamics similar to the concept of an HVDC (High Voltage Direct Current) transmission system in power systems. Since no electromechanical phenomenon occurs in the PV system, the PV generator could be considered as a static generator. However, PV systems and their controllers can negatively interact with other dynamic devices placed in close proximity. In order to capture the negative interaction and their influence, the PV system should be modelled as a dynamic device using a set of differential and algebraic equations. The IEEE guidelines for the interconnection of distributed resources suggest connecting PV at unity power factor [54]. Currently most inverters used in PV power conversion are designed to operate at unity power factor [57, 134], [6]. The solar irradiation is assumed constant throughout the analysis.

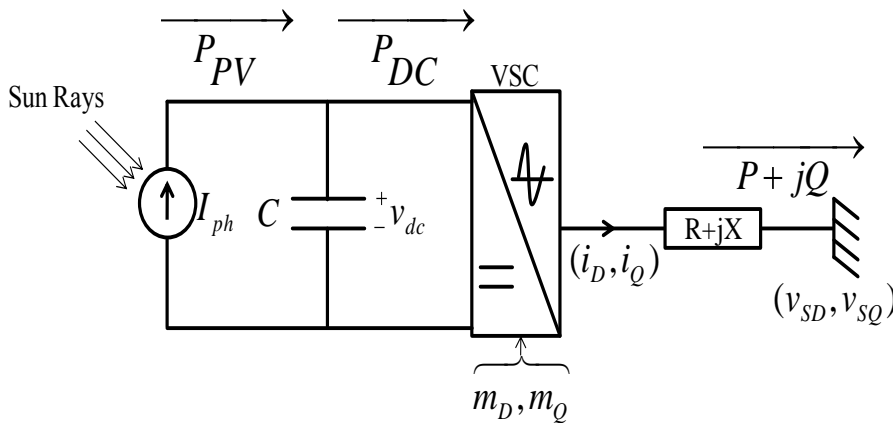
### 3.1.5. Model of Photovoltaic Generator

A schematic diagram of a grid-connected photovoltaic (PV) system is shown in Figure 4. The incidence of sun rays on PV panels induces photovoltaic current, which causes PV power flow ( $P_{PV}$ ) from PV panels to a DC link capacitor.  $P_{PV}$  can be given as (2.7) [16],[17]:

$$P_{PV} = n_p v_{dc} \left[ I_{ph} - I_{rs} \left\{ \exp \left( \frac{q}{kTA} \frac{v_{dc}}{n_s} \right) - 1 \right\} \right] \quad (2.7)$$

where  $n_p$  and  $n_s$  are numbers of parallel strings and number of series connected PV panels per string, respectively; and  $v_{dc}$  is the DC link capacitor voltage.

Figure 4: A schematic diagram of grid connected PV system



Quantities  $q, k, T$  and  $A$  denote the unit charge, Boltzmann's constant, cell temperature and p-n junction actuality factor, respectively. Now,  $I_{ph}$  is the photovoltaic current and is given by:

$$I_{ph} = [I_{SC} + k_T (T - T_R)] \frac{S}{100} \quad (2.8)$$

where  $T_R$  is the reference temperature of the cell;  $I_{SC}$  is the short circuit current of a unit cell of

PV at reference temperature and solar irradiation  $S$ ; and  $k_T$  is the temperature coefficient.

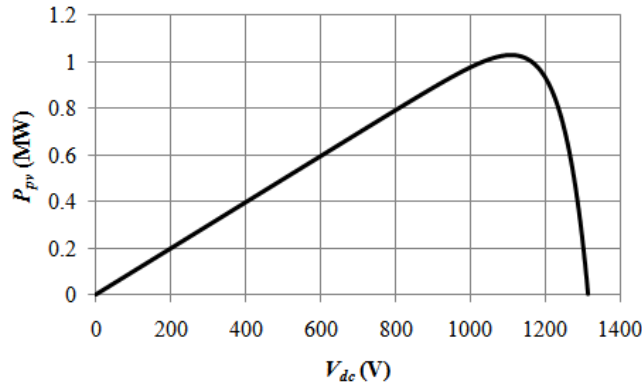
Similarly, cell reverse saturation current ( $I_{rs}$ ) is given as:

$$I_{rs} = I_{RR} \left[ \frac{T}{T_R} \right]^3 \exp \left( \frac{qE_G}{kA} \left[ \frac{1}{T_R} - \frac{1}{T} \right] \right) \quad (2.9)$$

where  $I_{RR}$  is the reverse saturation current at reference temperature  $T_R$ ; and  $E_G$  is the band gap energy of a cell.

For a particular grid-connected PV system,  $P_{PV}$  depends on  $v_{dc}$  for given conditions of solar irradiation and cell temperature. For the grid-connected PV system considered in this report, the variation  $P_{pv}$  with  $v_{dc}$  is assumed to be as shown in Fig. 2.5. It can be observed that the PV system output maximum of 1 MW at  $v_{dc}$  is set at 1.1 kV. The voltage of the DC link capacitor ( $v_{dc}$ ) is set to extract maximum power from the PV panel using maximum power point tracking (MPPT) control [17]. In this paper,  $v_{dc}$  is set to 1.1 kV. The irradiation level ( $S$ ) and cell temperature ( $T$ ) considered are  $700 \text{ W/m}^2$  and  $300\text{K}$ , respectively.

Figure 5: Relationship between DC link voltage and output power of a PV array



DC link capacitor voltage dynamics can be given by a power balance equation as:

$$\frac{C}{2} \frac{dv_{dc}^2}{dt} = P_{PV} - P_{DC} \quad (2.10) \text{ where } P_{DC} \text{ is the power transferred from capacitor to voltage source}$$

converter (VSC). VSC feeds the power into the grid by converting the DC signal into an

appropriate AC signal. If  $P$  is the power supplied to the grid, the expression for  $P_{DC}$  can be given

$$\text{as: } P_{DC} = P + P_{LOSS} \quad (2.11) \text{ where } P_{LOSS} \text{ is the power loss in VSC and interface impedance (R + j}$$

X). It is obvious from (2.10) and (2.11) that any disturbance in  $P$  will ultimately induce oscillations in  $v_{dc}$ , which must settle to  $v_{dc\text{ref}}$  determined by MPPT (maximum power point tracking) control.

### 3.1.6. Power factor control

The relationship of active power ( $P$ ) and reactive power ( $Q$ ) with voltages and currents in d- and q-axis reference can be given as:

$$\begin{cases} P = \frac{3}{2} (v_{sd} i_d + v_{sq} i_q) \\ Q = \frac{3}{2} (v_{sq} i_d - v_{sd} i_q) \end{cases} \quad (2.12)$$

where  $v_{sd}$  and  $v_{sq}$  are the d- and q- axis components of PV terminal voltage. Similarly,  $i_d$  and  $i_q$  are d- and q- axis components of PV current into the distribution network.

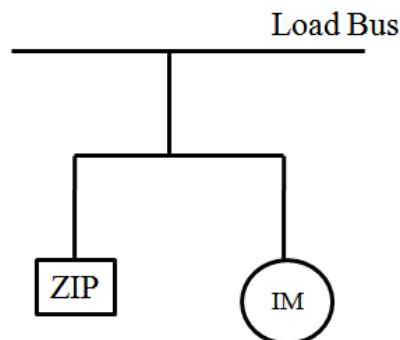
## 3.2. Load modelling

In steady state analysis, the loads are represented by constant power models [135]. However, in dynamic analysis, there is no uniformity in the literature regarding the choice of the proper load model. The IEEE task force [135] recommends that the active power loads be represented by constant current models and reactive power loads be represented by constant impedance models for dynamic simulation. On the other hand, induction motor dynamics is also popularly used to represent the load dynamics [136, 137]. In recent years, the composite load models have been widely used where static parts are represented by ZIP and dynamic parts are represented by induction machines [138, 139].

The selection of load model obviously affects the result of stability analysis [140-142]. Hence, all the loads of the studied system are modelled by constant impedance to achieve simplicity in analysis [142]. However, loads are modelled as a combination of static and induction motor (composite) to study the influence of loads on small signal stability of distribution system with DG units.

The composite dynamic load model, which consists of both ZIP and induction motor models, may be shown as Figure 6.

Figure 6: A composite dynamic load model



In a composite load model, the composition of a load may be expressed as (2.13).

$$S_{load} = (1-\gamma)S_{ZIP} + \gamma S_{IM} \quad (2.13)$$

where  $\gamma$  is the ratio of induction motor load to the total load;  $S_{ZIP}$  and  $S_{IM}$  are the complex powers consumed by static loads and induction motor loads respectively; and  $S_{load}$  is the complex power of the total load connected to the load bus. Now, the combination of ZIP may be expressed as (4.14).

$$S_{ZIP} = P + jQ \quad (2.14)$$

where

$$\begin{cases} P = P_o \left[ p_1 \left( \frac{V}{V_o} \right)^2 + p_2 \left( \frac{V}{V_o} \right) + p_3 \right], \\ Q = Q_o \left[ q_1 \left( \frac{V}{V_o} \right)^2 + q_2 \left( \frac{V}{V_o} \right) + q_3 \right] \end{cases} \quad (2.15)$$

Here,  $P_o$  and  $Q_o$  are nominal values of active and reactive powers at a load bus. Also,  $p_1, p_2, p_3$  and  $q_1, q_2, q_3$  are coefficients of constant impedance, constant current and constant power portions of active and reactive power respectively.

In this work, induction motor loads are modelled by a third-order model neglecting the stator flux dynamics [11]. The model for an induction motor is in principle the same as that for an induction generator as discussed above. The steady state equivalent circuit of an induction motor is shown

Figure 1 in Figure 1: Steady state equivalent circuit of induction generator

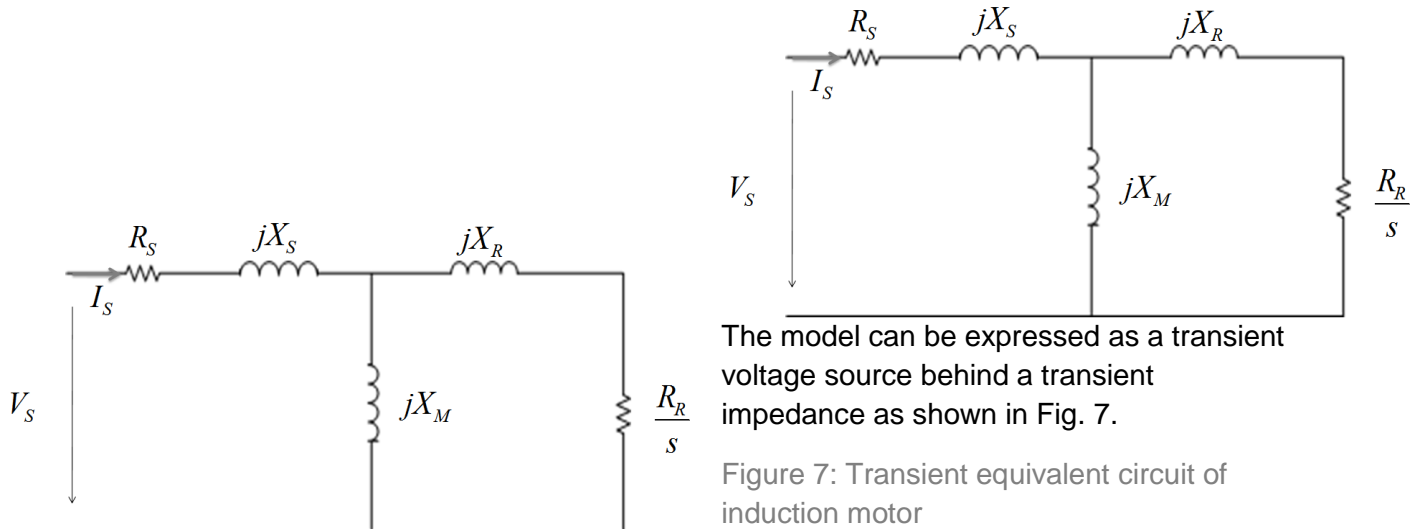


Figure 7: Transient equivalent circuit of induction motor

$$\text{where } \begin{cases} v_D = R_s i_{DS} - X' i_{QS} + e'_D \\ v_Q = R_s i_{QS} + X' i_{DS} + e'_Q \end{cases} \quad (2.16)$$

The real part of transient impedance is stator resistance and the imaginary part is the transient reactance, which is given by (2.3). In a third-order dynamic model of an induction motor, the transient voltage is expressed by dynamic equations as:

$$\begin{cases} \frac{de'_D}{dt} = -\frac{1}{T_o'} \left( e'_D + (X' - X'_{QS}) i_{QS} \right) + s e'_Q \\ \frac{de'_Q}{dt} = -\frac{1}{T_o'} \left( e'_Q + (X' - X'_{DS}) i_{DS} \right) - s e'_D \end{cases} \quad (2.17)$$

where  $X = X_M + X_s$  and  $T_o' = \frac{X_R + X_M}{\omega_E R_R}$  is the transient open circuit time constant expressed in radians.

Also, the rotor inertia dynamic is given by:

$$2H \frac{d}{dt} \left( \frac{\omega_R}{\omega_{BASE}} \right) = T_{EM} - T_{LOAD} \quad (2.18)$$

where  $\omega_E$  is the system frequency;  $\omega_{BASE}$  is the base frequency;  $s$  is the slip; and  $H$  is the acceleration constant of the induction motor.  $T_{EM}$  is the electromagnetic torque developed and  $T_{LOAD}$  is the load torque. The induction motor load is assumed to be operated in the linear region of torque speed characteristics.

In (2.17),  $e'_D$  and  $e'_Q$  are  $d$  – axis and  $q$  – axis back emfs induced in an induction motor.

$$\begin{cases} e'_D = \frac{-\omega_E}{\omega_{BASE}} \frac{X_M}{X_M + X_R} \psi_{QR} \\ e'_Q = \frac{\omega_E}{\omega_{BASE}} \frac{X_M}{X_M + X_R} \psi_{DR} \end{cases} \quad (2.19)$$

where  $\psi_{DR}$  and  $\psi_{QR}$  are the rotor fluxes.

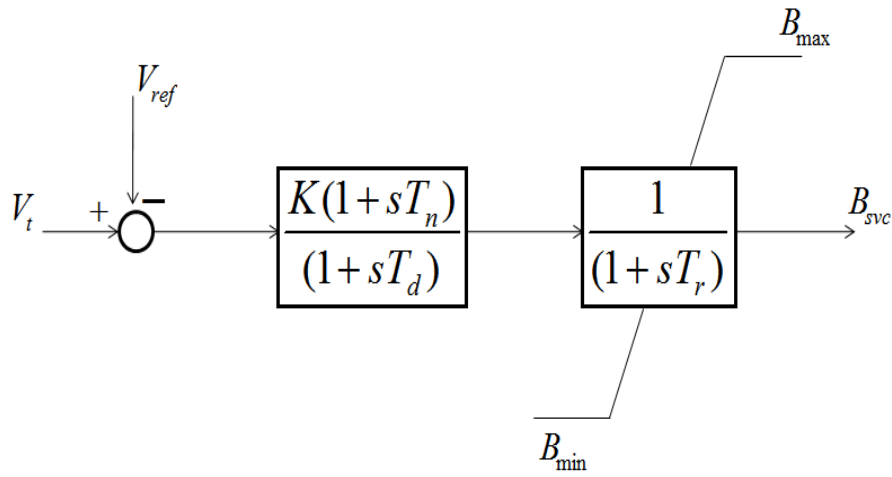
If an induction motor model is represented by the first-order model, the dynamics of transient voltage as described by (2.17) are neglected. In such a case, induction motor dynamics are represented by (2.18) only.

### 3.3. Static Var compensator (SVC)

SVC is a shunt-connected compensating device whose impedance is adjusted to control reactive power flow in the line. A thyristor-controlled reactor is connected in parallel to a fixed capacitor to control the effective reactance of the capacitor [11]. The block diagram of an SVC is shown in Fig.

8. Here,  $V_t$  and  $V_{ref}$  are the voltage magnitude at SVC terminal and voltage to be maintained by SVC, respectively.  $K$  is the gain of controller;  $T_n$  and  $T_d$  are used for gain adjustments; and  $T_r$  is the thyristor time constant.  $B_{max}$  and  $B_{min}$  specify the range of SVC compensation and  $B_{SVC}$  is the effective susceptance of SVC.

Figure 8: Block diagram of SVC control



### 3.4. Static synchronous compensator (STATCOM)

STATCOM is a Voltage Source Converter (VSC) based system that injects or absorbs reactive current, independent of grid voltage. Fig. 9 shows the basic block diagram of STATCOM. Reactive current injected or absorbed by STATCOM will profoundly influence grid node voltage. It is modelled either only as a reactive current source or as a current source with active and reactive components. The current injected by STATCOM depends on the pulse width modulation (PWM) method used along with operational limits and the characteristics of the Insulated Gate Bi-polar Transistors (IGBT) in use. Therefore, the current injected by STATCOM has appropriate limiters which are dynamic in nature [69]. The magnitude and/or phase shift of the voltage source converter (V) must be controlled to maintain the bus voltage (Vs) constant.

The STATCOM controller block is shown in Fig. 10 [143]. With  $i_d$  and  $i_q$  as reference currents in d-q reference frames, the active and reactive power injected by STATCOM can be expressed as

$$P_{STATCOM} = V(i_d \cos \theta + i_q \sin \theta) \quad (2.20)$$

$$Q_{STATCOM} = V(i_d \sin \theta - i_q \cos \theta) \quad (2.21)$$

Figure 9: Basic STATCOM model

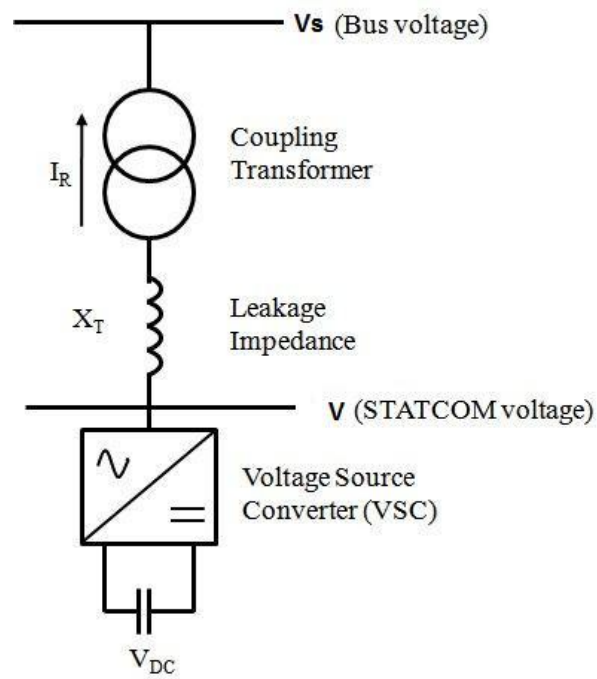
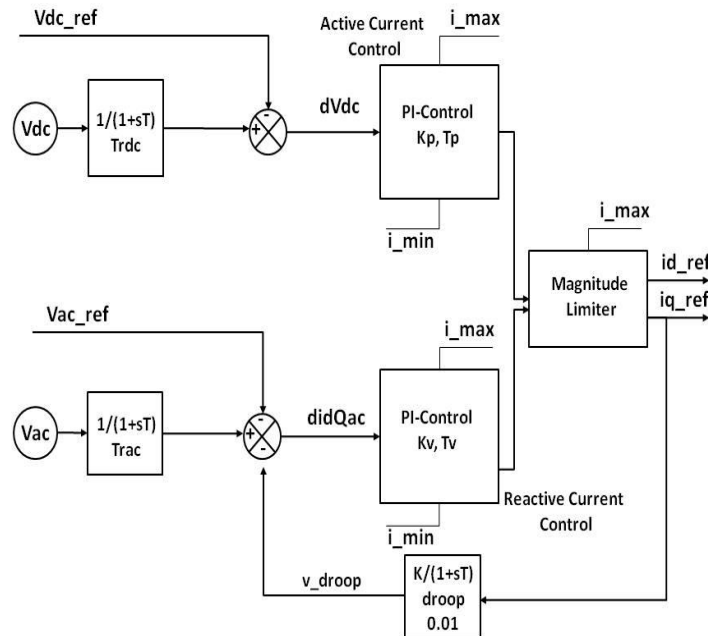


Figure 10: Block diagram of STATCOM controller.



### 3.5. Summary

In this chapter, models of different components of distribution systems have been briefly discussed. Stability studies require non-linear models of synchronous generators, asynchronous generators, static generators, loads, distribution networks and their associated controllers. The chapter summarised modelling practices adopted in our research for stability assessment. The basic function of voltage regulation is to keep the steady state voltage in the system stable within an acceptable range all the time. The desired voltages can be obtained by either directly controlling the voltage or by controlling the reactive power flow that in turn will affect the voltage drop. The next chapter will provide some novel techniques in terms of new indices for the placement of DG units and compensation devices in order to augment the voltage stability of MV/LV systems.

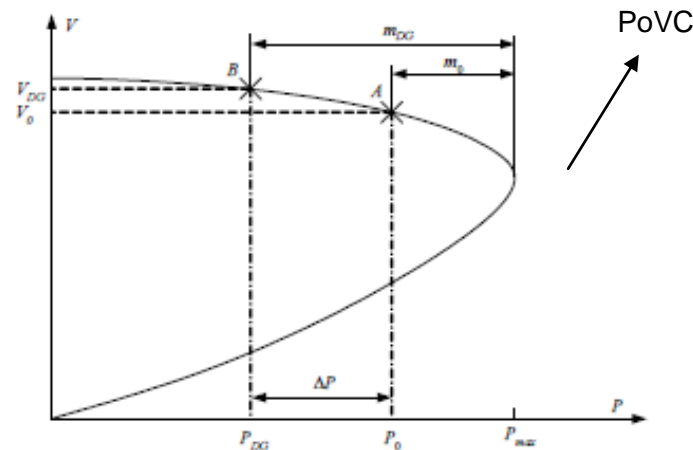
## 4. ENHANCEMENT OF VOLTAGE STABILITY WITH DG UNITS

A voltage stable power system is capable of maintaining post-fault voltages near the pre-fault values. If a power system is unable to maintain the voltage within acceptable limits the system undergoes voltage collapse. To facilitate the understanding of the various aspects of voltage instability mechanisms, the general and broad concept of 'voltage stability' is subdivided into two subcategories, namely Small and Large Disturbance Voltage Stability. Voltage collapse is the process by which a sequence of events accompanying voltage instability leads to an unacceptably low voltage profile in a significant part of the system. The time frame for this problem could range from a few seconds to several minutes. This usually occurs with heavily loaded lines which fail to meet reactive demands of local loads.

The most important factors determining the voltage stability of a power system are characteristics of the load, of reactive compensation devices and voltage control equipment of the network. To emphasise the importance of this fact, voltage stability is sometimes referred to as load stability. More specifically we can say that excessive load on a transmission line, a large distance between voltage sources and load centres, and a lack of sufficient reactive compensators are the principal causes behind voltage instability. Generally speaking, voltage stability is a dynamic phenomenon, which implies that full-scale modelling of the power system behaviour might be needed for rigorous analysis of voltage stability [25], [144].

As stated earlier, one of the most important factors affecting voltage stability is the ability of system generation and transmission to match the reactive power consumption due to the reactive load and losses. One of the most essential factors influencing the interaction between the DG and grid is the technology utilised in the DG, as well as the mode of DG control and operation. Similar to centralised generation, the following three generation technologies are normally used for distributed generation: synchronous generator, asynchronous generator and power electronic converter interface [145]. Comparisons have been made between these technologies from the perspective of their impact on grid voltage stability – that is, their ability to generate reactive power [146].

Figure 11: P-V curve: Enlargement of voltage stability margin



Synchronous generators are capable of both generating and absorbing reactive power. Therefore, the use of DGs utilizing overexcited synchronous generators will allow the production of reactive power onsite. The local generation of reactive power reduces its import from the feeder, thus reducing the associated losses and improving the voltage profile. As a consequence the voltage security is also improved, as can be seen from the P-V curve (Fig. 11). The installation of a distributed generator of  $\Delta P$  MW shifts the operation point on the associated P-V curve from point A to point B, which results in an increased stability margin from  $m_0$  to  $m_{DG}$ . So the installation of distributed generation will most likely enhance the voltage stability of the grid as long as the DG rating is smaller than twice the local loading level.

Although an asynchronous generator possesses a number of attractive features for DG, when directly connected to the grid this type of DG will consume reactive power, thus contributing to the factors increasing the probability of encountering voltage stability problems. The reactive power consumption of asynchronous generators is normally compensated for by shunt capacitor banks. This, however, is only a partial solution to the voltage stability problem, since a voltage reduction will decrease the amount of reactive power generated by the capacitor banks while increasing the reactive power consumption of the asynchronous generator. Therefore, there is a risk that instead of supporting the grid at an under voltage situation, the asynchronous generator will further lower the system voltage. This might in principle trigger a voltage stability problem.

It is a well known fact that conventional line-commutated converters always consume reactive power. The amount of the consumed reactive power can be as high as 30% of the rated power of the converter. To compensate for the Q demand, capacitor banks are normally installed on the AC side of the converter. This makes a line-commutated converter qualitatively equivalent to a directly connected induction generator. Therefore, under certain circumstances the presence of such a converter can negatively affect voltage stability.

Voltage instability is a local area phenomenon associated with the lack of reactive power in a significant part of the power network. Therefore, incorporation of VAR sources can increase the static voltage stability margin (VSM), which is defined as the distance between the nose point and the operational limit point. Optimal allocation of VAR sources such as capacitor banks, Static VAR Compensators (SVC) and STATCOM are key components for improving the voltage stability. Incorporation of shunt reactive power compensation in the power network provides voltage support, avoiding voltage instability or voltage collapse. In the past, locations of VAR sources were determined by estimation approach, but these methods are not effective.

The study of voltage stability in this work can be explained through the following steps.

1. Investigation of effective voltage stability indices
2. Improvement of static voltage stability margin with DG placement
3. Enhancement of static and dynamic voltage stability in view of present grid standards.

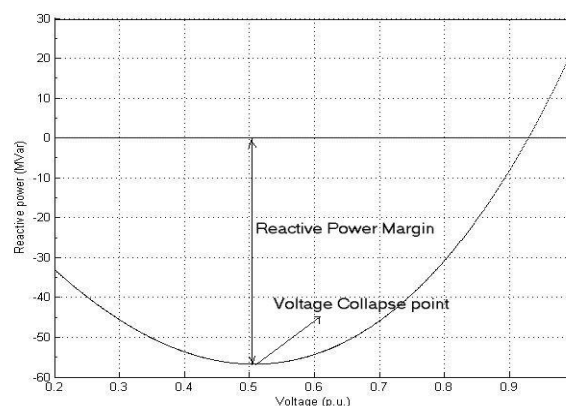
While analysing these issues, different load models and different types of DG have been utilised for the purposes of simulation.

### Investigation of effective voltage stability indices

One of the principal factors of voltage collapse has been identified as increased load demand, which is generally accompanied by an increase in reactive power demand. Distance to collapse can be measured in terms of different physical quantities such as loadability, and reactive power reserve. Also, a number of performance indices have been developed by researchers to understand proximity to voltage collapse [147]. Most of these indices are based on classical P-V and Q-V curve analyses. A typical Q-V curve is shown in

Figure 12, which depicts the variation in bus voltages with respect to changes in loading and reactive power support, respectively.

Figure 12: Sample Q-V curve and reactive power margin



### 4.1. System Loadability

Loadability limit is defined as the point where the load demand reaches a maximum value, beyond which the power flow solution fails to converge (Fig 11 PoVC) and the system can no longer operate [25]. If the load is considered as constant power, the loadability limit relates to the maximum deliverable power to a bus or a set of buses in a system [21]. So maximising loadability was a good choice for the distribution system operator to optimise their resources and maximise their profits.

### 4.2. Reactive power margin

Reactive power margin is measured as the distance between the lowest MVar point of the Q-V curve and voltage axis (Fig. 12) [144],[21]. The negative values of reactive supply indicate the increasing reactive load. Thus, the reactive power margin indicates how much further the loading on that particular bus can be increased before its loading limit is exceeded and voltage collapse takes place. Reactive power margins are used in [148] to evaluate voltage instability problems for coherent bus groups. These margins are based on the reactive reserve on generators, SVCs and synchronous condensers that exhaust reserves in the process of computing a Q-V curve at any bus in a coherent group or voltage control area. In this study, this index is used to measure the strength of buses of a primary distribution system with a single feeder. The validity of this index in our study will be justified by another index – the voltage sensitivity factor which has been used earlier for the same purpose [149].

### 4.3. Voltage Sensitivity Factor

Based on the general concept, SF (sensitivity factor) index for a system represented by  $F(\lambda)$  can

be defined as  $SF = \left\| \frac{dz}{d\lambda} \right\|$  [150]. When SF becomes large the system becomes insecure and can

lead ultimately to collapse. Here the system voltages are checked with respect to the change in loading as shown in Fig. 3.1, which results in a Voltage Sensitivity Factor (VSF) calculated as

$VSF = \left\| \frac{dV}{dP} \right\|$ . High sensitivity means that even small changes in loading result in large changes of

voltage magnitude. Therefore, high voltage sensitivities are indicative of a weak area in the system. With the combined results from the measurement of these two indices, the methodology described in the following section was used to identify the correct location and size of DG in the studied distribution system.

### 4.4. L-Index

The L-index has been established as a fast voltage stability indicator for transmission systems [151]. For an n-bus power system, buses can be separated into two groups, bringing all load buses to the head and denoting them as  $\alpha_L$  and putting the generator buses to the tail and denoting

them as  $\alpha_G$  i.e.  $\alpha_L = \{1, 2, \dots, n_L - 1, n_L\}$ ,  $\alpha_G = \{n_L + 1, n_L + 2, \dots, n - 1, n\}$ , where  $n_L$  is the number of load buses.

With a multi-node system,

$$I_{bus} = Y_{bus} \times V_{bus} \quad (3.1)$$

By arranging the load buses  $\alpha_L$  and generator buses  $\alpha_G$  as mentioned earlier, equation (3.1) can be written as

$$\begin{bmatrix} I_L \\ I_G \end{bmatrix} = \begin{bmatrix} Y_1 & Y_2 \\ Y_3 & Y_4 \end{bmatrix} \begin{bmatrix} V_L \\ V_G \end{bmatrix} \quad (3.2)$$

$$\begin{bmatrix} V_L \\ I_G \end{bmatrix} = H \begin{bmatrix} I_L \\ V_G \end{bmatrix} = \begin{bmatrix} Z_{LL} & F_{LG} \\ K_{GL} & Y_{GG} \end{bmatrix} \begin{bmatrix} I_L \\ V_G \end{bmatrix} \quad (3.3)$$

where  $Z_{LL}$ ,  $F_{LG}$ ,  $K_{GL}$  and  $Y_{GG}$  are sub-blocks of matrix  $H$ ;  $V_G$ ,  $I_G$ ,  $V_L$ ,  $I_L$  are voltage and current vector of generator and load buses respectively. For any load bus  $j \in \alpha_L$  stability index  $L_j$  can be expressed as

$$L_j = \left| \frac{S_j^+}{Y_{jj}^{+*} \cdot V_j^2} \right| \quad (3.4)$$

$$S_j^+ = \left( \sum_{k \in \alpha_L} \frac{Z_{jk}^*}{Z_{jj}^*} \cdot \frac{S_k}{V_k} \right) V_j \quad (3.5)$$

where  $S_k$  and  $V_k$  are complex power and complex voltage respectively of node  $k$ . The range of value is  $[0, 1]$ . Stability requires that  $L_j < 1$  and must not be violated on a continuous basis. A global system indicator  $L$  describes the stability of the complete system is  $L = \max(L_j)$ . When  $L$  approaches 1.0, the power system will approach voltage collapse. In practice  $L$  must be lower than a threshold value. The predetermined threshold value is specified at the planning stage depending on the system configuration and utility policy regarding quality of service.

#### 4.5. Impact of load model on voltage stability indices

The actual load below the sub-transmission level consists of a large variety of components like thermostatic, resistive and inductive loads, induction motors and lighting loads. Furthermore, the number and type of loads varies continuously through time as different load components are switched on or off in response to residential, commercial and industrial activities. The influence of load modelling on different voltage stability indices has been worked out in a few studies and it has been shown that with an increasing percentage of constant impedance load, indices related to P-V nose curves fail to measure the strength of nodes under a stressed condition [152], [153]. In this work, the impact of load uncertainties on reactive power margin as a voltage stability index was comprehensively examined. Reactive power margins of load buses have been calculated for a primary distribution system to measure the strength of each bus with different compositions of load. Results found in this study prove reactive power margin is a suitable index to identify the weakest bus irrespective of load pattern. Details of this work have been published in [154].

#### 4.6. Static load model

Most of the power system loads are connected to low or medium voltage distribution systems. In a transmission system, voltages are generally regulated by various control devices at the load/generator nodes. Therefore, in load flow calculations, loads can be represented by using constant power load models. In distribution systems however, voltages differ widely along system feeders due to non-availability of reactive power control devices. So in load flow studies of distribution systems, V-I characteristics play a very crucial role [155]. Load models are divided into two wide categories: static and dynamic. In load flow studies, static load models are used. They are typically classified as constant impedance, models constant current models and constant power load models. In general, a static load model is expressed by the following exponential equations:

$$P = P_0 \left( \frac{V}{V_0} \right)^{np} \quad (3.6)$$

$$Q = Q_0 \left( \frac{V}{V_0} \right)^{nq} \quad (3.7)$$

where  $P_0$  and  $Q_0$  stand for real and reactive power consumed at a reference voltage  $V_0$ . The exponents  $np$  and  $nq$  depend on the load type. Table 1 shows typical values of  $np$  and  $nq$  used in power system analysis/studies [144], [21]. Along with the exponential type as explained above, load can also be represented as polynomial load.

Table 1: Sample of load exponents

Load	$np$	$nq$
Fluorescent lighting	1	3
Resistance space heater	2	0
Room air conditioner	0.5	2.50
Incandescent lamp	1.54	0
Small industrial motors	0.1	0.6
Large industrial motors	0.05	0.5

#### 4.7. Test system and load composition

A 16-bus distribution system (see Figure 13) is used in this study. The system shown in Fig. 13 consists of a total load of 28.7MW and 17.3MVar respectively. The original system with three-feeder given in [156] is modified to a single feeder radial system with the same amount of base case load. All the results presented in this work were simulated with DigSilent PowerFactory 14.0 [157], power system simulators for engineers (PSSE), a commercial tool and have also been verified using the research analytical tool PSAT [158] and routines written in MATLAB. A wide variation of load composition is simulated through different sets of load models, which include both extreme and some intermediate conditions. In this work, three types of extreme load models have been considered along with three intermediate combinations represented by ZIP load model.

Figure 13: Single line diagram of 16-bus test distribution system.

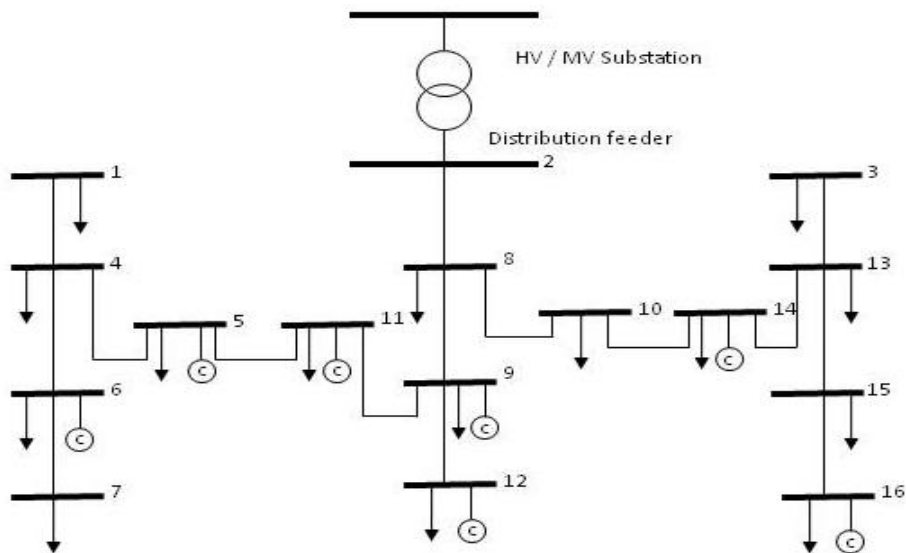


Table 2: Random load composition

Case	ZIP composition of loads		
	Z(%)	I(%)	P(%)
Extreme P	0	0	100
Extreme I	0	100	0
Extreme Z	100	0	0
Combination 1	0	50	50
Combination 2	30	20	50
Combination 3	80	20	0

Table 3: Typical load composition [3]

Load Class	Load composition (%)		
	<i>Residential</i>	<i>Commercial</i>	<i>Industrial</i>
Resistive	25	14	5
Small Motor	75	51	20
Large Motor	0	0	56
Discharge Lighting	0	35	19

This study then investigates practical scenarios. It is unlikely that a utility can easily divide customer loads directly into load components as mentioned in Table 1. Rather than doing that, utilities break their loads into three compositions with the presence of different percentages of loads. The breakdown typically used by utilities is shown in Table 3 [159]. Here, motors with power ratings greater than 100hp have been treated as large motors, which are principal loads in an industrial feeder. Residential and commercial loads are dominated by small motors representing air conditioners and water pumps. Fluorescent lighting comprises 35% of commercial feeders, whereas incandescent lights are the major illumination loads for residential feeders.

Along with reactive power margin ( $Q_{margin}$  in MVar) [144], voltage sensitivity factor (V p.u. / MW) [160] and L-index [151] have also been measured to show the comparison in their performance with load-type variation. Table 4 presents measured stability indices for three extreme types of loads. Table 5 shows the measured indices for three intermediate combinations with different proportions of loads as mentioned in Table 3. From the tabulated results, the lowest value of  $Q_{margin}$  and the highest value of VSF and L-index establish Bus 7 as the weakest bus. For example, for constant power load models the lowest  $Q_{margin}$  22.94, MVar was found with Bus 7, which establishes it as the weakest bus. This finding is in complete agreement with the VSF and L-index which have the highest values at 0.53 and 0.22 respectively, proving that Bus 7 is the weakest bus. VSF is found to be equally sensitive as the reactive power margin while L-index is less sensitive in identifying a weak bus. However, for a constant impedance load, VSF and L-index fail to provide any information on the strength of a bus because of the failure of convergence [152].

Table 4: Weak bus detection for extreme load types

Rank	Bus No	Constant power			Constant current			Constant impedance		
		$Q_{margin}$ (MVar)	VS	L-index	$Q_{margin}$ (MVar)	VSF	L-index	$Q_{margin}$ (MVar)	VS	L-index
1	Bu	22.94	0.5	0.22	26.36	0.07	0.49	28.25	-	-
2	Bu	24.41	0.5	0.22	28.16	0.06	0.44	30.19	-	-
3	Bu	32.54	0.3	0.19	38.07	0.02	0.28	40.93	-	-

Table 5: Weak bus detection for intermediate load types

Rank	Bus No.	Combination 1			Combination 2			Combination 3		
		$Q_{margin} (MVar)$	VSF	L-index	$Q_{margin} (MVar)$	VSF	L-index	$Q_{margin} (MVar)$	VSF	L-index
1	Bus	24.7	0.51	0.22	25.31	0.93	0.26	27.88	-	-
2	Bus	26.35	0.48	0.22	27	0.87	0.26	29.79	-	-
3	Bus	35.42	0.30	0.19	36.34	0.55	0.20	40.37	-	-

Q-V curve studies of Bus 7, the weakest bus, with three extreme load types, have been shown in Fig. 14. This figure shows that the highest reactive power margin of 28.25MVar occurs with constant Z type load whereas constant P type load offers the lowest reactive power margin i.e. 22.94MVar. With intermediate loads, it was observed that with increasing penetration of Z type load, reactive power margin improves, resulting in an improved stability of the system.

The work was extended to a practical scenario where the system was supplying demand to one of the three usual load compositions: residential, commercial and industrial (data taken from Table 3). Bus 7 was again identified as the weakest bus with the lowest reactive power margin among all the buses, followed by Buses 6 and 4. A comparison of  $Q_{margin}$  for different load compositions is shown in Figure 14.

Figure 14: Q-V curves for extreme types of loads.

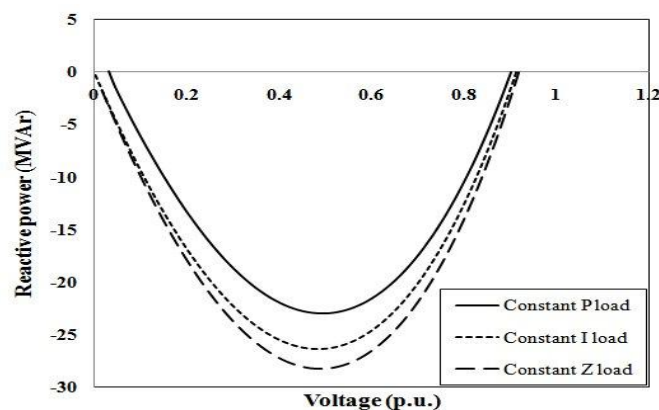
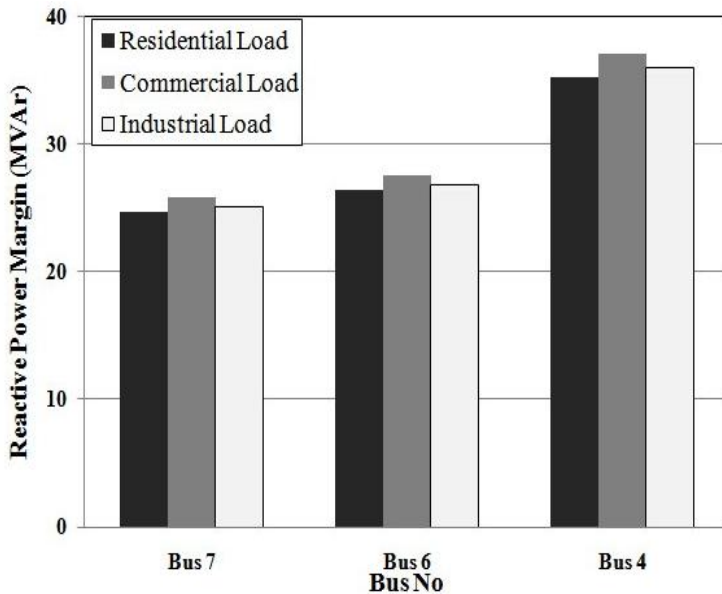


Figure 15: Reactive power margin with typical load composition



It was observed that the same distribution system offered improved stability when treated as a commercial feeder compared to a residential or an industrial feeder. For example, Bus 7 (the weakest bus as per finding) had a  $Q_{margin}$  of 26MVar with a commercial load, which is higher than with a residential or industrial load. This observation is more explicable with a loadability study. The test system offers the highest loadability of 4.3 p.u. with commercial load composition. Residential and industrial load compositions both offer a loadability of 3.5 p.u. From all the measured data it can be seen that constant P type load offers the lowest loadability and reactive power margin among all the compositions taken into account. But whatever the load composition is, the reactive power margin index works as a reliable index in identifying the weakest bus in a system. In our next study, the reactive power margin was utilised as an index along with the voltage sensitivity factor to find out bus strength. This study recommends proper placement of DG in a distribution system to ensure improved loadability.

#### 4.8. Improvement of static voltage stability margin with DG placement

A distributed generator is defined as an electric power source connected to a distribution system with generation from a few kW up to 50MW [4]. There are two control strategies adopted for synchronous machines – voltage regulation and power factor control strategies [161]. At present, distributed generators are not actively taking part in voltage regulation of distribution systems [1].

Power factor control strategies are usually adopted by independent power producers (IPPs) as their target is to maximise active power production [146]. So the second form of control (i.e. power factor control) has been employed in this research, where the controller set point was set to a fixed power factor. A number of static voltage stability indices have already been explored in this research and are presented in detail in section 4. This section aims at finding the best location of DG units, followed by an investigation of the sizing issue for loadability enhancement. The locations of DG units were ranked individually for two different types—Synchronous and Induction generators, with the objective of enhancing loadability and reactive power margins. The size of these machines has then been decided with a dual target of maximising loadability and minimising grid losses. A 16 bus test system (Fig. 13) was used in this study.

#### 4.9. Ranking of bus strength based on voltage stability indices

A ranking of buses in this test system is made using the calculation of the reactive power margin and the VSF of system buses. Figs 3.6 and 3.7 show the reactive power margin and VSF respectively for all the load buses in the 16 bus system. As can be observed from Fig. 3.6, Bus 8 has the highest margin of 150.35 MVar, whereas Bus 7 has the lowest margin of only 22.94 MVar. If we expand the concept of this index it can be argued that when an amount of reactive power equal to the reactive power margin is drawn from that bus by applied load then it may experience voltage collapse. So our study clearly defines Bus 8 as the strongest bus and Bus 7 as the weakest bus.

Figure 17 plots VSF of all load buses near to the point of collapse when the maximum value of loadability or loading point has been reached (here this value is 2.615 times the base load). High sensitivity means even small changes in loading can cause large changes in voltage magnitude. Therefore, high voltage sensitivities are indicative of a weak area in the system. Thus, Bus 7 comes out as the weakest bus while Bus 8 stands out as the strongest bus, even in terms of VSF. After closely examining these two plots together we can make a ranking of buses based on their strengths. Here, Table 6 represents the first four weak buses whereas Table 3 shows the first four strong buses. For example, in Table 6 Bus 7 stands out as the weakest bus with the lowest reactive power margin (22.94MVar) as well as the highest sensitivity factor (0.038161 p.u. voltage/MW). On the other hand, in Table 7 Bus 8 appears as the strongest bus with the highest reactive power margin (150.35 MVar) and the lowest VSF (0.002927 p.u. voltage/MW). Reactive power issues need extra attention while placing DGs on the buses listed in these tables.

Figure 16: Reactive power margin of load buses of the test system

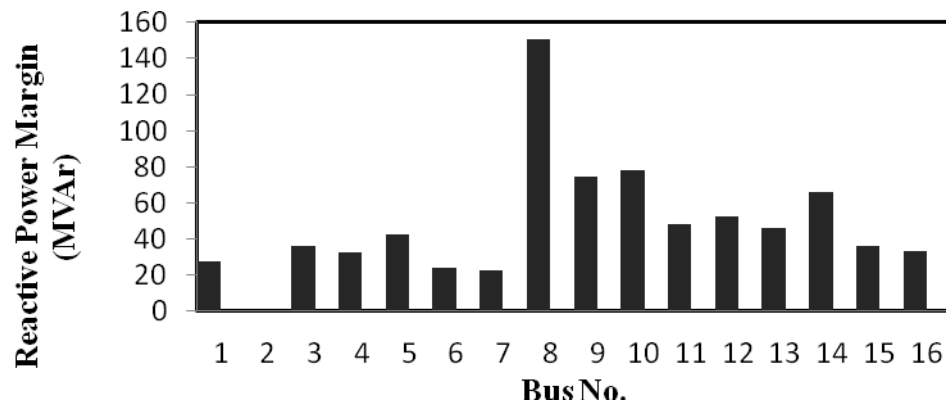


Figure 17: Voltage Sensitivity Factor of load buses of the test system.

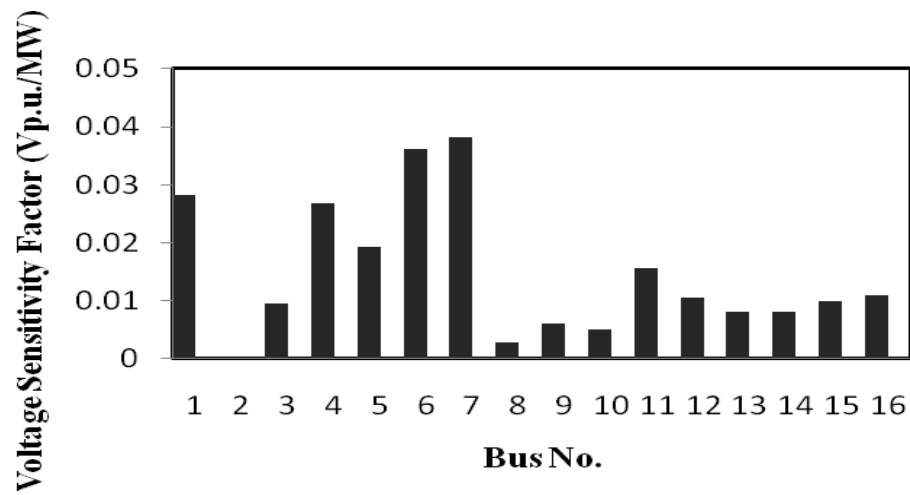


Table 6: Weak Buses

Bus No.	Reactive power Margin (MVar)	VSF (Voltage p.u./MW)
7	22.94	0.038161
6	24.41	0.036145
1	27.78	0.028193
4	32.54	0.026833

Table 7: Strong Buses

Bus No.	Reactive power Margin (MVar)	VSF (Voltage p.u./ MW)
8	150.35	0.002927
10	78.22	0.005134
9	74.34	0.006029
14	65.97	0.008107

### ***Selection of proper location for synchronous and induction generators***

According to results shown in Table 6, the weak buses having low reactive power margins are already operating with a deficiency in reactive power. So if some DG units which consume reactive power are placed on these buses it might cause voltage problems and instability. However, we can use the large reactive margin of strong buses to help these types of DG units. To find the effect of DG units on reactive power margin, induction generators (IG) and synchronous generators (SG) are placed separately on weak areas and the resulting reactive power margins are plotted in Figs. 18 and 19 respectively. Here we have considered the volatility of primary resources (i.e. wind) for IG which was reflected in the plot by taking three different levels of real power injection. These three levels of real power injection have been chosen based on different percentages of DG penetration into the system. The total system load was 28.7 MW – that is, in the order of 30 MW. So we have chosen two different machine sizes – 3 MW (around 10% of total demand), 6 MW (around 20% of total demand) and the base case with no DG (0 MW representing 0% penetration). This study can be extended for increasing penetration of DG based on the

availability of primary resources. To keep consistency in comparison of results we have assumed the same value of real power injection from the SG. As mentioned earlier the synchronous machines used in this study are operated in power factor control mode with a power factor of 0.8.

Figure 18: Change in Reactive Power Margin in weak area with inclusion of IG

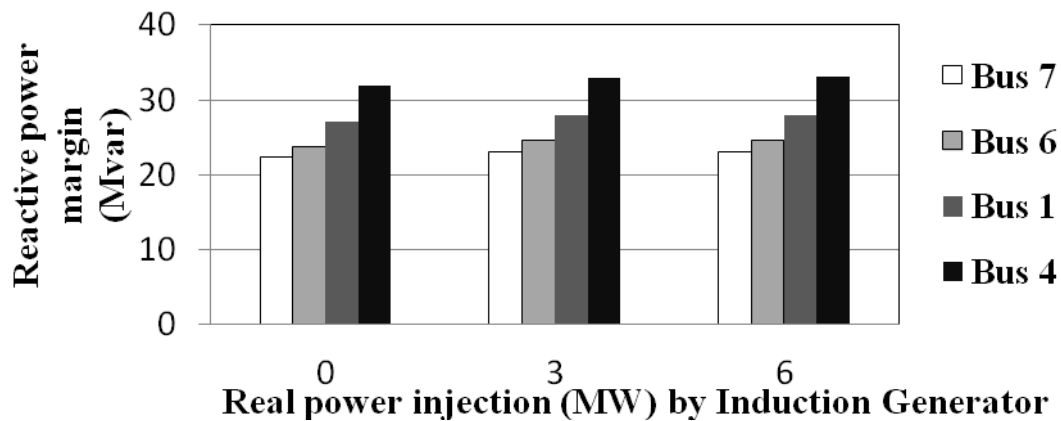
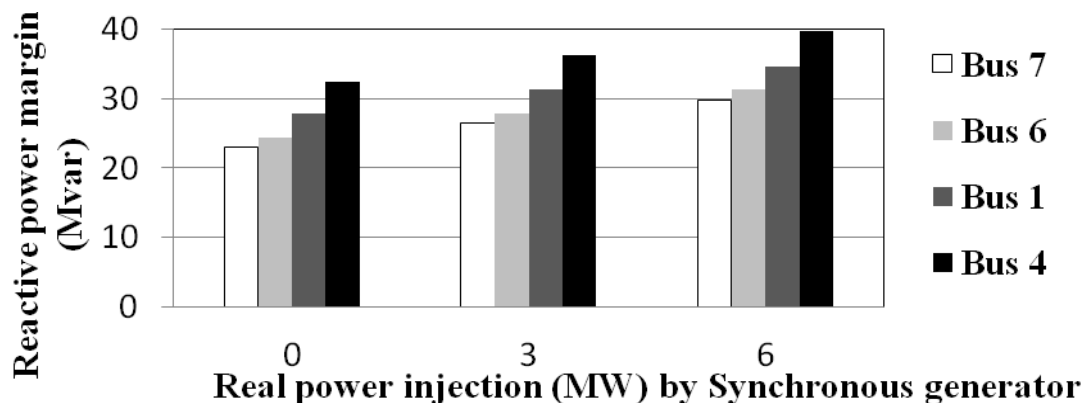


Figure 19: Change in Reactive Power Margin in weak area with inclusion of IG



These two plots clearly demonstrate that the inclusion of IG on the weak buses does not improve the reactive power margin or strength of these buses. For example, the reactive power margin of Bus 7 remains unchanged at around 23 MVAR with the change in real power injection. The same situation exists with other weak buses. But with the inclusion of SG this margin and strength shows great improvement, which is more prominent with higher real power injection by the machines. Here it is observed that the reactive power margin of Bus 7 increases from 22.94 MVAR to 29.74 MVAR with an increase in real power injection by the synchronous generator from 0 MW to 6 MW. So the increase in reactive power margin indicates the growing strength of the weak buses in the

presence of the synchronous generator, a result which is not achievable with an induction generator on weak buses.

System loadability is clearly affected by the inclusion of a DG into the system. The results have been shown for two different types of DG units with increasing sizes: a synchronous generator in Fig. 20 and an induction generator in Fig. 21. With increases of size in SG, loadability improves in every case (greater than the base case loading margin = 2.615 p.u.). But in this study, it was found that the rate of increase of loadability with respect to machine size is higher for the weak buses than for the strong buses. In a real scenario this loadability improvement due to increasing machine size is limited by the thermal limits of the network components.

As the size of the induction machine is increased the loadability decreases for almost every bus except strong buses. The rate of increase of loadability with IG is much lower than with SG and tends to decrease with machine size.

Figure 20: Variation in Loadability with the change of Synchronous machine size

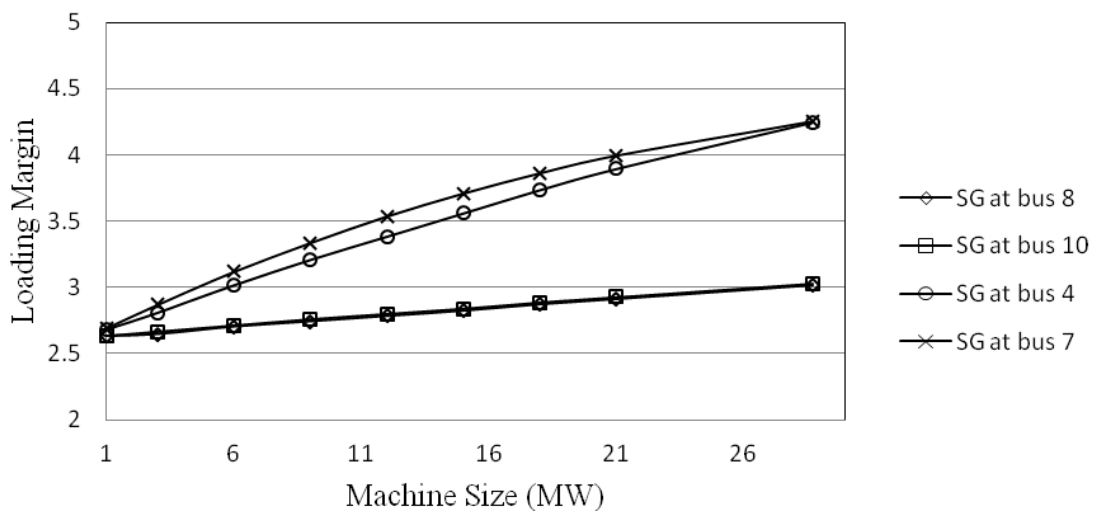
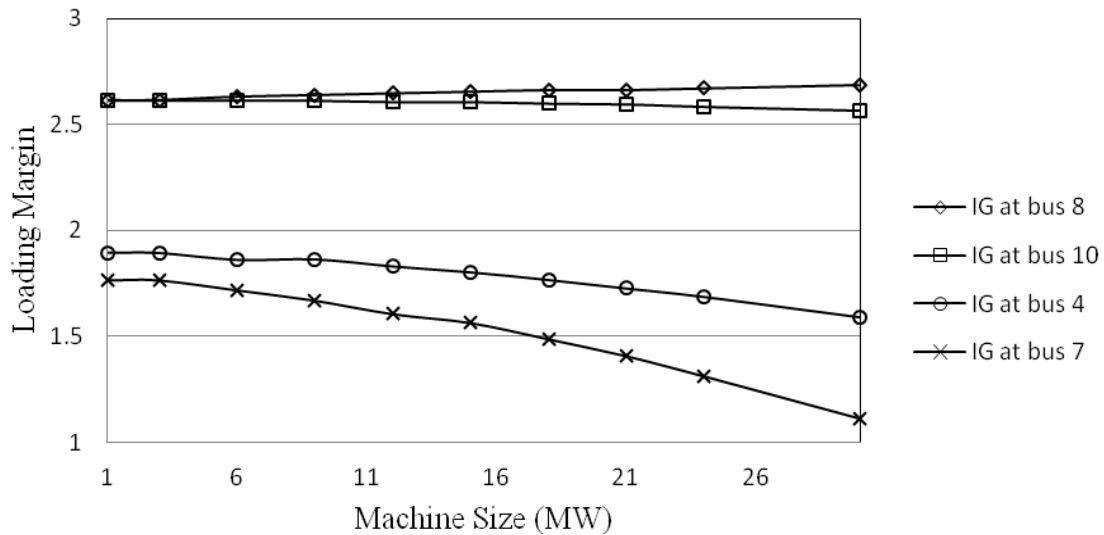


Figure 21: Variation in Loadability with the change of Synchronous machine size



It can be highlighted that in order to enhance the overall loadability and reactive power reserve of the studied distribution system, the synchronous generators need to be placed on weak buses (Buses 7, 6, 1 and 4) and the induction generators need to be placed on strong buses (Buses 8, 10, 9 and 14). The next section will demonstrate the results in the study for the determination of the size of synchronous generators, which will be followed by the induction generator for the 16 bus distribution system.

#### 4.9.1. Determining the size of the synchronous generators

As the synchronous machine loadability keeps on improving with increasing synchronous machine size, its optimal size is determined to minimise grid loss. It is obvious that with the inclusion of DG on a bus, losses in the system start to decrease, but beyond the optimal size the grid losses may increase again and may exceed the base case loss. So the optimal size of synchronous generators should be chosen based on loss minimisation. Figure 3.12 shows the variation of loss with increasing synchronous machine size on Bus 7. However, in practice another important factor that should be considered is that DG is not designed to supply reactive power. Usually, the grid/feeder is designed to supply the amount of reactive power required by system demand from the generator and compensating devices. So when SG units are placed in the system and the total reactive power demand of the system is delivered from that SG, then there will be zero reactive power flow from the remaining grid into the DG connected system. So this is the maximum size of

synchronous machine to be connected on a particular bus in the test system. Based on a number of load flows with increasing size of synchronous machine the optimal sizes for synchronous generators are determined and shown in Table 8 for all the weak buses in the test system. Any SG with a rated value lower/greater than this optimal value will result in a greater amount of real and reactive power loss in the system. With this optimal size, the reactive power intake of the feeder becomes zero as shown in Fig. 22. According to findings shown in Table 8, placement of a synchronous machine of around 10MW on any of the weak buses will reduce the grid loss by more than 50% of the original power loss.

Figure 22: Change in Grid losses and Reactive power intake with Synchronous machine size

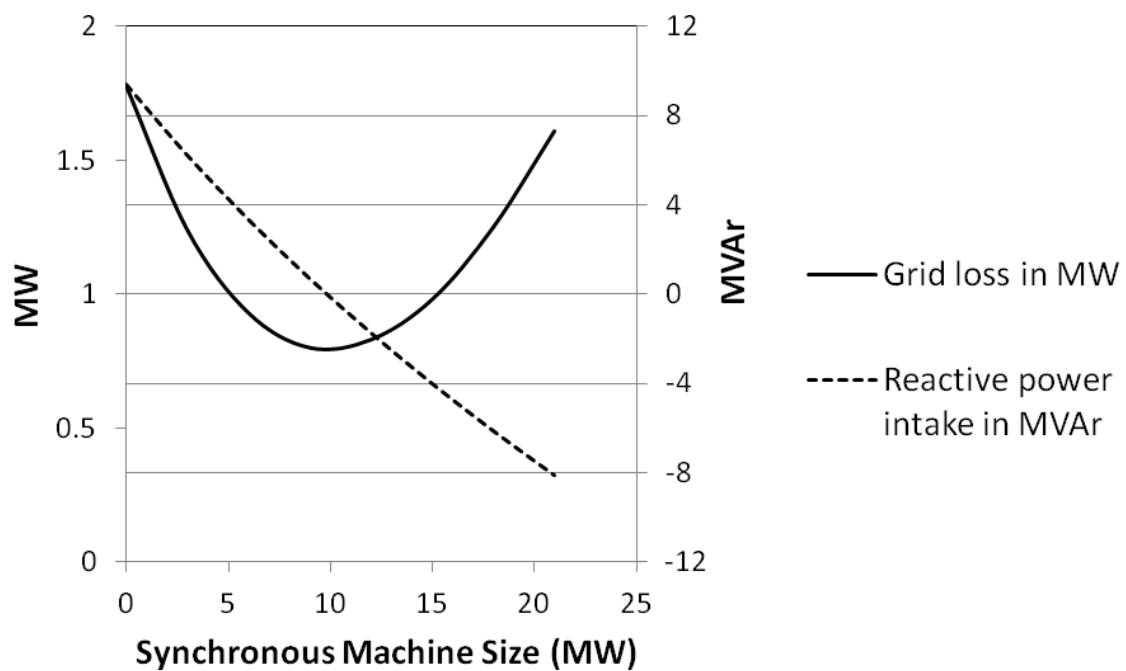


Table 8: Optimal Size of Synchronous Generator

Bus No.	Machine Size(MW) with p.f.=0.8	Grid loss (MW)		Grid loss (MVar)		$\lambda$ (p.u.)
		Without SG	With SG	Without SG	With SG	
7	9.81	1.78	0.80	1.95	0.93	3.39
6	9.76	1.78	0.76	1.95	0.89	3.38
1	9.86	1.78	0.81	1.95	0.91	3.22
4	9.68	1.78	0.70	1.95	0.77	3.23

#### 4.10. Determining the size of induction generators

With the placement of an induction generator the loadability of the system starts to decrease after a certain machine size as shown in Fig 23. So the optimal size would be that size of induction generator which corresponds to maximum loadability. The inclusion of an induction machine in the distribution system usually results in a greater amount of grid loss as mentioned earlier and this amount of loss is always more than with a SG in the system. Also, the reactive power consumption through the grid tends to increase with increasing machine size. Figure 23 shows the change in MW loss and reactive power intake in the system with the increase of induction machine size (rated mechanical power) placed on Bus 14. However, on any particular bus it is possible to keep grid loss to less than the base case so long as the induction machine is not larger than the optimal size. As a result these two issues of loadability and grid loss are combined to decide the optimal size of the induction generator. With the primary objective being to maximise loadability, the grid loss is calculated with increasing machine sizes. The optimal/maximum size as shown in Table 9 represents the machine for specified buses, which offers maximum loadability with grid loss lower than the base case.

It is interesting to note that the optimal size of induction generator at Bus 8, which is the strongest bus in the system, turns out to be 21MW though the system demand is around 30MW. However, in other locations the optimal sizes are in the range of 2.2MW up to 9MW which is around 30% of the total demand.

Figure 23: Change in Grid losses and reactive power intake with Induction machine size

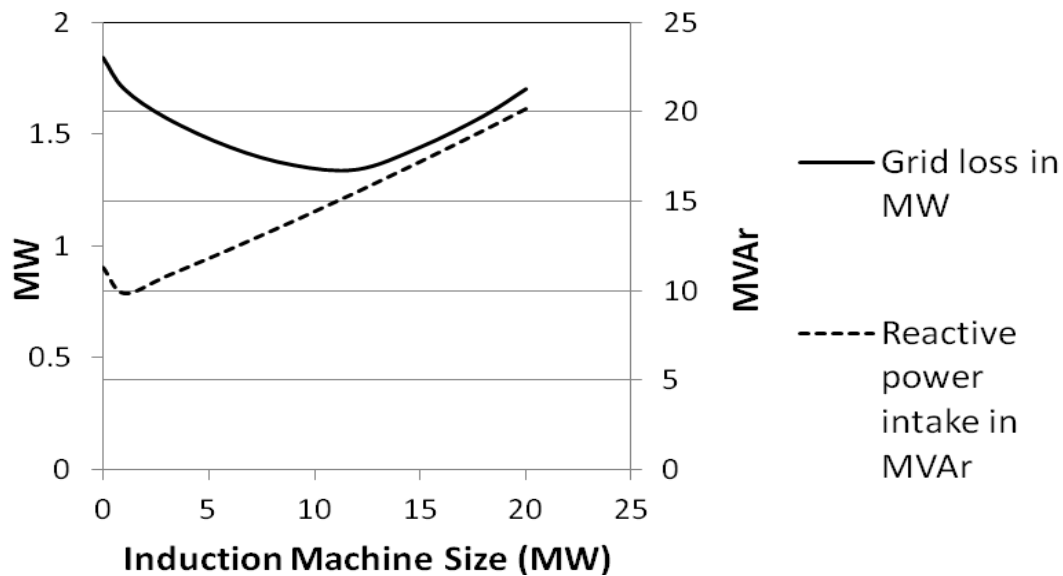


Table 9: Optimal Size of Induction Generator

Bus No.	Machine Size (MW)	Grid Loss (MW)		Grid Loss (MVar)		$\lambda$ (p.u.)
		With out IG	With IG	Without IG	With IG	
8	21	1.78	1.14	1.95	1.30	2.66
10	9	1.78	1.36	1.95	1.53	2.61
9	7.5	1.78	1.23	1.95	1.34	2.34
14	2.2	1.78	1.62	1.95	1.79	2.58

With an IG connected to the system, if the volatile primary resource (e.g. wind) becomes zero then the real power injection turns to zero. But the reactive power consumption is still there, which creates a grid loss greater than the base case. To keep the loss always lower than the base case loss we need to provide reactive power compensators on buses with IG in order to deal with the worst possible case. The minimum values of compensation which will result in a loss closest to the base case loss have been worked out and shown in Table 10. For example, placing a capacitor with a minimum value of 1.6MVar at Bus 9 (with the specified size of 7.5MW induction machine)

results in a grid loss of 1.78MW at zero real power injection. This loss equals the amount of loss found with 0% penetration of DG in the system. This will be further studied in the last section of the report with an optimisation tool.

Table 10: Minimum Size of Compensator

Bus No.	Induction Machine Size (MW)	Grid Loss (MW)		Compensator size (MVar)
		With out IG	With IG (Real power injection =0)	
8	21	1.78	1.78	3
10	9	1.78	1.78	1.9
9	7.5	1.78	1.78	1.6
14	2.2	1.78	1.78	0.5

### Case study: combined effect on system parameters

Depending on the available resources, there might be various types of DG units available in the same distribution system. So this part of the study investigates the combined effect of various DG units on the overall system loadability. Table 11 shows the voltage profile on the buses connected to different DG units. Here the synchronous and induction generators with different sizes have been connected to weak Bus 6 and strong Bus 10 respectively, as proposed in the earlier part of this study. Here 10% (3MW) and 20% (6MW) inclusion of DG real power was considered. Table 12 includes a photovoltaic plant of 1MW at Bus 7, which operates with a unity power factor and it goes through the same sets of combinations to get the voltage profile and system loadability.

Table 11: Combined Effect on voltage profile and LOADING margin by SG AND IG

<u>IG Size (MW) at Bus 10</u>	<u>SG Size (MW) at Bus 6 with pf = 0.8</u>	<u>PV Plant Size (MW) with pf=1.0</u>	<u>Loading margin (p.u.)</u>	<u>Voltage at Bus 10 (p.u.)</u>	<u>Voltage at Bus 6 (p.u.)</u>	<u>Voltage at Bus 7 (p.u.)</u>
0	0	0	2.615	0.948	0.902	0.901
0	3	0	2.855	0.955	0.938	0.937
3	0	0	2.615	0.951	0.904	0.903
3	3	0	2.791	0.959	0.940	0.939

0	6	0	3.094	0.962	0.972	0.970
6	0	0	2.615	0.954	0.906	0.905

Table 12: Combined EFFECTS on voltage profile and loading margin by SG, IG and PV Panel

<b>IG Size (MW) at Bus 10</b>	<b>SG Size (MW) at Bus 6 with pf = 0.8</b>	<b>PV Plant Size (MW) with pf=1.0</b>	<b>Loading margin (p.u.)</b>	<b>Voltage at Bus 10 (p.u.)</b>	<b>Voltage at Bus 6 (p.u.)</b>	<b>Voltage at Bus 7 (p.u.)</b>
0	0	1	2.663	0.949	0.909	0.908
0	3	1	2.919	0.957	0.944	0.944
3	0	1	2.662	0.953	0.911	0.91
3	3	1	2.831	0.96	0.946	0.945
0	6	1	3.159	0.964	0.977	0.976
6	0	1	2.655	0.956	0.913	0.912

From the results in Table 11, it can be concluded that with an increasing size of SG machine, both the loadability and voltage profiles improve significantly. The presence of both types of generators with 20% real power injection results in a loading margin of 2.791 p.u. which is obviously greater than the base case with no DG (2.615 p.u.). However, Table 12 shows that the inclusion of PV panels at Bus 7 results in increasing loadability with an increasing size of IG machine, which was almost fixed before the connection of the PV panels to the system. For example, from Table 11 it was found that a 6 MW IG on Bus 10 results in a loading margin of 2.615 p.u., whereas, if a PV panel of 1MW is present at Bus 7, the loading margin goes up to 2.665 p.u. Results from this study show that for the enhancement of the static voltage stability margin, SG needs to be placed at a weak bus and IG needs to be placed at a bus near to a substation which is strong enough to support reactive power requirement by IG. In recent years grid requirements and standards have been developed to shape the conventional control strategies and maintain static as well as dynamic voltage stability throughout a DG integrated system. The technical regulations or specific standards define the allowed voltage range that bounds the maximum permitted variation of every bus bar voltage under both transient and steady state conditions. Augmentation of both static and dynamic stability is examined in the next section considering current grid requirements.

#### 4.11. Enhancement of static and dynamic voltage stability in view of present grid standard

The post-fault voltage recovery time at the DG bus is the crucial part of available standards as it requests DG to trip, if recovery time exceeds a certain limit [106], [43]. It is well known that the voltage control issue in a power system has a strong correlation with reactive power compensation. Both static and dynamic compensators play an important role in voltage stability. Optimum allocation of static compensators (such as capacitor banks) considering location and size is one of the most important components of reactive power planning [78]. On the other hand, the SVC and STATCOM have inbuilt potential to offer both dynamic reactive power compensation for transient voltage stability improvement as well as steady state voltage regulation. For example, in a wind turbine integrated system, dynamic reactive power compensation is provided by a STATCOM or SVC located at the point of wind turbine connection [79], [80]. With a voltage source converter (VSC), STATCOM has the least delay associated with thyristor firing resulting in faster operation compared to an SVC [81]. However, these studies emphasize only the role of SVC and STATCOM in improving the voltage profile of DG bus.

In a few studies, On Load Tap Changing Transformers (OLTCs) and the reactive power generation capability of DG units have been utilised to maintain the voltage profile at a point of common coupling under all operating conditions [88], [89], [83], [84], [90]. These approaches allow plant operators to make large renewable energy-based power plants grid-code compliant. This issue takes on a new dimension when the penetration level of small-scale independent power producers in an area tends to increase. Due to the rapid growth of interest and investment in renewable energy, a widespread integration of small DG units is expected in coming years. With increased penetration of DG units, early tripping of DG due to local disturbance can further risk the stability of the whole system. Grid standards have addressed this issue by requesting distributed generators below a certain size to operate in constant power factor control mode [107]. Hence, the system operator becomes responsible for maintaining the voltage profile within an acceptable range at all nodes under all operating conditions. As a result, a fault-tolerant control algorithm is required for a DG integrated system, which improves the voltage recovery time to avoid tripping of small-scale DG units and also maintains acceptable voltage at all buses under all operating conditions. In this study, a methodology compatible with IEEE Std. 1547-2003 was used to control voltage and reactive power of the distribution test system, where a mixture of static as well as dynamic compensators was considered.

A sensitivity-based approach was used to decide and limit the location of high-cost dynamic compensator devices such as STATCOM. This unified approach not only reduces the loss but also ensures faster recovery time and thus improves uptime of DG. The effectiveness of the methodology is demonstrated on two distribution systems with different network and load configurations. The rest of this chapter is organised as follows: the following section provides a brief introduction to the available grid interconnection requirements for distributed resources by the utility grid, which is then followed by a detailed methodology to achieve an improved voltage profile in pre-fault and post-fault conditions.

## 4.12. Grid interconnection requirements and standards

Grid codes have been specified for wind power plants as well as for other distributed generators under both steady state and dynamic conditions. Normally, the operation requirements for DG units are specified at the point of common coupling. In general, the steady state operation requirements include power factor requirements for the DG units, a steady state voltage operating range, a frequency operating range and voltage quality [90].

### 4.12.1. *Reactive power generation capability*

In order to request increased real power generation in the system, different grid codes around the world have limited the reactive power capability of DG units to a minimum standard. IEEE Std 1547-2003 does not allow DG units to regulate voltage at the point of common coupling actively [107]. According to FERC orders 661 [98], the power factor at the coupling point must remain between 0.95 (leading) and 0.95 (lagging) for large wind parks generating over 20MW. In Australia, distributed generation with a capacity of less than 30MW shall not actively regulate the voltage at a coupling point and the power factor must lie between unity and 0.95, leading to both 100% and 50% real power injections [162].

### 4.12.2. *Steady state voltage; continuous operation range*

The steady state voltage level at each load connection point is one of the most important parameters for the quality of supply. The inclusion of DG has not affected this requirement. In general it is expected that the voltage of the DG bus and the load bus should remain within the range of  $\pm 10\%$  of nominal voltage [162].

### Interconnection system response to abnormal voltage

IEEE std. 1547-2003 states that any DG unit should cease energising the electric power system during abnormal system conditions according to the clearing times shown in **Error! Reference source not found.** 13. A clearing time is the time between the start of an abnormal condition (due to some fault) and the time at which the DG ceases to energise the local area [107]. The clearing time listed is a maximum threshold for DG units with capacities of 30 kW or less. For DG units with generation capacities greater than 30 kW, the listed clearing time is a default value though this can vary with different utility practices. Hence, the clearing time in **Error! Reference source not found.** 13 was taken as the default value for the present study. So DG can only remain connected to the system supplying the demand in pre-fault and post-fault conditions, if the voltage recovery time is less than the tabulated clearing time.

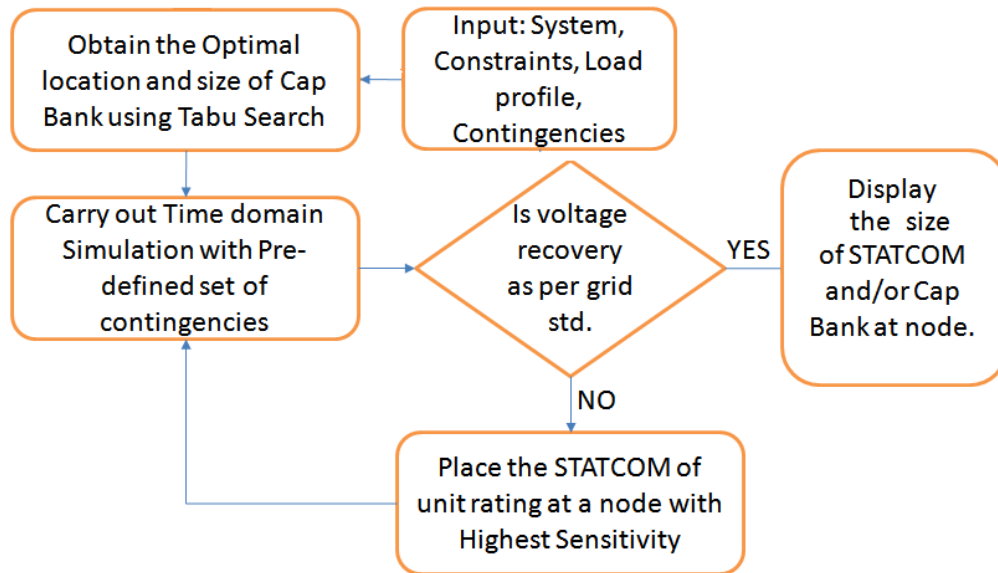
Table 13: Interconnection system response to abnormal voltages [107]

Voltage range (p.u.)	Clearing time (sec)
$V < 0.5$	0.16
$0.5 \leq V < 0.88$	2.00
$1.1 < V < 1.2$	1.00
$V \geq 1.2$	0.16

### 4.13. Methodology

Based on the literature review and existing grid requirements, a step-by-step methodology as shown in the flowchart of Figure 24 is used in this study to support a grid-compatible voltage profile of a DG integrated distribution system. A detail of the solution algorithm is described in section 3.4.3, followed by some other essentials information for implementing the proposed methodology.

Figure 24: Flow chart: determination of type, size and location of reactive power controller



#### 4.13.1. 3.4.3 Solution algorithm

The major steps to be followed to achieve regulated voltage throughout the system for pre-fault as well as post-fault conditions are depicted in **Error! Reference source not found.24**. All of the demand for real power is satisfied by the DG units in the system. This approach converts the test system to a normal interconnected micro grid. The position of the reactive power compensator was chosen with two objectives in mind: minimising grid loss and satisfying reactive power compensation requirements. A steady state voltage requirement (at generator and load terminals) is set as the constraint for the objective function. Static load models need to be considered for this part of the methodology. By changing the loading conditions, an optimal solution can be found which was suitable for both light loads and peak loads. For the present work, a peak load condition derived from a realistic load curve was utilised to determine the optimal location and size of capacitors. Time domain simulation was performed to check the dynamic voltage restoring capability of the generator and load bus when a range of faults were introduced into the system. A dynamic compensator (here STATCOM) is required only if static compensators fail to meet the grid requirement as mentioned above. A new sensitivity index  $dV/dI_R$  along its direction is used to find out the best location among optimal capacitor nodes to replace that capacitor with a STATCOM. After replacing the optimal capacitor by a STATCOM on the bus with the highest sensitivity, voltage recovery time is calculated with time domain simulation for the generator and

load buses. Performance of  $dV/dI_R$  is compared with an existing sensitivity index  $dV/dQ$ . The procedure repeats itself till the voltage excursion of all nodes concerned falls within the required range. Details of this procedure will be explained through simulation results.

#### 4.14. System model

Proper system modelling is required to investigate the feasibility of the proposed methodology. Commonly used power system dynamic equations are utilised in this modelling. For load flow studies and optimal compensation placement, static load models are relevant as they express active and reactive powers as functions of the bus voltages.

#### 4.15. Optimal capacitor placement

The capacitor problem considered in this work is how to determine the location, number and size of the capacitors to be installed in the test system. The objective function of the problem can be expressed to minimise the capacitor investment and system energy loss [163] as:

$$\text{Min} F = \sum_{i=1}^I C_i q_i + K \times \sum_{j=1}^L P_{\text{loss},j} \times T_j \quad (3.8)$$

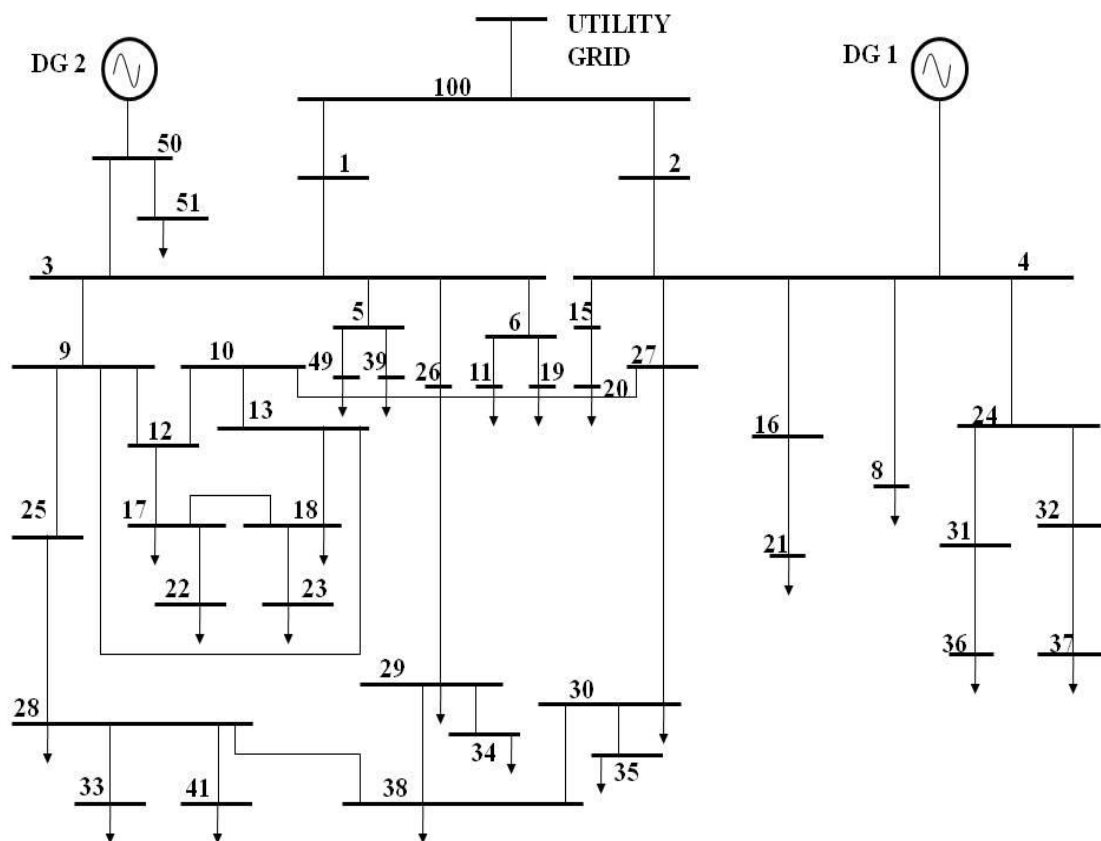
where power flow equations are used as equality constraints and VAR source placement restriction, reactive power generation restriction, transformer tap-setting restriction, bus voltage restriction and the power flow of each branch are used as inequality constraints. In the objective function,  $L$  represents the number of load levels;  $I$  represents the candidate locations for the capacitors;  $q_i$  stands for the set of fixed capacitors for an optimal solution; and  $q_j$  is the control scheme vector at load level  $j$  whose components are discrete variables. Investment cost associated with a capacitor installed at location  $i$  is given by  $C_i q_i$ . Power loss at a load level  $j$  with time duration  $T_j$  is given by  $P_{\text{loss}} \times T_j$  and  $K$  stands for the electricity price. Tabu search, a heuristic optimal search technique, was used as an optimisation tool for finding compensator placement and sizes [164] in the present work. DlgSILENT routine was used for this purpose [157].

#### 4.16. Results and analysis

To test the effectiveness of the proposed methodology, two distribution test systems with different configurations and load compositions were considered in this part of the research. The first distribution system used was a 23 kV radial distribution system with 16 nodes and a single line diagram of this test system is shown in Fig 3.15. An IEEE 43 bus mesh distribution system, with

total real and reactive power loads of 21.76MW and 9MVA<sub>r</sub> respectively, was studied as the second test system [165]. This test system is shown in Figure 25. The system has five different levels of rated voltage at 69 kV, 13.8 kV, 4.16 kV, 2.4 kV and as low as 0.48 kV. This system was treated as an industrial feeder.

Figure 25: Single line diagram of 43 bus test system.



#### 4.16.1. Load composition and load curves

This study considered practical scenarios of load composition as they have profound impacts on the dynamic voltage control of distribution nodes. Utilities divide their loads into various compositions with different percentages of loads. The breakdown typically used by the utilities for commercial and industrial feeders have been shown in **Error! Reference source not found.**<sup>14</sup>. Here, motors with a power rating greater than 100hp have been treated as large motors, which are the principal loads on an industrial feeder. For commercial feeders, on the other hand, 51% of the

load comes from small motors in air conditioners. These breakdowns of loads have been utilised for static load modelling of industrial and commercial feeders.

Table 14: Typical load composition [159]

Load type	Load Composition	
	Commercial Feeder (16 bus system)	Industrial Feeder (43 bus system)
<b>Resistive</b>	14	5
<b>Small Motor</b>	51	20
<b>Large Motor</b>	0	56
<b>Discharge Lighting</b>	35	19

For each type of feeder, the customer load has its typical daily load curve (DLC) set [166].

$P_{avg}/P_{max}$  found from these DLC sets is presented in Table 15: 15 and was used in this work.

Table 15: Peak load data [166]

Load type	Load Composition	
	Commercial Feeder (16 bus system)	Industrial Feeder (43 bus system)
<b><math>P_{avg}/P_{max}</math></b>	0.68	0.61
<b>Peak load (MW)</b>	42.72	28.82

#### 4.16.2. Distributed Generators and their size

The DG units considered in this study are conventional synchronous generators with unity power factor operation. The DG connection details for both systems are shown in

Table 16: at base load conditions. The locations of DG units in the 16 bus system have been chosen randomly at Bus 3 and Bus 6, whereas for the 43 bus system locations are given in the system data.

Table 16: Distributed Generation: capacity and location

Distributed Generation	Commercial Feeder (16 bus system)		Industrial Feeder (43 bus system)	
	DG1	DG2	DG1	DG2
Location bus	3	6	4	50
MVA rating	10	19.58	13	9.75
Power factor	1	1	1	1

#### 4.16.3. Optimal capacitor placement and sensitivity indices

The 'Tabu search' technique was used to determine the location of a fixed compensator in the system at the peak load conditions described in Table 15: 15. The number of candidate buses was chosen to be 50% with an objective function of minimising grid loss using as few of the available capacitor banks as possible. Voltage limits at the generator and the load bus have been set at between 0.90 pu and 1.1 pu according to the steady state voltage operating range in [107].

Table 17 summarises the results for the optimal location of capacitors for the 16 bus system and Table 18 shows the optimal location of capacitors for the 43 bus test system. Both tables contain sensitivity values  $dV/dQ$  and  $dV/dI_R$  at the optimal compensation nodes, which minimises the number of iterations needed to find the best node for dynamic compensation. These values are calculated numerically with small perturbations. For the 16 bus system, even at peak load, bus voltages do not exceed the specified limits. But along with maintaining the voltage limits at nodes, placing capacitors reduces the grid loss significantly. Grid loss was found to fall from 1.20 MW to 0.90 MW with the inclusion of a total 10.2MVar of fixed capacitors at the listed nodes in Table 17. In the 43 bus system, grid loss is reduced to 0.45MW from 0.54 MW with the inclusion of 11.20 MVar of fixed capacitors, which is not very significant. But the voltage profile along all the load buses has recovered to the specified limit.

Table 17: Optimal capacitor solution for the 16 bus system

Optimal Node	Capacitor Size (MVar)	Sensitivity index	
		$dV/dQ$ (Vp.u./MVar)	$dV/dI_R$ (Vp.u./Ip.u.)
7	1.8x2	0.0069	-0.1428 (Inductive)
5	1.8	0.0038	0.0769 (Capacitive)
11	1.8	0.0034	0.0667 (Capacitive)
15	1.8	0.0049	0.1 (Capacitive)
3	1.2	0.0048	0.11 (Capacitive)

Table 18: Optimal capacitor solution for 43 bus system

Optimal Node	Capacitor Size (MVar)	Sensitivity index	
		$dV/dQ$ (Vp.u./MVar)	$dV/dI_R$ (Vp.u./Ip.u.)
49	0.6	0.044	0.20 (Capacitive)
29	0.6	0.046	0.25 (Capacitive)
21	0.6	0.088	0.33 (Capacitive)
51	0.6	0.046	0.2 (Capacitive)
41	0.6	0.048	0.2 (Capacitive)
25	0.6	0.006	0.03 (Capacitive)
30	0.6	0.047	0.25 (Capacitive)
39	1.1	0.044	-0.25 (Inductive)
17	1.1	0.055	0.25 (Capacitive)
35	1.2	0.049	0.2 (Capacitive)
18	1.2	0.048	0.2 (Capacitive)
37	1.2	0.068	0.33 (Capacitive)
33	1.2	0.049	0.25 (Capacitive)

#### 4.17. Voltage recovery and STATCOM placement

According to [106] and [107], the voltage recovery requirement specifies that the DG terminal voltage must come back to 90% of its normal operating voltage within 2 second of a fault taking place. For the verification of the dynamic voltage restoring capability of generator and load buses, portions of the static loads were converted to dynamic motor loads according to proper

percentages (as given in Table 3.14). Then, to check the voltage profile under abnormal conditions, both systems were subjected to a three phase fault (with a fault reactance of  $0.05 \Omega$ ) near the generator bus and the fault was cleared after 12 cycles.

The following test cases were investigated to find out possible solutions for supporting the above requirements:

Case 1: without capacitors

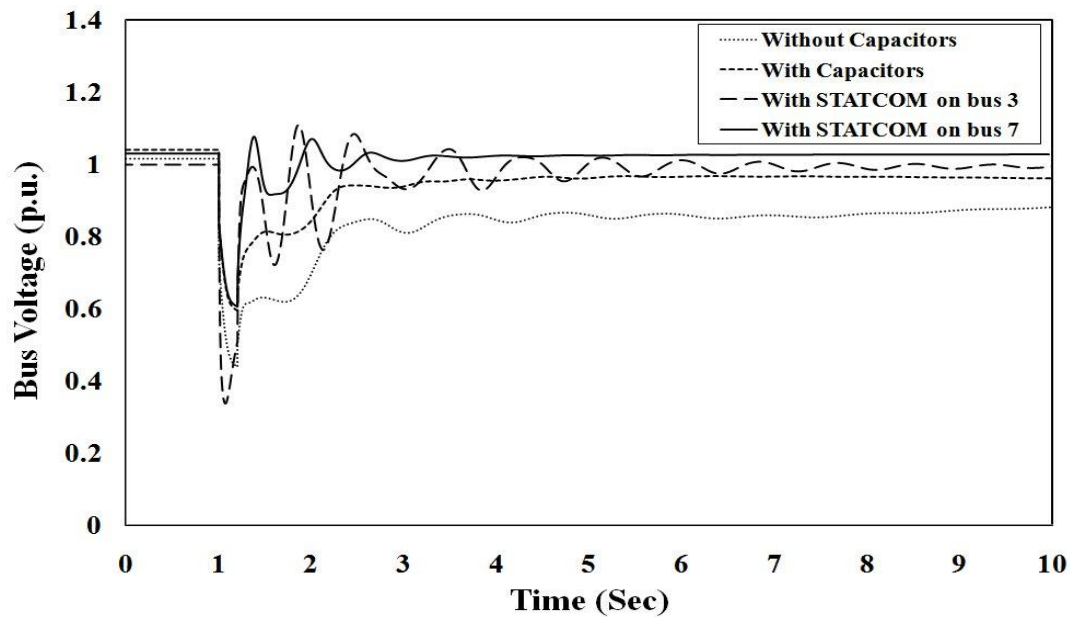
Case 2: with capacitors at optimal locations

Case 3: replacing capacitors with STATCOM at a bus with highest  $dV/dQ$

Case 4: replacing capacitors with STATCOM at a bus with highest  $dV/dI_R$  (for both inductive and capacitive values).

Figs 26 to 28 show the time domain simulation for the 16 bus system at peak load condition. Figs 26 and 27 show excursions in voltage at Buses 3 and 6 respectively with a fault at Bus 5. The load terminal voltage profile was plotted for the faulty Bus 5 in Figure 26. A STATCOM was placed at Bus 7 and then at Bus 3 to find the effect of placement on voltage recovery time and also to investigate the effectiveness of sensitivity indices  $dV/dQ$  and  $dV/dI_R$ . Without capacitors, the system fails to reach the required voltage after a three phase fault takes place. For a generator Bus 3, capacitors at optimal places with optimal sizes help to recover the bus voltage within 1.15sec. A STATCOM at Bus 7 reduces the restoring time significantly to only 0.26sec.

Figure 26: Voltage at Bus 3 for peak load (16 bus system)



It is interesting to see that although Bus 3 is a DG bus, placing a STATCOM on Bus 3 results in a longer recovery time (1.26sec) than when the STATCOM is placed on Bus 7. Table 19: 19 summarises the voltage recovery times for both generator buses of the 16 bus system. As the simulation results for the 16 bus system under peak load conditions do not reflect any problem of slow recovery of voltage on the DG buses, the base case study was not considered.

Figure 27: Voltage at Bus 6 for peak load (16 bus system)

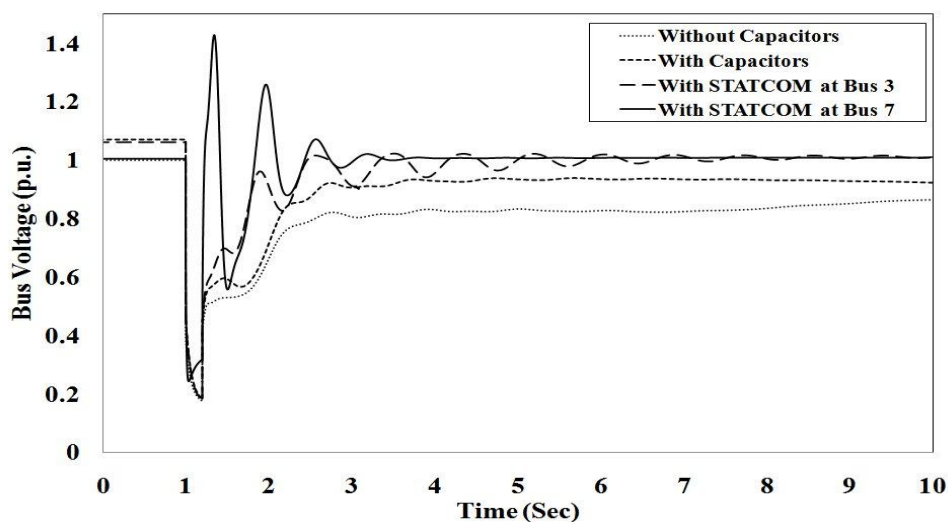


Figure 28: Voltage at Bus 5 for peak load (16 bus system)

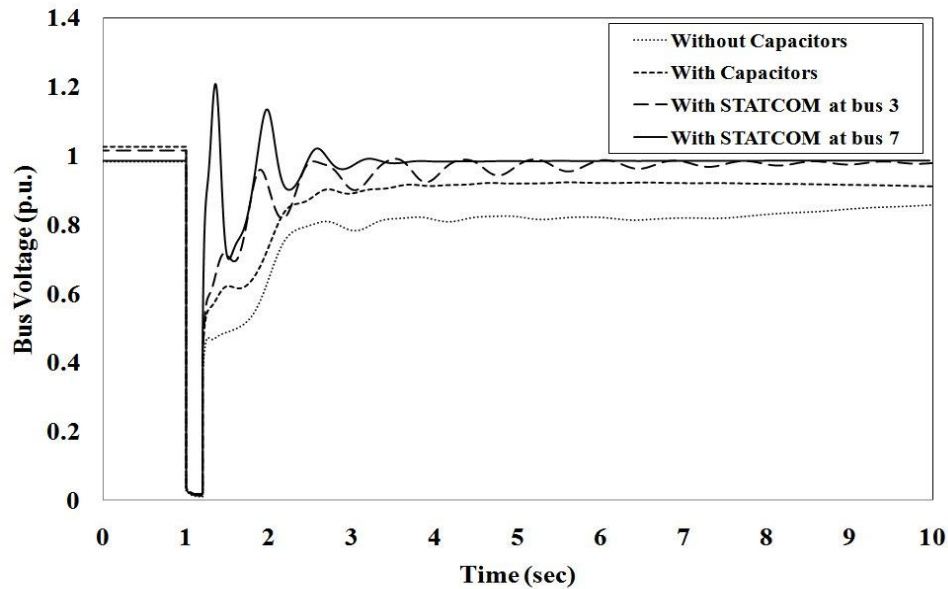


Table 19: Voltage recovery timeS for 16 bus system (peak load)

DG node	Without Capacitors	With Capacitors	With STATCOM at Bus 3	With STATCOM at Bus 7
3 (DG1)	N/A	1.15 Sec	1.26 Sec	0.26 Sec
6 (DG2)	N/A	1.59 Sec	1.97 Sec	1.26 Sec

Time domain simulations for the 43 bus system have been plotted for two cases – base load and peak load. Simulations were carried out for four cases (i) without capacitors, (ii) with capacitors at optimal locations, STATCOMs at with the highest  $dV/dQ$  and (iv) STATCOMS at STATCOM at a bus with the highest  $dV/dI_R$ . **Error! Reference source not found.** 29 and 30 show the simulation results for generator bus voltages with a three phase fault at Bus 31 for the base load condition. Sensitivity indices,  $dV/dQ$  and  $dV/dI_R$  (capacitive), both have their highest value at Bus 21.  $dV/dI_R$  (Inductive) is found only at Bus 39 with a value of 0.25 (Vp.u. /I p.u.) as shown in Table 20.

Figure 29: Voltage at Bus 4 for base load (43 bus system).

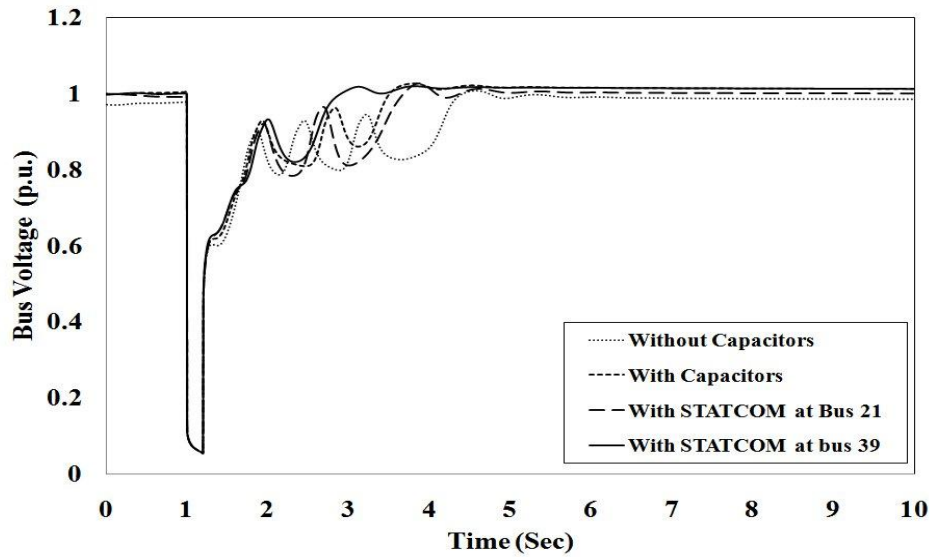


Figure 30: Voltage at Bus 50 for base load (43 bus system).

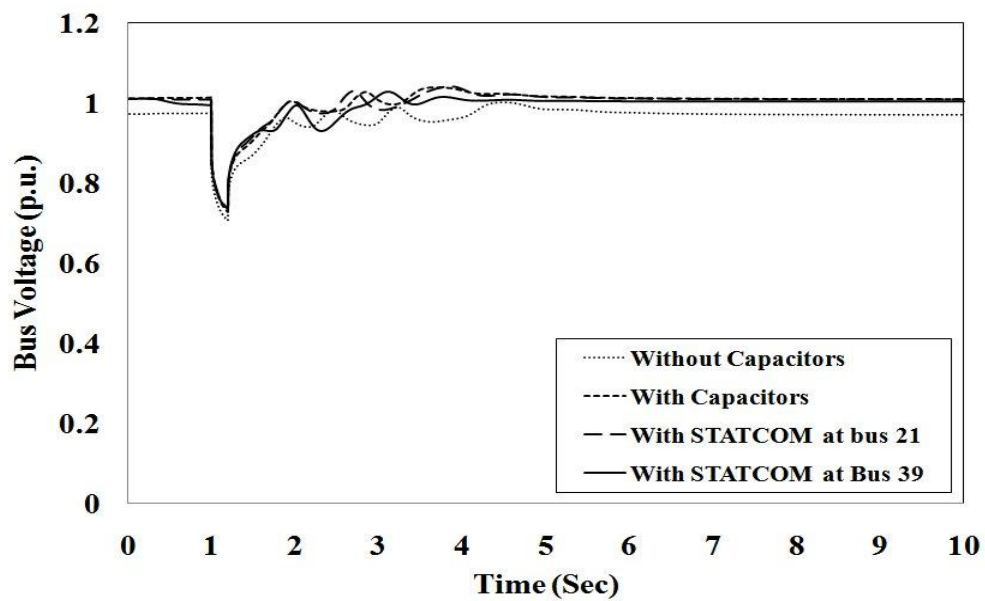


Table 20 summarises the voltage recovery time at base loading, which shows that other than a STATCOM at Bus 39, no controller arrangement could support grid requirements at Bus 4 as they had a recovery time greater than 2sec. For Bus 50, the recovery time was found to be less than

2sec in all arrangements considered. **Error! Reference source not found.** 31 and 32 show the simulation results with a three phase fault at Bus 31 for peak load condition. Table 20 summarises the voltage recovery times at peak load.

Table 20: Voltage recovery time for 43 bus system (base load)

DG node	Without Capacitors	With Capacitors	With STATCOM at Bus 21	With STATCOM at Bus 39
4 (DG1)	3.12 Sec	2.35 Sec	2.49 Sec	1.61 Sec
50 (DG2)	0.71 Sec	0.54 Sec	0.42 Sec	0.37 Sec

Figure 31: Voltage at Bus 4 for peak load (43 bus system).

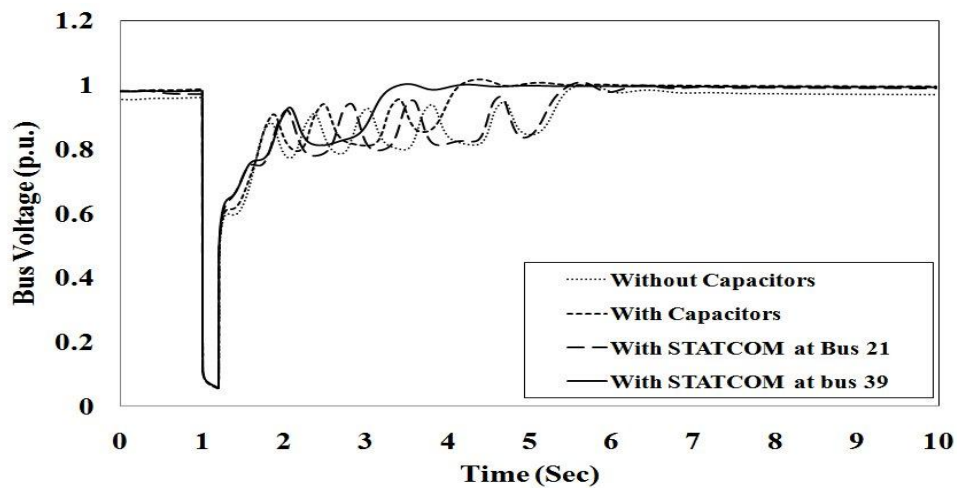


Figure 32: Voltage at Bus 50 for peak load (43 bus system).

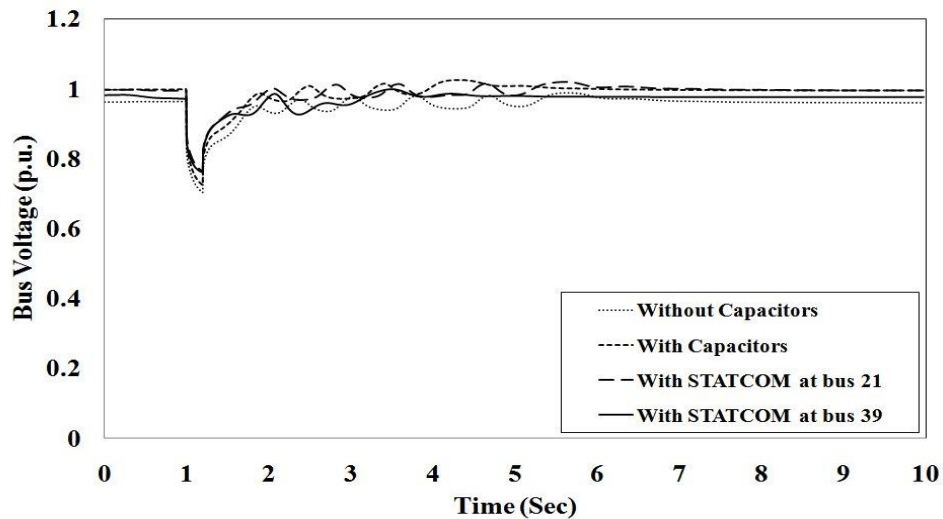


Table 21: Voltage recovery time for 43 bus system(peak load)

DG node	Without Capacitors	With Capacitors	With STATCOM at Bus 21	With STATCOM at Bus 39
4 (DG1)	4.25 Sec	2.94 Sec	4.18 Sec	2.06 Sec
50 (DG2)	0.68 Sec	0.52 Sec	0.36 Sec	0.36 Sec

Table 21 shows that placement of a STATCOM on Bus 39 results in reduced voltage recovery time though it fails to meet grid requirements, establishing the need for an optimal size of STATCOM and proper tuning of control parameters. Analysing the voltage recovery times from all three tables (Tables 19–21), it can be concluded that a STATCOM should be placed at the bus with the highest inductive  $dV/dI_R$  to support the voltage recovery requirements of DG units in the system. This scheme works efficiently as during the post fault recovery, capacitive VAR is required which is made available by a STATCOM. For a small radial system like a 16 bus system it was found that a STATCOM is not even necessary to support voltage recovery, though wrong placement of a STATCOM leads to longer recovery time. But for the 43 bus system with a large mesh configuration, a STATCOM is required at both base and peak loading conditions to enable the voltage recovery occurs within the specified limit.

#### 4.18. Summary of voltage stability study

This section summarises the findings of voltage stability studies of distribution systems with DG units. The studies can be classified into three broad categories as presented above, namely investigations of: (a) the effectiveness of voltage stability indices with various load models, (b) improvement of static voltage stability margin with proper placement of DG units and (c) enhancement of static and dynamic voltage stability considering present grid standards.

##### 4.18.1. Investigation of the effectiveness of voltage stability indices with various load models

Though load models play a significant role in investigating the occurrence of voltage collapse and instability problems, in the development of appropriate load models it is always a challenge to reflect the reality of a power system. So the stability index, which can be used irrespective of load type, is required to identify the weakest bus and take protective measures. In our study, the reactive power margin has been used as a stability index to determine the weakest node in a 16 bus primary distribution system and its performance has been compared with two other widely

used indices, VSF and L-index. Results show that the reactive power margin can be utilised as a reliable index to determine a critical or weak node while considering the influence of load uncertainties. The effectiveness of the reactive power margin index was proved using a modified 16 bus primary distribution system with a varied set of feeders and realistic load models. Identification of weak nodes leads to the optimal reactive power planning that would decide the candidate buses to have new reactive power sources installed.

#### *4.18.2. Improvement of static voltage stability margin with proper placement of DG units*

A methodology was developed based on Q-V curve analysis to determine the optimum location and size of two major classes of DG synchronous and induction generators taking into account the reactive power issues of the system and of these machines. P-V analysis was also carried out to investigate the loadability of the system. The algorithms proposed in this study have the potential to be used for ranking the buses, which leads to the final selection of sites for SG and IG for an overall improvement of reactive power reserve and loadability. It was observed that the placement of a synchronous generator on a weak bus improves the loadability of the system. It is interesting to note that the rate of improvement of loadability for SG on a weak bus is greater than when SG is placed on a strong bus. On the other hand it has been observed that induction generators need to be placed on strong buses in order to enhance loadability. In this study, sequential increases and decreases of SG and IG were investigated to observe their impact on loadability and system loss.

Once the locations were fixed, the sizes of these machines were calculated individually where loadability and grid loss were considered together to achieve an optimal solution. For fixing the synchronous machine size, preference was given to grid loss minimisation as loadability continues to improve with increasing machine size. It was found that at the optimal size of synchronous machines the reactive power intake from the feeder becomes zero.

#### *4.18.3. Enhancement of static and dynamic voltage stability considering present grid standards*

A new sensitivity index-based methodology for placement of shunt reactive power compensators has been developed. This approach helps in placing capacitor banks and STATCOM in a distributed manner to improve the voltage profile at the DG bus and load bus. Results show that dynamic compensation may not be necessary for a small radial distribution system but further investigation is required to generalise this finding. The new sensitivity index  $dV/dI_R$  has been proven to be effective in detecting the appropriate location of STATCOM in the presence of fixed compensation. As a result, small-scale DG units can remain connected to the grid under abnormal conditions, improving their uptime.

## 4.19. Software platform

A DlgSILENT PowerFactory R14.0-based model of a distribution system was constructed for this study. In the static analysis section, results were verified using the MatLab-based research analytical tool PSAT [158]. Following this, PowerFactory core functions were used with required modification and organization of cases.

### 4.19.1. Load Flow Analysis

Calculations of steady state initial conditions for stability simulations or short circuit calculations were carried out through load flow analysis. The calculation of branch loadings, system losses and voltage profiles has been utilised in system studies. Various features (for example: PV and QV curve and load flow sensitivity calculations) have been extensively used for the investigation of stability indices.

### 4.19.2. Optimisation Tools for Distribution Networks

By means of command edit dialogues it is possible to calculate the optimal placement, type and size of capacitors in radial distribution networks, the optimal separation points of meshed networks and the optimal type of reinforcement cables and overhead lines. PowerFactory applies two different optimisation approaches for capacitor placement:

**Gradient Search:** This search is fast and will mostly find a solution that performs well – even if it is not the mathematically exact global optimum.

**Reactive Tabu Search:** This search finds the exact optimum, but may be more time consuming.

In our work, the Reactive Tabu search algorithm was utilised to obtain the optimal location and size of capacitor banks.

### 4.19.3. Models for Stability Analysis

In the majority of cases the standard IEEE definitions for controllers, prime movers and other associated devices and functions are used. For systems and configurations for which no IEEE models exist, such as STATCOM, a composite model with a composite frame has been built to represent the device. The composite models are based on composite frames and are used to combine and interconnect several elements (built-in models) and/or common models. The composite frames enable the reuse of the basic structure of the composite model.

#### 4.19.4. Stability and EMT Simulations

The transient simulation functions available in DIgSILENT PowerFactory are able to analyse the dynamic behaviour of small and large power systems in the time domain. These functions therefore make it possible to model complex systems such as industrial networks and large transmission grids in detail, taking into account electrical and mechanical parameters. The process of performing a transient simulation typically involved the following steps:

- calculation of the initial condition with a load flow calculation
- definition of result variables and/or simulation events where a 2 phase short circuit fault has been considered
- optional definition of result graphs and/or other virtual instruments
- execution of simulation
- creating additional result plots or virtual instruments, or editing existing ones
- changing settings, parameters and repeating calculations.

## 5. SMALL SIGNAL STABILITY ASSESSMENT WITH DG UNITS

Traditional distribution systems are passive systems which only have loads and not generators and they consume power from the substations. With the influx of distributed generating (DG) sources and other power quality enhancing controllers, traditional distribution system are being transformed into active systems where there are possibilities for dynamic interactions. Moreover, as a result of the inclusion of DG units, power flow becomes bidirectional and the intermittent nature of some of the DG units' output power makes the system more vulnerable to collapse due to instability issues. Among dynamic instability issues, small signal instability which could lead to oscillatory instability problems could be considered as the most relevant to a distribution system compared to transient instability where generators lose the ability to remain connected due to a loss of synchronisation.

### 5.1. Methodology

Small signal stability analysis is typically performed with the help of eigenvalue analysis of the linearised model of a power system around the operating point of interest.

#### 5.1.1. Eigenvalue analysis

Consider the DAE model described in chapter 2. When the differential and algebraic equations are linearised around an equilibrium point of interest the following sets of equations (4.1) are obtained.

$$\begin{bmatrix} \Delta \dot{X} \\ 0 \end{bmatrix} = \begin{bmatrix} J_1 & J_2 \\ J_3 & J_4 \end{bmatrix} \begin{bmatrix} \Delta X \\ \Delta Y \end{bmatrix} \quad (4.1)$$

where  $J_1 = \partial f / \partial X|_o$ ,  $J_2 = \partial f / \partial Y|_o$ ,  $J_3 = \partial g / \partial X|_o$ , and  $J_4 = \partial g / \partial Y|_o$ . If  $J_3$  is a non-singular matrix, (4.1) can be reduced to (4.2).

$$\Delta \dot{X} = A_{sys} \Delta X \quad (4.2)$$

where  $A_{sys} = (J_1 - J_2 J_3^{-1} J_4)$  represents the system state matrix of the distribution system with DG units.

In this case, the DAE system is reduced to a set of ordinary differential equation (ODE) equations. The eigenvalues of system state matrix  $A_{sys}$  gives information on “the small signal stability of the distribution system. The complex eigenvalues of  $A_{sys}$  represent the oscillatory modes of the system. If all the eigenvalues have a negative real part, the system, if considered stable, is also

known as asymptotically stable. If at least one of the eigenvalues or a pair of eigenvalues has a positive real part the system is said to be unstable. The real part and imaginary part of the complex eigenvalues give information on the damping and frequency of the oscillatory modes respectively. The low damped and low frequency modes are critical modes, which need to be handled carefully to enhance the small signal stability of the system. Power utilities' practice is to keep the damping ratio of the critical modes at least 5%.

#### 5.1.2. Extended eigenvector

The characteristics of loads are included in the admittance (Y) matrix. Hence, it is important to investigate the relationships between the system critical mode and elements of Y matrix. In this research, the extended eigenvector method has been used to rank the loads based on their relative influence on the critical mode. Using extended eigenvector, the eigenvalue  $\lambda$  can be restated as (4.3) [167].

$$\begin{bmatrix} J_1 & J_2 \\ J_3 & J_4 \end{bmatrix} \begin{bmatrix} v_1 \\ v_2 \end{bmatrix} = \lambda \begin{bmatrix} v_1 \\ 0 \end{bmatrix} \quad (4.3)$$

where  $\begin{bmatrix} v_1 \\ v_2 \end{bmatrix}^T$  is the extended eigenvector of  $\lambda$  and

$$v_2 = -J_4^{-1} J_3 v_1 \quad (4.4)$$

The elements of  $v_2$  correspond to the algebraic variables at each bus, such as voltages and angles or real and imaginary voltages. Hence, a load bus corresponding to the maximum entry of  $v_2$  and critical mode can be ranked as the most influential load to the critical mode. Similarly, a load bus corresponding to the minimum element of  $v_2$  and critical mode can be ranked as the least influential load to the critical mode.

Once the load ranking is done, then the highly ranked loads are modelled by composite loads to investigate their impact on oscillatory stability and dynamic loadability of the distribution system. The dynamic loadability is defined as the closest oscillatory point from the base case loading point for a given load direction [2].

#### 5.1.3. Participation factor

The contributions of different state vectors and hence machines participating on oscillation modes can be identified by evaluating the participation factors (PFs) of each state on a particular mode.

PFs give the relationships between the states and eigenmodes in a dynamic system. The participation of  $k_{th}$  state in the  $i_{th}$  eigenmode is given by:

$$p_{ki} = \phi_{ki} \psi_{ik} \quad (4.5)$$

where:

$\phi_{ki}$  :  $k_{th}$  entry of right eigenvector  $\phi_i$

$\psi_{ik}$  :  $k_{th}$  entry of left eigenvector  $\psi_i$

#### 5.1.4. Eigenvalue sensitivity

The sensitivity of an eigenvalue  $\lambda_i$  to a system parameter  $K_j$  may be defined as

$$\frac{\partial \lambda_i}{\partial K_j} = \frac{\omega_i^T \left( \frac{\partial A}{\partial K_j} \right) v^i}{\omega_i^T v^i} \quad (4.6)$$

where  $\omega_i^T$  and  $v^i$  are the left and right eigenvectors of eigenvalue  $\lambda_i$ . The eigenvalues representing the oscillatory modes can be written as:  $\lambda_i = \alpha_i \pm j\beta_i$ , where  $\alpha_i$  is the real part and  $\beta_i$  is the imaginary part. The real part indicates the damping and the imaginary part indicates the frequency of oscillations.

The distributed generators, whether they are renewable energy-based or not, mostly produce unregulated power. As a result, the distribution system experiences fluctuating power injection into the system, which may have a significant impact on system oscillations. The impact of uncontrolled power fluctuations on system oscillations may be evaluated by eigenvalue sensitivity. In this study, the sensitivity of the real part of the eigenvalue with respect to active power is chosen to be the sensitivity parameter. The sensitivity  $\partial \alpha_i / \partial P$  (where  $P$  is the total active power generated by the distributed generators) can be calculated numerically by performing two eigenvalue calculations with the total generator outputs at  $P$  and at a slightly perturbed value of  $P + \Delta P$  [168, 169], [4].

In a distribution system, active and reactive power loads are continuously changing as a result of consumer action. The changes in active and reactive power loads in the system affect the damping performance on different modes. However, the impact on some oscillatory modes is more significant than others; such modes are identified as critical modes.

The impacts on individual modes may be compared by evaluating the sensitivity of complex eigenvalues with respect to small perturbations in active and reactive power loads of the system. In this paper the sensitivity of the real part with respect to active power load ( $\partial\alpha/\partial P$ ), and reactive power load ( $\partial\alpha/\partial Q$ ), have been proposed as sensitivity parameters to identify the critical mode. The total sensitivity of a critical mode  $\lambda_i = \alpha_i \pm j\beta_i$  with respect to active power load ( $TS_p$ ) and reactive power load ( $TS_Q$ ) may be calculated using (4.7) and (4.8).

$$TS_p = \frac{\partial\alpha_i}{\partial\left(\sum_{j=1,n} P_j\right)} \quad (4.7)$$

$$TS_Q = \frac{\partial\alpha_i}{\partial\left(\sum_{j=1,n} Q_j\right)} \quad (4.8)$$

where  $n$  is the number of load buses in a system. The modes with the highest values of  $TS_p$  and  $TS_Q$  may be selected as critical modes of the system.

#### 5.1.5. Time domain simulation

Eigenvalue analysis results can be corroborated with the non-linear time domain simulation for small disturbances such as a load increase. In the time domain simulation, the behaviour of power system elements and power systems is observed by calculating the state variables using some robust numerical integration techniques.

## 5.2. Simulation results

### 5.2.1. Oscillatory stability assessment

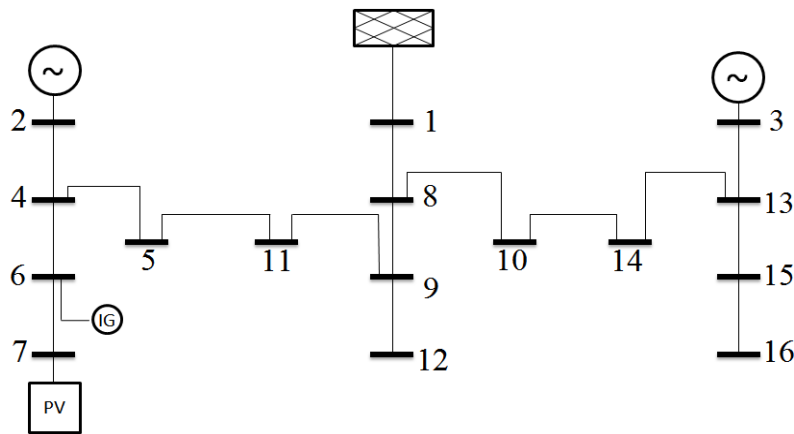
#### Description of distribution system

The configuration of the distribution system which is under study is shown in Fig. 33. It is a modified version of the distribution system presented in [156]. In this system, three radial feeders are connected by tie lines. The total real power load of the system is 28.7 MW and the reactive power load is 17.3 MVAR. The distribution network is modelled by a  $\pi$ -model similar to that of transmission system models.

A synchronous generator operating in voltage control mode is connected at Bus 2, supplying 4 MW. It has a reactive power limit of 3 MVAR. Another synchronous generator operating in power factor control mode is connected at Bus 3, supplying 5 MW at unity power factor. The system is fed

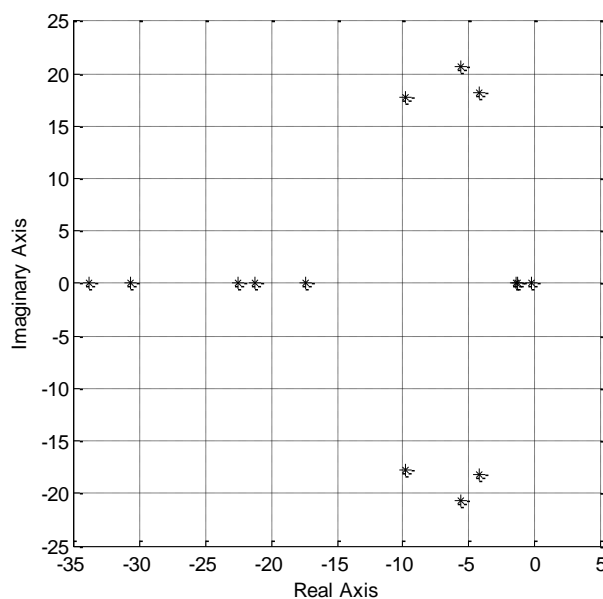
by the grid substation at Bus 1. The grid substation is supposed to supply power at a constant power factor and should not propagate any low frequency oscillations into the distribution system [170]. A 2 MW wind generator is connected at Bus 6 and a 1 MW solar PV generator is connected at Bus 7. The wind generator is compensated for by a shunt capacitor supplying reactive power equal to one-third of the active power generated [146].

Figure 33: Single line diagram of the 16 bus test distribution system



### 5.3. Oscillatory modes observed in distribution system

Figure 34: Eigenvalues of the 16 bus test distribution system.



The system under study has fifteen eigenvalues as shown in Fig. 34. Since all the eigenvalues lie on the left side of the imaginary axis, the system is said to be asymptotically stable. Eigenvalue analysis can be used to determine acceptable renewable energy penetration before the system loses small signal stability. The limiting criteria for penetration could be either the damping ratio or a point of Hopf bifurcation condition which triggers the onset of oscillation and limits the loading. In this system, three pairs of complex low frequency oscillatory modes were observed. They are summarised in Table 22.

Table 22: the oscillatory modes existing in the distribution system

Modes	Real Part (1/s)	Imaginary Part (rad/sec)	Damping Ratio	Frequency (Hz)
1, 2	-5.57	20.64	0.26	3.28
3, 4	-4.23	18.15	0.23	2.89
5, 6	-9.81	17.72	0.48	2.82

It is interesting to note that the oscillatory frequencies of all the modes are around 3 Hz, which is more than the frequency of electromechanical modes of large generators observed in transmission systems, typical values of which are 0.1 to 2 Hz [11]. Some studies with induction generator applications also show similar frequencies of oscillation in distribution systems [171-173]-[11]. Further lower frequency modes are not observed in the present study.

The modes presented in Table 22 are local modes, which are very important for local stability of the generators. However, when a large number of generators is scattered in a large distribution system, this may create some small groups of generators oscillating against each other, creating a problem of inter-area oscillations.

#### 5.4. Participation factor

Table 23 shows the participation factors of state vectors of the distribution system on oscillatory modes. It is observed that the PFs contributed by state 1 and state 14 for Modes 1, 2 and Modes 3, 4 are 0.2 and 0.46 respectively. Similarly, the PFs of state 10 and state 13 for Modes 1, 2 and Modes 3, 4 are 0.48 and 0.19 respectively. So the dominant states for Modes 1, 2 are the rotor angle and speed deviation of the generator at Bus no. 3. The dominant states for Modes 3, 4 are

rotor angle and speed deviation of the generator at Bus no. 2.

The PFs of state 12 and state 15 on Modes 5, 6 are 0.61 and 0.58 respectively. Other states have negligible participation on this mode, so the dominant states for Mode 5, 6 are the induced emf and rotor speed of the induction generator. It may be observed that an induction generator contributes significantly to system oscillation.

In the literature [174],[12] presents similar results for a large power system with induction machine applications. The modes dominated by wind generator states are highly damped as compared to the modes dominated by synchronous generator states. Solar PV generators do not participate in the oscillatory modes.

Table 23: Participation factors of state variables

States	Modes	Modes 3,	Modes 5,
1	<b>0.20</b>	<b>0.46</b>	0.09
2	0.00	0.00	0.00
3	0.05	0.09	0.03
4	0.00	0.01	0.00
5	0.05	0.10	0.03
6	0.00	0.00	0.00
7	0.11	0.03	0.00
8	0.01	0.00	0.00
9	0.12	0.04	0.00
10	<b>0.48</b>	<b>0.19</b>	0.01
11	0.00	0.00	0.01
12	0.00	0.08	<b>0.61</b>
13	<b>0.48</b>	<b>0.19</b>	0.01
14	<b>0.20</b>	<b>0.46</b>	0.09
15	0.00	0.07	<b>0.58</b>

## 5.5. Impact of penetration

With the worldwide concern about environmental issues and legislative changes, more renewable energy resources are likely to be integrated into distribution systems in the future. Many countries have set a target of supplying at least 20% of their load demand from renewable energy within the next 10 years [175]. Based on these facts, the research has investigated three cases for small signal stability analysis.

- Base case: This is the case of the existing scenario.

- 20% wind: The wind power in the system is increased to 6 MW. It is assumed that more wind generators are connected in parallel at Bus 6. Solar PV output is set constant at 1 MW.
- 20% solar: The solar power in the system is increased to 6 MW. Here also it is assumed that more solar PV output is connected in parallel at Bus 7. The wind power is set constant at 2 MW.

An objective of this work is to determine the contribution of different types of generators on different oscillation modes. Participation factor and eigenvalue sensitivity approaches have been chosen for analysis. This will further help to choose the most effective generator to be controlled to suppress unwanted oscillations in the distribution system.

### 5.6. Impact of penetration on mode participations

The participation of the states was evaluated for increased penetration of wind and solar power into the system.

Table 24: Impact of the penetration of renewable resources on participation factors of state variables

States	Modes 1, 2			Modes 3, 4			Modes 5, 6		
	Base Case	20% Wind	20% Solar	Base Case	20% Wind	20% Solar	Base Case	20% Wind	20% Solar
1	0.20	0.16	0.17	0.46	0.68	0.44	0.09	0.64	0.05
2	0.00	0.00	0.00	0.00	0.00	0.00	0.00	0.00	0.00
3	0.05	0.01	0.01	0.09	0.04	0.01	0.03	0.02	0.01
4	0.00	0.01	0.01	0.01	0.02	0.01	0.00	0.02	0.00
5	0.05	0.06	0.07	0.10	0.23	0.13	0.03	0.17	0.02
6	0.00	0.00	0.00	0.00	0.00	0.00	0.00	0.00	0.00
7	0.11	0.11	0.11	0.03	0.05	0.02	0.00	0.03	0.01
8	0.01	0.01	0.01	0.00	0.01	0.00	0.00	0.00	0.00
9	0.12	0.12	0.12	0.04	0.05	0.03	0.00	0.04	0.00
10	0.48	0.48	0.47	0.19	0.23	0.17	0.01	0.20	0.02
11	0.00	0.00	0.00	0.00	0.01	0.00	0.01	0.02	0.01
12	0.00	0.00	0.00	0.08	0.88	0.06	0.61	0.88	0.60
13	0.48	0.48	0.47	0.19	0.23	0.17	0.01	0.20	0.02
14	0.20	0.16	0.17	0.46	0.68	0.44	0.09	0.64	0.05

15	0.00	0.00	0.00	0.07	0.77	0.05	0.58	0.78	0.58
----	------	------	------	------	------	------	------	------	------

Table 24 shows the participation factors for Modes 1, 2, Modes 3, 4 and Modes 5, 6 respectively with increased wind and solar penetration. For Modes 1, 2 the impact of penetration is not significant. However, the penetration has a significant impact on state contributions in Modes 3, 4 and Modes 5, 6.

For Modes 3, 4, the PFs of state 1 and state 14 increased from 0.46 to 0.68. Furthermore, the PFs of state 12 increased significantly from 0.08 to 0.88 and the PFs of state 15 increased significantly from 0.07 to 0.77. The dominant states of Modes 3, 4 changed from state 1 and state 14 to state 12 and state 15.

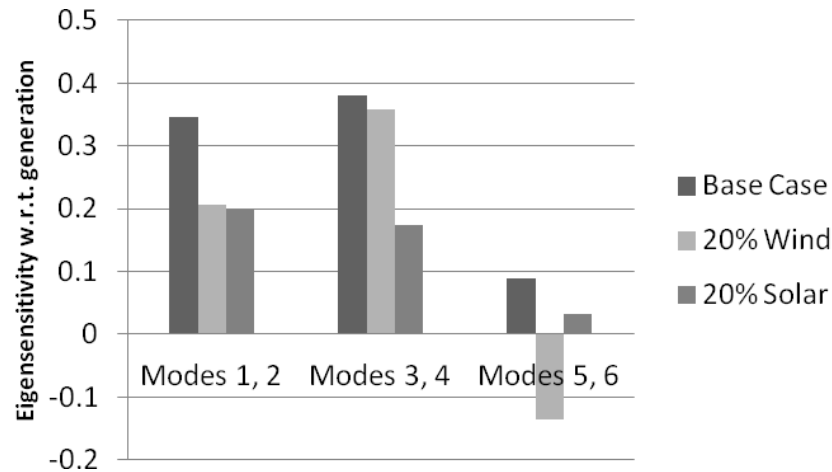
The dominant states of some modes may alter after significant wind penetration. Similarly, the PFs of state 1 and state 14 on Modes 5, 6 increase significantly from 0.09 to 0.64. Apart from these dominant states, the PFs of state 12 and state 15 also increase for corresponding modes after significant wind penetration. So, the increased wind penetration has a significant impact on the dynamics of a distribution system.

Table 24 also indicates that the solar penetration has less impact than wind penetration. The PFs of all the states do not change significantly when solar penetration is increased. The impact of solar PVs on the low frequency electromechanical oscillations should be very low because unlike wind generators, the photovoltaic generators do not have rotating parts. However, the PV controllers may have some impact on system dynamics following significant PV penetration. The effect of controllers has not been presented in this paper and is left for future study.

### 5.7. Impact of penetration on eigenvalue sensitivity

The impact of wind and solar power penetration on system damping has been assessed by evaluating the sensitivity of eigenvalues with respect to small perturbations of generation by DGs. The perturbation parameter used is 0.5%. The results are shown in Fig. 35.

Figure 35: Eigen sensitivities with generation for increased penetration.

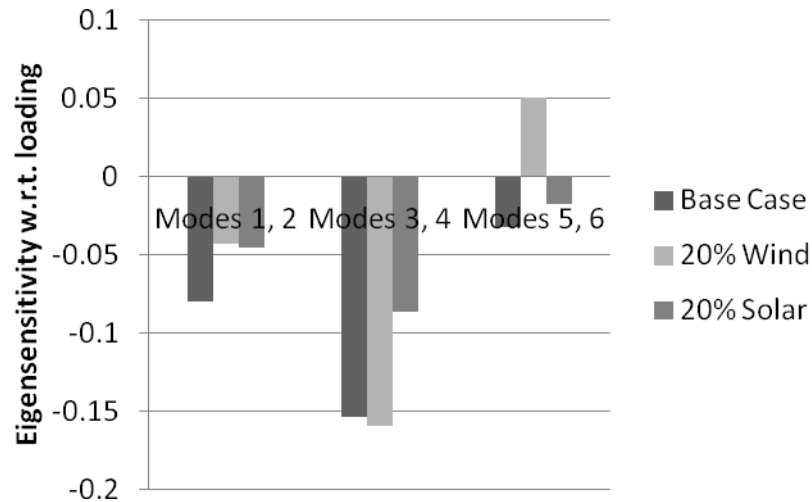


With increased solar penetration, the eigensensitivity of Modes 1, 2 with respect to active power generation decreases from 0.34 to 0.2. Similarly, the eigensensitivity of Modes 3, 4 decrease from 0.38 to 0.17 and that of Modes 5, 6 decreases from 0.09 to 0.03. It may be observed that eigensensitivity of all the modes decreases with an increase of PV penetration. This indicates that the modes become stronger with increased solar penetration.

On the other hand, with increased wind penetration, the eigensensitivity of Modes 1, 2 decreased from 0.34 to 0.2. The eigensensitivity of Modes 3, 4 decreased from 0.38 to 0.35 and that of Modes 5, 6 decreased from 0.08 to -0.13. Therefore, it can be seen that a wind generator can decrease the sensitivity of some modes; they may help in the damping of some modes of oscillations in distribution systems. Also, the eigensensitivity of Modes 5, 6 was changed from a low positive value to a high negative value. This indicates that wind generator dynamics are significant in the oscillations of distribution systems.

As discussed previously, most of the generated power in a renewable energy-based distribution system is unregulated and the eigensensitivity with respect to generated power gives the indication of small signal stability of the distribution system when the injected power is randomly fluctuating with time. In the same way, the loads on a distribution system also change with time. So, the sensitivities of eigenvalues with respect to active power loading were also evaluated. The results are shown in Fig. 36.

Figure 36: Eigen sensitivities with loading for increased penetration.



Similarly, as in the previous case, the penetration of solar PV decreases the magnitude of the eigensensitivity of Modes 1, 2, Modes 3, 4 and Modes 5, 6. So, penetration of solar PV generators makes the system more stable for small signals. This is similar to the observation from Fig. 9. For increased wind penetration, the sensitivities of some modes are decreased while others are increased. The significant changes in sensitivities indicate that the wind generator dynamics are still very prominent.

Figs. 35 and 36 also show that Modes 3, 4 are the most sensitive modes and Modes 5, 6 are the least sensitive modes. So, the oscillatory modes dominated by wind generator states are less sensitive as compared to the modes dominated by synchronous generator states. This indicates that the location of damping controllers should be in the vicinity of synchronous generators in the distribution system.

### 5.8. Time domain analysis

Time domain analysis was performed to visualize the rotor oscillations of synchronous generators under different wind and solar PV penetrations. For this, a three phase short circuit fault was applied at Bus 15 and cleared after 70 ms to trigger the mode. The rotor speeds of the synchronous generators at Buses 2 and 3 were observed.

Fig. 37 shows the rotor speed of the synchronous generator at Bus 2. This generator is operating in voltage control mode. It is observed that the damping of the oscillations is improved as wind and solar penetration is increased. Damping is more pronounced with solar penetration than with wind penetration. This is because the output of the PV generator is constant while the reactive power of a wind generator varies based on the bus voltage and active power generated.

Figure 37: Response of voltage controlled synchronous generator for increased penetration.

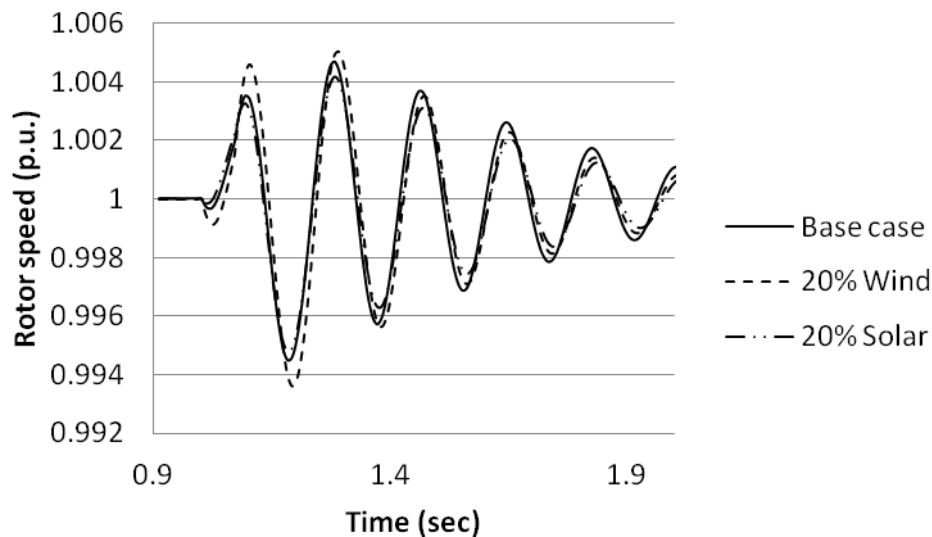
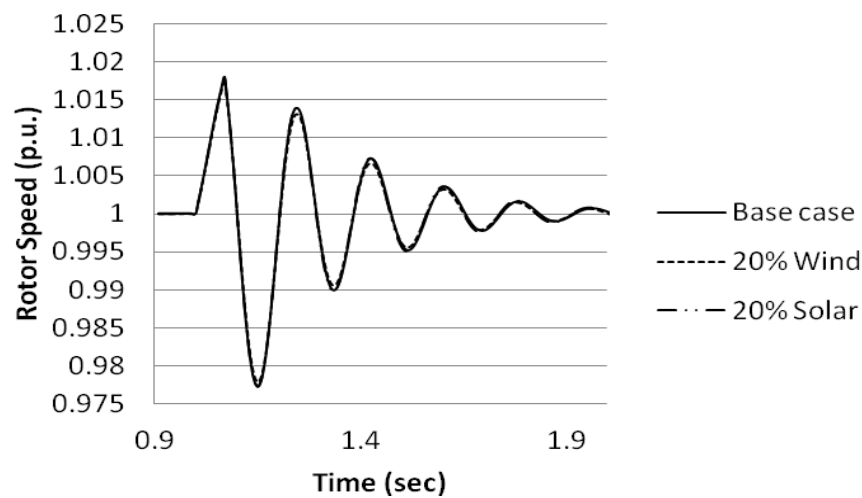


Fig. 4.5.

Fig. 386 shows the response of generator rotor speed of the generator at Bus 3. The generator at Bus 3 is operated in power factor control mode with a unity power factor. It is interesting to observe that the response does not change even if wind and solar penetration is increased. The power factor of the synchronous generator was reduced to 0.8 (lag) and the response of the system to a fault was again simulated. The results are shown in Fig. 38. The response also shows that the

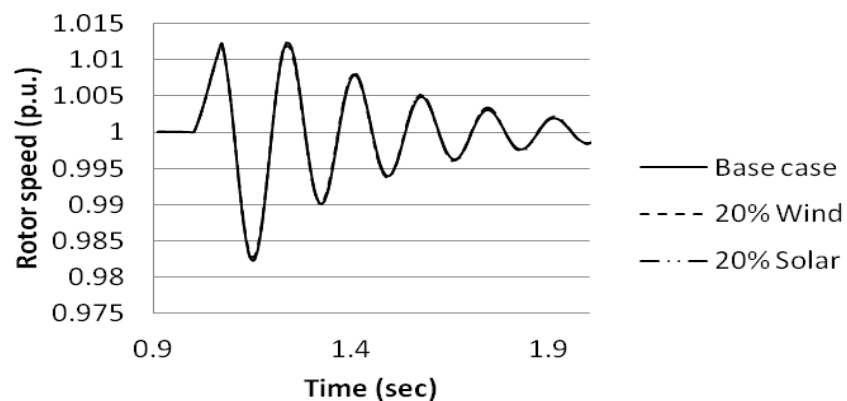
penetration of renewable resources does not affect the damping of the power factor controller generator. It is likely that the machine dynamics are not affected by penetration of renewable energy resources if the synchronous generator is operating at power factor control mode.

Figure 38: Response of power factor controlled synchronous generator for increased penetration (power factor = unity).



If the synchronous generator is supporting reactive power required by the system, the other generators are likely to have an effect on it. On the other hand, other generators do not affect the synchronous generator if it is operating in a power factor control mode. Again, the time domain responses, shown in Figs. 37-39 have frequencies of oscillation of around 3 Hz, which is also the range shown by modal analysis (Table 22). Hence, it is likely that the frequency of electromechanical oscillations observed in the distribution system is slightly higher than those observed in transmission systems.

Figure 39: Response of power factor controlled synchronous generator for increased penetration (power factor = 0.8, lag).



## 5.9. Influence of composite loads on oscillatory stability

### 5.9.1. Test System

The configuration of the distribution system which is under study is shown in Fig. 33. The distribution system is connected to an external utility through Bus 1. The distribution system is supplied by local generators located at different buses. It is assumed that generators are located based on the location of renewable resources and so the selection of location is random. The description of the generators is summarised in Table 25.

Table 25: SUMMARIES of Generators of the System

Gen	Power	Operation	Model	Bus
SG1	5 MW	Power factor	Sixth order	3
SG2	4 MW	Terminal voltage	Sixth order	2
IG	2 MW	Reactive power	Third	6
PV	1 MW	Unity power	Static	7

Here, synchronous generator SG2 has a reactive power limit of  $\pm 3$  MVAR. Capacitor banks are located at different buses to maintain voltage stability of the distribution system. In this paper, the distribution network is considered to be a strong network and there is no influence of an external system on the oscillation of the distribution system. The distribution system is supposed to oscillate with local distributed generators. The distribution system under study has three pairs of oscillatory modes, which are summarised in Table 26.

Table 26: THE OSCILLATORY MODES OF THE DISTRIBUTION SYSTEM

Modes	Real Part (1/s)	Imaginary Part (rad/sec)	Damping Ratio	Frequency (Hz)	Dominant Generator
1, 2	-5.57	20.64	0.26	3.28	SG1
3, 4	-4.23	18.15	0.23	2.89	SG2
5, 6	-9.81	17.72	0.48	2.82	IG

The dominant generators are identified by evaluating the participation factors of state variables to the oscillatory modes. These modes are categorised as ‘system modes’, as all the rotary generators of the system participate in them. Although all the modes seem to be well damped, the damping of the modes may weaken owing to the fluctuating nature of loads, intermittent output of DG units and capacitor compensation [112]. The damping of some modes may be severely affected compared to others. Those critical modes should be handled carefully to improve the small signal performance of the system.

### 5.10. Identification of critical modes

The critical modes of the system (Modes 1, 2 given in Table 26) are identified by calculating the values of  $TS_p$  and  $TS_Q$  for each mode of the system. The total active and reactive power of the system was perturbed by 0.5%. The results are shown in Figs. 40 and 41. It can be observed that the total sensitivities of Modes 1, 2; Modes 3, 4 and Modes 5, 6 with respect to active power load ( $TS_p$ ) at base load are 0.08, 0.15 and 0.03 respectively. Similarly the total sensitivities of Modes 1, 2; Modes 3, 4 and Modes 5, 6 with respect to reactive power load ( $TS_Q$ ) at base load are 0.06, 0.15 and 0.03 respectively. Hence, any change in system loads affects the damping of Modes 3, 4 significantly as compared to other modes. Similar results are obtained for 50% loading and 50% overloading of the distribution system. Hence, Modes 3, 4 are identified as the critical modes of the system.

Figure 40: Comparison of eigenvalue sensitivities of different modes with respect to active power loading.

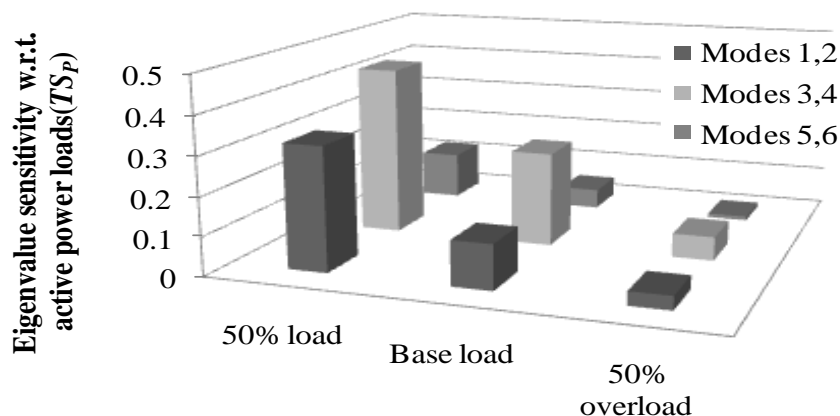
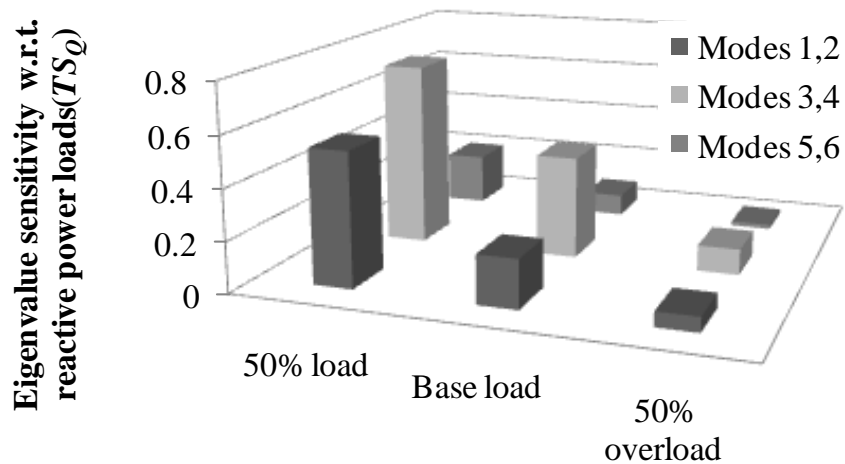


Figure 41: Comparison of eigenvalue sensitivities of different modes with respect to reactive power loading.



It should be noted that the behaviour of critical modes depends on the nature of a particular power system. They may change with different loading conditions [176]. Hence, to have confidence in small signal stability analysis, searching for critical modes should be done at different loading conditions of a power system.

### 5.11. Identification of most influential load

The loads are ranked for composite load modelling on the basis of their highest influence on the critical modes. Table 27 shows the sensitivities of modes with respect to perturbations of active and reactive powers at Bus 4 to Bus 16. Sensitivities were calculated for different loading conditions of the distribution system. Buses 1, 2 and 3 do not have loads.

Table 27: Critical Modes sensitivity At Different Loadings of Distribution System

Bus	50% Base Load		Base Load		50% Overload	
	$\partial\alpha/\partial P$	$\partial\alpha/\partial Q$	$\partial\alpha/\partial P$	$\partial\alpha/\partial Q$	$\partial\alpha/\partial P$	$\partial\alpha/\partial Q$
4	0.265	0.230	0.301	0.337	0.074	0.100
5	0.215	0.166	0.244	0.251	0.064	0.089
6	0.265	0.231	0.303	0.343	0.077	0.103
7	0.265	0.231	0.303	0.344	0.077	0.104
8	0.062	0.017	0.068	0.053	0.036	0.067
9	0.116	0.079	0.131	0.135	0.041	0.071
10	0.057	0.010	0.064	0.048	0.038	0.069
11	0.189	0.143	0.214	0.220	0.058	0.084
12	0.117	0.079	0.134	0.134	0.043	0.071
13	0.053	0.000	0.058	0.042	0.030	0.063
14	0.056	0.007	0.062	0.046	0.039	0.070
15	0.053	0.000	0.059	0.042	0.031	0.063
16	0.053	0.000	0.059	0.042	0.031	0.063

It can be observed that the sensitivities with loads at Buses 7, 6 and 4 are approximately the same, with Bus 7 being the most sensitive followed by Bus 6 and then Bus 4. The loads at these buses have the greatest influence on the small signal stability of the system. In this case, Bus 7 is the most influential on critical mode and is the highest ranked; hence it is considered for dynamic load modelling. At base load, the sensitivity with respect to active power ( $\partial\alpha/\partial P$ ) is 0.303 and the sensitivity with respect to reactive power ( $\partial\alpha/\partial Q$ ) is 0.344. On the other hand it can also be observed from Table 27 that the critical modes have the least eigenvalue sensitivities with respect to the loads at Bus 13, Bus 15 and Bus 16. In this case the load at Bus 13 is the least ranked in terms of its influence on critical modes. At base load, the sensitivities  $\partial\alpha/\partial P$  and  $\partial\alpha/\partial Q$  of critical modes with respect to load at Bus 13 are 0.058 and 0.041 respectively. Load ranking was the same under all loading conditions. However, from a practical viewpoint the load ranking sometimes does depend on loading conditions. Hence, different operating conditions should be considered to gain a reliable load ranking for a distribution system. Once the ranking of the loads is done, a composite dynamic load model, in which only the highly ranked loads are represented, can be used to examine the impact of loads on the small signal stability of the system.

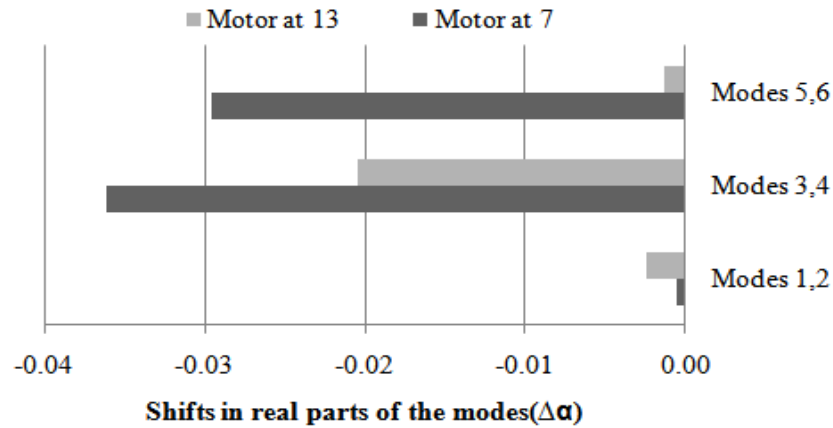
### 5.12. Load Representation by composite load model

The highly ranked loads are represented by the composite load model which comprises static and third-order dynamic induction motors. The ratio of induction motor load ( $\gamma$ ) is assumed to be 20% of the total active power load of the bus [138]. The reactive power consumed by an induction motor is calculated as a function of bus voltage and slip of the induction motor. The total reactive power load of a bus is divided into the reactive power consumption of the induction motor and the reactive power consumption of static loads.

Representing the load at Bus 7 by composite load model shows an additional oscillatory mode (Modes 7, 8) in the system. Modes 7, 8 have eigenvalues  $-0.83 \pm j3.58$  with a damping ratio of 0.23 and a frequency of 0.57 Hz. This is a low frequency oscillation mode, which is well damped from a system stability point of view. Hence, Modes 7, 8 are not problematic for stability of the distribution system. The results of composite load modelling at the highest and the least ranked buses are compared. Replacing a static load by a composite load model results in changes in the distribution of oscillatory modes.

The representation of the load at Bus 7 in the composite load model results in the shift of real parts of oscillatory modes. Similarly, composite load modelling of the least ranked load – that is, the load at Bus 13, also results in the shift of real parts of oscillatory modes. The shifts of real parts of the modes ( $\Delta\alpha$ ) confirms the influence of load modelling on small signal stability of the distribution system. Here, a negative shift in the real part ( $\Delta\alpha$ ) means that eigenvalues are moving away from an imaginary axis in the negative direction. Hence, damping of the modes is improved. The shifts of real parts of oscillatory modes ( $\Delta\alpha$ ) are compared for composite load modelling at Bus 7 and Bus 13. The results are shown in Fig. 42.

Figure 42: Real part of critical modes with different load models.



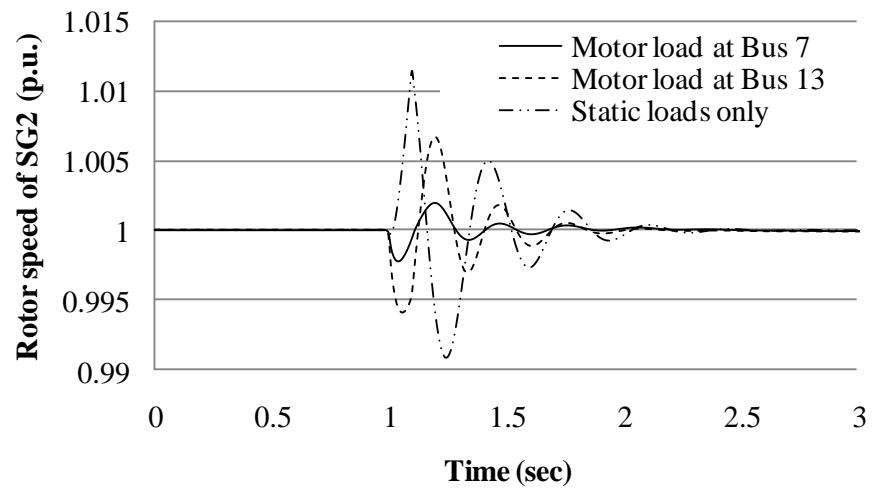
It can be seen that the shift of the real part of oscillatory modes ( $\Delta\alpha$ ) is more significant when the load at Bus 7 is modelled by composite load model rather than when the load at Bus 13 is modelled by composite load model. This shows that the load at Bus 7 is a more appropriate load for composite load modelling than the load at Bus 13.

### 5.13. Influence of composite load model on oscillation of generators

The results obtained from eigenvalue analysis were compared with the time domain analysis. The ratio of induction motor load ( $\gamma$ ) to total bus load was assumed to be 100% in this case. At  $t = 1$  sec, power injection from Bus 1 was interrupted. Power injection was resumed after 100 milliseconds. Fig. 43 shows the response (changes in rotor speed) of the synchronous generator at Bus 2 against the disturbance at Bus 1.

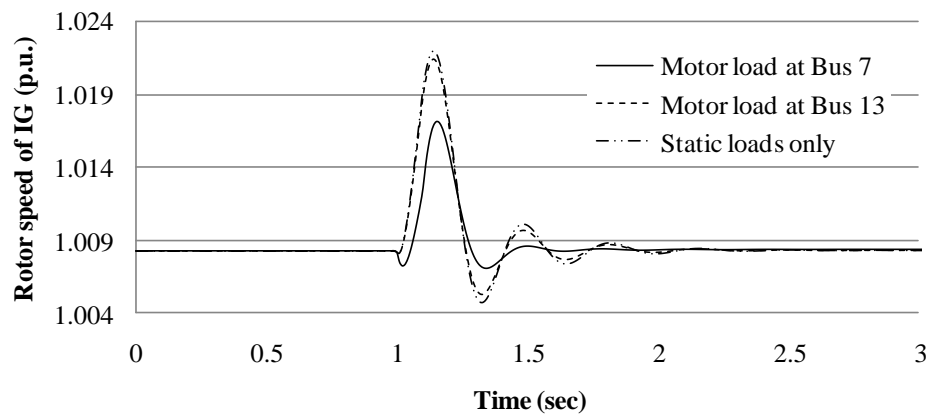
It can be seen that the damping of rotor oscillation improves when the loads are modelled by composite load models rather than static load models. The damping is more pronounced when the load is modelled by a composite load at Bus 7 rather than by a composite load at Bus 13. This suggests that damping is better for a system with high penetration of induction motor loads. Using static load models for small signal stability analysis of such systems may yield pessimistic results for stability assessment.

Figure 43: Response of rotor speed of SG2 (100% motor).



Similarly, under the same disturbance scenario, rotor oscillations of the wind generator was observed with composite load modelling at Bus 7 and Bus 13. The results are shown in Fig. 44.

Figure 44: Response of rotor speed of induction generator (100% motor).

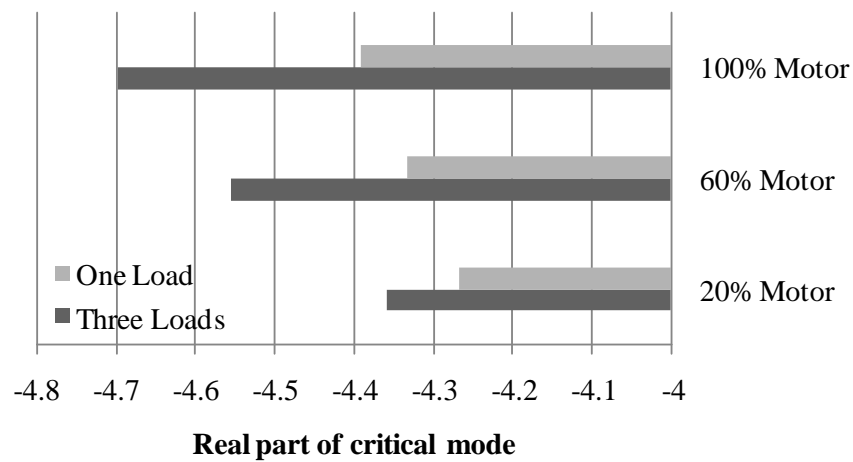


It can be seen that oscillation is better damped when the load at Bus 7 is modelled by composite load. The responses of rotor speed are similar when the loads at Bus 13 are modelled by induction motor load and static loads.

#### 5.14. Composite load modelling of multiple loads

In this case, the more highly ranked loads, as discussed in Section 4.3.2, were modelled by the composite dynamic load model. The selected load buses are Bus 7, Bus 6 and Bus 4. The real parts of critical modes ( $\alpha$ ) were plotted for different percentages of motor loads in the composite load model. The results are shown in Fig. 45.

Figure 45:. Comparison of real part of critical modes for composite load modelling at single load and three loads.

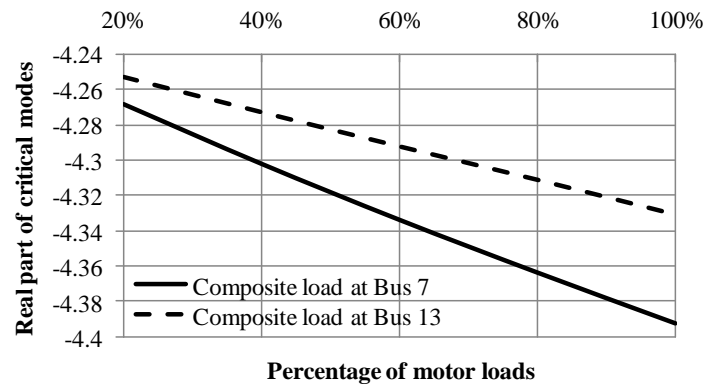


It can be seen that modelling more than one load bus by composite loads results in higher values of the real part of critical modes ( $\alpha$ ) as compared to modelling one bus by critical mode. As the percentage of motor loads ( $\gamma$ ) increases, the magnitude of the real part of critical modes ( $\alpha$ ) also increases. However, the increase in  $\alpha$  is more sensitive when multiple buses are represented by composite load models. This suggests that increasing the proportion of induction motor loads in the system enhances damping of critical modes.

### 5.15. Impact of percentage of motor load

In the results presented in the previous subsections, the ratio of motor loads to total load ( $\gamma$ ) considered was between 20% and 100% in all cases. Owing to the variation of load composition over time, the percentage of dynamic loads in a system changes continuously. The impact on small signal stability of changes in composite loads may differ depending on its composition. A comparison of impacts of variation of percentage of motor loads ( $\gamma$ ) on critical mode was observed. In this case, the percentage of motor loads ( $\gamma$ ) at Bus 7 and Bus 13 are varied from 20% to 100%. The real part of critical modes ( $\alpha$ ) with respect to percentage of motor loads is plotted in Fig. 46.

Figure 46: Real part of critical modes with different motor ratio.



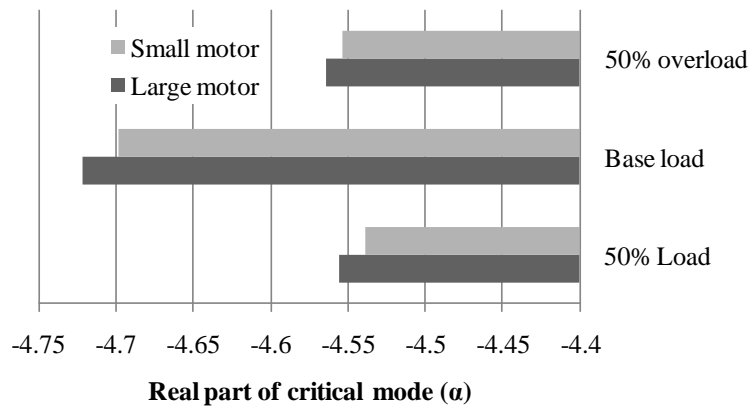
It can be observed that the impact of changing the motor percentage at two different buses is different. Critical modes are more sensitive to change in motor percentage at Bus 7 than at Bus 13. So, loads at Bus 7 are more influential on critical modes than the loads at Bus 13. So Bus 7 is a better choice for composite load modelling than Bus 13. This further supports the load ranking results presented above. The results also show that the greater the induction motor load, the better the damping on critical mode.

### 5.16. Impact of the size of an induction motor

The induction machine part of composite load models may be represented by either 'small' or 'large' motors [177]. The 'large' motors are characterised by higher values of inertia constant ( $H_m$ ) and lower values of operating slip as compared to the 'small' motors. The results with the

application of 'large' and 'small' motors were compared to observe the impact of motor size on the oscillatory modes of the distribution system. The composite load model was implemented at Bus 7. The percentage of the total bus load produced by the induction motor ( $\gamma$ ) is taken as 100%. The real part of the critical mode was compared for 'small' and 'large' motor representations of the composite load model. Observations were made for different loading conditions of the distribution system. The results are shown in Fig. 47

Figure 47: Comparison of real part of critical modes for composite load modelling with 'large' and 'small' induction motor.

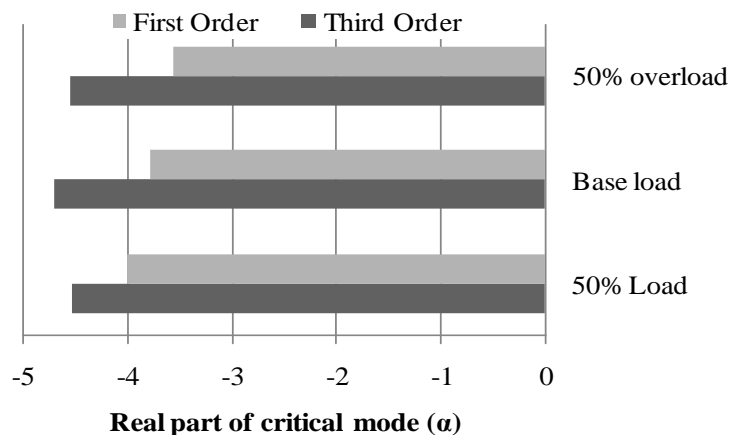


It can be seen that critical modes are better damped when 'large motors' were used for composite load modelling of a distribution system. Similar results were obtained in all the loading conditions of the distribution system.

### 5.17. Impact of lower order model

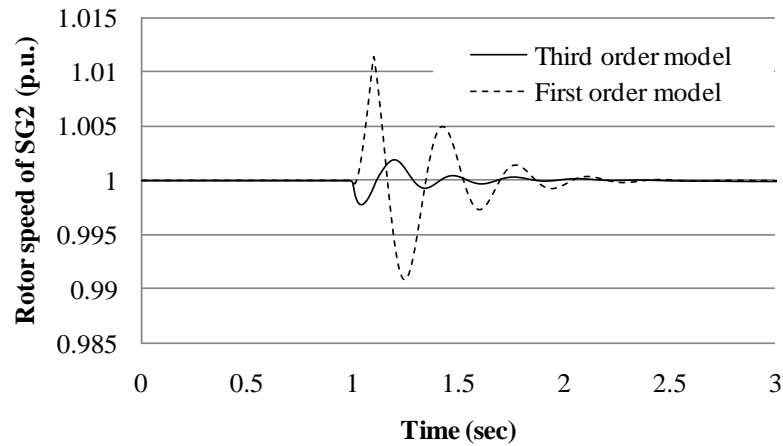
In this case, the third order induction motor model of the composite load model was replaced by the first order model. The first order model represents induction motor dynamics by a single dynamic equation for rotor inertia [177]. The composite load model was implemented at Bus 7 and the motor ratio ( $\gamma$ ) was assumed to be 100%. Real parts of critical mode were compared for first and third order representations of induction motors of composite load models. Comparisons were made for different loading conditions of the distribution system. The results are shown in Fig. 48. It can be seen that the third order model of induction motor results in more damping of the critical mode than the first order model.

Figure 48: Comparison of real part of critical modes for composite load modeling with third and first order induction motor model.



The results can be verified by comparing the time domain responses in the first order and third order models of the induction motor. The power injection from Bus 1 was interrupted at  $t = 1$  sec, and it was resumed after 100 milliseconds. The response of rotor speed of SG2 was observed, and the result is shown in Fig. 49. It can be observed that the third order model of induction motor gives a better damped response than the first order model.

Figure 49: Comparison of time domain responses for third order and first order models of induction motor.

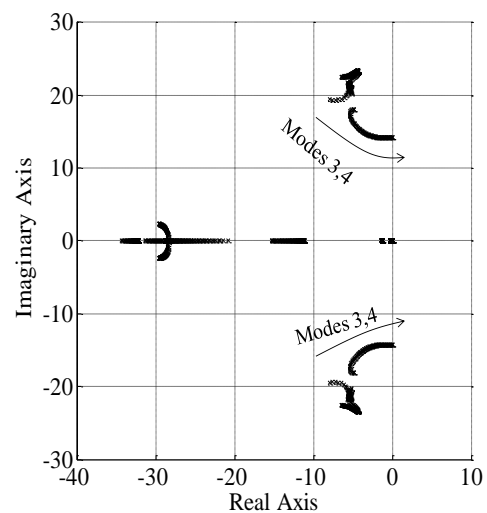


Although all the modes are well damped, the damping of the modes may weaken owing to the fluctuating nature of loads and the output of DG units. The damping of some modes may be more severely affected in some modes than in others. Those critical modes should be handled carefully to improve the small signal performance of the system.

### 5.18. Critical modes

The movement of oscillatory modes on a complex plane was observed by increasing the system loading. The modes which first cross the imaginary axis as the system loading is increased are identified as the critical modes of the system. In the system under study, the trajectories of oscillatory modes as the system loading is increased are shown in Fig. 50.

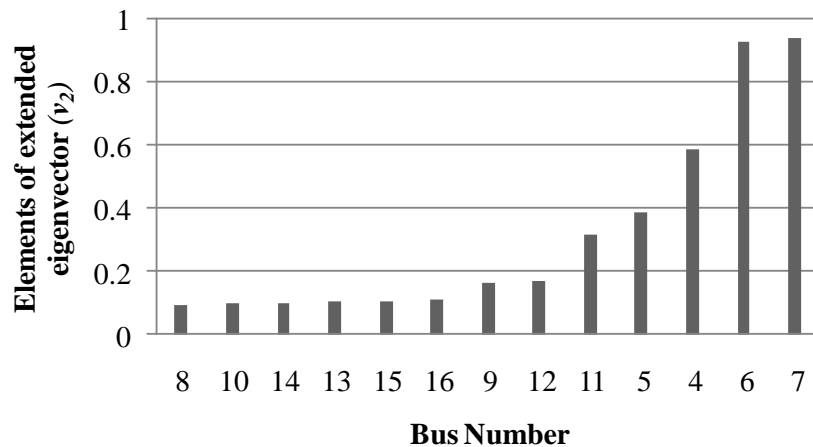
Figure 50: Trajectories of oscillatory modes and HB condition.



It can be seen that modes 3, 4 cross the imaginary axis from the left towards the right. This point of loading is the HB point of the system, which occurs at the total system loading of 53.6 MW. Hence, 53.6 MW is the dynamic loading limit of the distribution system and beyond this load the system experiences oscillatory instability. At increased system loading, modes 3, 4 are the critical modes of instability. The other modes 1, 2 and 5, 6 are more stable under increased system loads.

### 5.19. Identification of the most influential load

Figure 51: Load ranking at HB point of system loading

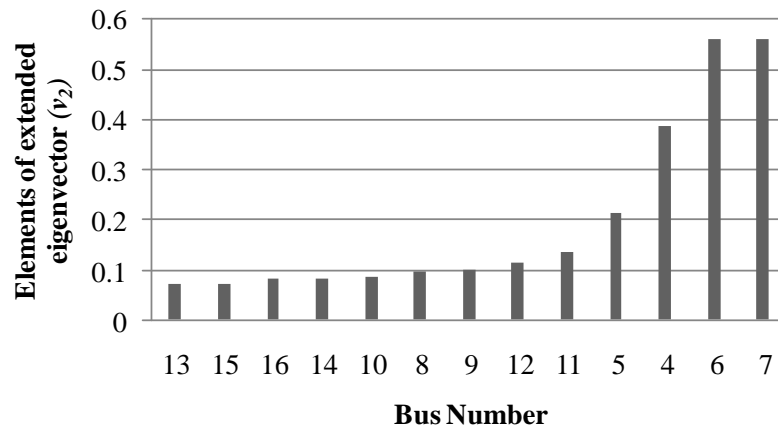


The loads are ranked based on their influence on critical modes.

First, load ranking was done at the HB point of the system. The elements of extended eigenvectors for the critical modes  $v_2$  were evaluated at the HB point. The elements of  $v_2$  corresponding to the load buses are shown in Fig. 51. It can be seen that the load at Bus 7 has the highest  $v_2$ . Hence, loads at Bus 7 are ranked as the most influencing load to the critical mode at the HB point.

Secondly, load ranking was also done at base loading of the system. The results are shown in Fig. 52. It can be seen that the load ranking was different at the base loading compared to the system HB point. While the highly ranked loads were similar, low ranked loads were different at base load. This suggests that system loading has a significant impact to load ranking for small signal stability. Some of the loads may be highly ranked at higher loading, showing their significance in stability performance.

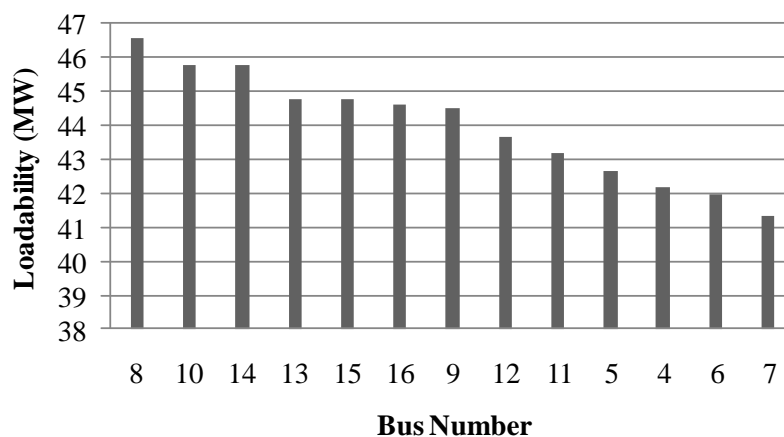
Figure 52: Load ranking at base load of test distribution system.



### 5.20. Influence of composite loads on loadability

The dynamic loadability as indicated by HB phenomena was re-evaluated by modelling all bus loads with composite load models. The induction motor ratio ( $\gamma$ ) was taken as 20% for each load. The system loadability for different cases was compared. The results are shown in Fig. 53.

Figure 53: System loadability with composite loads at different buses

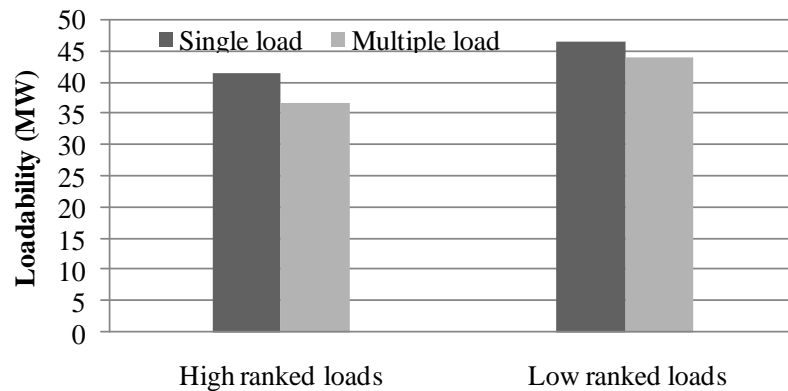


It can be seen that loadability was highest for composite loads at Bus 7 and lowest for composite loads at Bus 8. Comparison of Figs. 51 and 53 shows that loadability magnitudes at different buses are in close agreement with the load ranking. Hence, the loadability magnitudes for composite load

modelling at different loads support the load ranking results. It is apparent that an extended eigenvalue approach can be used for load ranking for small signal stability analysis.

Next, the influence of composite load models at multiple loads of the distribution system was tested. Both the high and low ranked loads were modelled by composite loads and corresponding system loadability was evaluated. Buses 4, 6 and 7 were identified as highly ranked loads and modelled by composite loads. Similarly, Buses 8, 10 and 14 were selected as low ranked loads and also modelled by composite loads. The results are shown in Fig. 54.

Figure 54: System loadability with composite load models at multiple loads.

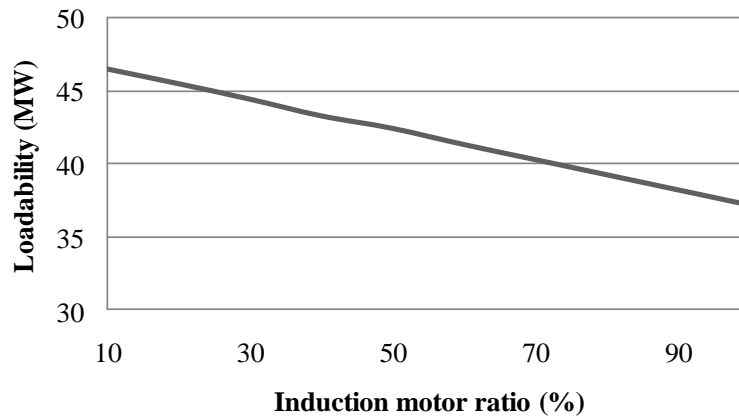


It can be seen that representing multiple loads by composite loads reduces the loadability of the system. Also, loadability is lower for composite load models at multiple highly ranked loads as compared to the results with multiple low ranked loads.

### 5.21. Influence of load composition on loadability

The ratio of the power produced by the induction motor was increased from 10% to 100% and dynamic loadability was reassessed as the percentage increased. The results are shown in Fig. 55. It can be seen that increasing the percentage of induction motor decreases the dynamic loadability of the system.

Figure 55: Variation of loadability with motor ratio of composite loads



Next, the induction motor part of composite loads was represented in both the third order and the first order dynamic models. In both models the induction motor was represented by parameters for 'large' and 'small' motors. The per unit values of induction motor parameters used in this study for 'large' and 'small' motors are shown in Table 28.

Table 28: TYPICAL INDUCTION MOTOR DATA

	Stator resistance ( $R_S$ )	Stator reactance ( $X_S$ )	Rotor resistance ( $R_R$ )	Rotor reactance ( $X_R$ )	Mutual reactance ( $X_M$ )	Inertia constant (H)
Large motors	0.023	0.085	0.013	0.085	3.14	1.6
Small motors	0.068	0.15	0.037	0.123	2.57	0.17

The impact of different load compositions on dynamic loadability is shown in Table 29. It can be observed that the third order model gives a higher value of dynamic loadability than the first order model. Similarly, 'large' motors give a higher value of dynamic loadability than 'small' motors.

Table 29: THE OSCILLATORY MODES OF THE DISTRIBUTION SYSTEM

First Order		Third Order	
Large Motors	Small Motors	Large Motors	Small Motors
43 (MW)	42.4 (MW)	45.7 (MW)	43.8 (MW)

### ***Enhancement of oscillatory stability using shunt controllers***

The simulation was carried out on a radial distribution system, which is shown in Fig. 33. There were three pairs of complex eigenvalues as shown in Table 30 (the same results are shown in Table 22). These results represent the oscillatory modes that exist in the distribution system in the base case. The oscillatory modes in the base case were better damped than those of high voltage transmission systems.

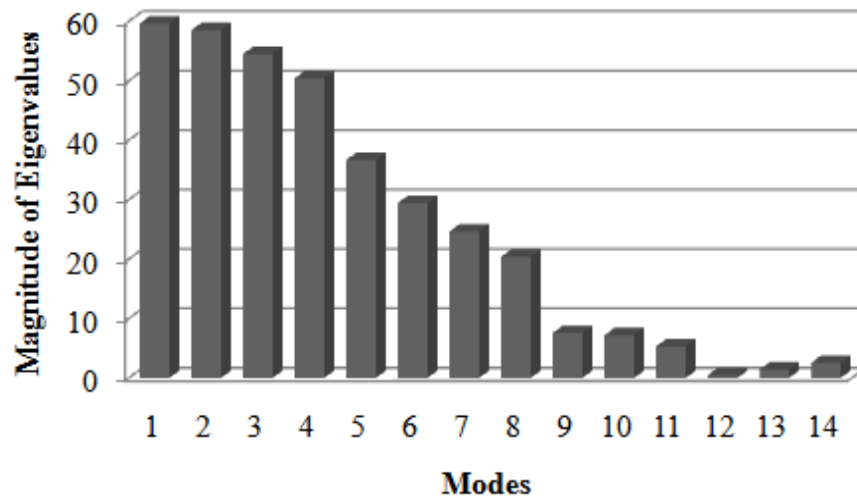
Table 30: THE OSCILLATORY MODES OF THE DISTRIBUTION SYSTEM

Modes	Real Part (1/s)	Imaginary Part (rad/sec)	Damping Ratio	Frequency (Hz)
1, 2	-5.57	20.64	0.26	3.28
3, 4	-4.23	18.15	0.23	2.89
5, 6	-9.81	17.72	0.48	2.82

## **5.22. Identification of significant buses**

The voltage instability of the modes was calculated using modal analysis and the results are given in Fig. 56. The lowest voltage stability was found at Mode 12, which had an Eigenvalue of 0.4932.

Figure 56: Modes of voltage stability



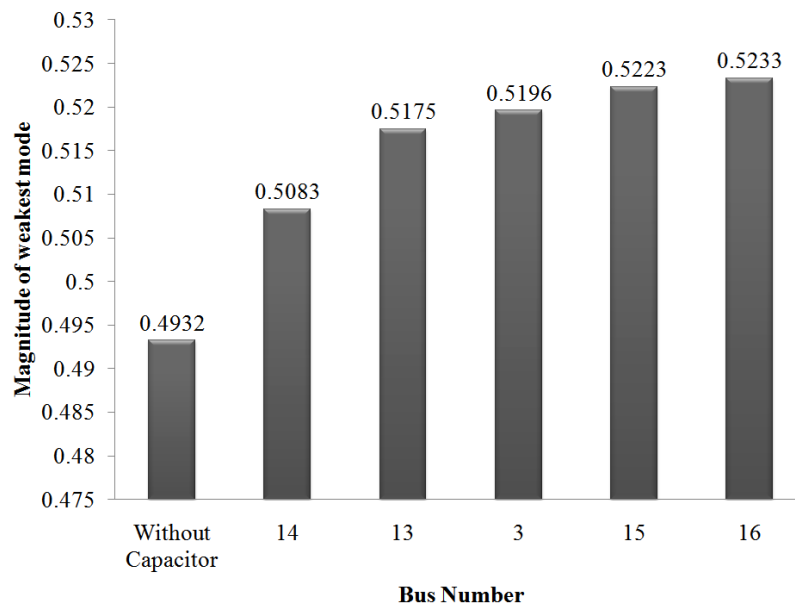
Bus participation factors to the weakest modes are given in Table 4.10. It can be seen that Bus 16 has the highest bus participation factor for Mode 12. Hence, Bus 16 is the most appropriate location for a shunt compensator for voltage stability improvement. The ranking of candidate buses as given in Table 31 in descending order of their normalised participation factors is 16, 15, 3, 13, and 14. These buses are the possible locations for a shunt controller for small signal stability enhancement.

Table 31: BUS PARTICIPATION FACTOR

Bus#	Bus Participation	Normalised participation
3	0.1848	0.8391
4	0.0016	0.0073
5	0.0058	0.0262
6	0.0025	0.0114
7	0.0026	0.0119
8	0.0157	0.0714
9	0.0128	0.0582
10	0.0656	0.2979
11	0.0076	0.0345
12	0.0143	0.065
13	0.1658	0.7525
14	0.089	0.4038
15	0.2116	0.9603
16	0.2203	1

### 5.23. Impact of capacitor placement

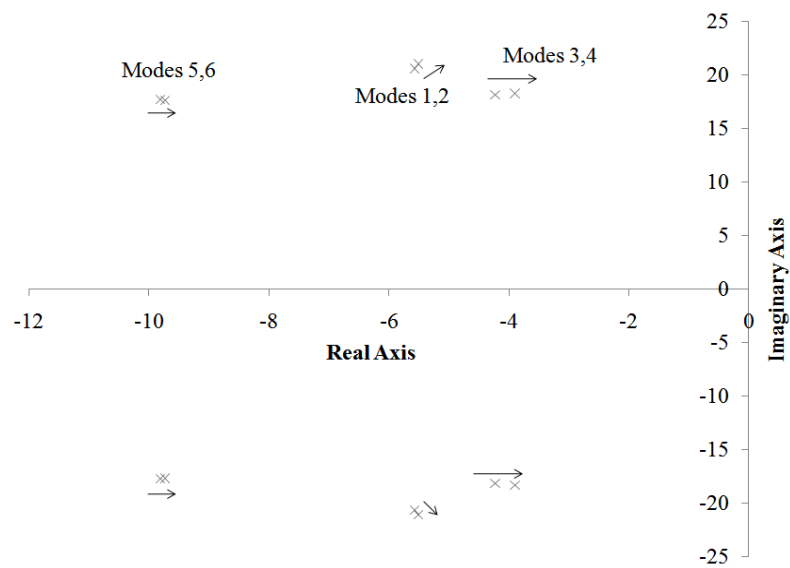
Figure 57: Magnitudes of the weakest modes with different capacitor locations.



A shunt capacitor of 5 MVar was placed at each of the candidate buses in turn and its impact was tested in each case. The results are presented in Fig. 57. It can be seen that the magnitude of the weakest mode increases as the shunt capacitor is placed in the system. This means the voltage stability of the system increases [114],[11]. Furthermore, the magnitude of the weakest mode increases as the capacitor is moved from lower to higher ranked buses. This supports the bus ranking results obtained using modal analysis.

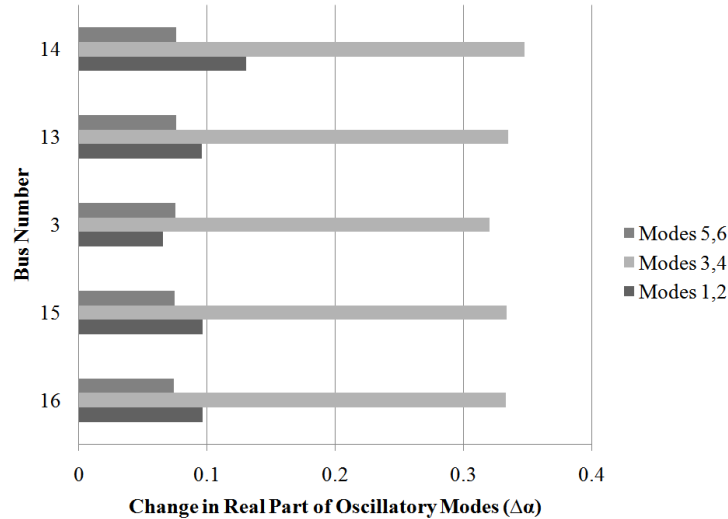
Next, the impact of capacitor placement on small signal stability was studied by placing the capacitor at Bus 16, which is the highest ranked bus. The result is presented in Fig. 58. It can be seen that the placement of capacitors pushes the system eigenvalues towards the right side in the complex plane. As a result, the damping of oscillatory modes is weakened. The reason for this is the negative damping imposed by shunt compensators on synchronising and damping torques of the system oscillations [112],[113].

Figure 58: Oscillatory modes with and without capacitor at Bus 3.



The impact of a shunt capacitor on the oscillatory modes of a distribution system varies depending on which bus it is placed at. However, the primary objective of a shunt capacitor in a distribution system is voltage control. So, of the candidate buses identified using modal analysis, the one that is the best location for a shunt capacitor is the one which has the least detrimental impact on the damping of oscillatory modes. This means the bus which gives the least shift of eigenvalues towards the right side of the complex plane would be the best location. The differences between the real parts of eigenvalues with and without the additional shunt capacitors are taken to be the shifts of the eigenvalues. The shifts of oscillatory modes when shunt capacitors are placed at different candidate buses are shown in Fig. 59.

Figure 59: Change in real part of oscillatory modes with different capacitor placements.



It can be seen that placement of a capacitor at Bus 3 results in the least shift of Modes 3, 4 by 0.319 towards the right on the complex plane. So, Bus 3 would be the best location of shunt capacitor for the least detrimental impact on system modes. With a capacitor at Bus 3, the shifts of Modes 1, 2 and Modes 5, 6 are 0.065 and 0.075 respectively. The shifts of Modes 1, 2 and Modes 5, 6 do not vary significantly according to the location of the shunt capacitor.

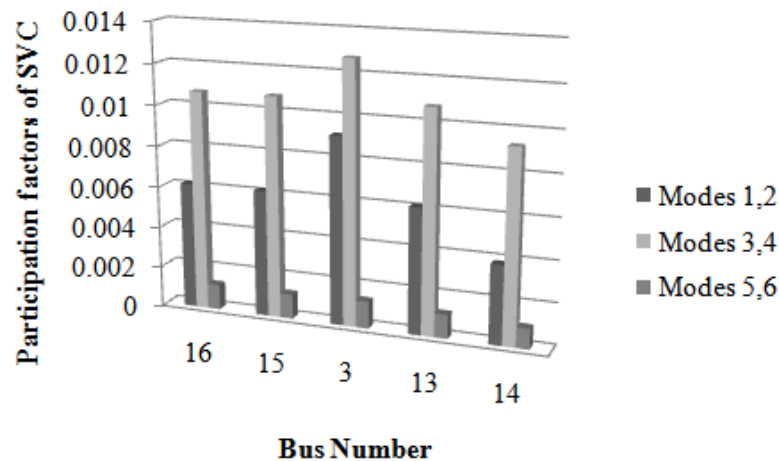
## 5.24. Placement of SVC

The primary controller of an SVC may support damping of the electromechanical oscillations of a power system [113]. The influence of an SVC to the system oscillation modes can be observed by evaluating the participation factor. In this research, participation factor is used as an index to determine the best location of an SVC. The location for which the SVC state has the highest participation factor to the system oscillatory modes is selected as the best location of SVC to support small signal stability of the system. For a particular value of  $T_r$ , SVC participation depends on its location.

The participation factors of SVC states on different modes are shown in Fig. 60. The gain and thyristor time constants are assumed to be 1.00 and 0.02 seconds respectively [11]. The gain

adjustment may be discarded to see the effectiveness of an SVC on system damping [178]. It can be seen that locating an SVC at Bus 3 results in the highest participation of SVC state on Modes 1, 2 and Modes 3, 4. The participation on Modes 5, 6 is 0.0013, which is very small but is still the highest among all the SVC locations. So, Bus 3 is a suitable place for installing an SVC to support the small signal stability of the system. It is important to note that the best location of an SVC is the same as the best location of a capacitor which would have the least detrimental impact on system modes as explained above.

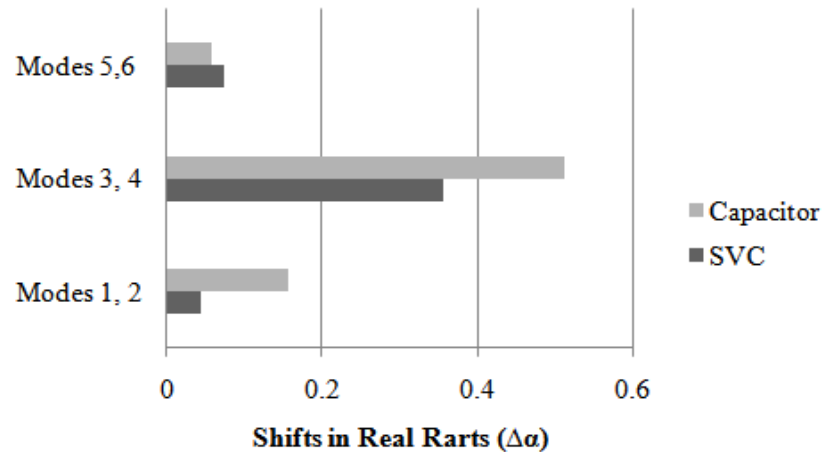
Figure 60: Participation factors of SVC states on system modes with different locations of SVC.



### 5.25. Comparison of SVC and shunt capacitor placement

The negative damping effect of shunt compensators can be minimised by the properly designed primary controller of an SVC. The effectiveness of an SVC can be observed by comparing the shifts of the real part of modes with respect to the base case for an SVC and capacitor placements. The size of both capacitor and SVC were taken as 5 MVAR. The gain and thyristor time constants were again 1.00 and 0.02 seconds respectively. The effectiveness may be improved by the proper setting of the gains and time constants of the SVC. Here, the SVC and capacitor were placed at Bus 3 and a corresponding shift of oscillatory modes was observed. The results are shown in Fig. 61.

Figure 61: Comparison of real part shift with shunt capacitor and SVC at Bus 3.



It can be seen that placement of an SVC results in smaller shifts of the real part of Modes 1, 2 and Modes 3, 4 towards the right of the complex plane as compared to the placement of a capacitor. The shifts of Modes 5, 6 are very small in both cases and that indicates that shunt controllers have negligible impact on these modes. It is important to note that placement of an SVC also reduces the stability of oscillation modes in the same way as a capacitor does. For this reason, some additional controllers are suggested for an SVC to improve the stability of oscillatory modes in addition to voltage stability[113],[115]. This paper is concerned with the best location of an SVC without an additional controller which can serve for enhancing voltage stability as well as minimising the negative damping effect of the shunt capacitor.

The effectiveness of an SVC and capacitor for improving the time domain response of the distribution system was observed. A sudden increase in wind power output by 10% was taken as a disturbance to the system. The responses of voltage at Bus 3 and the rotor speed of the synchronous generator at Bus 3 were observed. The results are shown in Figs. 62 and 63. It can be seen that the response of voltage is slightly less damped with a capacitor than without any controller at Bus 3. Also, the damping of oscillations in bus voltage and generator rotor speed has been improved with SVC placement compared to capacitor placement. This is because of the primary controller of the SVC, which adjusts its total susceptance to generate the reactive power required to maintain the voltage magnitude.

Figure 62: Comparison of response of voltage at Bus 3 with and without shunt controller.

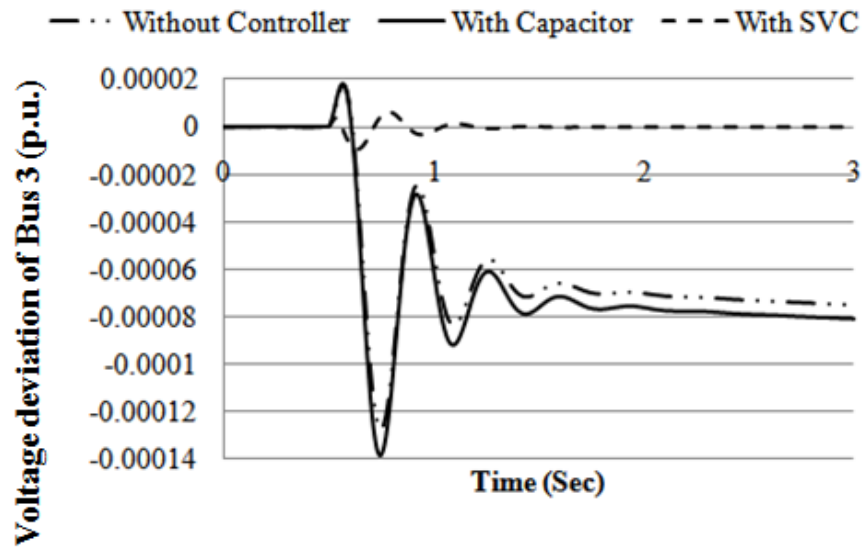
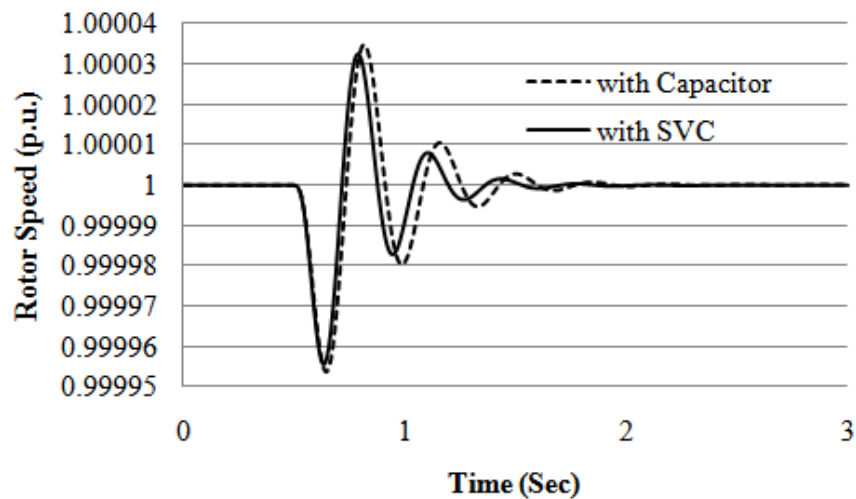


Figure 63: Comparison of response of rotor speed of generator at Bus 3 with shunt capacitor and SVC.



## 5.26. Summary

This section summarises the findings of a small signal stability study of distribution systems with DG units. The studies can be classified into three broad categories as presented above, namely (a) Oscillatory Stability Assessment, (b) Influence of Composite Loads on Oscillatory Stability and (c) Enhancement of Oscillatory Stability.

### 5.26.1. *Oscillatory stability assessment*

The oscillatory stability or small signal stability of a distribution system was investigated for situations involving the penetration of renewable energy resources like wind and solar. Eigensensitivity with respect to active power fluctuations was used as a sensitivity parameter to study the impact of penetration. The level of penetration was varied to study the impact on small signal stability. The sensitivity parameter and time domain simulation were used for stability analysis.

Low frequency oscillation modes with an approximate frequency of 3 Hz were observed. The results show that rotor flux variables of wind generators have a significant impact on the system oscillations. The oscillatory modes dominated by wind generator states were less sensitive to power fluctuations and were relatively well damped compared to the modes dominated by synchronous generator states. Similarly, increased solar PV penetration decreased the eigensensitivity, improving the small signal performance of the distribution system.

The time domain simulation also confirmed the frequency of oscillations (3 Hz) suggested by modal analysis. The increased penetration of wind and solar power had a positive impact on the oscillation damping of the voltage controlled synchronous generator. However, the damping of the power factor controlled synchronous generator was not affected. In system currently in use the controllers are not installed and the results purely reflect the dynamics of machines only.

### 5.26.2. *Influence of composite loads on oscillatory stability*

Loads are considered to be the major determinants of small signal stability of the system and each node may consist of a wide variety of loads, including induction motor loads. In this research, a sensitivity based approach was used for ranking the load buses to select the most influential bus for composite load modelling on power system oscillatory stability. The indices presented in this study for load ranking were computed numerically using perturbations in active and reactive power

loads. In this study the results were verified and compared by modelling the high ranked and low ranked loads using composite load models. Also, the impact of varying the composition of the load in the composite load model on small signal stability was presented. The conclusions drawn in this paper are summarised as follows.

- A distribution system with distributed generation has a number of oscillatory modes. The modes which are highly sensitive at different operating conditions of the system may be selected as critical modes for load ranking.
- The sensitivity-based indices proposed in this research can identify the critical modes of the distribution system. These indices can also be used to rank the loads based on their relative influence on the small signal stability of the distribution system.
- Strategies for damping both synchronous and induction generators should be based on modelling using the composite load model. Composite load modelling shows that good results can be obtained for small signal stability. Hence, composite load modelling gives accurate results for small signal stability.
- Modelling multiple loads using the composite load model gives more accurate results for small signal stability of a renewable energy-based distribution system.
- Representing induction motors by a higher order model gives a more accurate result for small signal stability than lower order models.

It is obvious that the selection of a load model will have an influence on the stability assessment of a distribution system. Any distribution system has its unique composition of loads, which ultimately influences the results of stability assessment. The stability assessment will include a dynamic loading margin.

In addition to the eigenvalue sensitivity method for load ranking, an extended eigenvector technique was used. Although both are linear methods, the sensitivity approach may be computationally demanding as the sensitivities need to be calculated for each load bus. The Hopf bifurcation criterion was used to evaluate dynamic loadability. The induction motor was used as a dynamic part of the composite load model. The conclusions derived from the paper are summarised below.

- The extended eigenvector method can be used for load ranking and composite load modelling of emerging distribution systems.
- Increasing system loading induces Hopf bifurcation, which limits system loadability in emerging distribution systems.
- Load ranking at different system loadings may be different, making some loads important for small signal stability under particular loading conditions.
- Modelling a load by composite load with an induction motor reduces the dynamic loadability of the system. Similarly, representing multiple loads by using a composite load model further reduces dynamic loadability.
- Increasing induction motor percentage in a composite load model decreases the system loadability. Similarly, representing an induction motor by the third order and 'large motors' gives higher values of loadability as compared to first order and 'small motor' representations.

Appropriate load modelling in a distribution system is very important for system planning and operation. The dynamic loads should be properly represented to provide better approximations of system behaviour. Neglecting load dynamics may yield results in planning studies which are too optimistic. This in turn, results in a weaker design for the distribution network. On the other hand, considering detailed load dynamics may yield stability analysis results that are too pessimistic. This may result in an unnecessarily strong design for the distribution network and more investment on network assets. Hence, appropriate modelling of load dynamics is very important in planning and designing future distribution networks.

#### 5.26.3. *Enhancement of oscillatory stability*

Oscillatory stability can be improved by adding damping on the critical mode and this can be done with a wide variety of devices and controllers. However, some important questions to be addressed are: what controller or device should be used? At which location should it be placed? And what is the best control approach?

In this chapter an approach for finding the best locations for shunt controllers to enhance small signal stability of distribution systems with DG units was presented. First, buses were ranked according to their effectiveness as locations for shunt compensators to increase voltage stability. Then, the location for which a shunt compensator had the least detrimental impact on oscillation damping was selected as an appropriate location for small signal stability enhancement. A minimum eigenvalue shift-based index was used for placement of a static shunt compensator such as a capacitor. Participation factors were used to identify the best location for a dynamic compensator such as an SVC. The following conclusions were made based on the observations.

- The integration of DG units into a distribution system generates some oscillatory modes, which need to be well damped to ensure small signal stability of a system.
- $V-Q$  Sensitivity analysis may be used to rank the buses of a distribution system for compensator placement. The installation of a shunt compensator at a highly ranked bus effectively improves the overall voltage stability of the system. On the other hand, such a compensator may weaken the damping of oscillatory modes. A shift of eigenvalues towards the imaginary axis of a complex plane may occur.
- Locating a shunt capacitor at one of the highly ranked buses provides a minimum eigenvalue shift towards the imaginary axis. Locating an SVC at the same bus also shows

the highest participation of SVC to the oscillatory modes. Hence, the bus may be taken as an appropriate location of such shunt controllers for small signal stability.

- The installation of an SVC results in less negative damping of oscillatory modes than the installation of a capacitor of the same rating. Also, SVCs provide better transient and steady state responses of bus voltage and generator rotor angle in the event of system disturbances.

Hence, an SVC is a better choice than a shunt capacitor of the same rating for small signal stability enhancement of a distribution system. A controller, in addition to the primary voltage controller of an SVC, can be designed for the SVC to eliminate its negative damping effect. The design aspects will be addressed in future works.

Future power distribution requires extra expansion capability and flexibility in the integration of DG. This is why the control strategy in the interconnected grids should be combined with a control methodology of inverters. The next chapter will provide control methodologies for controlling converters in DG units, for example, DFIG, DDWG and PV systems for the enhancement of stability under both small and large disturbances.

## 6. CONTROL METHODOLOGIES FOR DISTRIBUTED GENERATION

Traditionally, distributed network design did not consider the issue of stability as networks were considered to be passive [179]. The integration of large Distributed Generation (DG) units has a significant impact on the performances of power systems. The main technical challenges to increased penetration of DGs into an existing grid are voltage regulation, power quality, protection against faults, dynamic voltage and small signal stability. In this chapter we concentrate mainly on the issues of dynamic voltage and small signal stabilities. Suitable control methodologies must be applied to ensure the stability of the system.

There are a number of approaches to controlling distributed generation for enhanced network stability. This chapter explains some of the advanced control approaches that may be useful for maintaining the stability of distributed generation. These control schemes include designing a shunt controller for a selected capacitor bank and/or designing additional controllers for DG units such as PV and DFIG. A coordinated control approach for different DG units is also proposed and discussed. A number of cases are analysed to gain a deeper insight into the issues involved. Depending on the nature of the control problem, we propose a control algorithm that can significantly enhance the penetration level of DG units.

This chapter is organised as follows: Section 5.2 provides an approach to controlling a shunt capacitor bank in order to adjust the damping of the critical modes. Section 5.3 discusses a supplementary control for photovoltaic (PV) generators for augmenting small signal stability of distributed systems. Section 5.4 provides a robust control algorithm for a doubly-fed induction generator (DFIG) for enhancing small disturbance stability of a distributed system. Section 5.5 proposes a robust decentralized control approach for different types of DG including DFIGs, PV generators and direct drive wind generators (DDWGs) in order to enhance both dynamic voltage and transient stabilities for the flexible integration of DG units. Finally, the conclusions drawn from the results and contributions of the chapter are summarised in Section 5.6.

## 6.1. Controlling a capacitor bank using a thyristor control reactor (TCR)

Flexible AC transmission system (FACTS) controllers are widely used in conventional transmission systems for stability enhancement [167]. However conventional distribution networks are usually compensated for by mechanically switched capacitor banks to support node voltages. Mechanically switched capacitor banks are incapable of handling the dynamics of distribution networks containing distributed generators. Furthermore, capacitor banks are reported to be detrimental to oscillation damping [180]. Hence, dynamic compensation devices such as FACTS with supplementary control loops may be required to ensure the small signal stability of a distribution network. Alternatively, existing capacitor banks may be utilised in combination with a TCR to ensure small signal stability by dynamically controlling their susceptance instead of investing in an additional device. This combination is popularly known as SVC. The next section presents a systematic approach to controller design. However, before designing a controller it is important to determine the critical modes to ensure an optimum controller performance.

### 6.1.1. Critical mode

The system under study is a 16 bus distribution system as discussed in Chapter 4. The system has four pairs of complex low frequency oscillatory modes, which are summarised in Table 32. It can be seen that Modes 7 and 8 have the lowest damping ratio of nearly 2%, which is undesirable for power system small signal stability. Hence, this mode has been considered as a critical mode. The dominant states and corresponding generators for different oscillatory modes were identified using normalised participation factors which are shown in Table 33.

Table 32: OSCILLATORY MODES EXISTING IN THE TEST SYSTEM

Modes	Real Part (1/s)	Imaginary Part (rad/sec)	Damping Ratio	Frequency (Hz)
1, 2	-4.85	20.50	0.23	3.26
3, 4	-2.90	10.40	0.23	1.66
5, 6	-10.30	17.40	0.50	2.77
7, 8	-0.44	24.00	0.02	1.82

It can be seen that induction generators also participate in system oscillatory modes along with synchronous generators. Also, two synchronous generators participate equally to Modes 1, 2 and Modes 3, 4. Participation factors are indicative of the location of stabilisers used to add damping on the weakest mode. However, owing to the unregulated operation of distributed generators, stabilizers are not always an effective means of stability enhancement [167]. So damping can be effectively controlled by a controller installed at the distribution network. In the following sections, the location and design of such a controller is discussed.

Table 33: DOMINANT GENERATORS AND STATES FOR DIFFERENT MODES

Mode	Dominant Generator	Dominant states (PF%)
1, 2	SG1	Rotor angle (28%)
		Speed Deviation (12%)
	SG2	Rotor angle (12%)
		Speed Deviation (28%)
3, 4	SG1	Rotor angle (11%)
		Speed Deviation (27%)
	SG2	Rotor angle (27%)
		Speed Deviation (11%)
5, 6	IG	Rotor speed (40%)
		q-axis rotor flux (42%)
7, 8	SG1	Rotor angle (21%)
		d-axis rotor flux (22%)
		Speed deviation (21%)
		Exciter (22%)

### 6.1.2. Selecting a capacitor bank for controller

The state space model of a distribution system with a shunt capacitor controller connected at a remote bus can be written as:

$$\begin{bmatrix} \Delta \dot{X} \\ 0 \\ 0 \end{bmatrix} = \begin{bmatrix} A & B & 0 \\ -C & D - Y_{GG} & Y_{GR} \\ 0 & Y_{RG} & Y_{RR} \end{bmatrix} \begin{bmatrix} \Delta X \\ \Delta V_G \\ \Delta V_R \end{bmatrix} + \begin{bmatrix} 0 \\ 0 \\ 1 \end{bmatrix} \Delta I_R \quad (5.1)$$

where  $\Delta I_R$  is the vector of currents absorbed by a damping controller at the remote bus. Now, if  $\beta_R$  is the shunt susceptance of a capacitor bank at bus  $r$  with voltage  $V_R$ , current injected to the bus by shunt capacitor can be written as:

$$I_R = \beta_R V_R \quad (5.2)$$

Linearising (5.2) at an operating point of interest gives

$$\Delta I_R = \beta_{R0} \Delta V_R + V_{R0} \Delta \beta_R \quad (5.3)$$

where  $\beta_{R0}$  and  $V_{R0}$  are steady state capacitive susceptance and bus voltage respectively. Now,

(5.3) can be rewritten as

$$\Delta I_R = B_C \Delta V_R + b_{\Delta\beta,R} \Delta \beta_R \quad (5.4)$$

where  $B_C$  represents the steady-state susceptance of the controllable shunt capacitor and  $b_{\Delta\beta,R}$  represents the steady state voltage of the shunt capacitor bus. Substituting (5.4) into (5.3) yields

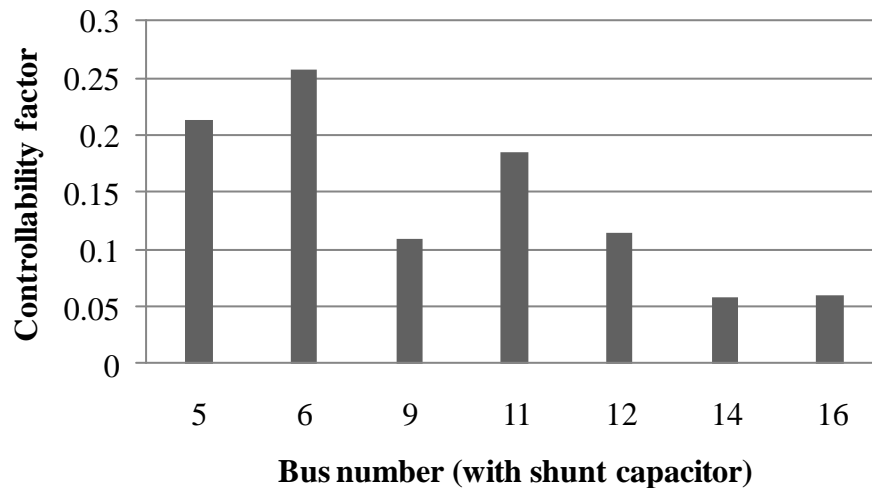
$$\begin{bmatrix} \Delta \dot{X} \\ 0 \\ 0 \end{bmatrix} = \begin{bmatrix} A & B & 0 \\ -C & D - Y_{GG} & Y_{GR} \\ 0 & Y_{RG} & Y_{RR} + B_C \end{bmatrix} \begin{bmatrix} \Delta X \\ \Delta V_g \\ \Delta V_R \end{bmatrix} + \begin{bmatrix} 0 \\ 0 \\ b_{\Delta\beta,R} \end{bmatrix} \Delta \beta_R \quad (5.5)$$

Hence,  $b_{\Delta\beta,R}$  represents the controllability vector of shunt capacitor control. Now, controllability factor of mode  $i$  for the shunt capacitor control at any arbitrary bus  $j$  can be written as

$$w_{ij} = b_{\Delta\beta,j} \psi_i \quad (5.6)$$

where,  $\psi_i$  is the  $i^{th}$  left eigenvector. The controllability factors of critical modes for shunt susceptance modulations were evaluated for all the shunt capacitors of the test distribution network. The results are shown in Figure 64.

Figure 64: Controllability factors of susceptance modulation of shunt capacitors of the test distribution system for the critical mode.

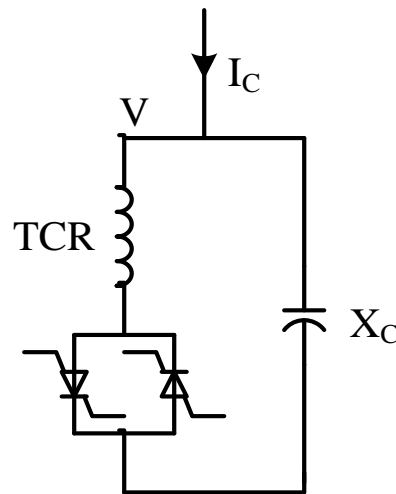


It can be seen that the shunt capacitor at Bus 6 has the highest controllability factor for shunt susceptance modulation. Hence, controlling the susceptance of this capacitor is the most effective means of damping control of the critical mode.

#### 6.1.3. Control methodology

A power electronic reactance controller has a thyristor in series with an inductor, whose value can be adjusted by controlling the thyristor firing angle. Such a scheme is known as thyristor-controlled reactor (TCR). The controller, when connected in parallel with a capacitor bank, is able to exchange capacitive or inductive current so as to maintain the bus voltage. In this section a scheme of controlling an appropriate shunt capacitor using a TCR is presented. A block diagram of such a scheme is shown in Figure 65.

Figure 65: A schematic diagram of thyristor-controlled reactor for controlling the susceptance of a capacitor bank



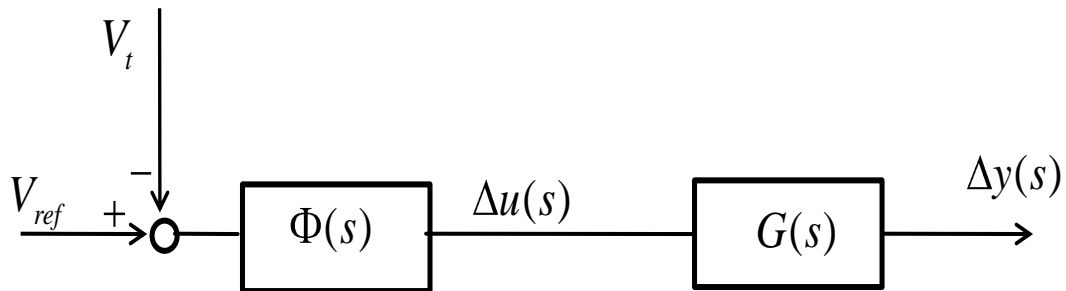
The transfer function of such a controller is given as:

$$\Phi(s) = \frac{1}{1 + T_r s} \quad (5.7)$$

where  $T_r$  is the thyristor time constant. Usually,  $T_r$  is selected in the range of 0.02 to 0.05 seconds [11]. In this work,  $T_r$  is selected to be 0.02 seconds.

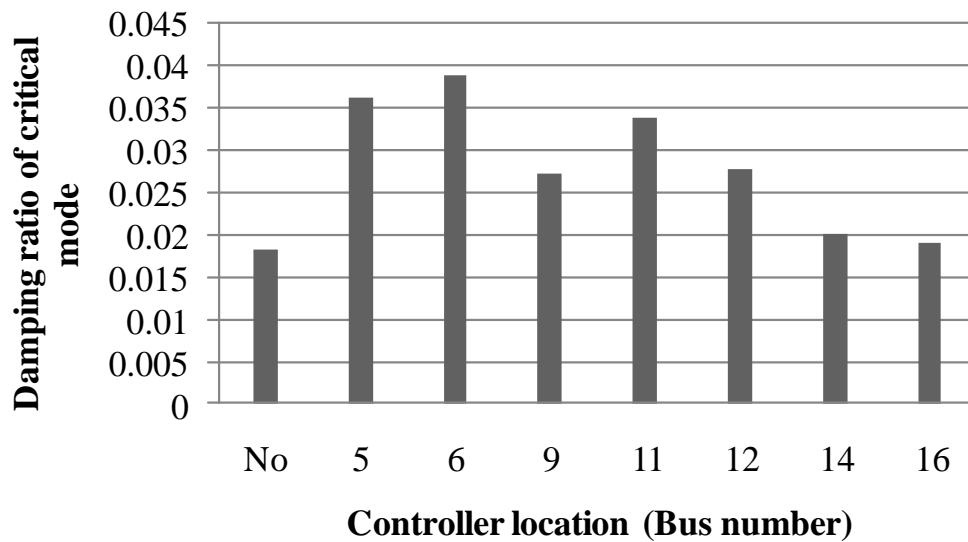
The system with a controller can be represented as Fig 66, where  $V_t$  is the terminal voltage,  $V_{ref}$  the reference terminal voltage,  $\phi(s)$  the controller function,  $u(s)$  the control input,  $G(s)$  the system transfer function and  $y(s)$  the measured output.

Figure 66: Block diagram of the distribution system with converter control.



Depending on the location of the controller, the influence may be either beneficial or detrimental to system modes [178]. In this case the impact of the controller location on the damping ratio of the critical mode was observed. The results are shown in **Error! Reference source not found.67**.

Figure 67: Impact of controller location on damping ratio of the critical modes.

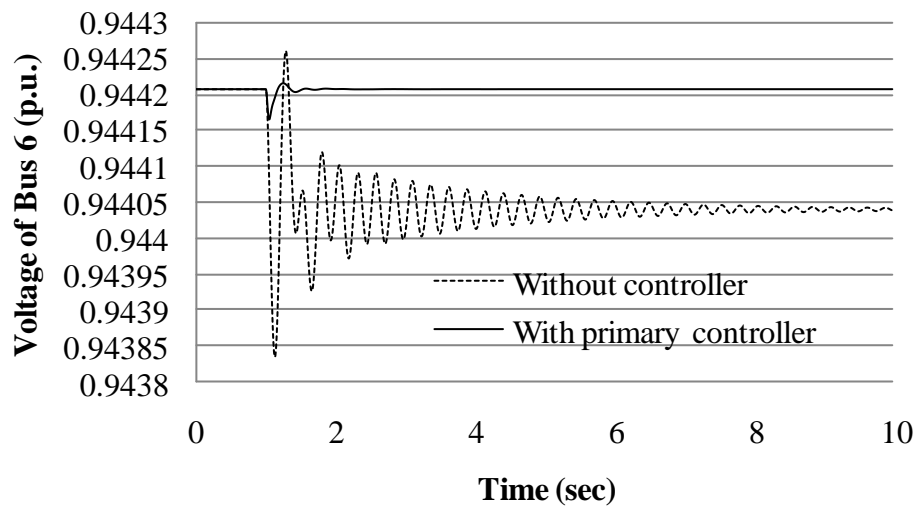


It can be seen that the damping ratios of the critical modes with a controller installed at a bus are larger than the damping ratios with no controller. This shows that the controller has a positive impact on the damping of the critical mode. Also, the damping ratio is highest for the controller installed at Bus 6. However, the damping ratio after installation of a controller is still very low i.e. less than 4%. This is regarded as a low damped case in a power system. Hence, an additional

controller should be designed to make the damping ratio at the desired value, i.e. 5% in this case. This will be discussed in the next subsection.

The effectiveness of the controller was also observed by time domain simulation. A controller was installed at Bus 6. A step change in mechanical torque of the wind generator of 10% was applied as a disturbance to the system and the response of voltage magnitude at Bus 6 was observed. The results are shown in figure 68. It can be seen that the controller effectively improves the transient and steady state voltage profile of the system.

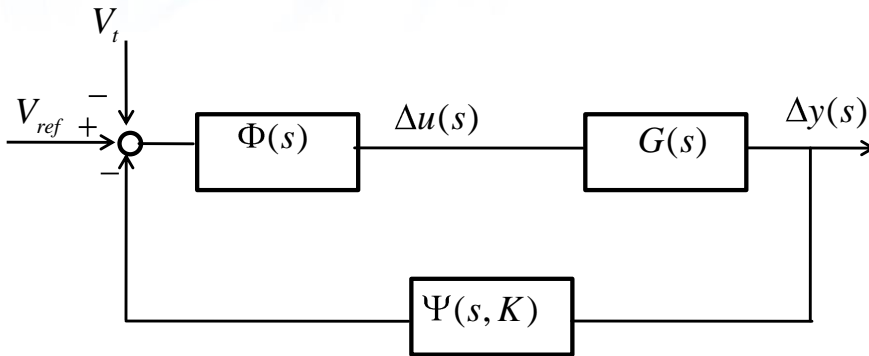
Figure 68: Impact of controller on time domain response of the system.



#### 6.1.4. Performance of controller

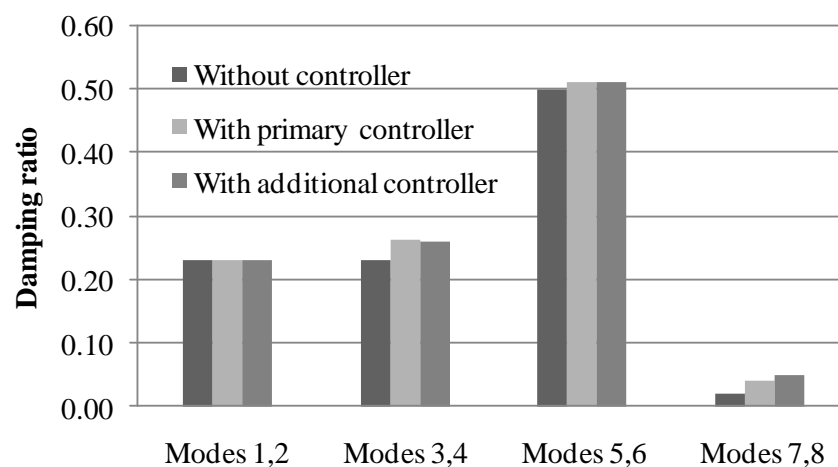
An additional controller was designed to enhance the damping of the critical mode to a desired value. The block diagram representation of the additional controller in association with the primary controller of the system is shown in figure 69 with  $\psi(s)$  as the additional controller function.

Figure 69: Block diagram of the distribution system with converter control and additional controller.



Using the procedure explained in section above, an additional controller was designed to achieve a desired damping ratio of the critical mode, i.e. 5% in this case. The washout time constant was taken as 5 seconds. The effectiveness of having an additional controller was evaluated by observing the damping ratios with and without the controllers. The results are shown in Figure 70. It can be seen that an additional controller can effectively improve the damping of the critical mode so that it reaches 5%. It can also be seen that the primary controller has an impact on all the modes of the system, while the additional controller does not affect the damping of system modes, except the critical mode. Hence, an additional damping controller design is useful for targeting the damping of a particular mode of interest without hampering the damping of other modes.

Figure 70: Comparison of damping ratios of different modes with and without controllers.



Although the power system stabilizer in a synchronous generator is mainly used to improve damping in power systems, appropriate control of PV can also contribute to the enhancement of small signal stability.

## DESIGN OF SUPPLEMENTARY CONTROLLER FOR PV GENERATORS

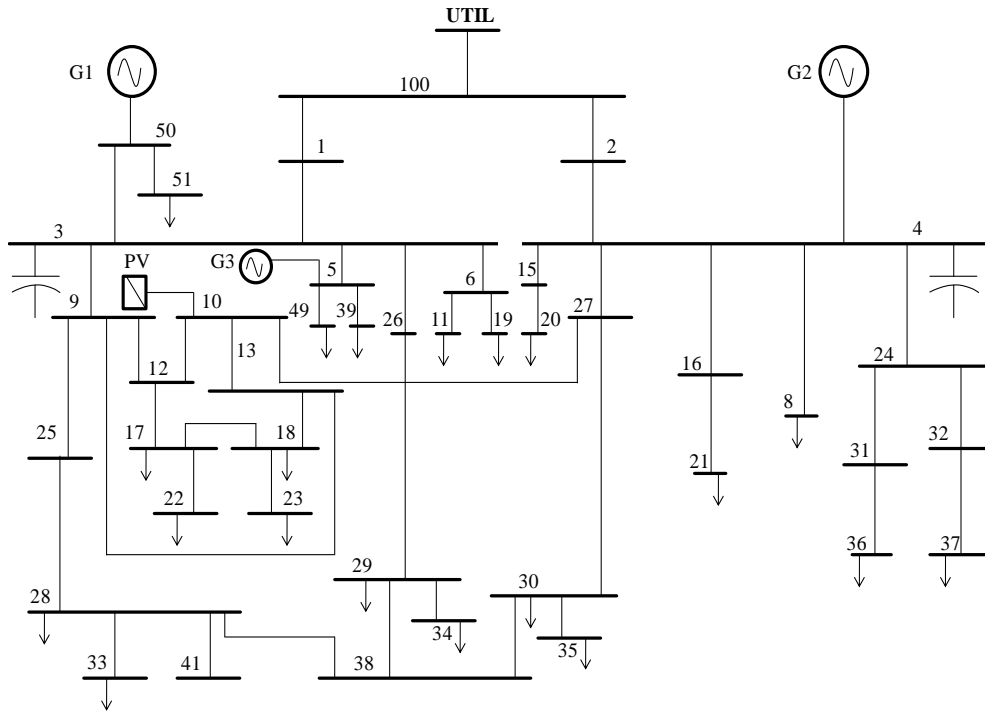
Oscillatory instabilities in the form of low frequency oscillations are highly undesirable. These oscillations must have acceptable damping ratios to ensure stable operation of a power system [47]. In case of transmission systems, various controllers such as power system stabilisers (PSSs), static VAR (volt-ampere reactive) compensators (SVCs) and static compensators (STATCOMs) are commonly used for oscillation damping [50]. There are various methods reported in the literature for determining suitable locations and design approaches for incorporating these damping controllers in a power system [178]. However, the installation of such devices in a low voltage distribution system may not always be technically and economically attractive. Instead, one of the DG units in the system may be controlled to improve system stability [118]. Given the structure of DG units (such as PV and DFIG), which are dominated by controllers, one of the controllers of the DG units may be employed for improving the oscillation damping. The network consists of synchronous generators, a fixed speed induction generator, a DFIG and a PV. A control methodology was proposed for a PV system to enhance the damping of low frequency oscillations.

### 6.1.5. Test system

The distribution system under study is shown in figure 71. This is a 43 bus distribution network with a total load of 21MW and 8 MVAR [165]. The system is connected to an external utility grid through Bus 100. The system is supplied by two synchronous generators (G1 and G2) located at Buses 50 and 4, respectively. In this study, a squirrel cage induction generator (SCIG) is added as a source

(G3) of wind power at Bus 5. Similarly, a VSC-based photovoltaic generator (PV) is added at Bus 10 as a source of solar power.

Figure 71: Single line diagram of a case distribution system.



#### 6.1.6. Power factor control

The relationship of active power ( $P$ ) and reactive power ( $Q$ ) with voltages and currents in d- and q-axis reference can be given as:

$$\begin{cases} P = \frac{3}{2} (v_{SD} i_D + v_{SQ} i_Q) \\ Q = \frac{3}{2} (v_{SQ} i_D - v_{SD} i_Q) \end{cases} \quad (5.8)$$

where  $v_{SD}$  and  $v_{SQ}$  are the d- and q- axis components of PV terminal voltage. Similarly,  $i_D$  and  $i_Q$  are the d- and q- axis components of PV current into the distribution network.

In this chapter, the aim is to operate PV in power factor control mode. Since,  $v_{SD}$  and  $v_{SQ}$  are determined by the distribution network, power factor control can be achieved by independent control of  $i_D$  and  $i_Q$ . For a given network condition, the PV power factor can be set to a desired

value by appropriate values of currents, i.e.  $i_{Dref}$  and  $i_{Qref}$ . Then,  $i_D$  and  $i_Q$  can be controlled to follow  $i_{Dref}$  and  $i_{Qref}$  by using proportional and integral (PI) controllers as shown in **Error! Reference source not found.72** and **Error! Reference source not found.73**. The outputs of the controllers, i.e.  $m_D$  and  $m_Q$ , are control parameters of the VSC.

Figure 72: d- axis current controller

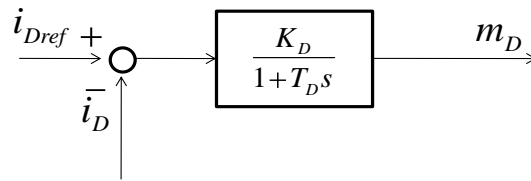
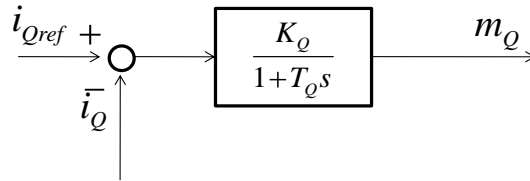


Figure 73: q-axis current controller.



#### 6.1.7. Design of a lead lag controller for PV

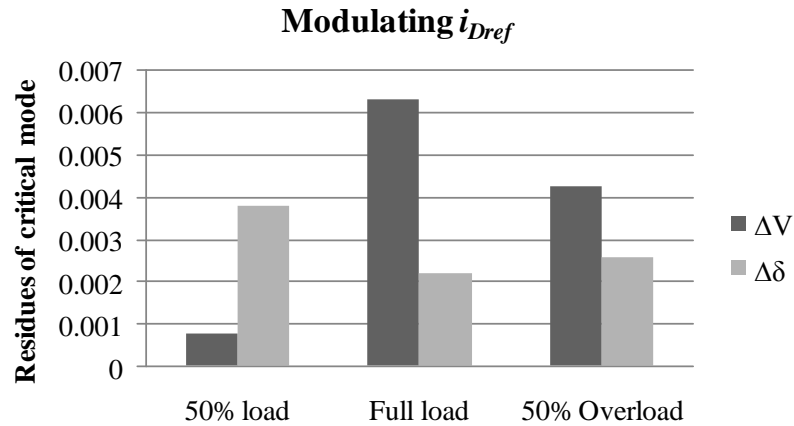
In this section, a design procedure for an additional controller for PV is presented in order to enhance the system damping. The first step towards the controller design is selection of the most appropriate control signals.

#### 6.1.8. Selection of control signals

Residue method presented in chapter 4 was used as an index for selection of control signals. The combination of signals giving the highest magnitude of residue was selected for the input modulation signal and feedback signal for the controller.

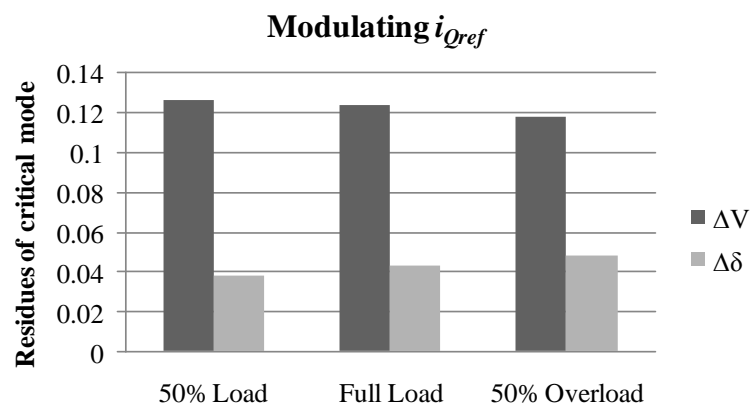
In this work, two local signals i.e. deviations of PV terminal voltage magnitude ( $\Delta V$ ) and angle ( $\Delta \delta$ ) were taken as possible signals for feedback to the controller. The outputs of the controller were used to modulate the reference signals, i.e.  $i_{Dref}$  and  $i_{Qref}$ . The residues at critical modes, when  $i_{Dref}$  is modulated, are shown in **Error! Reference source not found.74**.

Figure 74: Residues of system when d-axis current of PV is modulated.



It can be seen that using  $\Delta V$  as a feedback signal gives larger values of residues at full load and at 50% overload of the distribution system than at 50% loads. However,  $\Delta \delta$  as a feedback signal gives a larger value of residue at 50% load of the distribution system than at full load and 50% overload. Hence, the controller designed for full load using  $\Delta V$  as a feedback signal may not be effective at 50% load of the distribution system. Similarly, the residues of critical mode when  $i_{Qref}$  is modulated are shown in Fig. 75.

Figure 75: Residues of system when q-axis current of PV is modulated.



It can be seen that  $\Delta V$  has a greater magnitude of residue than  $\Delta\delta$  in different loading conditions of the distribution system. Hence,  $\Delta V$  is an appropriate feedback signal for a controller when  $i_{Qref}$  is modulated.

It is obvious from Equation (5.8) that power factor control can be achieved by modulating either  $i_{Dref}$  or  $i_{Qref}$ . Hence, the input signal that gives larger values of residues when  $\Delta V$  or  $\Delta\delta$  is used as the feedback signal can be used as an input modulating signal. It can be seen from **Error! Reference source not found.** 5.11 and 5.12 that using  $i_{Qref}$  as a modulating signal gives larger values of residues in all cases. Hence,  $i_{Qref}$  has been used as the modulating signal.

#### 6.1.9. Controller design

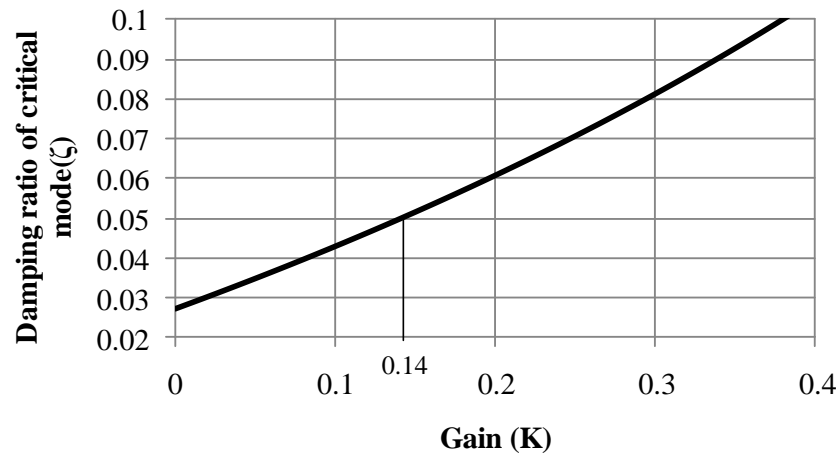
A controller was designed for modulating  $i_{Qref}$  to improve damping of the critical mode. The calculated values of constants of the controller are given in **Error! Reference source not found.** 34.

Table 34: PARAMETERS OF THE POWER FACTOR CONTROLLER.

$\phi$ (degree)	$m$	$\alpha$ (degree)	$T_1$ (seconds)	$T_2$ (seconds)
102.8°	2	7.02°	1.78	0.22

The gain of the controller (K) was obtained by using the root-locus technique. The trace of  $\zeta$  with K is shown in Fig. 5.13. Here, K was gradually increased from zero until the desired damping ratio of the critical mode was obtained. It can be seen from fig 76 that  $\zeta$  can be increased by increasing the value of K. When K equals zero,  $\zeta$  has the initial value of 2.74%. Similarly, when K equals 0.38,  $\zeta$  equals 10%. In this chapter, K is set at 0.14 to make  $\zeta$  equal to 5%.

Figure 76: Variation of damping ratio of critical mode with controller gain.



#### 6.1.10. Effectiveness of the controller

The effectiveness of the controller was evaluated by observing the damping ratios before and after installing the controller for PV. The results are shown in **Error! Reference source not found.77**. It can be seen that the supplementary controller effectively improves the damping ratio of critical modes to the targeted value of 5%. The damping ratios of other modes are unaffected. Similarly, the time domain response was observed by applying a three phase fault at Bus 3. The fault was cleared after 90 ms. The responses of voltage at Bus 10 with and without a controller were observed as shown in fig 77. It can be seen that the controller effectively improves time domain response of the system.

Figure 77: Comparison of damping ratios with and without controller.

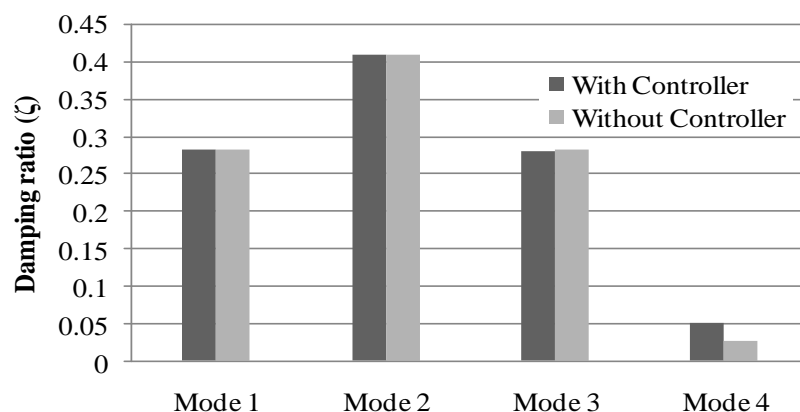
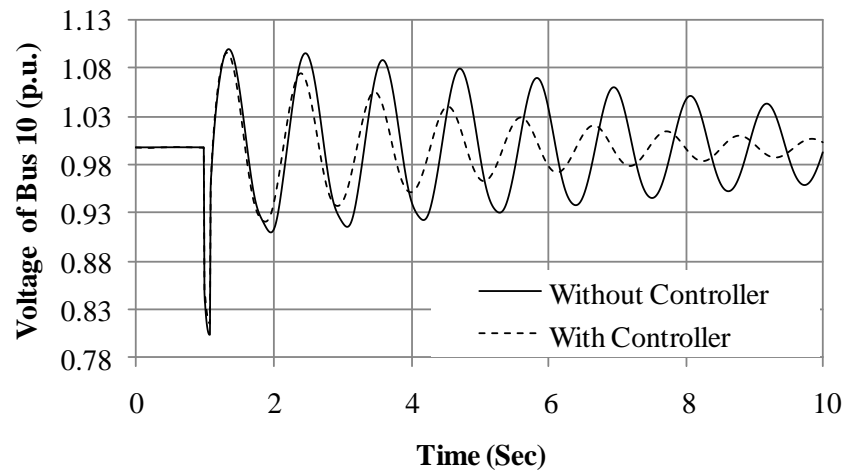
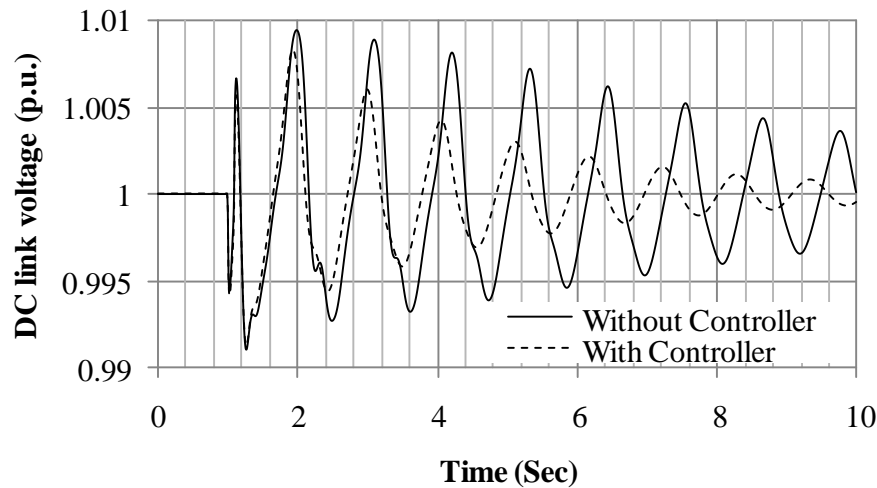


Figure 78: Comparison of time domain responses of voltage at Bus 10 with and without controller.



Similarly, time domain response of the DC-link voltage of the PV was observed under a similar disturbance scenario. The result is shown in Figure 79. It can be seen that oscillation in the DC-link voltage is better damped with the controller than without. It should be noted that emerging distribution systems typically have a number of renewable energy-based distributed generators, whose outputs depend upon the weather conditions. A PV system generates power based on available solar radiation and temperature as discussed in section 3.2. Hence, oscillation damping from a PV generator is not possible on a cloudy day, unless there is a provision for energy storage. In such a scenario, a wide area coordinated control of a number of DG units and reactive power compensators may be designed. Then, any of the DG units may utilise their available energy to support oscillation damping based on wide area measurement data. This issue will be addressed in future works.

Figure 79: Comparison of time domain responses of DC-link voltage with and without controller.



Generally, PI control is used for both rotor and stator converters in DFIG to control direct and quadrature (q) axis currents for the enhancement of system stability. However, it is difficult to find the PI parameters systematically and this type of controller cannot guarantee stability under different operating conditions. In the next section a robust control methodology is presented for the enhancement of small signal stability which ensures stability under varying operating conditions.

#### 6.1.11. Control of DFIG

Given the structure of a doubly-fed induction generator (DFIG) based wind generation system, which is dominated by controllers, one of the controllers of DFIG may also be employed for improving the oscillation damping. In this section also, damping of a low frequency oscillation in a distribution network is discussed. The network consists of synchronous generators, a squirrel cage induction generator, a photovoltaic (PV) generator and a DFIG. The impact of DFIG power on a low frequency mode is systematically assessed. Then, a robust control methodology is proposed for a DFIG system to enhance the damping of low frequency oscillations.

As a DG unit, DFIG is usually operated at a desired power factor. It is obvious that active and reactive power output of a DFIG is determined by terminal voltage and input current. In a distribution network, terminal voltage is governed by the operating condition of the distribution network and input current is determined by the availability of real power on the generator shaft. Therefore, it is convenient to control rotor currents to obtain a desired ratio of active to reactive

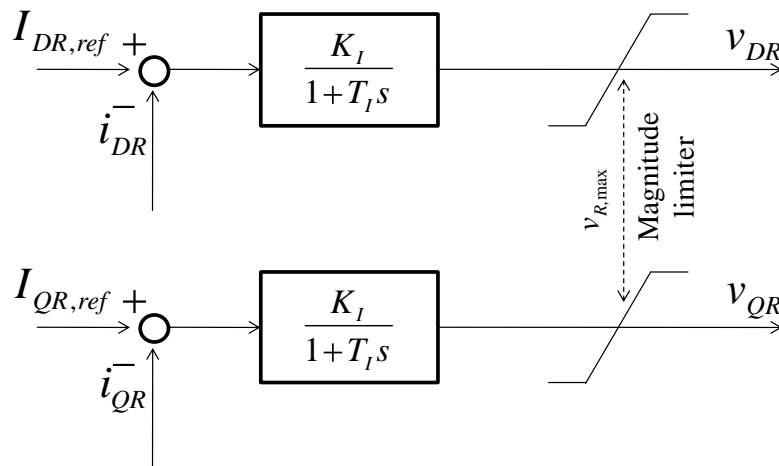
power. Based on the desired output powers  $P_{DFIG}$  and  $Q_{DFIG}$ , rotor reference currents can be calculated as:

$$I_{DR,ref} = -\frac{P_{DFIG}}{|v_s|} \frac{L_s}{L_m} \quad (5.9)$$

$$I_{QR,ref} = \frac{Q_{DFIG}}{|v_s|} \frac{L_s}{L_m} - \frac{|v_s|}{L_m} \quad (5.10)$$

Once the reference currents are determined, rotor current control can be achieved by PI controllers, which generate reference values for the rotor side converter (RSC). The block diagram of the scheme is shown as Fig. 80.

Figure 80: Scheme for rotor current control.



The corresponding rotor voltages are provided by the RSC based on so called vector control. It should be noted that outputs of the current controllers have to be transformed to the common reference frame before using as a reference for an RSC.

### 6.1.12. Design for a robust damping controller

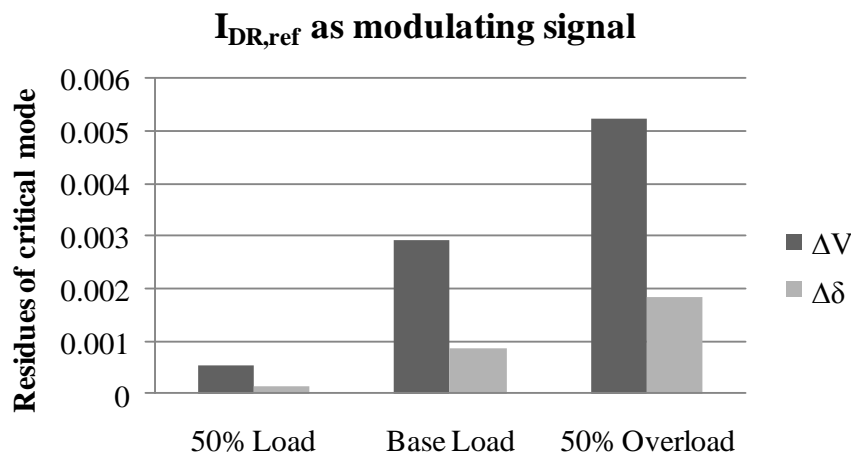
The controllers designed by classical control techniques have their validity restricted to a nominal operating point at which the system is linearised. But a power system constantly experiences changes in operating conditions due to variations in load generation patterns and variations in transmission networks. In addition, some uncertainty is introduced into the power system model due to inaccurate approximations of the power system parameters, neglecting high frequency dynamics and assumptions made in the modelling process. Hence it is desirable to have a robust damping controller to ensure adequate damping under a range of system operating conditions.

In this study, Glover-McFarlane  $H_\infty$  loop shaping design has been employed for a robust controller design [116].  $H_\infty$  optimal design was preferred as this technique has less computational burden than other robust control techniques [117]. The design approach for the robust controller is discussed in this section.

### 6.1.13. Selection of control signals

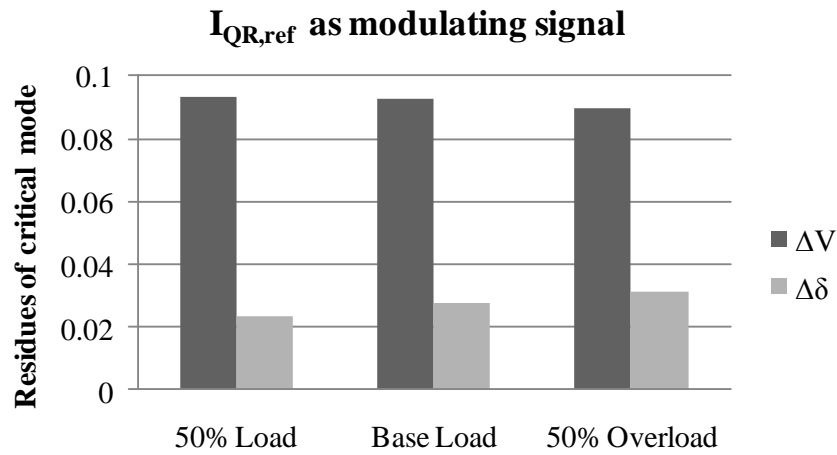
The residue method is used to select the best control signal for the robust controller. Two local signals, i.e. deviations of magnitude of DFIG terminal voltage ( $\Delta V$ ) and phase angle ( $\Delta\delta$ ), were taken as possible signals for a feedback controller. The residues of critical mode when  $I_{DR,ref}$  is used as a modulating signal is shown in 81.

Figure 81: Residues of system when d-axis rotor current of DFIG is modulated.



It can be seen that using  $\Delta V$  as a feedback signal gives larger residue values at loading conditions of a distribution system. Hence,  $\Delta V$  is an appropriate feedback signal for a controller when  $I_{DR,ref}$  is used as a modulating signal. Similarly, the residues of critical mode when  $I_{QR,ref}$  is used as an input signal are shown in **Error! Reference source not found.82**. It can be seen that  $\Delta V$  has a larger magnitude of residue than  $\Delta\delta$  in different loading conditions of the distribution system. Hence,  $\Delta V$  is an appropriate feedback signal for a controller when  $I_{QR,ref}$  is used as a modulating signal.

Figure 82: Residues of system when d-axis rotor current of DFIG is modulated.



It is obvious from Equations (5.9) and (5.10) that power factor control can be achieved by modulating either  $I_{DR,ref}$  or  $I_{QR,ref}$ . Hence, the input signal which gives larger values of residues when  $\Delta V$  or  $\Delta\delta$  is used as a feedback signal can be used as the input modulating signal. It can be seen from **Error! Reference source not found.5.18** and **Error! Reference source not found.5.19** that using  $I_{QR,ref}$  as a modulating signal gives larger values of residues in all cases, hence,  $I_{QR,ref}$  has been used as a modulating signal.

#### 6.1.14. Controller design

Robust controller design procedure involves two steps – loop shaping and controller synthesis.

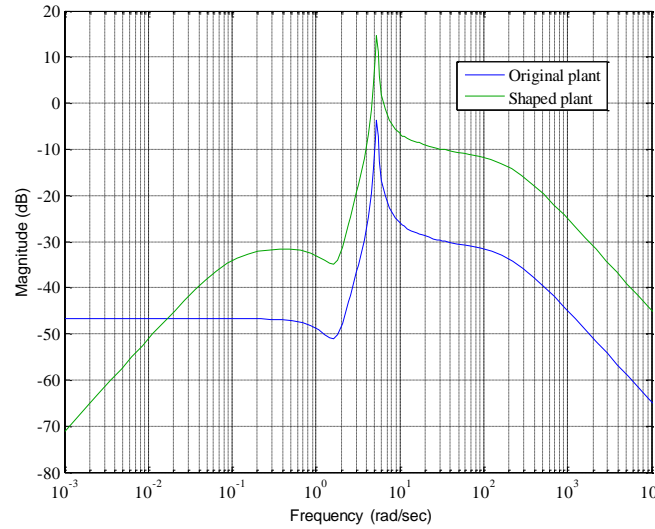
##### Loop shaping

In this case, the open loop system is shaped by a weighting function  $W_a$  to increase the open loop gain around the frequency of critical mode. The weighting function used in this paper is given as:

$$W_a = \frac{6 \times 5s(1 + 0.33s)}{(1 + 5s)(1 + 0.2s)} \quad (5.11)$$

The weighting function  $W_a$  was determined by adding poles and zeros to the open loop system so that gain was increased only at the desired frequency range. The addition of a zero ensures that the controller has zero DC gain. Similarly, a washout filter with a time constant of  $5s$  ensures that the controller only works in a transient state. The addition of a pole at  $1+j0.2$  and a zero at  $1+j0.33$  increases the gain around the frequency of interest so that disturbances get attenuated effectively. The response of the shaped plant was compared with the response of the original plant, and the result is shown in Fig. 83. It can be seen that the open loop gain of the shaped plant is significantly improved at the frequencies of interest.

Figure 83: Comparison of open loop gains of the original and the shaped plant.



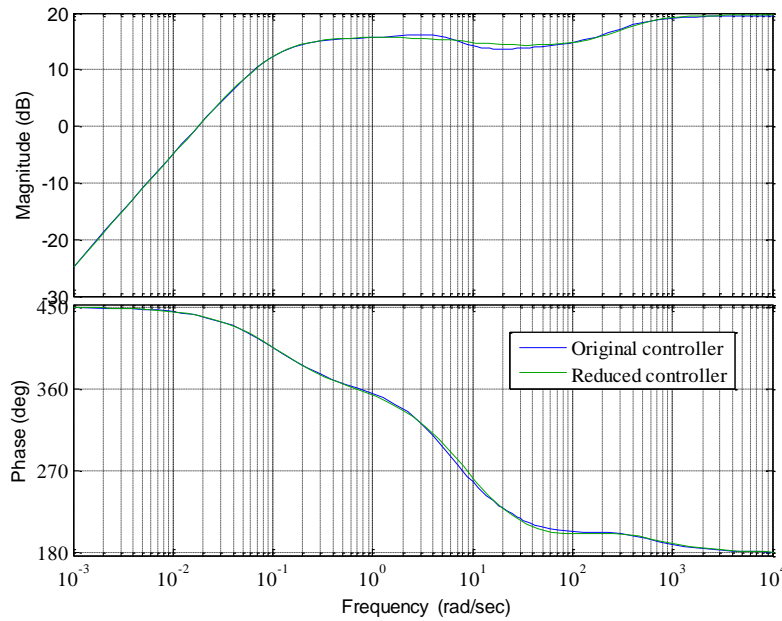
### Controller Synthesis

In this case,  $\varepsilon_{\max}$  was found to be 0.956. Hence, a robust controller was defined by selecting  $\varepsilon \leq 0.956$  and synthesizing a controller, which is given as:

$$\left\| \begin{bmatrix} I \\ K_{\infty} \end{bmatrix} \left( -P_s K_{\infty} \right)^{-1} \tilde{M}_s^{-1} \right\|_{\infty} \leq 0.956^{-1} \quad (5.12)$$

For easy implementation, the controller was further reduced to a third order using the method of balanced model reduction. The responses of the reduced and original controllers are similar to those shown in Fig. 84, hence the reduction of order of the controller is justified.

Figure 84: Comparison of responses of original and reduced controller.

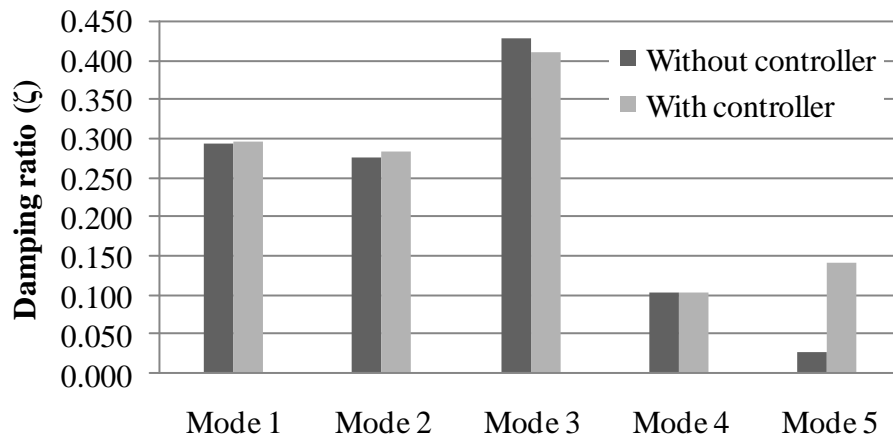


### Performance evaluation

#### Damping ratios

The effectiveness of the controller was evaluated by observing its effect on the damping ratios of all the modes of the distribution system. The damping ratios of all modes for base case and after controller installation are compared and the results are shown in Fig 85. It can be seen that the robust controller effectively improves the damping ratio of critical mode to 0.141. The impacts on damping ratios of the other modes are negligible. Hence, the controller effectively improves the damping of the critical mode without adversely affecting the damping of the other modes.

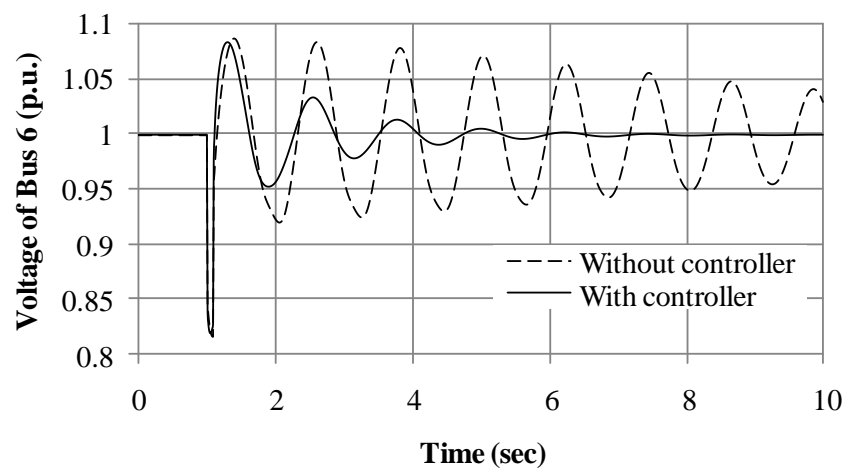
Figure 85: Comparison of damping ratios of the modes with and without robust controller.



### ***Time domain response***

The effectiveness of the controller for reducing time domain response of the system was observed. A three phase fault was applied at Bus 3 and cleared after 100 ms. The response of voltage at Bus 6 was observed, and the result is shown in Fig 86. It can be seen that the originally low damped oscillation damps out within 10s of the controller being installed. Hence the controller significantly improves the damping of low frequency oscillations.

Figure 86: Comparison of time domain response of the bus voltage with and without robust controller.



### Robustness

Eigenvalue analysis was carried out at different operating points of the system to verify the robustness of the controller. In this paper, the system loading and output powers from PV and wind have been considered as uncertain parameters of the system. Accordingly, different operating points have been derived based on their extreme cases. When any of the system parameters i.e. system loading, PV output or wind speed fall below 50% of their normal values, it is considered to be a 'low' case. On the other hand, when they increase beyond 50% of the normal value, it is considered to be a 'high' case.

Damping ratios were calculated for different operating points. The results are tabulated in **Error! Reference source not found.**<sup>35</sup>. It can be seen that the controller maintains the damping ratio of the critical mode at different system operating conditions. Hence, the result proves the robustness of the controller.

Table 35: COMPARISON OF DAMPING RATIOS AT DIFFERENT OPERATING CONDITIONS OF THE DISTRIBUTION SYSTEM.

PV power	Wind power	System Load	Damping ratio ( $\zeta$ ) of critical mode
Low	Low	Low	0.148
Low	Low	High	0.137
Low	High	Low	0.148
Low	High	High	0.137
High	Low	Low	0.148
High	Low	High	0.137
High	High	Low	0.148
High	High	High	0.137

There are different types of DG units, for example, PV, DFIG and DDWG present in distribution systems and operating simultaneously. It is obvious that the interactions between different controllers can degrade the overall performance of the system under certain operating conditions. Next a coordinated robust decentralised controller is presented that ensures stability in the

presence of load and interconnection uncertainties, enhancing both dynamic voltage and transient stabilities.

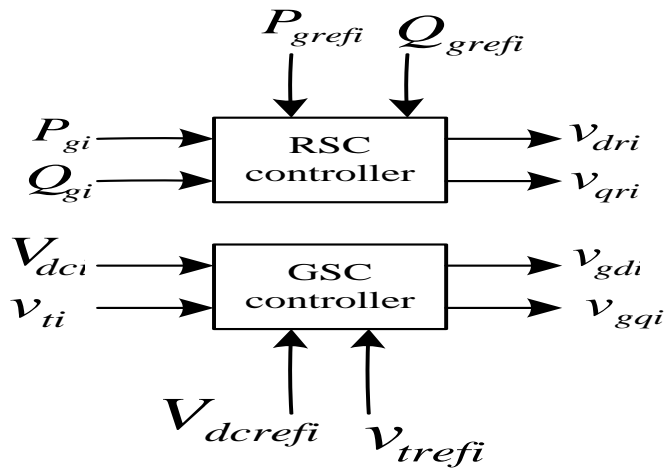
## 6.2. Robust decentralised control for flexible DG integrations

This section presents a decentralised control strategy for integrating distributed generators without violating system operating constraints. A systematic procedure is developed and a robust control designed to ensure both dynamic voltage and transient stability for a specified integration level. A robust output feedback linear quadratic control is synthesized for both wind turbines and photovoltaic (PV) generators. It is shown that the penetration levels of DG units are not only limited by the voltage constraints but also, in certain cases, by the dynamic voltage stability. This designed control scheme enhances the integration level in a distributed system. Its effectiveness is verified on a three feeder test of a system experiencing large disturbances. This test system is modified by connecting DFIG ( $DG_1$ ) at Bus 6, DDWG at Bus 1 ( $DG_3$ ) and PV at Bus 3 ( $DG_2$ ).

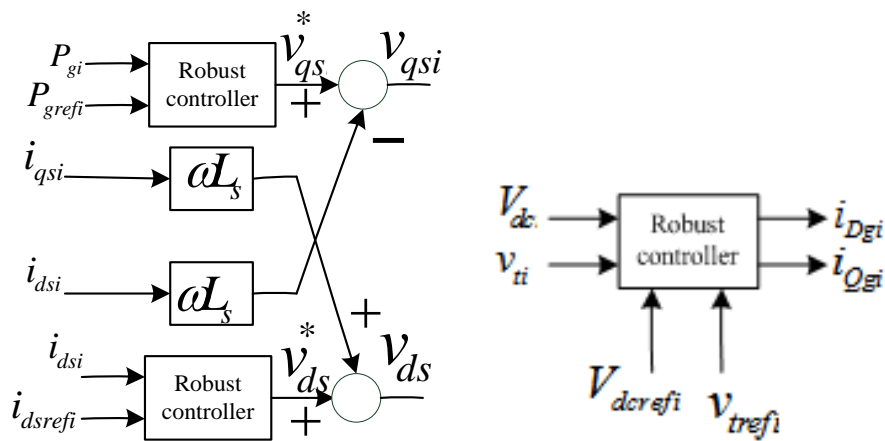
### 6.2.1. Control strategies for DG units

In this section we propose a decentralised control for DG accommodation where the system includes DFIGs, DDWGs and PV generators. The controllers, both GSC and RSC of a DFIG are shown in Fig. 87 (a). The function of the rotor side converter control is to limit the rotor fault current and to increase the damping of stator flux and consequently to enhance the ride-through capability. The main objective of the GSC control is to keep the DC voltage constant and to regulate the reactive current for controlling generator reactive power. Since the DC link dynamics are nonlinear, the conventional linear control cannot properly limit the DC voltage under severe voltage dips. Therefore, by using the proposed control approaches the wind generator contributes to grid stability by controlling both active and reactive power taking into account the nonlinearity of wind generators.

Figure 87: (a) Control strategy for DFIG.

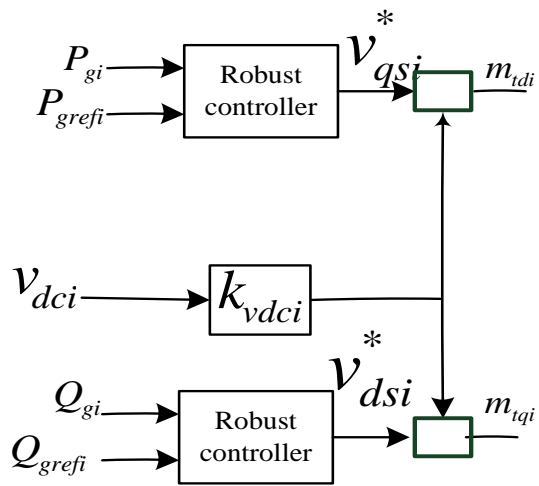


(b) Generator-side converter control and 5.24. (c) and grid-side converter control.



The functions of the generator-side converter of a DDWG are: to control the output power, to track the input of the wind input torque and to minimise the power loss of the generator. On the other hand the grid-side converter control maintains the DC and terminal voltages. The control strategies are shown in Figs. 87 (b) and 87 (c).

(d) Control strategy for PV.



In the voltage control mode of PV,  $P$  is controlled by the phase angle and  $Q$  is controlled by the amplitude of the VSC terminal voltage. The control strategy in the  $d$ - $q$  frame is shown in Fig. 87 (d).

### 6.2.2. Problem formulation

The power system model used in this paper is described by the following large-scale system ( $S$ ) comprising  $N$  subsystems  $S_i, i=1, 2, \dots, N$  [181], [182]:

$$S_i : \dot{x}(t) = A_i x_x(t) + B_i u_i(t) + E_i \xi_i(t) + L_i r(t) \quad (5.13)$$

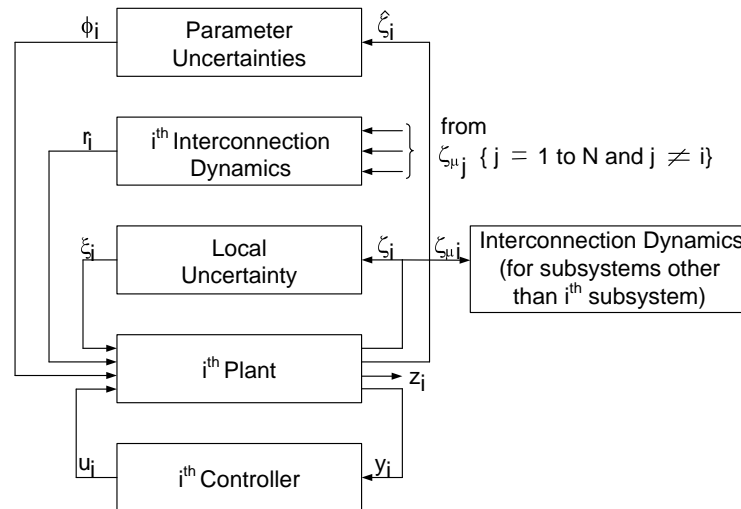
$$z_i(t) = C_i x_x(t) + D_i \xi_i(t) \quad (5.14)$$

$$\zeta_i(t) = G_i x_x(t) + H_i u_i(t) \quad (5.15)$$

$$y_i(t) = C_{yi} x_x(t) + D_{yi} \zeta_i(t) \quad (5.16)$$

where  $x_i \in R^{n_i}$  is the state vector,  $u_i \in R^{m_i}$  the control input,  $\xi_i \in R^{p_i}$  the perturbation,  $\zeta_i \in R^{h_i}$  the uncertainty output,  $z_i \in R^{q_i}$  the controlled output,  $y_i \in R^{g_i}$  the measured output, and the input  $r_i$  describes the effect of the other subsystems ( $S_1, \dots, S_{i-1}, S_{i+1}, \dots, S_N$ ) on subsystem  $S_i$ . The structure of system  $S$  is shown in Fig. 88.

Figure 88: Block diagram of decentralised control.



The system models (5.13) to (5.16) reflect the nature of a generic interconnected uncertain system in which each subsystem is affected by uncertainties that have two sources. Local uncertainties in the large-scale system arise from the presence of uncertain dynamics in each subsystem. Such dynamics are driven only by the uncertainty output ( $\zeta_i$ ) of subsystem  $S_i$ . A second source of uncertainties arises from interactions between the subsystems of the large-scale system. Indeed, the partitioning of a complex uncertain system into a collection of subsystems ( $S_i$ ) results in the uncertainty of the original system being distributed among the subsystems. This provides the motivation for treating the interconnections as uncertain perturbations.

The power system under consideration satisfies the assumptions of:

- (i)  $D_i^T D_i + G_i^T G_i > 0$  and  $D_{yi} D_{yi}^T > 0$ ;
- (ii) the pair  $(A_i, C_i^T C_i)$  is observable; and
- (iii) the pair  $(A_i, B_i^T B_i)$  can be stabilised.

We define  $\zeta_i = \Delta_i \xi_i$  and  $r_i = \Delta_{ij} \xi_i$  where  $\Delta_i$  and  $\Delta_{ij}$  are the uncertain gain matrices. The uncertainty and interconnection must satisfy the following conditions:

$$\|\zeta_i\|^2 \leq \|\xi_i\|^2 \text{ and } \|r_i\|^2 \leq \|\xi_i\|^2. \quad (5.17)$$

The robust output-feedback controller designed in this paper minimises the cost (Equation 5.18) subject to the above Equation (5.17) bounds on the local uncertainty and interconnections. Associated with the uncertain system [Equations (5.13)-(5.16)], we consider a cost function of the form:

$$\int_0^\infty \sum_{i=1}^N \|z_i(t)\| dt \quad (5.18)$$

The min-max optimal control finds the controller which minimises the above cost function over all admissible uncertainties which satisfy the following relationship:

$$\inf_{u_i, i=1 \dots N} \sup_{\Xi, \Pi} \int_0^\infty \sum_{i=1}^N \|z_i(t)\| dt \leq \inf_{\Gamma} \sum_{i=1}^N x_{i0}^T [X_i + \tau_i M_i + \theta_i \bar{M}_i] x_{i0} \quad (5.19)$$

where  $[x_{i0} \dots x_{N0}]$  is the initial condition vector,  $\Xi$  is a set of all admissible uncertainties,  $\Pi$  is a set of interconnection inputs,  $\Gamma = \{\{\tau_i, \theta_i\}_{i=1}^N \in R^{2N}\}$ , is a set of vectors, and  $M_i > 0$  and  $\bar{M}_i > 0$  are two positive definite symmetrical matrices. Matrices  $X_i$  and  $Y_i$  are the solutions to the following pair of parameter-dependent coupled algebraic equations [181]:

$$A_i^T Y_i + Y_i A_i + Y_i \bar{B}_{2i} \bar{B}_{2i}^T Y_i - [C_{yi}^T W_i^{-1} C_{yi} - \bar{C}_i^T \bar{C}_i] = 0, \quad (5.20)$$

$$A_i^T X_i + X_i A_i + \bar{C}_i^T \bar{C}_i - X_i [B_i R_i^{-1} B_i^T - \bar{B}_{2i} \bar{B}_{2i}^T] X_i = 0, \quad (5.21)$$

where  $R_i = \bar{D}_i^T \bar{D}_i$ ,  $W_i = \bar{D}_{yi} \bar{D}_{yi}^T$  and  $\bar{\theta}_i = \sum_{n=1, n \neq i}^N \theta_n$ ,

$$\bar{C}_i = \begin{bmatrix} C_i \\ \mathbf{e}_i + \bar{\theta}_i \mathbf{r}_i^2 H_i \end{bmatrix}, \quad \bar{D}_i = \begin{bmatrix} D_i \\ \mathbf{e}_i + \bar{\theta}_i \mathbf{r}_i^2 G_i \end{bmatrix},$$

$$\bar{B}_{2i} = \begin{bmatrix} \mathbf{I}_i^{-1/2} E_i & \theta_i^{-1/2} L_i \end{bmatrix}, \quad D_{yi} = \begin{bmatrix} \mathbf{I}_i^{-1/2} D_{yi} & 0 \end{bmatrix}.$$

These solutions are required to satisfy the following conditions:

$$\tau_i > 0, \theta_i > 0, X_i \geq 0, Y_i \geq 0 \text{ and } Y_i > X_i.$$

Then, the controller is designed using the equations:

$$\dot{x}_{ci} = \{A_i - [B_i R_i^{-1} B_i^T - \bar{B}_{2i} \bar{B}_{2i}^T] X_i\} x + [Y_i - X_i]^{-1} C_{yi}^T W_i^{-1} [y_i(t) - C_{yi} x_{ci}] \quad (5.22)$$

$$u_i = -R_i^{-1} B_i^T X_i x_{ci}. \quad (5.23)$$

### 6.2.3. Case studies

Before designing a controller, we consider a number of hypothetical situations in order to gain a deeper insight into the complex issues involved and to consider the factors that might limit the DG integration level. A few of them are presented below.

#### 6.2.4. Integration level with voltage control capability

It is well known that IEEE Std 1547-2003 does not allow DG units to actively regulate voltage at the point of common coupling (PCC). This is true in Australia for a DG with a capacity of less than 30 MW and also the power factor of DG units must lie between unity and 0.95 (leading) for both 100% and 50% real power injections. However, a DG embedded with a voltage control capability can significantly enhance the penetration level.

In this analysis, we consider two cases: (i) DG units without a voltage control capability (operated at unity power factor as suggested by IEEE 1547); and (ii) DG units with a voltage control capability. We allow a maximum  $\pm 10\%$  voltage variation in the DG buses. The maximum penetration levels for the DGs in three different buses, which are limited due to the voltage rise problem, are given in Table 36. The penetration level at Bus 6 can be increased by 54.16% and 66.67% if the DG units are operated in power factor and voltage control modes respectively. From Table 36 it is clear that more DG units can be accommodated if they are installed with voltage control operating modes.

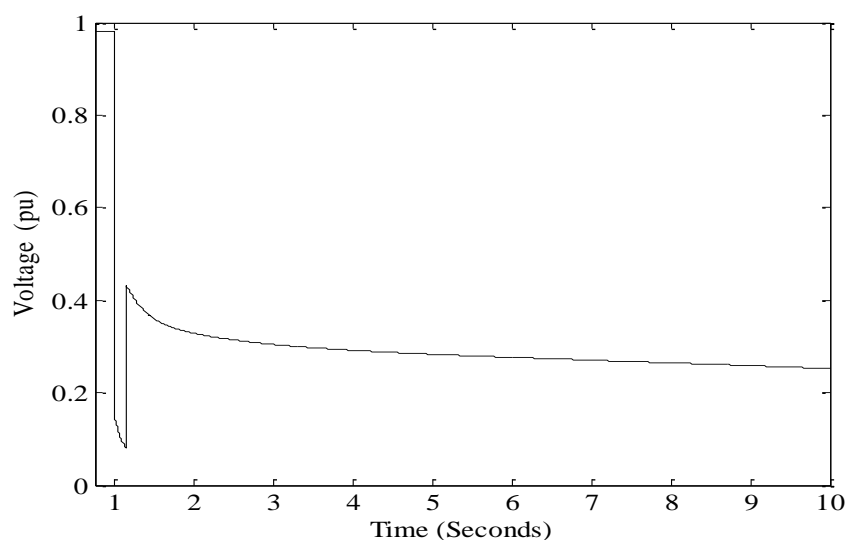
Table 36: PENETRATION LEVELS AT DIFFERENT OPERATING MODES

Control mode	Bus 1 (MW) DG <sub>3</sub>	Bus 3 (MW) DG <sub>1</sub>	Bus 6 (MW) DG <sub>2</sub>
No control (unity pf)	9.15	7.75	12
Power factor	12.5	11.5	18.5
Voltage	15.75	13.5	20

#### 6.2.5. Transient voltage variation and voltage stability

Although in general DG integration is only limited by voltage rise, the transient and voltage stabilities can also limit large-scale DG integration under very stressed operating conditions. To study this, the test system is congested by increasing the load demand and transmission line length to twice those given in [156]. Under these stressed conditions, a wind farm comprised of DFIGs with a total capacity of 30 MW can be accommodated at Bus 6 without violating the voltage constraint. Fig. 89 shows the terminal voltage of a DFIG for a three phase fault at Bus 6 which is subsequently cleared after 0.15s. It is clear that although it satisfies a steady state voltage variation, the system becomes unstable due to its nonlinear dynamics.

Figure 89: Terminal voltage of DFIG for three-phase fault at Bus 7.



### 6.2.6. Control algorithm

In this section, a controller for accommodating DG units that ensures dynamic stability and provides the required steady state voltage is designed. The test system is divided into three subsystems: (i) a DFIG (ii) a DDWG and (iii) a PV with a controller designed for each subsystem. The structure of the controller is shown in Fig. 88 and the control design algorithm is as follows:

- (i) Solve the base case power flow and monitor the bus voltage;
- (ii) First, linearise the complete system about the desired equilibrium point: one part consists of the states of the devices in the subsystem ( $x_i$ ) and the other part consists of the rest of the states ( $r_i$ ). The matrices  $A_i$  and  $L_i$  are appropriately chosen from the complete linearised model equations. Second, determine the other matrices given in the problem formulations in Section 5.5.2 corresponding to the control input, measured output and control variable;
- (iii) Increase the generation profile, perform a power flow and check the bus voltage again; if the bus voltage is within the statutory limit ( $\pm 10\%$  of nominal voltage), go to (iv). Otherwise go to (ix);
- (iv) Obtain the uncertain matrix ( $E_i$ ) taking the difference between the matrices of subsystem  $A_i$  for the nominal and the increased generations;
- (v) Solve the optimisation problem using the line search technique for the positive values of  $\tau_i$  and  $\theta_i$  which can be achieved by the MATLAB function *fmincon* with a proper initialisation;
- (vi) Substitute the values of  $\tau_i$  and  $\theta_i$  and solve the Riccati equations given in (5.20) and (5.21);
- (vii) Design the controller according to Equations (5.22) and (5.23); if a feasible controller is obtained, go to the next section, otherwise go to (x);
- (viii) Perform a time domain simulation and evaluate the controller's performance for the worst case scenario;
- (ix) If the controller satisfies both the static and dynamic constraints, go to (ii), otherwise go to (x);
- (x) Stop and specify the upper level of DG integration.

### 6.2.7. Controller performance evaluation

The upper levels of DG penetration using the abovementioned procedure are given in Table 5.6. To assess the performance of the designed controller, the integration level using a conventional PI controller was also determined. The controller's performance was verified for the upper integration

level for a three phase fault at Bus 6 using  $DG_1=18.5$  MW,  $DG_2=30$  MW and  $DG_3=16.25$ . A symmetrical three phase fault was applied at 1s and cleared after 0.15 s. Fig. 5.28 shows the terminal voltage of the DFIG using both the proposed robust control and the conventional control from which it is clear that, when using the PI control, the voltage collapses. However, the robust performance of the designed controller ensures stability.

Table 37: Penetration levels using proposed controls

Control	Bus 1 (MW) PV	Bus 3 (MW) DDWG	Bus 6 (MW) DFIG
Robust control	16.25	18.5	30
PI control	14.65	16.75	26.5

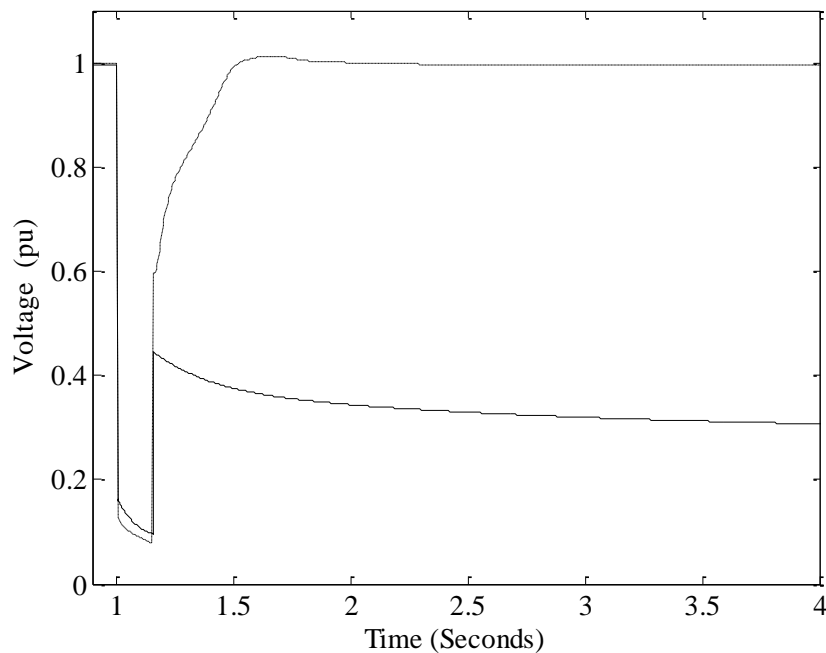


Figure 90: Terminal voltage of DFIG (solid line proposed control and dotted line conventional control).

Figs. 90 and 91 show the terminal voltage and speed response of the DFIG during islanding from which it is clear that, although both controllers ensure stable operation, the designed controller provides better performance in terms of damping oscillations and settling time. The terminal voltage of the PV generator during sudden islanding is shown in Fig. 92 from which it is clear that the proposed control strategy provides better performance for PV as well.

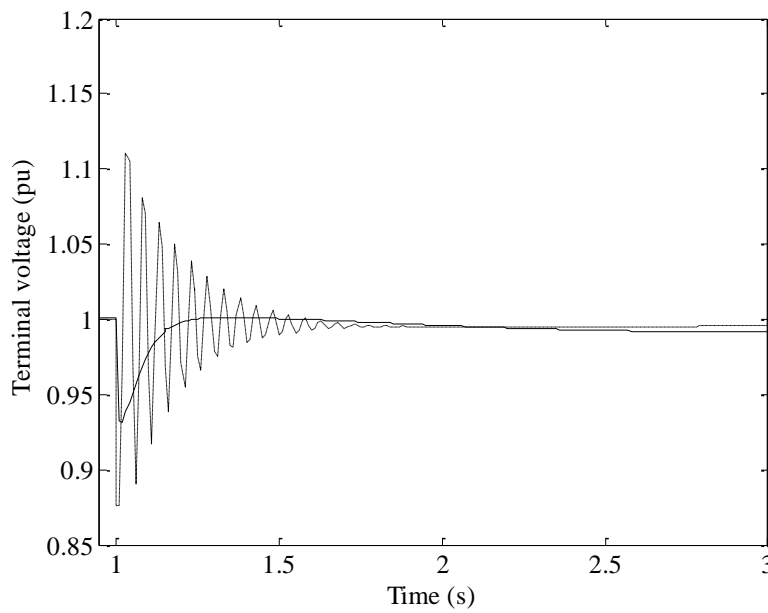


Figure 91: Terminal voltage of DFIG during islanding (solid line proposed control and dotted line PI).

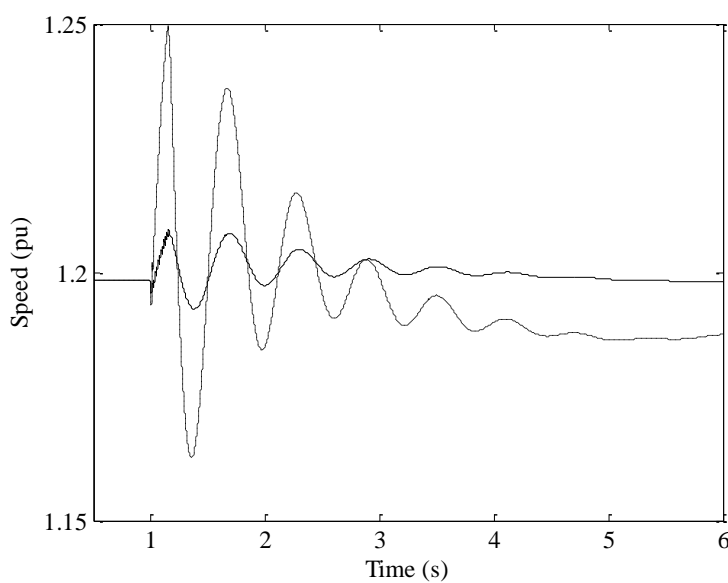


Figure 92: Speed response of DFIG during islanding (solid line proposed control and dotted line PI).

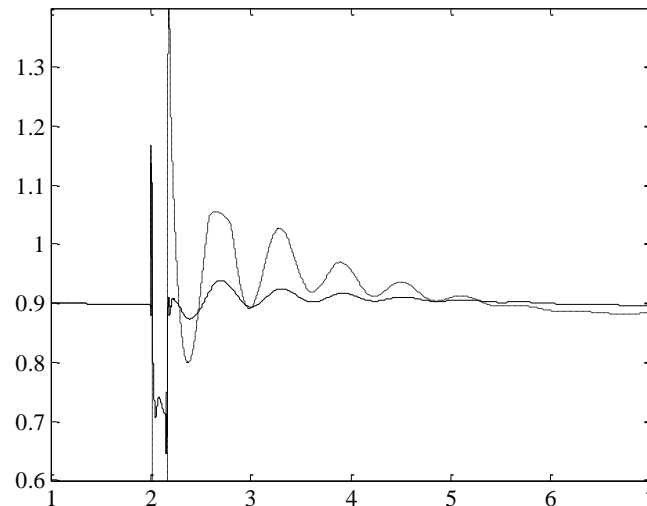


Figure 93: Terminal voltage of PV during islanding (solid line proposed control and dotted line PI).

### 6.3. Summary

This section summarises the findings on the performance of the proposed controller of a distribution system with DG units. The studies can be classified into three broad categories as presented above, namely enhancement of (a) small signal stability through shunt control and DG control (b) dynamic voltage stability and transient stability with coordinated decentralised control of DG units.

#### 6.3.1. Enhancement of small signal stability

Oscillatory modes with frequencies of 1.5 Hz to 4 Hz were observed for the distribution system with DG units. Some of them are low damped modes which may be harmful to the stability of a system. This study also demonstrated that the induction generator along with synchronous generator participated positively on oscillatory modes.

It was shown that the small signal stability of the distribution network can be ensured by installing a damping controller at a capacitor bank. The controllability index identified the best capacitor bank for installing such a controller. It was demonstrated that the proposed controller could improve the damping ratio of a low damped mode. The desired damping ratio can be achieved by selecting

appropriate values of time constants and gain of the controller. The designed controller improved the damping ratio from 2% to the desired value, i.e. 5%. Hence, it can be concluded that regulating susceptance of a capacitor bank is an effective means of small signal stability enhancement in a renewable energy-based distribution system.

In different loading conditions of the distribution system, the q-axis component of PV current has been found to be a better modulating signal compared to other measurable signals for designing an additional damping controller. The critical mode was better damped when there was reactive power support from a PV generator in a distribution system. Hence, operating PV at a lower factor than unity has a better impact on damping of the critical mode. In different loading conditions of a distribution system, the critical mode has a higher sensitivity with respect to the reactive power of PV as compared to the active power. So, reactive power control of PV seems to be better for damping of low damped excitation modes.

The chapter also demonstrates that reactive power support from DFIG is beneficial to the damping of the critical mode. The critical mode is more sensitive to reactive power modulation than is active power modulation. Furthermore, active and reactive powers can be modulated by controlling the rotor currents. The  $Q$ –axis component of rotor current is a more effective control signal than the  $D$ –axis component of rotor current.

Also, the additional controllers were found to be able to improve the damping of the critical mode effectively by shifting the eigenvalues to desired locations. A desired damping ratio was achieved by selecting an appropriate value of controller gain. The controller was found to affect only the critical mode while the other modes are unaffected. While the damping ratio of the critical mode was significantly improved, damping ratios of other modes were not significantly affected. The controllers improved the time domain response of the distribution system. The robust controller for DFIG performed excellently at different operating conditions of the distribution system, i.e. different conditions of wind, solar irradiation and system loading.

### 6.3.2. *Augmentation of dynamic voltage and transient stabilities*

DG's penetration level can be significantly enhanced when it operates in a voltage control mode instead of the unity power factor recommended by the IEEE 1547 standard. Transient voltage variations and dynamic voltage instability can also limit DG penetration although voltage rise is a major constraint when accommodating DG units. From the simulation results it is shown that the

proposed robust control method can augment the potential penetration of DGs without requiring network reinforcements or violating a system operating constraints.

#### 6.4. Software section

A MATLAB/Simulink-based dynamic model of a distribution system was constructed for this study. This software utilises some of the MatLab commands and other user defined routines for the analysis. It has the flexibility to expand in the future as per requirements. Currently the software has the following major capabilities applicable for small signal stability analysis.

##### ***Initialisation***

This command initialises the dynamic variables of the machines for dynamic simulation. Inputs to this command are line data, bus data, generator data and constants of the controllers.

##### ***Networksolver***

Network solver is a Simulink model of the distribution system with DG units and controllers. It has the facility to observe time domain responses of the bus voltages, generator rotor angles and rotor speeds.

##### ***Eigensensitivity***

This command calculates eigenvalue sensitivity of a mode with the specified parameter of the distribution system.

##### ***Participation***

This command calculates participation factors of the state variables on different modes.

##### ***Rlplot***

This command generates the root-locus plot of the steady state system.

##### ***Controller design***

This command evaluates the parameters of controller design based on classical residue technique.

##### ***Robust controller***

A routine called 'eihinfy' has been developed to determine the parameters of a robust controller designed for a DG unit. This function also includes an embedded routine for system reduction.

##### ***Decentralised controller***

In this work, the controllers were designed using Matlab and then simulations were carried out with the nonlinear dynamic models and widely used power system simulator (PSSE).

## 7. CONCLUSIONS AND KEY FINDINGS FROM THIS PROJECT

Penetration of Distributed Generation (DG) is gradually increasing in power systems all around the world and they are typically integrated into distribution systems. The increasing integration of DG has raised many concerns and challenges about the operation and control of distribution and entire power systems. Voltage instability and small signal instability are the two major concerns for DG-integrated distribution systems. Although distributed generation integration has a number of obvious benefits such as loss reduction and reliability improvement, it may give rise to some voltage instability issues as a result of the source characteristics and the ways they are asked to operate. With increased penetration of DG, small signal instability can also be a critical issue due to its cumulative behaviour and interactions which can limit the penetration level. Advanced control methodologies need to be developed to address these issues. In this research, a number of studies were carried out to gain a deeper understanding of the instability problems and to develop methodologies to mitigate them. The key findings from this work are highlighted in the next section.

### 7.1. Key findings

#### 7.1.1. *Voltage stability study*

With increased penetration of DG units, early tripping of DG due to local disturbances can reduce the stability of the whole system. The grid standards which have been developed to address this issue require system stability under steady state and fast voltage recovery under abnormal conditions. In this research, a grid compatible methodology was proposed to control voltage and reactive power.

#### 7.1.2. *Reactive power margin index*

An accurate representation of loads in a distribution system plays a significant role in understanding voltage instability and system collapse. Developing a proper load model is always a challenge due to factors such as a large number of loads and time/weather dependence of these loads. A number of commonly used stability indices have failed to detect a weak bus with specific load models. This research found that reactive power margin is a reliable index to determine critical or weak buses while considering the influence of load uncertainties.

### 7.1.3. *Proper DG placement*

A methodology was developed to determine the optimal location and size of synchronous and induction generator-based DG units, taking into account their reactive power capabilities. It has been found that placing synchronous generators (SG) on weak buses improves voltage stability and increases loadability of the distribution system. The rate of increase of loadability is greater with an SG at a “weak bus” rather than a “strong bus”. To avoid a reduction of loadability and to improve voltage stability, induction generator-based DG units need to be placed at strong buses. The notion of weak and strong buses is defined based on the reactive power margin available at the node. The node with the largest reserve of reactive power is identified as a strong bus while the node with the lowest margin is defined as a weak bus.

### 7.1.4. *Enhancement of steady state and dynamic voltage stability*

A complete methodology based on the index, have been formulated for the normal operation and post-fault voltage recovery according to current practices of grid codes and standards. The index is based on the sensitivity of terminal voltage with respect to the reactive current injection. Grid codes demand voltage recovery within a short time frame (e.g. 2sec in the IEEE grid code 1547 and in AEMO requirements) after a fault takes place near to a generator bus. This methodology can identify the minimum number of shunt compensation devices required to prevent DG units tripping and allow them to remain connected. The methodology also identifies the correct locations of these devices, which can be capacitor banks and/or STATCOMs.

Our research work shows that appropriate location of DG units can in most cases improve voltage stability. However, for a weakly connected network, proper placement of compensation devices needs to be considered. In many cases, fixed capacitors help to improve the voltage profile in the steady state as well as under abnormal conditions. However, in a few cases, a shunt FACTS device is required to ensure fast voltage recovery. DG in voltage control mode can resolve many issues regarding voltage stability. System specific analysis is required to devise the best solution for actual systems.

### 7.1.5. *Small signal stability study*

Small signal instability could lead to oscillatory instability problems and is considered to be more relevant than the problem of transient instability. This research work shows oscillatory problems can arise with high penetration of DG units in sub-transmission/distribution systems.

#### 7.1.6. *Stability Assessment*

This research attempts to identify possible small signal stability issues which can arise due to a high penetration of DG units in distribution networks. It has been found that a distribution network with DG units oscillates with a frequency around 3 Hz. This frequency of oscillation is slightly higher than that found in similar studies on transmission systems. DG units, not only conventional synchronous generators but also emerging induction generators, can participate in the oscillation in a positive or a negative way. It has been found that a higher penetration of wind and solar DG units enhances damping of oscillatory modes because these units positively participate in oscillation.

#### **Influence of loads on oscillation**

In distribution or sub-transmission networks, the composition of a load has a significant impact on small signal stability and this impact is more pronounced when DG units are present in the system. The percentage of induction motor load and its size influences the damping on critical modes. An increase in percentage of induction motor load increases the damping ratio of the critical mode. Similarly, for small signal stability a detailed dynamic model of an induction motor yields a more optimistic result than a simplified model. This once again confirms the influence of an induction motor on a critical mode and suggests the importance of modelling such loads in small signal stability studies of distribution and sub-transmission systems.

#### 7.1.7. *Control strategy*

##### ***Enhancement of small signal stability***

Shunt compensation devices such as capacitor banks, SVCs and STATCOMs are normally installed for voltage stability enhancement. However, the placement of such dynamic compensating devices with an auxiliary controller can improve the small signal stability. It was found that static reactive power compensating devices may reduce the small signal stability of a network. For example, a shunt capacitor yields a poorer damping ratio on critical mode. On the other hand, DG units installed in a network can be utilised to enhance the network's small signal stability. Given the controller-dominated structure of renewable energy-based DG units such as solar photovoltaic and wind, one or more of the controllers may be employed to support oscillation damping. In this research, a pole placement control strategy for shunt capacitor bank, lead/lag

control of solar photovoltaic and robust control of DFIG were proposed. The controller designed in this research improved the damping ratio from 2% to the desired value, i.e. 5%.

### ***Robust coordinated control for DG units***

The penetration level of DG units is generally constrained by a voltage rise problem in distribution systems. However, transient voltage variations and dynamic voltage instability can also limit DG penetration in stressed systems. When DG operates in voltage control mode instead of at the unity power factor recommended by the IEEE 1547 standard, more DG units can be accommodated. A robust coordinated control method was developed for enhancing dynamic stability of PVs, DFIGs and DDWG-based DG units. This method can augment the potential penetration of DGs without requiring network reinforcements and without violating a system's operating constraints.

Appropriate control of DG can improve the performance of DG units without violating network constraints and it can facilitate the effective participation of DG in a power system and its market operation.

## 8. APPENDIX-A

TABLE A.1: Data of A 16 bus Test System

Bus to Bus	Section Resistance (p.u.)	Section Reactance (p.u.)	End Bus Load (MW)	End Bus Load (MVar)	End Bus Capacitor (MVar)
4-1	0.075	0.1	0.0	0.0	
5-4	0.08	0.11	2.0	1.6	
4-6	0.09	0.18	2.0	0.8	1.2
6-7	0.04	0.04	1.5	1.2	
2-8	0.11	0.11	4.0	2.7	
8-9	0.08	0.11	5.0	3.0	1.2
8-10	0.11	0.11	1.0	0.9	
9-11	0.11	0.11	0.6	0.1	0.6
9-12	0.08	0.11	4.5	2.0	3.7
13-3	0.11	0.11	0.0	0.0	
14-13	0.09	0.12	1.0	0.9	
13-15	0.08	0.11	1.0	0.9	
15-16	0.04	0.04	2.1	1.0	1.8
11-5	0.04	0.04	3.0	1.5	1.1
10-14	0.04	0.04	1.0	0.7	1.8

## Appendix-B

**8.1. List of publications from this project**

1. T. Aziz, T. K. Saha, N. Mithulananthan, "Distributed Generators Placement for Loadability Enhancement Based on Reactive Power Margin," Proceedings of the 9th International Power and Energy Conference IPEC2010, 27–29 October 2010, Singapore.
2. T. Aziz, T. K. Saha, and N. Mithulananthan, "Identification of the Weakest Bus in a Distribution System with Load Uncertainties Using Reactive Power Margin, Proceedings of the 2010 Australasian Universities Power Engineering Conference, Christchurch, New Zealand, 5–8 December 2010.
3. S. Dahal, N. Mithulananthan, and T. K. Saha, "Investigation of Small Signal Stability of a Renewable Energy Based Electricity Distribution System," Proceedings of the IEEE Power and Energy Society General Meeting, 2010, USA, July 2010.
4. S. Dahal, N. Mithulananthan, T. Saha, "Enhancement of small signal stability of a renewable energy based electricity distribution system using shunt controllers", Proceedings of Australasian Universities Power Engineering Conference (AUPEC 2010), Dec 5–8, Christchurch, New Zealand.
5. T. Aziz, Sudarshan Dahal, N. Mithulananthan and Tapan K. Saha, "Impact of Widespread Penetrations of Renewable Generation on Distribution System Stability", Proceedings of 6th International Conference on Electrical & Computer Engineering 2010 (ICECE'10), December 18–20, 2010, Dhaka, Bangladesh.
6. T. Aziz, U. P. Mhaskar, T. K. Saha and N. Mithulananthan. "A Grid Compatible Methodology for Placement of Reactive Power Compensation in Renewable Based Distribution System"-proceedings of the IEEE Power & Energy Society General Meeting (PESGM) 2011, Detroit, Michigan, USA during 24–28 July 2011.
7. S. Dahal, N. Mithulananthan, T. Saha, "An approach to control a photovoltaic generator to damp low frequency oscillations in an emerging distribution system", proceedings of the IEEE Power & Energy Society General Meeting (PESGM) 2011, Detroit, Michigan, USA, 24–28 July 2011.
8. T. Aziz, U. P. Mhaskar, T. K. Saha and N. Mithulananthan. "An Index and Grid Compatible Methodology for Reactive Power Compensation in Renewable Based Distribution System" IEEE transactions on Power systems (2nd review completed).
9. M. J. Hossain, T. K. Saha, and N. Mithulananthan, "Impacts of wind and solar integrations on the dynamic operation of distribution systems", Accepted for the 2011 Australasian Universities Power Engineering Conference, to be held in Brisbane, 25–28 September 2011
10. S. Dahal, N. Mithulananthan, T. Saha, "Impact of Composite Loads on Dynamic Loadability of Emerging Distribution Systems", Accepted for the 2011 Australasian Universities Power Engineering Conference, to be held in Brisbane, 25–28 September 2011.

11. S. Dahal, N. Mithulananthan, T. Saha, "Influence of Composite Loads on Small Signal Stability Performance of Renewable Energy Based Distribution System", Paper submitted for publication in IET Generation, Transmission & Distribution Transaction.
12. S. Dahal, N. Mithulananthan, T. Saha, "Assessment and Enhancement of Small Signal Stability of a Renewable Energy Based Electricity Distribution System", Paper Accepted for publication in the IEEE Transactions on Sustainable Energy (July 2011).
13. J. Hossain, T. K. Saha, N. Mithulananthan, " A Control Methodology for Renewable Energy Integrations in Distribution Systems", Proceedings of IEEE PES Innovative Smart Grid Technology Conference (ISGT2011 Asia), 13-16 November 2011, Perth Australia.

## 9. REFERENCES

- [1] N. Jenkins and Institution of Electrical Engineers., *Embedded generation*. London: Institution of Electrical Engineers, 2000.
- [2] A.-M. Borbely and J. F. Kreider, *Distributed generation : the power paradigm for the new millennium*. Boca Raton: CRC Press, 2001.
- [3] "Draft Standard for Interconnecting Distributed Resources with Electric Power Systems," IEEE.
- [4] T. Ackermann, G. Andersson, and L. Söder, "Distributed generation: a definition," *Electric Power Systems Research*, vol. 57, pp. 195-204, 2001.
- [5] H. Bevrani, Y. Mitani, and K. Tsuji, "Robust load frequency regulation in a new distributed generation environment," in *Power Engineering Society General Meeting, 2003, IEEE*, 2003, p. 553 Vol. 2.
- [6] U. D. o. Energy, "2009 Renewable Energy Data Book " 2010.
- [7] G. X. Luo and A. Semlyen, "Efficient load flow for large weakly meshed networks," *Power Systems, IEEE Transactions on*, vol. 5, pp. 1309-1316, 1990.
- [8] C. S. Cheng and D. Shirmohammadi, "A three-phase power flow method for real-time distribution system analysis," *Power Systems, IEEE Transactions on*, vol. 10, pp. 671-679, 1995.
- [9] Y. Zhu and K. Tomsovic, "Adaptive Power Flow Method for Distribution Systems with Dispersed Generation," *Power Engineering Review, IEEE*, vol. 22, pp. 72-72, 2002.
- [10] S. M. Moghaddas-Tafreshi and E. Mashhour, "Distributed generation modeling for power flow studies and a three-phase unbalanced power flow solution for radial distribution systems considering distributed generation," *Electric Power Systems Research*, vol. 79, pp. 680-686, 2009.
- [11] P. Kundur, "Power System Stability and Control," *Electric Power Research Institute*.
- [12] N. Jenkins, R. Allan, P. Crossley, D. S. Kirschen, and G. Strbac, *Embedded Generations*, 1st ed. London, U.K., 2000.
- [13] B. M. Nomikos and C. D. Vournas, "Investigation of induction Machine contribution to power system oscillations," *IEEE Transactions on Power Systems*, vol. 20, pp. 916-925, 2005.
- [14] L. Holdsworth, X. G. Wu, J. B. Ekanayake, and N. Jenkins, "Comparison of fixed speed and doubly-fed induction wind turbines during power system disturbances," in *IEE Proceedings of Generation, Transmission and Distribution*, vol. 150, pp. 343-352, 2003.
- [15] V. Akhmatov, *Induction Generators for Wind Power*: Multi-Science Publishing Company Ltd, 2005.
- [16] A. Yazdani and P. P. Dash, "A Control Methodology and Characterization of Dynamics for a Photovoltaic (PV) System Interfaced With a Distribution Network," *IEEE Transactions on Power Delivery*, vol. 24, pp. 1538-1551, 2009.
- [17] T. Yun Tiam, D. S. Kirschen, and N. Jenkins, "A model of PV generation suitable for stability analysis," *IEEE Transactions on Energy Conversion* vol. 19, pp. 748-755, 2004.
- [18] R. Shah, N. Mithulananthan, A. Sode-Yome, and K. Y. Lee, "Impact of large-scale PV penetration on power system oscillatory stability," in *Proceedings of IEEE Power and Energy Society General Meeting, 2010* pp. 1-7.
- [19] L. Dong-Jing and W. Li, "Small-Signal Stability Analysis of an Autonomous Hybrid Renewable Energy Power Generation/Energy Storage System Part I: Time-Domain Simulations," *IEEE Transactions on Energy Conversion*, vol. 23, pp. 311-320, 2008.

- [20] M. H. Haque, "Load flow solution of distribution systems with voltage dependent load models," *Electric Power Systems Research*, vol. 36, pp. 151-156, 1996.
- [21] T. Van Cutsem and C. Vournas, *Voltage Stability of Electric Power Systems*: Kluwer, 1998.
- [22] S. A. Y. Sabir and D. C. Lee, "Dynamic Load Models Derived from Data Acquired During System Transients," *Power Apparatus and Systems, IEEE Transactions on*, vol. PAS-101, pp. 3365-3372, 1982.
- [23] C. Concordia and S. Ihara, "Load Representation in Power System Stability Studies," *Power Apparatus and Systems, IEEE Transactions on*, vol. PAS-101, pp. 969-977, 1982.
- [24] W. W. Price, K. A. Wirgau, A. Murdoch, J. V. Mitsche, E. Vaahedi, and M. El-Kady, "Load modeling for power flow and transient stability computer studies," *Power Systems, IEEE Transactions on*, vol. 3, pp. 180-187, 1988.
- [25] P. Kundur, N. J. Balu, and M. G. Lauby, *Power system stability and control*. New York: McGraw-Hill, 1994.
- [26] P. C. Krause, *Analysis of Electric Machinery*: McGraw-Hill, 1986.
- [27] O. H. Abdalla, M. E. Bahgat, A. M. Serag, and M. A. El-Sharkawi, "Dynamic load modelling and aggregation in power system simulation studies," in *Power System Conference, 2008. MEPCON 2008. 12th International Middle-East*, 2008, pp. 270-276.
- [28] L. Shao-Hua, C. Hsiao-Dong, and L. Sheng, "Analysis of Composite Load Models on Load Margin of Voltage Stability," in *Power System Technology, 2006. PowerCon 2006. International Conference on*, 2006, pp. 1-7.
- [29] P. W. Sauer and M. A. Pai, *Power system dynamics and stability*, Updated ed. Champaign, IL.: Stipes Publishing L.L.C., 2006.
- [30] L. L. Lai and T. F. Chan, *Distributed generation : induction and permanent magnet generators*. Chichester: John Wiley / IEEE, 2007.
- [31] E. J. Coster, J. M. A. Myrzik, B. Kruimer, and W. L. Kling, "Integration Issues of Distributed Generation in Distribution Grids," *Proceedings of the IEEE*, vol. 99, pp. 28-39, 2011.
- [32] E. F. Mogos and X. Guillaud, "A voltage regulation system for distributed generation," in *Power Systems Conference and Exposition, 2004. IEEE PES*, 2004, pp. 787-794 vol.2.
- [33] K. Miyong, R. Hara, and H. Kita, "Design of the Optimal ULTC Parameters in Distribution System With Distributed Generations," *Power Systems, IEEE Transactions on*, vol. 24, pp. 297-305, 2009.
- [34] M. Chakravorty and D. Das, "Voltage stability analysis of radial distribution networks," *International Journal of Electrical Power & Energy Systems*, vol. 23, pp. 129-135, 2001.
- [35] S. K. Salman, "The impact of embedded generation on voltage regulation and losses of distribution networks," in *Embedded Generation on Distribution Networks (Digest No. 1996/194), IEE Colloquium on the Impact of*, 1996, pp. 2/1-2/5.
- [36] C. L. T. Borges and D. M. Falcao, "Impact of distributed generation allocation and sizing on reliability, losses and voltage profile," in *Power Tech Conference Proceedings, 2003 IEEE Bologna*, 2003, p. 5 pp. Vol.2.
- [37] T. K. S. Tareq Aziz , N. Mithulanathan, "Distributed Generators Placement for Loadability Enhancement based on Reactive Power Margin," in *IPEC, 2010*. Singapore.
- [38] L. F. Ochoa and G. P. Harrison, "Minimizing Energy Losses: Optimal Accommodation and Smart Operation of Renewable Distributed Generation," *Power Systems, IEEE Transactions on*, vol. 26, pp. 198-205, 2011.
- [39] M. J. J. Scheepers, "Transitions in Electricity Supply Systems: Challenges for Policy and Regulation," *OTTI* pp. 148-155, 2004.
- [40] A. Bhowmik, A. Maitra, S. M. Halpin, and J. E. Schatz, "Determination of allowable penetration levels of distributed generation resources based on harmonic limit considerations," *Power Delivery, IEEE Transactions on*, vol. 18, pp. 619-624, 2003.

- [41] P. P. Barker and R. W. De Mello, "Determining the impact of distributed generation on power systems. I. Radial distribution systems," in *Power Engineering Society Summer Meeting, 2000. IEEE*, 2000, pp. 1645-1656 vol. 3.
- [42] S. P. T. H. Boutsika, N. Drossos, "Calculation of fault current contribution of distributed generation according to IEC Standard 60909," in *CIGRE Symposium on Power Systems with Dispersed Generation*, 2005.
- [43] "International Grid Code Comparison (IGCC-list) online available at [http://www.gl-group.com/pdf/IGCC\\_list.pdf](http://www.gl-group.com/pdf/IGCC_list.pdf)."
- [44] P. M. Anderson, *Power system protection*. New York: McGraw-Hill : IEEE Press, 1999.
- [45] J. L. Blackburn and T. J. Domin, "Protective relaying : principles and applications," 3rd ed Boca Raton, FL: CRC Press, 2007.
- [46] A. Ipakchi and F. Albuyeh, "Grid of the future," *Power and Energy Magazine, IEEE*, vol. 7, pp. 52-62, 2009.
- [47] "Australian Energy Market Operator (AEMO), "National Electricity Amendment (Technical Standards for Wind Generation and other Generator Connections) Rule 2007," 2007.
- [48] S. M. Mueeen, R. Takahashi, T. Murata, and J. Tamura, "A Variable Speed Wind Turbine Control Strategy to Meet Wind Farm Grid Code Requirements," *IEEE Transactions on Power Systems* vol. 25, pp. 331-340.
- [49] S. Dahal, N. Mithulananthan, and T. Saha, "Investigation of small signal stability of a renewable energy based electricity distribution system," in *Proceedings of IEEE Power and Energy Society General Meeting, 2010* pp. 1-8.
- [50] N. Mithulananthan, C. A. Canizares, and J. Reeve, "Tuning, performance and interactions of PSS and FACTS controllers," in *Proceedings of IEEE Power Engineering Society Summer Meeting*, 2002, pp. 981-987 vol.2.
- [51] F. P. de Mello, J. W. Feltes, L. N. Hannett, and J. C. White, "Application of Induction Generators in Power Systems," *Power Apparatus and Systems, IEEE Transactions on*, vol. PAS-101, pp. 3385-3393, 1982.
- [52] B. M. Nomikos and C. D. Vournas, "Investigation of induction Machine contribution to power system oscillations," *Power Systems, IEEE Transactions on*, vol. 20, pp. 916-925, 2005.
- [53] R. Stern and D. W. Novotny, "A Simplified Approach to the Determination of Induction Machine Dynamic Response," *Power Apparatus and Systems, IEEE Transactions on*, vol. PAS-97, pp. 1430-1439, 1978.
- [54] H. L. Willis, "Analytical methods and rules of thumb for modeling DG-distribution interaction," in *Power Engineering Society Summer Meeting, 2000. IEEE*, 2000, pp. 1643-1644 vol. 3.
- [55] J. G. Slootweg and W. L. Kling, "The impact of large scale wind power generation on power system oscillations," *Electric Power Systems Research*, vol. 67, pp. 9-20, 2003.
- [56] R. D. Fernández, R. J. Mantz, and P. E. Battaiotto, "Impact of wind farms on a power system. An eigenvalue analysis approach," *Renewable Energy*, vol. 32, pp. 1676-1688, 2007.
- [57] T. Yun Tiam and D. S. Kirschen, "Impact on the Power System of a Large Penetration of Photovoltaic Generation," in *Power Engineering Society General Meeting, 2007. IEEE*, 2007, pp. 1-8.
- [58] D. Gautam, V. Vittal, and T. Harbour, "Impact of Increased Penetration of DFIG-Based Wind Turbine Generators on Transient and Small Signal Stability of Power Systems," *Power Systems, IEEE Transactions on*, vol. 24, pp. 1426-1434, 2009.
- [59] B. C. Pal and F. Mei, "Modelling adequacy of the doubly fed induction generator for small-signal stability studies in power systems," *Renewable Power Generation, IET*, vol. 2, pp. 181-190, 2008.
- [60] C. A. Canizares, "On bifurcations, voltage collapse and load modeling," *Power Systems, IEEE Transactions on*, vol. 10, pp. 512-522, 1995.
- [61] H. G. Kwatny, R. F. Fischl, and C. O. Nwankpa, "Local bifurcation in power systems: theory, computation, and application," *Proceedings of the IEEE*, vol. 83, pp. 1456-1483, 1995.
- [62] M. A. Pai, P. W. Sauer, and B. C. Lesieutre, "Static and dynamic nonlinear loads and structural stability in power systems," *Proceedings of the IEEE*, vol. 83, pp. 1562-1572, 1995.

- [63] A. H. Nayfeh, A. M. Harb, and C. Char-Ming, "Bifurcations in a power system model," in *Circuits and Systems, 1995. ISCAS '95., 1995 IEEE International Symposium on*, 1995, pp. 283-286 vol.1.
- [64] C. A. Canizares, N. Mithulananthan, F. Milano, and J. Reeve, "Linear performance indices to predict oscillatory stability problems in power systems," *Power Systems, IEEE Transactions on*, vol. 19, pp. 1104-1114, 2004.
- [65] A. Kumar, S. C. Srivastava, and S. N. Singh, "Available transfer capability assessment in a competitive electricity market using a bifurcation approach," *Generation, Transmission and Distribution, IEE Proceedings-*, vol. 151, pp. 133-140, 2004.
- [66] C. D. Vournas and G. A. Manos, "Modelling of stalling motors during voltage stability studies," *Power Systems, IEEE Transactions on*, vol. 13, pp. 775-781, 1998.
- [67] T. A. Short, *Electric Power Distribution Handbook*: CRC Press LLC, 2004.
- [68] T. Gonen, *Electric Power Distribution System*: McGraw-Hill Book Company, 1986.
- [69] N. G. Hingorani and L. Gyugyi, *Understanding FACTS : concepts and technology of flexible AC transmission systems*. Delhi: IEEE Press, 2001.
- [70] K. R. Padiyar, *Facts controllers in power transmission and distribution*. New Delhi: New Age International, 2007.
- [71] S. Kincic, X. T. Wan, D. T. McGillis, A. Chandra, O. Boon-Teck, F. D. Galiana, and G. Joos, "Voltage support by distributed static VAR systems (SVS)," *Power Delivery, IEEE Transactions on*, vol. 20, pp. 1541-1549, 2005.
- [72] S. Kincic and A. Chandra, "Impact of distributed compensators on power system voltages," in *Electrical and Computer Engineering, 2003. IEEE CCECE 2003. Canadian Conference on*, 2003, pp. 547-552 vol.1.
- [73] S. Kincic and A. Chandra, "Distribution level STATCOMs (DSTATCOMs) for load voltages support," in *Power Engineering, 2003 Large Engineering Systems Conference on*, 2003, pp. 30-37.
- [74] N. M. Arthit Sode-Yome, "Comparison of shunt capacitors, SVC and STATCOM in static voltage stability margin enhancement," *International Journal of Electrical Engineering Education*, vol. 41, pp. 158-171, April, 2004.
- [75] T. Niknam, A. M. Ranjbar, and A. R. Shirani, "Impact of distributed generation on volt/Var control in distribution networks," in *Power Tech Conference Proceedings, 2003 IEEE Bologna*, 2003, p. 7 pp. Vol.3.
- [76] L. A. Kojovic, "Modern techniques to study voltage regulator - DG interactions in distribution systems," in *Transmission and Distribution Conference and Exposition, 2008. T&D. IEEE/PES*, 2008, pp. 1-6.
- [77] A. Keane, L. F. Ochoa, E. Vittal, C. J. Dent, and G. P. Harrison, "Enhanced Utilization of Voltage Control Resources With Distributed Generation," *Power Systems, IEEE Transactions on*, vol. 26, pp. 252-260, 2011.
- [78] Z. Wenjuan, L. Fangxing, and L. M. Tolbert, "Review of Reactive Power Planning: Objectives, Constraints, and Algorithms," *Power Systems, IEEE Transactions on*, vol. 22, pp. 2177-2186, 2007.
- [79] C. Chompoo-inwai, C. Yingvivatanapong, K. Methaprayoon, and L. Wei-Jen, "Reactive compensation techniques to improve the ride-through capability of wind turbine during disturbance," *Industry Applications, IEEE Transactions on*, vol. 41, pp. 666-672, 2005.
- [80] N. K. Ardeshta and B. H. Chowdhury, "Supporting islanded microgrid operations in the presence of intermittent wind generation," in *Power and Energy Society General Meeting, 2010 IEEE*, 2010, pp. 1-8.
- [81] M. Noroozian, N. A. Petersson, B. Thorvaldson, A. B. Nilsson, and C. W. Taylor, "Benefits of SVC and STATCOM for electric utility application," in *Transmission and Distribution Conference and Exposition, 2003 IEEE PES*, 2003, pp. 1143-1150 vol.3.
- [82] K. Tanaka, T. Senjyu, S. Toma, A. Yona, T. Funabashi, and K. Chul-Hwan, "Decentralized voltage control in distribution systems by controlling reactive power of inverters," in *Industrial Electronics, 2009. ISIE 2009. IEEE International Symposium on*, 2009, pp. 1385-1390.

- [83] S. Foster, L. Xu, and B. Fox, "Coordinated reactive power control for facilitating fault ride through of doubly fed induction generator- and fixed speed induction generator-based wind farms," *Renewable Power Generation, IET*, vol. 4, pp. 128-138, 2010.
- [84] A. Keane, L. F. Ochoa, E. Vittal, C. J. Dent, and G. P. Harrison, "Enhanced Utilization of Voltage Control Resources With Distributed Generation," *Power Systems, IEEE Transactions on*, vol. PP, pp. 1-1, 2010.
- [85] M. V. A. Nunes, J. A. P. Lopes, H. H. Zurn, U. H. Bezerra, and R. G. Almeida, "Influence of the variable-speed wind generators in transient stability margin of the conventional generators integrated in electrical grids," *Energy Conversion, IEEE Transactions on*, vol. 19, pp. 692-701, 2004.
- [86] K. M. Rogers, R. Klump, H. Khurana, A. A. Aquino-Lugo, and T. J. Overbye, "An Authenticated Control Framework for Distributed Voltage Support on the Smart Grid," *Smart Grid, IEEE Transactions on*, vol. 1, pp. 40-47, 2010.
- [87] M. Singh, V. Khadkikar, A. Chandra, and R. K. Varma, "Grid Interconnection of Renewable Energy Sources at the Distribution Level With Power-Quality Improvement Features," *Power Delivery, IEEE Transactions on*, vol. 26, pp. 307-315, 2011.
- [88] R. Caldon, S. Spelta, V. Prandoni, and R. Turri, "Co-ordinated voltage regulation in distribution networks with embedded generation," in *Electricity Distribution, 2005. CIRED 2005. 18th International Conference and Exhibition on*, 2005, pp. 1-4.
- [89] F. A. Viawan and D. Karlsson, "Voltage and Reactive Power Control in Systems With Synchronous Machine-Based Distributed Generation," *Power Delivery, IEEE Transactions on*, vol. 23, pp. 1079-1087, 2008.
- [90] Qiuwei Wu, Zhao Xu, and J. Ostergaard, "Grid integration issues for large scale wind power plants (WPPs)," in *Power and Energy Society General Meeting, 2010 IEEE*, 2010, pp. 1-6.
- [91] F. A. Viawan and D. Karlsson, "Coordinated voltage and reactive power control in the presence of distributed generation," in *Power and Energy Society General Meeting - Conversion and Delivery of Electrical Energy in the 21st Century, 2008 IEEE*, 2008, pp. 1-6.
- [92] F. A. Viawan and D. Karlsson, "Combined Local and Remote Voltage and Reactive Power Control in the Presence of Induction Machine Distributed Generation," *Power Systems, IEEE Transactions on*, vol. 22, pp. 2003-2012, 2007.
- [93] W. Yi and X. Lie, "Coordinated Control of DFIG and FSIG-Based Wind Farms Under Unbalanced Grid Conditions," *Power Delivery, IEEE Transactions on*, vol. 25, pp. 367-377, 2010.
- [94] W. Li, W. Kuo-Hua, L. Wei-Jen, and C. Zhe, "Power-Flow Control and Stability Enhancement of Four Parallel-Operated Offshore Wind Farms Using a Line-Commutated HVDC Link," *Power Delivery, IEEE Transactions on*, vol. 25, pp. 1190-1202, 2010.
- [95] S. Teleke, M. E. Baran, S. Bhattacharya, and A. Q. Huang, "Optimal Control of Battery Energy Storage for Wind Farm Dispatching," *Energy Conversion, IEEE Transactions on*, vol. PP, pp. 1-8, 2010.
- [96] S. Teleke, M. E. Baran, A. Q. Huang, S. Bhattacharya, and L. Anderson, "Control Strategies for Battery Energy Storage for Wind Farm Dispatching," *Energy Conversion, IEEE Transactions on*, vol. 24, pp. 725-732, 2009.
- [97] S. M. Mueen, R. Takahashi, T. Murata, and J. Tamura, "Integration of an Energy Capacitor System With a Variable-Speed Wind Generator," *Energy Conversion, IEEE Transactions on*, vol. 24, pp. 740-749, 2009.
- [98] Federal Energy Regulatory Commission (FERC), "Interconnection for Wind Energy " Issued June 2, 2005.
- [99] I. J. Balaguer, L. Qin, Y. Shuitao, U. Supatti, and P. Fang Zheng, "Control for Grid-Connected and Intentional Islanding Operations of Distributed Power Generation," *Industrial Electronics, IEEE Transactions on*, vol. 58, pp. 147-157, 2011.
- [100] J. E. Hill, "A practical example of the use of distribution static compensator (D-STATCOM) to reduce voltage fluctuations," in *Power Electronics for Renewable Energy (Digest No: 1997/170), IEE Colloquium on*, 1997, pp. 7/1-7/5.

- [101] M. A. Eldery, E. F. El-Saadany, and M. M. A. Salama, "Effect of distributed generator on the allocation D-STATCOM in distribution network," in *Power Engineering Society General Meeting, 2005. IEEE*, 2005, pp. 2360-2364 Vol. 3.
- [102] M. Molinas, J. A. Suul, and T. Undeland, "Extending the Life of Gear Box in Wind Generators by Smoothing Transient Torque With STATCOM," *Industrial Electronics, IEEE Transactions on*, vol. 57, pp. 476-484, 2010.
- [103] Z. Saad-Saoud and N. Jenkins, "Models for predicting flicker induced by large wind turbines," *Energy Conversion, IEEE Transactions on*, vol. 14, pp. 743-748, 1999.
- [104] Z. Saad-Saoud, M. L. Lisboa, J. B. Ekanayake, N. Jenkins, and G. Strbac, "Application of STATCOMs to wind farms," *Generation, Transmission and Distribution, IEE Proceedings-*, vol. 145, pp. 511-516, 1998.
- [105] P. Brady, C. Dai, and Y. Baghzouz, "Need to revise switched capacitor controls on feeders with distributed generation," in *Transmission and Distribution Conference and Exposition, 2003 IEEE PES*, 2003, pp. 590-594 vol.2.
- [106] "IEEE Application Guide for IEEE Std 1547, IEEE Standard for Interconnecting Distributed Resources with Electric Power Systems," *IEEE Std 1547.2-2008*, pp. 1-207, 2009.
- [107] "IEEE Standard for Interconnecting Distributed Resources With Electric Power Systems," *IEEE Std 1547-2003*, pp. 0\_1-16, 2003.
- [108] T. Aziz, U. P. Mhaskar, Tapan K. Saha, N. Mithulanathan, "A Grid Compatible Methodology for Reactive Power Compensation in Renewable Based Distribution System " in *PESGM*, Detroit, Michigan, 2011.
- [109] L. Rouco and F. L. Pagola, "An eigenvalue sensitivity approach to location and controller design of controllable series capacitors for damping power system oscillations," *Power Systems, IEEE Transactions on*, vol. 12, pp. 1660-1666, 1997.
- [110] N. Martins and L. T. G. Lima, "Determination of suitable locations for power system stabilizers and static VAR compensators for damping electromechanical oscillations in large scale power systems," *Power Systems, IEEE Transactions on*, vol. 5, pp. 1455-1469, 1990.
- [111] D. Masand, S. Jain, and G. Agnihotri, "Control Algorithms for Distribution Static Compensator," in *Industrial Electronics, 2006 IEEE International Symposium on*, 2006, pp. 1830-1834.
- [112] J. Hongjie, Y. Xiaodan, S. Xiaoyan, C. Jianhua, W. Wei, and Y. Yixin, "Relationship between shunt capacitor and small signal stability of power systems," in *Electrical and Computer Engineering, 2005. Canadian Conference on*, 2005, pp. 1708-1713.
- [113] H. F. Wang and F. J. Swift, "Capability of the static VAR compensator in damping power system oscillations," *Generation, Transmission and Distribution, IEE Proceedings-*, vol. 143, pp. 353-358, 1996.
- [114] B. Gao, G. K. Morison, and P. Kundur, "Voltage stability evaluation using modal analysis," *Power Systems, IEEE Transactions on*, vol. 7, pp. 1529-1542, 1992.
- [115] N. Mithulanathan, C. A. Canizares, J. Reeve, and G. J. Rogers, "Comparison of PSS, SVC, and STATCOM controllers for damping power system oscillations," *Power Systems, IEEE Transactions on*, vol. 18, pp. 786-792, 2003.
- [116] D. McFarlane and K. Glover, "A loop-shaping design procedure using  $H_\infty$  synthesis," *Automatic Control, IEEE Transactions on*, vol. 37, pp. 759-769, 1992.
- [117] Z. Chuanjiang, M. Khammash, V. Vittal, and Q. Wenzheng, "Robust power system stabilizer design using  $H_\infty$  loop shaping approach," *Power Systems, IEEE Transactions on*, vol. 18, pp. 810-818, 2003.
- [118] F. Katiraei, M. R. Iravani, and P. W. Lehn, "Micro-grid autonomous operation during and subsequent to islanding process," *IEEE Transactions on Power Delivery*, vol. 20, pp. 248-257, 2005.
- [119] E. Muljadi, C. P. Butterfield, B. Parsons, and A. Ellis, "Effect of Variable Speed Wind Turbine Generator on Stability of a Weak Grid," *Energy Conversion, IEEE Transactions on*, vol. 22, pp. 29-36, 2007.

- [120] N. R. Ullah and T. Thiringer, "Effect of operational modes of a wind farm on the transient stability of nearby generators and on power oscillations: a Nordic grid study," *Wind Energy*, vol. 11, pp. 63-73, 2008.
- [121] J. J. Sanchez-Gasca, N. W. Miller, and W. W. Price, "A modal analysis of a two-area system with significant wind power penetration," in *Power Systems Conference and Exposition, 2004. IEEE PES*, 2004, pp. 1148-1152 vol.2.
- [122] A. Mendonca and J. A. P. Lopes, "Impact of large scale wind power integration on small signal stability," in *Future Power Systems, 2005 International Conference on*, 2005, pp. 5 pp.-5.
- [123] F. M. Hughes, O. Anaya-Lara, N. Jenkins, and G. Strbac, "A power system stabilizer for DFIG-based wind generation," *Power Systems, IEEE Transactions on*, vol. 21, pp. 763-772, 2006.
- [124] S. Muller, M. Deicke, and R. W. De Doncker, "Doubly fed induction generator systems for wind turbines," *Industry Applications Magazine, IEEE*, vol. 8, pp. 26-33, 2002.
- [125] M. Zhixin, F. Lingling, D. Osborn, and S. Yuvarajan, "Control of DFIG based wind generation to improve inter-area oscillation damping," in *Power and Energy Society General Meeting - Conversion and Delivery of Electrical Energy in the 21st Century, 2008 IEEE*, 2008, pp. 1-7.
- [126] M. Zhixin, F. Lingling, D. Osborn, and S. Yuvarajan, "Control of DFIG-Based Wind Generation to Improve Interarea Oscillation Damping," *Energy Conversion, IEEE Transactions on*, vol. 24, pp. 415-422, 2009.
- [127] O. Wasynczuk and N. A. Anwah, "Modeling and Dynamic Performance of a Self-Commutated Photovoltaic Inverter System," *Power Engineering Review, IEEE*, vol. 9, pp. 33-34, 1989.
- [128] L. Wu, Z. Zhao, and J. Liu, "A Single-Stage Three-Phase Grid-Connected Photovoltaic System With Modified MPPT Method and Reactive Power Compensation," *Energy Conversion, IEEE Transactions on*, vol. 22, pp. 881-886, 2007.
- [129] Z. Shi-cheng, W. Pei-zhen, and G. Lu-sheng, "Study on Pwm Control Strategy of Photovoltaic Grid-connected Generation System," in *Power Electronics and Motion Control Conference, 2006. IPEMC 2006. CES/IEEE 5th International*, 2006, pp. 1-5.
- [130] E. Figueres, G. Garcera, J. Sandia, and F. J. Gonzalez-Espin, "Modelling and control of a 100kW photovoltaic inverter with an LCL grid filter for distributed power systems," in *Power Electronics and Applications, 2007 European Conference on*, 2007, pp. 1-10.
- [131] Y. Guangya, G. Hovland, R. Majumder, and D. ZhaoYang, "TCSC allocation based on line flow based equations via mixed-integer programming," in *Power and Energy Society General Meeting - Conversion and Delivery of Electrical Energy in the 21st Century, 2008 IEEE*, 2008, pp. 1-1.
- [132] R. W. Chang and T. K. Saha, "Maximizing power system loadability by optimal allocation of svc using mixed integer linear programming," in *Power and Energy Society General Meeting, 2010 IEEE*, pp. 1-7.
- [133] W. Feng, Z. Xiao-Ping, and J. Ping, "Modeling and control of the wind turbine with the Direct Drive Permanent Magnet Generator integrated to power grid," in *Electric Utility Deregulation and Restructuring and Power Technologies, 2008. DRPT 2008. Third International Conference on*, 2008, pp. 57-60.
- [134] T. Yun Tiam, D. S. Kirschen, and N. Jenkins, "A model of PV generation suitable for stability analysis," *Energy Conversion, IEEE Transactions on*, vol. 19, pp. 748-755, 2004.
- [135] "Load representation for dynamic performance analysis [of power systems]," *Power Systems, IEEE Transactions on*, vol. 8, pp. 472-482, 1993.
- [136] A. Borghetti, R. Caldon, A. Mari, and C. A. Nucci, "On dynamic load models for voltage stability studies," *Power Systems, IEEE Transactions on*, vol. 12, pp. 293-303, 1997.
- [137] L. Pereira, D. Kosterev, P. Mackin, D. Davies, J. Undrill, and Z. Wenchun, "An interim dynamic induction motor model for stability studies in the WSCC," *Power Systems, IEEE Transactions on*, vol. 17, pp. 1108-1115, 2002.
- [138] J. Wang, R. He, and J. Ma, "Load Modeling Considering Distributed Generation," in *Power Tech, 2007 IEEE Lausanne*, 2007, pp. 1072-1077.

- [139] H. Renmu, J. Ma, and D. J. Hill, "Composite load modeling via measurement approach," *Power Systems, IEEE Transactions on*, vol. 21, pp. 663-672, 2006.
- [140] M. A. Pai and P. Sauer, *Power System Dynamics and Stability*. Champaign: Stipes Publishing L.L.C., 2006.
- [141] M. A. Pai, P. W. Sauer, B. C. Lesieutre, and R. Adapa, "Structural stability in power systems-effect of load models," *Power Systems, IEEE Transactions on*, vol. 10, pp. 609-615, 1995.
- [142] P. M. Anderson and A. A. Fouad, *Power System Control and Stability* IEEE Press, 2003.
- [143] D. P. 13.2, "Technical documentation on dynamic modeling of Doubly-Fed Induction Machine wind-generators," 30 Sept 2003.
- [144] C. W. Taylor, N. J. Balu, and D. Maratukulam, *Power system voltage stability*. New York: McGraw Hill, 1994.
- [145] N. Jenkins, *Distributed generation*. London: Inst Of Engin And Tech, 2009.
- [146] W. Freitas, J. C. M. Vieira, A. Morelato, L. C. P. da Silva, V. F. da Costa, and F. A. B. Lemos, "Comparative analysis between synchronous and induction machines for distributed generation applications," *Power Systems, IEEE Transactions on*, vol. 21, pp. 301-311, 2006.
- [147] "Voltage stability assessment, procedures and guides " IEEE/PES Power System Stability Subcommittee Technical Report January 2001.
- [148] R. A. Schlueter, "A voltage stability security assessment method," *Power Systems, IEEE Transactions on*, vol. 13, pp. 1423-1438, 1998.
- [149] N. Mithulananthan and T. Oo, "Distributed Generator Placement to Maximize the Loadability of Distribution System " *IJEEE* vol. 43, pp. 107-118, April 2006.
- [150] Y. Mansour, "Suggested techniques for voltage stability analysis," IEEE/PES, Technical Report 1993.
- [151] P. Kessel and H. Glavitsch, "Estimating the Voltage Stability of a Power System," *Power Delivery, IEEE Transactions on*, vol. 1, pp. 346-354, 1986.
- [152] J. Hongjie, Y. Xiaodan, and Y. Yixin, "An improved voltage stability index and its application," *International Journal of Electrical Power & Energy Systems*, vol. 27, pp. 567-574, 2005.
- [153] P. K. Satpathy, "Impact of Various Load Models in Power System Bifurcation Analysis," *Electric Power Components and Systems*, vol. 31, pp. 653 - 669, 2003.
- [154] Tareq Aziz, T. K. Saha and N. Mithulananthan, "Identification of the weakest bus in a distribution system with load uncertainties using reactive power margin " in *submitted in AUPEC*, Newzealand, 2010.
- [155] M. M. A. S. N. Mithulananthan, C. A. Canizares and J. Reeve, "Distribution system voltage regulation and var compensation for different static load models," *International Journal of Electrical Engineering Education*, vol. 37, pp. 384-395, 2000.
- [156] S. Civanlar, J. J. Grainger, H. Yin, and S. S. H. Lee, "Distribution feeder reconfiguration for loss reduction," *Power Delivery, IEEE Transactions on*, vol. 3, pp. 1217-1223, 1988.
- [157] DIgSILENT GmbH, "DIgSILENT PowerFactory V14.0 -User Manual," *DIgSILENT GmbH*, 2008.
- [158] F. Milano, "PSAT, Matlab-based Power System Analysis Toolbox," 2002.
- [159] K. Morison, H. Hamadani, and W. Lei, "Load Modeling for Voltage Stability Studies," in *Power Systems Conference and Exposition, 2006. PSCE '06. 2006 IEEE PES*, 2006, pp. 564-568.
- [160] T. Aziz, "Investigation of Voltage Stability Issues of Distribution Network with Large Scale Integration of Renewable Energy Based Distributed Generation," PhD Confirmation report, School of ITEE, The University of Queensland, Internal Report, 2010.
- [161] S. J. van Zyl and C. T. Gaunt, "Control strategies for distributed generators operating on weak distribution networks," in *Power Tech Conference Proceedings, 2003 IEEE Bologna*, 2003, p. 7 pp. Vol.3.

- [162] A. E. M. Commission, "National Electricity Amendment (Technical Standards for wind and other generators connections) Rule 2007," 8 March, 2007, [www.aemc.gov.au](http://www.aemc.gov.au).
- [163] H. Yann-Chang, Y. Hong-Tzer, and H. Ching-Lien, "Solving the capacitor placement problem in a radial distribution system using Tabu Search approach," *Power Systems, IEEE Transactions on*, vol. 11, pp. 1868-1873, 1996.
- [164] Z. Wen, L. Yutian, and L. Yuanqi, "Optimal VAr planning in area power system," in *Power System Technology, 2002. Proceedings. PowerCon 2002. International Conference on*, 2002, pp. 2072-2075 vol.4.
- [165] "IEEE Recommended Practice for Industrial and Commercial Power Systems Analysis," *IEEE Std 399-1997*, p. I, 1998.
- [166] G. Levitin, A. Kalyuzhny, A. Shenkman, and M. Chertkov, "Optimal capacitor allocation in distribution systems using a genetic algorithm and a fast energy loss computation technique," *Power Delivery, IEEE Transactions on*, vol. 15, pp. 623-628, 2000.
- [167] N. Mithulanathan, C. A. Canizares, J. Reeve, and G. J. Rogers, "Comparison of PSS, SVC, and STATCOM controllers for damping power system oscillations," *IEEE Transactions on Power Systems*, vol. 18, pp. 786-792, 2003.
- [168] C. Y. Chung, W. Lei, F. Howell, and P. Kundur, "Generation rescheduling methods to improve power transfer capability constrained by small-signal stability," *Power Systems, IEEE Transactions on*, vol. 19, pp. 524-530, 2004.
- [169] K. W. Wang, C. Y. Chung, C. T. Tse, and K. M. Tsang, "Multimachine eigenvalue sensitivities of power system parameters," *Power Systems, IEEE Transactions on*, vol. 15, pp. 741-747, 2000.
- [170] F. Mei and B. Pal, "Modal Analysis of Grid-Connected Doubly Fed Induction Generators," *Energy Conversion, IEEE Transactions on*, vol. 22, pp. 728-736, 2007.
- [171] L. Rouco and J. L. Zamora, "Dynamic patterns and model order reduction in small-signal models of doubly fed induction generators for wind power applications," in *Power Engineering Society General Meeting, 2006. IEEE*, 2006, p. 8 pp.
- [172] L. Sigrist and L. Rouco, "Design of damping controllers for doubly fed induction generators using eigenvalue sensitivities," in *Power Systems Conference and Exposition, 2009. PSCE '09. IEEE/PES*, 2009, pp. 1-7.
- [173] F. Mei and B. C. Pal, "Modelling and small-signal analysis of a grid connected doubly-fed induction generator," in *Power Engineering Society General Meeting, 2005. IEEE*, 2005, pp. 2101-2108 Vol. 3.
- [174] S. Ahmed-Zaid and O. Awed-Badeeb, "Dynamic interaction of synchronous generators and induction motor loads," in *Circuits and Systems, 1992., Proceedings of the 35th Midwest Symposium on*, 1992, pp. 1432-1435 vol.2.
- [175] A. Kent and D. Mercer, "Australia's mandatory renewable energy target (MRET): an assessment," *Energy Policy*, vol. 34, pp. 1046-1062, 2006.
- [176] W. Xiaoyu and V. Ajjarapu, "Application of a novel eigenvalue trajectory tracing method to identify both oscillatory stability margin and damping margin," *IEEE Transactions on Power Systems*, vol. 21, pp. 817-824, 2006.
- [177] "IEEE Task Force on Load Representation for Dynamic Performance , "Load representation for dynamic performance analysis [of power systems]," *IEEE Transactions on Power Systems*, vol. 8, pp. 472-482, 1993.
- [178] G. J. Rogers, *Power System Oscillations*. Boston/London/Dordrecht: Kluwer Academic Publishers, 2000.
- [179] J. A. P. Lopes, N. Hatziaargyriou, J. Mutale, P. Djapic, and N. Jenkins, "Integrating distributed generation into electric power systems: A review of drivers, challenges and opportunities," *Electric Power Systems Research*, vol. 77, pp. 1189-1203, 2007.
- [180] J. Hongjie, Y. Xiaodan, S. Xiaoyan, C. Jianhua, W. Wei, and Y. Yixin, "Relationship between shunt capacitor and small signal stability of power systems," in *In Proceedings of Canadian Conference on Electrical and Computer Engineering, 2005*, 2005, pp. 1708-1713.

- [181] L. Li, V. A. Ugrinovskii, and R. Orsi, "Decentralized robust control of uncertain Markov jump parameter systems via output feedback," *Automatica*, vol. 43, pp. 1932-1944, 2007.
- [182] M. J. Hossain, H. R. Pota, and C. Kumble, "Decentralized robust static synchronous compensator control to augment dynamic transfer capability," *Journal of Renewable and Sustainable Energy*, vol. 2, p. 20, March 2010.

## 10. REFERENCE LIST

AHN, S. J., PARK, J. W., CHUNG, I. Y., MOON, S. I., KANG, S. H. & NAM, S. R. 2010. Power-Sharing Method of Multiple Distributed Generators Considering Control Modes and Configurations of a Microgrid. *IEEE Transactions on Power Delivery*, 25, 2007-2016.